

**HIGH PERFORMANCE SEPARATION STUDIES ON
LANTHANIDES AND SOME ACTINIDES**

By

ARPITA DATTA

Enrolment No: CHEM02200704002

**Indira Gandhi Centre for Atomic Research, Kalpakkam,
Tamil Nadu, India**

*A thesis submitted to the
Board of Studies in Chemical Sciences*

*In partial fulfillment of requirements
For the Degree of*

DOCTOR OF PHILOSOPHY

of

HOMI BHABHA NATIONAL INSTITUTE



May, 2012

**HIGH PERFORMANCE SEPARATION STUDIES ON
LANTHANIDES AND SOME ACTINIDES**

By

ARPITA DATTA

Enrolment No: CHEM02200704002

**Indira Gandhi Centre for Atomic Research, Kalpakkam,
Tamil Nadu, India**

*A thesis submitted to the
Board of Studies in Chemical Sciences*

*In partial fulfillment of requirements
For the Degree of*

DOCTOR OF PHILOSOPHY

of

HOMI BHABHA NATIONAL INSTITUTE

Research Supervisor

Dr. P. R. Vasudeva Rao

Director, Chemistry Group

Indira Gandhi Centre for Atomic Research

Kalpakkam-603 102, Tamil Nadu, India.



May, 2012

Homi Bhabha National Institute

Recommendations of the Viva Voce Board

As members of the Viva Voce Board, we certify that we have read the dissertation prepared by **Arpita Datta** entitled “**High Performance Separation Studies on Lanthanides and Some Actinides**” and recommend that it may be accepted as fulfilling the dissertation requirement for the Degree of Doctor of Philosophy.

Chairman – Dr. T.G. Srinivasan

Date: 29.10.12

Supervisor/Convener - Dr. P.R. Vasudeva Rao

Date: 29/10/12

Member – Dr. N. Sivaraman

Date:

N. Sivaraman

29/10/2012

Date:

Member– Dr. K. Nagarajan

K. Nagarajan

29/10/12

Date:

External Examiner-Prof. M.L.P. Reddy (Senior Scientist, National Institute for Interdisciplinary Science and Technology, CSIR, Kerala)

29/10/2012

Final approval and acceptance of this dissertation is contingent upon the candidate's submission of the final copies of the dissertation to HBNI.

I hereby certify that I have read this dissertation prepared under my direction and recommend that it may be accepted as fulfilling the dissertation requirement.

Date: 29.10.2012

Place: Kalpakkam

**Department of Atomic Energy
Indira Gandhi Centre for Atomic Research
Kalpakkam**

Ref: HBNI / PhD / Arpita / 2012 / 1

Date: 29-10-2012

Certificate

I, Dr. P.R. Vasudeva Rao, certify that there have been no corrections suggested by the external examiners for the dissertation entitled, "High Performance separation studies on lanthanides and some actinides" by Ms. Arpita Datta. The thesis submitted to the examiners has been bound and submitted to HBNI for the award of the degree of Doctor of Philosophy to Ms. Arpita Datta based on the recommendation of the viva-voce examiner and after due approval by competent authority at HBNI.



Dr. P.R. Vasudeva Rao
(Guide & Convener)

Dean-Academic, Chemical Sciences
HBNI, Kalpakkam

STATEMENT BY AUTHOR

This dissertation has been submitted in partial fulfillment of requirements for an advanced degree at Homi Bhabha National Institute (HBNI) and is deposited in the Library to be made available to borrowers under rules of the HBNI.

Brief quotations from this dissertation are allowable without special permission, provided that accurate acknowledgement of source is made. Requests for permission for extended quotation from or reproduction of this manuscript in whole or in part may be granted by the Competent Authority of HBNI when in his or her judgment the proposed use of the material is in the interests of scholarship. In all other instances, however, permission must be obtained from the author.

Kalpakkam

May 15, 2012

Arpita Datta

ARPITA DATTA

DECLARATION

I, hereby declare that the investigation presented in the thesis has been carried out by me. The work is original and has not been submitted earlier as a whole or in part for a degree / diploma at this or any other Institution / University.

Arpita Datta

ARPITA DATTA

Dedicated to

*My Parents
&
Husband*

ACKNOWLEDGEMENTS

I, wish to express my deep and sincere gratitude to my research supervisor **Dr. P.R. Vasudeva Rao**, Director, Chemistry Group, Indira Gandhi Centre for Atomic Research for his excellent supervision, support and valuable discussion for the work related to this thesis.

I would like to express my gratitude to my co- supervisor, **Dr. N. Sivaraman**; I am pleased to thank him for his valuable guidance, constructive advice, a constant encouragement, timely enlightening discussions and fruitful suggestion through out the course of my PhD work. I thank him for teaching me various aspects of chromatography, theoretical and instrumental part of High performance liquid chromatography (HPLC).

I express my sincere gratitude to my Doctoral committee members **Dr. T. G. Srinivasan**, **Dr. K. S. Viswanathan** (formerly Doctoral committee member) and **Dr. K. Nagarajan** for their valuable suggestions during my doctoral committee meetings. I also thank to **Dr. T. Gnanasekaran**, **Dr. V. Ganesan** (Dean academic, Chemical Sciences, HBNI, IGCAR, Kalpakkam) for useful discussions during my project presentation in Chemistry Group.

My sincere special thanks to **Dr. K. S. Viswanathan** for several discussions and fruitful suggestions for theoretical part of my PhD work. I am also thankful to **Mr. Suddhasattwa Ghosh** for his help regarding Matlab software.

I extend my sincere thanks to **Dr. Baldev Raj**, former Director and **Shri S. C. Chetal**, present Director of Indira Gandhi Centre for Atomic Research.

I would like to thank **Mr. K. A. Venkatesan**, for his help and discussion during my ionic liquid work. I also thank **Dr. Jagadeeswara Rao** for his help during ionic liquid synthesis.

I would like to thank **Mr. R. Kumar**, **Dr. S. Vijayalakshmi**, **Mr. R. Balasubramanian**, **Mrs. K. Sujatha**, **Dr. A. Suresh**, and **Mr. Brahmananda Rao** for the useful discussions. I would like to thank **Dr. K. N. Sabharwal** for his help during “radioactive handling” training. I also thank **Mr. S. Sriram** for his help in analysing samples using ICP-AES. I would like to thank **Mrs. Jayalakshmi**, **Mr. Chinaraga Pitchaiah** and **Ms. Toni Kumari** for their help.

I am personally thankful to my friends **Mr. Prasanta Jana, Ms. Lipika Rani Bairi, Mr. Debasish Saha and Mr. Muffazal Badshahwala**. They had extended their moral support and help as friends whenever I had difficulties during my stay in kalpakkam.

I would like to thank **IGCAR Management**, for providing me nice accommodation and Research fellowship.

I express my sincere gratitude to my mother **Mrs. Swarnalata Datta**, father **Mr. Badari Narayan Datta** not only for my PhD degree but also for the entire education I have had till this day. I owe my entire education to them in some sense. Their inspiration led me to the stage where I am today. It's my pleasure to thank my sister **Ms. Sumana Datta**. Besides my parents, I like to thank my father in law **Mr. Sibaram Konar**, my mother in law **Mrs. Manju Konar**, and grandma in law **Mrs. Geeta Rani Konar**, whose support also worth mentioning. I thank all the teachers in my primary school, secondary school, under graduate college and University. I would like to thank my husband **Dr. Chiranjib Konar** for his continuous support and encouragement. Without his support, it was impossible for me to finish my PhD work successfully.

ARPITA DATTA
May, 2012

CONTENTS

S. No.	Contents	Page No.
	SYNOPSIS	i-x
	LIST OF FIGURES	xi-xvii
	LIST OF TABLES	xviii-xx
	<u>CHAPTER-1</u>	
	Introduction	
1.1	Chromatography	1
1.1.1	Applications of chromatography	1-2
1.1.2	Types of chromatography	2-3
1.1.3	Historical development of chromatography	4-6
1.1.4	Principle of chromatography	6
1.1.5	Retention in chromatography	7-9
1.1.6	Efficiency of chromatographic column	9-12
1.1.7	Resolution (R_s) in chromatography	13-14
1.2	High Performance Liquid Chromatography (HPLC)	14-15
1.2.1	HPLC column packing material	15
1.2.2	HPLC separation modes	15
1.2.2.1	Normal phase liquid chromatography (NPLC)	15-16
1.2.2.2	Reversed phase liquid chromatography (RPLC)	16-17
1.2.2.3	Ion chromatography (IC)	17
1.2.3	Chromatography with $< 2 \mu\text{m}$ particle size	17-18
1.2.4	Separation using monolith based stationary phase	18-19
1.3	Separation chemistry in nuclear industry	19
1.3.1	Nuclear power-An alternative clean source of energy	19-20
1.3.2	Chemistry of lanthanides	20-23
1.3.3	Actinides	23-25
1.3.4	Burn-up (Atom percent fission)	25-26
1.3.4.1	Methods for atom percent burn-up determination	26-27

1.3.5	Importance of separation of lanthanides and actinides	27-28
1.3.5.1	Methods for lanthanides and actinides separation	28
1.3.5.2	High performance liquid chromatography (HPLC) for the separation of lanthanides	29-32
1.3.5.3	Retention of actinides	32
1.4	Methods for the determination of stability constant of lanthanides and actinides	33
1.5	Ionic liquid and its applications in chromatography	33-34
1.6	Scope of Present work	34-36
<u>CHAPTER-2</u>		
Experimental		
2.1	HPLC Instrumentation	37-40
2.1.1	Solvent (mobile phase) reservoir	41
2.1.2	High pressure pump	41
2.1.3	Tubing and fittings	42
2.1.4	Gradient mixer	42
2.1.5	Sample Injector	42
2.1.6	HPLC Columns	43
2.1.7	HPLC Detector	43-44
2.2	Post-column derivatisation method for detection	45
2.3	Preparation of standard solution of lanthanides, U, Th, Pu and Am	45-47
2.4	Calibration studies	47
2.5	Mobile phase preparation	47-48
2.6	Preparation of “dynamically” coated columns	48
2.7	Preparation of “Permanently” coated columns	48
<u>CHAPTER-3</u>		
Rapid Separation of Lanthanides and Actinides on Small Particle Based Chromatographic Supports		
3.1	Introduction	49-50
3.1.1	Need for development of ultra-fast separations	50-51
3.2	Experimental	52

3.3	Results and discussion	52
3.3.1	Lanthanides separation-gradient elution	52-61
3.3.2	Lanthanides separation-isocratic elution	61-65
3.3.3	Retention behaviour of uranium and thorium	65
3.3.3.1	Retention behaviour without modifier	65-72
3.3.3.2	Separation of U from Th using dynamic ion-exchange technique	72-75
3.4	Application of small particle based support (3 cm length with particle size of 1.8 μm)	75
3.4.1	Determination of lanthanides in uranium matrix	75-76
3.5	Conclusion	76-77
<u>CHAPTER-4</u>		
Liquid Chromatographic Behavior of Lanthanides and Actinides on Monolith Based Supports		
4.1	Introduction	78-80
4.2	Experimental	80
4.2.1	Modification of monolith column	80
4.2.2	Determination of the BEHSA content on monolith column	81-82
4.3	Results and discussion	82
4.3.1	Separation of lanthanides using a monolith column of 10 cm length	82
4.3.1.1	Gradient elution	82-89
4.3.1.2	Isocratic elution	90-91
4.3.2	Lanthanide separation using monolith support of 5 cm length	91
4.3.2.1	Gradient elution	91-92
4.3.2.2	Isocratic elution from 5 cm support	92-94
4.3.3	Retention studies on uranium and thorium from 10 cm length monolith column	94
4.3.3.1	Retention behavior under dynamic ion-exchange condition	94-96
4.3.3.2	Retention of U and Th without CSA modifier-reversed phase condition	96-99
4.3.3.3	Retention of U and Th on modified monolith support: Studies on BEHSA coated monolithic column	99-100
4.3.3.3.1	Influence of BEHSA concentration	100-102

4.3.3.3.2	Uranium and Thorium separation with HNO ₃ as mobile phase	102-103
4.3.4	Comparison of performance of monolithic column with 1.8 micron particle based column during dynamic ion-exchange chromatographic studies	103-105
4.4	Conclusion	105-106
<u>CHAPTER-5</u>		
Burn-up Measurement on Dissolver Solution of Nuclear Reactor Fuels using HPLC		
5.1	Atom percent determination on dissolver solution of a fast reactor fuel	
5.1.1	Introduction	107-109
5.1.2	Experimental	109
5.1.2.1	Studies involving dissolver solution of spent fuel (FBTR)	109
5.1.3	Results and discussion	110
5.1.3.1	Estimation of lanthanides in dissolver solution of fast reactor fuel using small particle (1.8 µm) based support	110
5.1.3.2	Separation and determination of lanthanides in dissolver solution of fast reactor fuel using monolith support	110-114
5.1.3.3	Separation and determination of U and Pu in dissolver solution of fast reactor fuel using small particle (1.8 µm) based support	114-116
5.1.3.4	Separation and determination of uranium and plutonium using monolithic column	116-118
5.1.3.5	Identification of americium in dissolver solution	119
5.1.3.6	Minimisation of radiation exposure and waste	119-120
5.1.4	Conclusion	120
5.2	Determination of lanthanides in uranium matrix using single stage double column chromatography and its application to burn-up measurement of nuclear reactor fuels	
5.2.1	Introduction	121-123
5.2.2	Experimental	123
5.2.2.1	Column-1	123
5.2.2.1.1	Preparation of TOPO modified reversed phase (5 cm length) support	123
5.2.2.1.2	Preparation of TOPO modified 25 cm (4.6 mm dia) length reversed phase support	124

5.2.2.2	Column-2: Modification of 10 cm reversed phase monolithic support into a dynamic ion-exchange column	125
5.2.2.3	Dissolution of spent fuel (PHWR)	125
5.2.3	Results and discussion	125
5.2.3.1	Separation of lanthanides in U matrix on analytical column	125-126
5.2.3.2	Separation of lanthanides from uranium matrix using single stage double column chromatographic method	127-129
5.2.3.3	Breakthrough studies on TOPO coated column	129-130
5.2.3.4	Separation of lanthanides from uranium matrix: Influence of TOPO content on the separation	130-135
5.2.3.4.1	Lanthanides in uranium matrix (1:10 ⁶)	136-137
5.2.3.5	Significance of use of 5 cm length TOPO coated column	137-138
5.2.3.6	Regeneration of “uranium sorbed TOPO coated column”	138-139
5.2.3.7	Retention behavior of fission products, Pu(III), Pu(IV) and Am(III) on TOPO coated reversed phase support	139-141
5.2.3.8	Burn-up determination of PHWR fuel by single stage double column chromatography	141-145
5.2.3.9	Elution behaviour of U, Pu, Am and lanthanide fission products present in the dissolver solution of fast reactor fuel	145-147
5.2.3.10	Advantages of Burn-up measurements with HPLC technique	147-148
5.2.4	Conclusion	148
	<u>CHAPTER-6</u>	
	Correlation of Retention of Lanthanide and Actinide Complexes with Stability Constants and their Speciation	
6.1	Introduction	149-151
6.2	Experimental	151
6.3	Results and discussion	151
6.3.1	Estimation of capacity factor of lanthanides and actinides based on their species	151-157
6.3.2	Estimation of stability constant and its validation (method-1)	157-165
6.3.2.1	Estimation of β_3	161
6.3.2.2	Influence of column length, mobile phase flow rate, RSO_3^- , $[\text{A}^-]$ on Y	165-167
6.3.3	Estimation of stability constant of unknown complexing agent with metal ion	167-168

6.3.4	Estimation of stability constant from speciation data (method-2)	169-173
6.3.4.1	Influence of RSO ₃ H on retention	173-174
6.3.5	Correlation of retention with stability constant – estimation of stability constant at different ionic strengths	174-178
6.3.6	Estimation of stability constant of transition metal ions, Th(IV) and Pu(IV)	178-180
6.3.7	The advantages and limitations of estimation of stability constant by chromatographic retention correlation	180
6.3.8	Speciation of actinides and their retention behavior on reversed phase chromatography	181-185
6.4	Conclusion	185
<u>CHAPTER-7</u>		
Influence of Temperature on the Elution Behaviour of Lanthanides and Some Actinides on Reversed Phase Supports		
7.1	Introduction	186-187
7.2	Experimental	187
7.3	Results and discussion	188
7.3.1	Effect of temperature on chromatographic separation of lanthanides and some actinides on reversed phase support	188
7.3.1.1	Isocratic elution of lanthanides on 25 cm (5 µm) and 3 cm length reversed phase support	188-194
7.3.1.2	Separation of U & Th on 25 cm (5 µm) and 3 cm length reversed phase supports as a function of temperature	194-204
7.4	Conclusion	205
<u>CHAPTER-8</u>		
Task-Specific Ionic Liquids in Liquid Chromatography-Studies on the Retention Behaviour of Lanthanides and Some Actinides		
8.1	Introduction	206-207
8.2	Experimental	207-208
8.3	Results and discussion	208
8.3.1	Retention behavior of U and Th in the presence of TSIL + α-HIBA system	208-212
8.3.1.1	Retention mechanism of U and Th in the presence of TSIL on the reversed phase support	212-213

8.3.2	Retention behavior of lanthanides using ionic liquid, Betaine NTf ₂ as mobile phase	213-215
8.4	Conclusion	215
	<u>CHAPTER-9</u>	
9.1	Summary and Conclusion	216-222
9.2	Future Studies	222-223
	REFERENCES	224-237
	LIST OF PUBLICATIONS, AWARDS / HONORS	238-240

SYNOPSIS

Lanthanides and actinides have many applications in diverse fields including nuclear industry [1-4]. Individual separation of lanthanides and actinides is challenging due to similar chemical properties i.e. same charge and similarity in size. Various separation methods [5-8] were developed and reported in literature for separation of lanthanides and actinides. Among these, high performance liquid chromatographic (HPLC) technique [9] is more efficient and offers fast separation for the isolation of lanthanides and actinides. A major advantage of HPLC technique is its ability to provide rapid and high performance separations with sensitive detection. Liquid chromatographic techniques based on ion exchange, ion pairing / ion-interaction have been developed for the isolation of individual lanthanides. In all these studies reported in literature, the separation of individual lanthanides from each other was not less than 8 min using dynamic ion-exchange chromatographic technique [10-13].

Lighter lanthanides (La, Ce, Pr, Nd, Sm and Eu) constitute about one fourth of the total fission products produced in the nuclear fission of uranium or plutonium. Individual separation of lanthanides and actinides is mandatory for burn-up measurement on dissolver solution of nuclear reactor fuel. Lighter lanthanides such as La and Nd were employed as burn-up monitors as they fulfil the major requirements of fission product monitor [14]. Thus accurate determination of Nd or La in the dissolver solution of spent fuel can be used to determine total number of fissions. The burn-up measurement on dissolver solution of nuclear reactor fuel subjected to high burn-up, poses a great challenge due to the association of high level of radioactivity. Therefore, isolation of lanthanides as well as actinides from these solutions demands a rapid and high-resolution separation to ensure minimization of the radiation exposure to the operator and minimisation of waste generation. The reversed phase HPLC separation

technique is a powerful chromatographic method for isolation of actinides from each other [15-17]. The separation of actinides such as Th and U was studied in literature using reversed phase chromatographic technique.

The aim of the present study is to develop high performance separations of lanthanides and actinides and to reduce the separation time. Therefore, the thesis is focused on development of rapid separation of lanthanides and actinides using various liquid chromatographic techniques.

In this context, elution behaviour of lanthanides and actinides was investigated on small particle (1.8 μm) reversed phase supports and monolith based reversed phase supports. These methods were employed for the burn-up measurement on dissolver solutions of nuclear reactor fuels. A single stage double column chromatographic technique was developed and the same was applied for burn-up measurement of dissolver solution of PHWR (Pressurised Heavy Water Reactor, MAPS, Kalpakkam, India). The dynamic ion-exchange HPLC technique was employed to estimate the stability constant of lanthanides and actinides in a single run. Speciation data for plutonium (in different oxidation states), and americium were obtained with α -hydroxy isobutyric acid (α -HIBA) from stability constant data. These studies were employed to explain the elution behaviour of plutonium, americium, uranium and thorium during their chromatographic separation. Elution behaviour of lanthanides and actinides was also investigated as a function of temperature. Retention behaviour of lanthanides and actinides was investigated using task specific ionic liquids as mobile phase. This thesis comprises of nine chapters and contents of the different chapters in the present thesis are briefly given below.

Chapter-1: This chapter describes the history of development of chromatographic technique and principles of various chromatographic methods and their applications. The liquid chromatographic technique has revolutionised separation chemistry due to

the invention of high performance liquid chromatographic technique (HPLC). Historical developments of HPLC, various types and its applications in different areas are discussed. Applications of lanthanides in various fields such as alloys, catalysts, phosphors, lasers, batteries, chemicals, ceramics, glass, glazes, lighting, medical imaging, thermal spray powders etc are discussed. Separation and determination of lanthanides is important for measuring the burn-up of nuclear reactor fuels and also in geological studies. Various separation methods for individual separation of lanthanides have been described. Developments and advances in the field of lanthanides and actinides separation by liquid chromatographic technique have been discussed in detail. Estimation of the stability constant of metal ions using chromatographic methods as well as traditional methods (potentiometry, polarography, conductometry, spectrophotometry, solvent extraction and ion exchange methods) is discussed. An introduction to ionic liquid and its applications in liquid chromatography is also briefed in this chapter.

Chapter-2: This chapter describes the experimental techniques and methods that are used in the present work. Instrumentation details of HPLC are discussed. The use of post-column derivatisation method for the detection and determination of metal ions is discussed. Preparations of standard solutions of metal ions such as lanthanides, uranium and thorium are discussed.

Chapter-3: Particle size of the support materials employed in HPLC influences separation efficiency and affects the back-pressure of column. The column efficiency increases with decrease in particle size. It is evident from van Deemter curve for particle size versus resolution that packing materials with particle size less than 2 μm provide better resolution compared to 5 μm based supports for high speed separations. The use of small particle size e.g. 1.8 micron results in a high back pressure and needs systems to deliver solvents at high pressures, typically in the range of 500 bar with precise flow

rates. The separation of individual lanthanides and actinides was investigated using 1.8 μm based support as it offers high column efficiency compared to the 5 μm support. This chapter describes results on the use of short columns (3-5 cms long) with small particle size (1.8 μm) for high performance liquid chromatographic separation of individual lanthanides, uranium from thorium as well as uranium from plutonium. Lanthanides could be separated from each other in ~ 3.6 min, thorium-uranium in 1 \sim min and uranium from plutonium in ~ 4.2 min. A dynamic ion-exchange chromatographic separation technique was developed using camphor-10-sulfonic acid (CSA) as the ion-pairing reagent and α -hydroxy isobutyric acid (α -HIBA) as the complexing reagent for the isolation of individual lanthanides as well as the separation of uranium from thorium. A reversed phase HPLC technique was developed for the isolation of uranium from thorium as well as lanthanide group from uranium. The reversed phase HPLC separation technique with small particle based support was demonstrated for separation of lanthanides as a group from uranium matrix. Lanthanides (e.g. La, Nd) were separated and estimated in uranium matrix of samples of LiCl-KCl eutectic salt containing chlorides of lanthanides in uranium matrix (typical La to U ratio of 1:2000). The results on the use of small particle support for the burn-up measurements are discussed later.

Chapter-4: Monolith support consists of a single piece of porous, rigid material containing mesopores and micropores, which provide fast analyte mass transfer. Higher separation efficiency is obtained for higher permeability and higher flow rates, which leads to shorter separation times on monolith columns compared to traditional HPLC supports. This chapter describes the liquid chromatographic behaviour of lanthanides and actinides on monolith based support. A dynamic ion-exchange technique was developed using monolith based reversed phase support for the individual separation of lanthanides as well as actinides, and has led to the separation of all 14 lanthanides in

about 2.8 minutes and this is the fastest LC technique reported as of now in literature. The sorption behaviour of uranium and thorium was examined on a reversed phase monolith support as well as modified (bis-2-ethylhexyl succinamic acid (BEHSA)) monolith support. In these studies, α -HIBA as well as HNO_3 were employed as the mobile phase. Rapid separation of uranium from thorium could be achieved in about 20 sec from a modified monolith support using 0.01 N HNO_3 as mobile phase. The individual separation of lanthanides and actinides was demonstrated for the burn-up measurement on the dissolver solution of FBTR and the results are discussed in Chapter 5.

Chapter-5: This chapter deals with burn-up measurement on dissolver solution of nuclear reactor fuels. Dynamic ion-exchange HPLC technique using small particle support (1.8 μm) was developed for the determination of burn-up of fast reactor spent fuel (FBTR, India), discharged at 155 GWd/ton. In this method, U and Pu present in the dissolver solution of FBTR fuel were removed by an ion-exchange chromatography and assayed subsequently. The fission product fraction after the removal of U and Pu was subsequently injected into HPLC for the assay of burn-up monitors i.e. La and Nd. A reversed phase chromatographic technique was employed for the determination of uranium and plutonium in the dissolver solution. HPLC technique using monolith support was also demonstrated for the first time for the direct injection of dissolver solution from fast reactor fuel without any pre-separation. The atom% fission was determined based on these measurements and the results are discussed. Reversed phase chromatographic technique using monolith based support was also developed for the determination of uranium and plutonium in the dissolver solution. A single stage double column chromatographic technique was developed and demonstrated for the separation and determination of lanthanides fission products such as La, Ce, Pr, Nd and Sm in the dissolver solution of PHWR fuel without removal of “matrix uranium” for the burn-up

measurements. In this technique, two columns were connected in a series, first column (reversed phase 5 cm length support) modified with tri-n-octylphosphine oxide (TOPO) and the second one (reversed phase 10 cm length monolith support) modified with an ion pairing reagent for individual separation of lanthanides. Uranium was retained in the first column and lanthanide fission products were transferred to the second column during chromatographic runs. About 45 consecutive injections could be carried out for the assay of lanthanides in uranium matrix, prior to elution of uranium. Retention behaviour of Pu(III) and Pu(IV) was investigated on TOPO modified 5 cm length reversed phase support. The elution behaviour of fission products such as Zr, Mo, Cs, Ba, Sr, Ru, Rh, Pd and Nd was also studied on TOPO coated reversed phase support and the results are discussed.

Chapter-6: A method for the correlation of retention of lanthanide and some actinide complexes with the stability constant is described in this chapter. In these studies, an ion-pairing reagent, e.g. camphor-10-sulphonic acid (CSA) was used as the modifier and organic acids such as α -hydroxy isobutyric acid (α -HIBA) and lactic acid were employed as complexing reagent for elution. The retention times as well as capacity factors of lanthanides and actinides were measured as a function of CSA, organic acid concentrations and mobile phase pH. From these studies, a correlation has been established between capacity factor of a metal ion, concentrations of ion-pairing reagent and complexing agent with the stability constant of lanthanide/actinide complex. Based on these studies, it has been shown that the stability constant of lanthanides and actinides can be estimated using a single lanthanide calibrant. The method was validated by the estimation of stability constant of lanthanides with the organic acids such as HIBA, lactic acid, mandelic acid and tartaric acid. These studies have established that a single chromatogram can be used for estimation of stability constant at various ionic strengths and the estimated data are found to be in very good agreement with the

experimentally determined values. These studies also demonstrated that the method can be applied for estimation of stability constant of actinides with a ligand whose value is not reported yet, e.g., ligands of importance in the lanthanide - actinide separations, chelation therapy etc. The chromatographic separation method is fast and the estimation of stability constant can be done in a very short time, which is a significant advantage especially in dealing with radioactive species. The stability constant data was used to derive speciation data of plutonium in different oxidation states as well as that of americium with α -HIBA. The elution behaviour of actinides such as Pu and Am from reversed phase chromatographic technique could be explained based on the speciation data

Chapter-7: This chapter describes the effect of temperature (25°C to 85°C) on the retention of lanthanides and actinides on chromatographic supports. Dynamic ion-exchange and reversed phase chromatographic techniques were carried out using reversed phase support of 25 cm (5 μ m particle size) and 3 cm (1.8 μ m particle size) length. Influence of temperature was studied for (a) isocratic elution of lanthanides and (b) separation of uranium and thorium. It was observed from these studies that the retention was reduced to approximately half of its initial time at 85°C compared to that at 25°C for individual separation of lanthanides. A temperature gradient was also employed to separate the individual lanthanides in an isocratic mode in ~ 16 min. The retention of actinides such as uranium and thorium was also investigated on a reversed phase based support using α -HIBA, mandelic acid and lactic acid as a function of temperature (25 to 85°C). Capacity factors of lanthanides, U and Th were correlated with temperature using van't Hoff plot and linear correlation was established; from this study, enthalpy of sorption ($\Delta H_{\text{sorption}}$) of lanthanides, uranium and thorium was computed.

Chapter-8: Task-specific ionic liquids such as 1-butyl-3-methylimidazolium benzoate, protonated betaine bis(trifluoromethylsulfonyl)imide [Hbet][NTf₂] and its precursor [Hbet] Cl, were employed as the mobile phase along with α -HIBA using a reversed phase support to study the sorption behaviour of uranium, thorium and lanthanides. Individual separation of all 14 lanthanides was studied using ionic liquid, bis(trifluoromethylsulfonyl)imide. The separation factors for U-Th as well as adjacent lanthanide pairs were measured. In the case of isolation of uranium from thorium, highest separation factor was achieved with 1-butyl-3-methylimidazolium benzoate as an ionic liquid. For the first time, the use of ionic liquids was demonstrated for separation of lanthanides and also for the separation of uranium from thorium.

Chapter-9: This chapter summarises the highlights of studies carried out in the present work. This includes, (a) development of dynamic ion-exchange based HPLC technique for the rapid separation of individual lanthanides using 1.8 μ m as well as monolith based supports (b) reversed phase as well as modified reversed phase methods for the rapid separation of uranium and thorium, (c) separation of uranium and plutonium etc. The advantage of dynamic ion-exchange technique for measuring the concentrations of fission product lanthanides such as La, Ce, Pr, Nd and Sm in the dissolver solution of nuclear reactor fuel is highlighted. The advantage of dynamic ion-exchange HPLC technique for stability constant determination of lanthanides and actinides is discussed. The potential applications of high temperature liquid chromatographic technique and use of ionic liquids for the development of high performance separations are highlighted.

References

- [1] F. H. Spedding, A. H. Daane, *The rare earths*, Wiley, New York, 1961.
- [2] C. H. Knight, R. M. Cassidy, B. M. Recoskie, L.W. Green, *Anal. Chem.*, 56 (1984) 474-478.
- [3] N. R. Larsen, *J. Radioanal. Chem.* 52 (1979) 85-91.
- [4] P. Henderson, *Rare earth element geochemistry*, Elsevier, Amsterdam, 1984.
- [5] K. Robards, S. Clarke, E. Patsalides, *Analyst*, 113 (1988) 1757-1779.
- [6] K. L. Nash, M. P. Jensen, *Sep. Sci. and Tech.*, 36 (2001) 1257-1282.
- [7] J. Korkisch, *Modern methods for the separation of rarer metal ions*, chapter 3, Pergamon Press, Oxford, 1969.
- [8] M. Kumar, *Analyst*, 119 (1994) 2013-2024.
- [9] L. R. Snyder, J. J. Kirkland, *Introduction to modern Liquid chromatography*, 2^{ed} Edn, John Wiley & Sonc, Inc, New York, 1979.
- [10] D. J. Barkley, M. Blanchette, R. M. Cassidy, S. Elchuk, *Anal. Chem.*, 58 (1986) 2222-2226.
- [11] R. M. Cassidy, S. Elchuk, *Anal. Chem.*, 54 (1982) 1558-1563.
- [12] R. M. Cassidy, S. Elchuk, N. L. Elliot, L. W. Green, C. H. Knight, B. M. Recoskie, *Anal. Chem.*, 58 (1986) 1181-1186.
- [13] P. R. Vasudeva Rao, N. Sivaraman, T. G. Srinivasan, *Studies on the lanthanide separation using HPLC*, *Encyclopedia of Chromatography*, (2005).
- [14] *Atomic data and nuclear data tables: Fission product yields from neutron induced fission*, E. A. C. Crouch, Academic Press, New York and London, 1977.
- [15] S. Elchuk, K. I. Burns, R. M. Cassidy, C. A. Lucy, *J. Chromatogr* 558, (1991) 197-207.

[16] F. Hao, P. R. Haddad, P. E. Jackson, J. J. Carnevale, *J. Chromatogr.*, 640, (1993)
187-194.

[17] F. Hao, B. Paull, P. R. Haddad, *J. Chromatogr.*, 739, (1996) 151-161.

LIST OF FIGURES

Figure No.	Title	Page No.
1.1	Chromatogram of substances A and B	9
1.2	Influence of particle size on HETP	12
1.3	Influence of mobile phase flow rates on HETP-Contribution of eddy diffusion (A), longitudinal diffusion (B), mobile phase, stationary phase and stagnant mobile phase mass transfer (C) terms to HETP; X is resultant plot	12
1.4	Measurement of resolution	13
1.5	Electron micrographs of the (a) macroporous and (b) mesoporous structures in a monolithic silica rod	19
1.6	Variation of ionic radii of lanthanides and actinides with atomic number	23
1.7	Schematic illustration of (a) the ion-pair (b) the dynamic ion-exchange and (c) the ion-interaction models for the retention of anionic solutes in the presence of a lipophilic cationic ion-interaction reagent (IIR)	31
2.1	Schematic diagram of High Performance Liquid Chromatography(HPLC)	38
2.2	Photograph of HPLC system used in present study	39
2.3	Schematic diagram of HPLC system for radioactive sample analysis	40
2.4	Schematic diagram of HPLC reciprocating pump	41
2.5	HPLC Rheodyne Sample injector	42
3.1	Separation of lanthanides using gradient elution-(A) Present work (B) Vasudeva Rao <i>et al</i> , 2005 wok (C) Cassidy <i>et al</i> , 1984 work	53
3.2	Separation of lanthanides on 1.8 μm particle size of 5 cm length column using gradient elution	57

3.3	Separation of lanthanides on 1.8 μm particle size of 3 cm length column using gradient elution	58
3.4	Variation of capacity factor of some lanthanides as a function of α -HIBA concentration on 1.8 μm based support	58
3.5	Variation of capacity factor of some lanthanides as a function of CSA concentration on 1.8 μm based support	59
3.6	Variation of capacity factor of some lanthanides as a function of mobile phase pH on 1.8 μm based support	59
3.7	Variation of capacity factor of some lanthanides as a function of mobile phase flow rate on 1.8 μm based support	60
3.8	Separation of lanthanides by isocratic elution from 1.8 μm , 5 cm length reversed phase column	63
3.9	Separation of lanthanides by isocratic elution from 1.8 μm , 3 cm length reversed phase column	63
3.10	Separation of lanthanum from other lanthanides on 1.8 μm , 3 cm length reversed phase column in about 2.5 min	65
3.11	Retention behaviour of U and Th on 1.8 μm , 3 cm length reversed phase column with 0.1 M α -HIBA as a function of pH	66
3.12	Retention behaviour of U and Th on 1.8 μm , 3 cm length reversed Phase column with 0.15 M α -HIBA as a function of pH	67
3.13	Speciation of (a) uranium-HIBA and (b) thorium-HIBA complexes as a function of mobile phase (0.05 M α -HIBA) pH	67
3.14	Speciation of (a) uranium-HIBA and (b) thorium-HIBA complexes as a function of mobile phase (0.15 M α -HIBA) pH	68
3.15	Retention behaviour of U and Th on 1.8 μm , 5 cm length reversed phase column with 0.1 M α -HIBA as a function of pH	68
3.16	Retention behaviour of U and Th on 1.8 μm , 5 cm length reversed phase column with 0.15 M α -HIBA as a function of pH	69
3.17	Retention behaviour of Nd, Th and U on 1.8 μm , 3 cm length reversed phase column at pH 3	70
3.18	Separation factor of U/Th. Separation factors as a function of mobile phase (α -HIBA) pH and its concentration for 3 (1.8 μm), 5 (1.8 μm) and 25 cm (5 μm) length reversed phase columns	71

3.19	Separation of U and Th on 1.8 μm , 3 cm length support using dynamic ion-exchange chromatography	73
3.20	Separation of U from Th on a 1.8 μm , 5 cm length reversed phase column using dynamic ion-exchange chromatography	74
3.21	Influence of α -HIBA concentration and pH on the retention behaviour of U and Th in the presence of CSA	75
4.1	Plate height (H) vs flow rate (u) for monolith and particle packed HPLC columns	79
4.2	Structure of bis-2-ethylhexyl succinamic acid (BEHSA)	80
4.3	Calibration plot for bis-2-ethylhexyl succinamic acid (BEHSA) using HPLC with UV-Vis detection (Det: 215 nm)	82
4.4	Separation of lanthanides on a monolith column using dynamic ion-exchange chromatography	85
4.5	Variation of capacity factor of lanthanides as a function of α -HIBA concentration on monolith column	87
4.6	Variation of capacity factor of lanthanides as a function of mobile phase pH on monolith column	88
4.7	Variation of capacity factor of lanthanides as a function of CSA concentration on monolith column	89
4.8	Separation of lanthanides by isocratic elution from 10 cm length monolith column	90
4.9	Separation of lanthanides on a 5 cm length monolith column using dynamic ion-exchange chromatography	92
4.10	Separation of lanthanides by isocratic elution from 5 cm length fast gradient monolith column	94
4.11	Retention behaviour of U and Th on dynamically modified 10 cm length reversed phase monolith column as a function of mobile phase pH	95
4.12	Separation factor for Th/U as a function of mobile phase pH and concentration from 10 cm length monolith support	96
4.13	Retention behaviour of U and Th on 10 cm length reversed phase monolith column as a function of mobile phase pH	97
4.14	Retention behaviour of U and Th on 10 cm length reversed phase monolith column as a function of mobile phase flow rate	99

4.15	Retention behaviour of U and Th on BEHSA modified reversed Phase column as a function of mobile phase flow rate	100
4.16	Capacity factor (k') of U and Th on the BEHSA modified support	101
4.17	Influence of BEHSA concentration on the separation factor of U/Th	101
4.18	Retention behavior of U & Th on a BEHSA modified 10 cm and 5 cm length monolith support	102
5.1	Schematic of mass spectrometric technique for burn-up determination on nuclear reactor fuels	108
5.2	Separation of individual lanthanide fission products from dissolver solution using 1.8 μm based support	110
5.3	Direct injection of dissolver solution (burn-up~ 155 Gwd/ton) using monolith support	111
5.4	Separation and estimation of lanthanum from uranium and plutonium present in dissolver solution in 1.8 min using monolith support	112
5.5	Injection of dissolver solution into small particle (1.8 μm) based reversed phase support after separation from fission products by anion exchange	115
5.6	Direct injection of dissolver solution into small particle (1.8 μm) based without any pre-separation	116
5.7	Direct injection of dissolver solution for uranium and plutonium assay by dynamic ion-exchange	117
5.8	Direct assay of uranium present in dissolver solution using reversed phase monolith support	118
5.9	Direct plutonium assay from dissolver solution using reversed phase monolith support	118
5.10	Identification of Am from dissolver solution	119
5.11	Separation of individual lighter lanthanides on a monolithic column in the presence of uranium	126
5.12	Schematic of single stage dual column chromatographic technique for separation of lanthanides in uranium matrix	127

5.13	Separation of lanthanides using dynamic ion-exchange chromatography with and without connecting TOPO coated column	128
5.14	Breakthrough profile of uranium on TOPO coated support	130
5.15	Elution behaviour of lanthanum in the presence of matrix uranium in a dual coupled column chromatography	133
5.16	Separation of lanthanides from uranium matrix using single stage double column chromatographic technique	134
5.17	Uranium loading on TOPO coated supports	135
5.18	Separation of lanthanide impurities in uranium matrix (1 part lanthanides in 10^6 parts of uranium) using dual column chromatographic support	137
5.19	Elution behaviour of fission products on TOPO coated reversed phase support	140
5.20	Retention behavior of Pu(III), Pu(IV) and Am(III) on TOPO coated reversed phase support	141
5.21	Separation of simulated dissolver solution containing lanthanides from uranium matrix using single stage double column chromatographic support	143
5.22	Direct assay of lanthanide fission products present in the dissolver solution of PHWR spent fuel using single stage double column chromatographic technique	144
5.23	Identification of Am(III)/Pu(III) from dissolver solution of PHWR spent fuel using single stage double column chromatographic support	145
5.24	Elution behavior of plutonium and lanthanide fission products present in the dissolver solution of fast reactor fuel by single stage double column chromatography	146
6.1	Retention of lanthanides, Am(III) and Pu(III) as a function of mobile phase pH	152
6.2	Retention of lanthanides, Am(III) and Pu(III) as a function of CSA concentration	153
6.3	Plot of uncomplexed (M^{+3}), dipositive (MA^{+2}), monopositive (MA_2^{+1}), neutral (MA_3) & anionic (MA_4^{-1}) species of lanthanides (Pr, Gd, Ho, Lu)- HIBA complexes against capacity factor (k')	171

6.4	Plot of uncomplexed $[M^{+3}]$ against capacity factor for all the lanthanides	174
6.5	Stability constant of lanthanide-HIBA complexes ($\log\beta_1$) at two different ionic strengths	178
6.6	Speciation of (a) Pu(III)-HIBA, (b) Pu(IV)-HIBA and (c) PuO_2^{+2} -HIBA complexes as a function of mobile phase (0.1 M α -HIBA) pH	182
6.7	Speciation of Nd(III)-HIBA and Am(III)-HIBA complexes as a function of mobile phase (0.1 M α -HIBA) pH	182
6.8	(A) Elution behavior of Pu(III), Pu(IV), PuO_2^{+2} , Am(III), UO_2^{+2} and Th(IV) on a reversed phase HPLC as a function of pH; (B) Elution behavior at pH: 4	183
7.1	Isocratic elution of lanthanides on 25 cm length support as a function of temperature	189
7.2	Plot of $\ln(k')$ vs $1/T$ for lanthanides from a 25 cm length column	190
7.3	Elution behaviour of lanthanides on 3 cm length support as a function of temperature	192
7.4	Plot of $\ln(k')$ vs $1/T$ for lanthanides from a 3 cm length (1.8 μ m) column	193
7.5	Elution of lanthanides using temperature gradient (25 ⁰ C-90 ⁰ C)	194
7.6	Retention behaviour of U & Th-HIBA complexes on a 25 cm length reversed phase support as a function of temperature	195
7.7	Plot of $\ln(k')$ vs $1/T$ for U and Th for 25 cm length column	197
7.8	Retention of U & Th – HIBA complexes on 1.8 micron reversed phase support as a function of temperature	198
7.9	Plot of $\ln(k')$ vs $1/T$ for U and Th for 3 cm length 1.8 micron reversed phase column	199
7.10	Retention of U & Th – mandelate complexes on a reversed phase HPLC as a function of temperature	201
7.11	Speciation of U & Th with mandelic acid as a function of pH	202
7.12	Plot of $\ln(k')$ vs $1/T$ for U and Th with mandelic acid	202
7.13	Retention behaviour of U & Th- lactate complexes on a reversed phase chromatography as a function of temperature	203

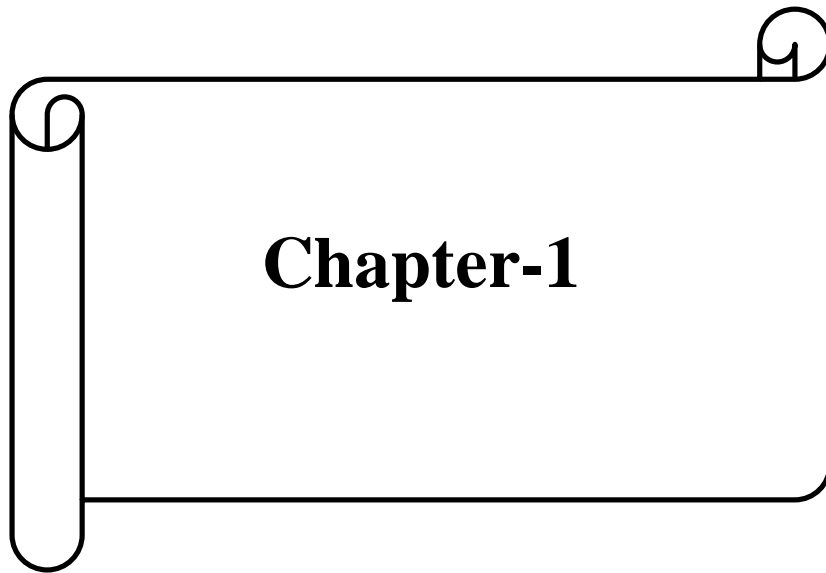
7.14	Plot of $\ln(k')$ vs $1/T$ for U and Th with lactic acid	204
8.1	Structure of (A) Betaine NTf ₂ (B) Bmim-benzoate	207
8.2	Calibration plot of U and Th using ionic liquid as mobile phase	208
8.3	Separation of uranium from thorium (~25 ppm) using ionic liquid, betaine chloride	209
8.4	Separation of uranium from thorium (25 ppm) using ionic liquid, betaine NTf ₂	210
8.5	Separation of uranium from thorium (~ 50 ppm) using bmim-benzoate + α -HIBA	211
8.6	Separation factors for U-Th as a function of mobile phase pH	212
8.7	Separation of lanthanides using ionic liquid [Hbet][NTf ₂] with α -HIBA as mobile phase on reversed phase support	213
8.8	Retention behavior of lutetium using ionic liquid [Hbet] [NTf ₂] with α -HIBA as mobile phase on reversed phase support	214

LIST OF TABLES

Table No.	Title	Page No.
1.1	Percentage (%) cumulative yield for some fission products	21-22
2.1	Detection limits of some lanthanides (La, Ce, Pr, Nd and Sm) and some actinides (U and Th)	44
3.1	Gradient elution for separation of lanthanides- a comparison	54
3.2	Gradient programming for separation of lanthanides on 3 cm length reversed phase support	55-57
3.3	Separation factors for adjacent lanthanides on 3 cm length (1.8 μ m) column under various experimental conditions	61
3.4	Isocratic elution for separation of lanthanides – a comparison	62
3.5	Column efficiency of lanthanides-a comparison	64
4.1	Modifier content on 10 cm and 5 cm length monolith coated support	81
4.2	Gradient programming for separation of lanthanides on 10 cm length monolith support	83-84
4.3	Efficiency of 10 cm length monolith column for separation of lanthanides	86
4.4	Separation factor of adjacent lanthanides as a function of α -HIBA concentration from 10 cm length monolith support	87
4.5	Separation factor of adjacent lanthanides as a function of mobile phase pH from 10 cm length monolith support	88
4.6	Separation factor of adjacent lanthanides as a function of CSA concentration from 10 cm length monolith support	89
4.7	Gradient and isocratic elution for separation of lanthanides using monolith column	91
4.8	Separation factor of adjacent lanthanides from 5 and 10 cm length monolith support	93

4.9	Separation factor for U and Th as a function of mobile phase pH and concentration from 10 cm length monolith support	98
4.10	Comparison of column parameters for separation of lanthanides	104
5.1	Estimation of lanthanides, uranium and plutonium in dissolver solution using (A) small particle and (B) monolith supports for measurement of atom% burn-up	113
5.2	Preparation of TOPO modified 5 cm and 25 cm length support: coating solutions and % sorption	124
5.3	Separation factors for some adjacent lanthanides on a monolithic column with and without TOPO coated column	129
5.4	Separation of lanthanides in the presence of uranium matrix- Influence of uranium and TOPO contents on separation behavior	132-133
5.5	Predicted and experimentally observed number of injections on the TOPO coated support	135
5.6	Estimation of lanthanides and actinides in dissolver solution of PHWR spent fuel – determination of atom percent burn-up	144
5.7	Estimation of lanthanide fission products, U and Pu in dissolver solution of Fast Reactor Fuel	147
6.1	Comparison of experimentally measured capacity factor (k') of lanthanides and some actinides with the predicted one	157
6.2	Stability constant of lanthanides with α -HIBA estimated for 0.2 M ionic strength at 25 ⁰ C (method-I)	162
6.3	Stability constant of lanthanides with lactic acid estimated for 2 M ionic strength at 25 ⁰ C (method-1)	163
6.4	Stability constant of lanthanides with mandelic acid estimated for 0.1 M ionic strength at 25 ⁰ C	164
6.5	Stability constant of lanthanides with tartaric acid estimated for 0.015 M ionic strength at 25 ⁰ C (method-1)	165
6.6	Variation of Y (K_s, X) as a function of mobile phase flow rates for calibrant, Sm	166

6.7	Estimation of stability constant of lanthanides with a ligand (method-1) whose data is not reported: Validation of the method	168
6.8	Stability constant of lanthanides with α -HIBA (method-2), estimated for 0.2 M ionic strength at 25 ⁰ C	172
6.9	Stability constant of lanthanides with lactic acid (method-2), estimated for 2 M ionic strength & 0.1 M ionic strength at 25 ⁰ C	173
6.10	Stability constant of lanthanide - HIBA complexes (method-1), estimated at 0.5 M ionic strength at 25 ⁰ C	175
6.11	Stability constant of lanthanide -HIBA complexes (method-1 & method-2), estimated at 0.2 M ionic strength at 25 ⁰ C	176
6.12	Stability constant of lanthanide-HIBA complexes (method-1 & method-2), estimated at 0.5 M ionic strength at 25 ⁰ C	177
6.13	Stability constant of transition metal complexes with HIBA (method-2), estimated for 1 M ionic strength	179
6.14	Percentage of total species (neutral + anionic) of Nd(III)-HIBA, Am(III)-HIBA, Pu(III)-HIBA, Pu(IV)-HIBA, Th(IV)-HIBA, UO ₂ ⁺² -HIBA and PuO ₂ ⁺² -HIBA – elution sequence of lanthanide and actinides	184
7.1	Slope from van't Hoff plot, and enthalpy of sorption of all 14 lanthanides on 25 cm and 3 cm length supports	191
7.2	Enthalpy of sorption of U & Th on 25 cm length reversed phase support	197
7.3	Enthalpy of sorption of U & Th on 3 cm length (1.8 μ m) reversed phase support	199
8.1	Separation factors for adjacent lanthanides	215



Chapter-1

Chapter-1

Introduction

1.1 Chromatography

Chromatography is a separation technique [1-2] which is used for the isolation of a pure sample component from a mixture. This technique can analyse sample molecules (gaseous, liquid or solid) in a range of simple to complex mixtures. The principle of separation by this method is based on the distribution (adsorption, partition, ion exchange or size exclusion) of sample molecules between two phases. One is a stationary phase and the other is a mobile phase, which moves over the stationary phase in a definite direction. The stationary phase can be a solid or a liquid coated on an inert solid support, while the mobile phase can be gas or liquid or a supercritical fluid.

Quantitative as well as qualitative information about analytes can be obtained from chromatography. Qualitative information of analyte is obtained from retention time data, obtained experimentally. Quantitative information of analyte can be obtained from its corresponding peak area or peak height of a chromatogram using a calibration plot, which is generally prepared using standard solutions of an analyte.

1.1.1 Applications of chromatography

Chromatographic methods were employed for the separation and purification of various samples in different fields such as chemical industry, pharmaceutical industry, biotechnology, forensic science and nuclear industry [3]. In chemical industry, chromatographic methods are employed for the removal of pesticides and insecticides like dichlorodiphenyltrichloroethane (DDT) and polychlorinated biphenyl (PCB) from the

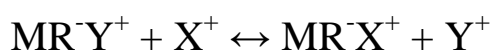
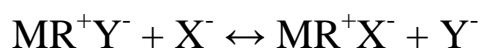
groundwater. In pharmaceutical industries, chromatographic technique is employed for purification of materials that are required in making drugs/medicines. This technique is also employed for separation of enantiomers. Important applications of chromatography are in the field of food industry, where proper food maintenance is necessary to ensure quality. Chromatography is used as a technique to separate the additives, vitamins, preservatives, proteins and amino acids. In forensic science, chromatography is a very popular technique for investigations such as (i) to determine substances that are present in the human body, (ii) to determine the presence of drugs or drug byproducts in urine/blood samples, (iii) analyse samples of crime scenes and (iv) detect samples of explosives.

1.1.2 Types of chromatography

Chromatographic methods are classified according to the nature of mobile phase, stationary phase, and retention mechanism. Based on the nature of mobile phase, chromatographic technique can be classified as gas chromatography (GC), liquid chromatography (LC), and supercritical fluid chromatography (SFC). In gas chromatography, the mobile phase is gas and solid adsorbent or a nonvolatile liquid coated on a solid support is employed as the stationary phase. Separation of sample components depends on the relative partial pressure of the sample components and their affinity onto the stationary phase. In the case of liquid chromatography, mobile phase is a liquid and a solid support is used as the stationary phase. Separation is based on partition/adsorption of sample molecule between a stationary phase and mobile phase. Supercritical fluid chromatography is a separation technique in which the mobile phase employed is a supercritical fluid (to prepare a supercritical fluid, its $T > T_c$ and $P > P_c$, where T_c and P_c are critical temperature and critical pressure respectively).

Depending on the separation mechanism, chromatography can be classified as adsorption chromatography, partition chromatography, ion exchange chromatography and size-exclusion chromatography. In adsorption chromatography, mobile phase is a liquid or gas that is adsorbed onto the surface of a solid stationary phase. The separation of different solute molecules depends on the equilibrium distribution of solute molecules between the mobile phase and stationary phase, which in turn depends on their relative polarity. In partition chromatography, the surface of a solid support is coated with a liquid stationary phase. Solute molecules distribute between the mobile phase and the stationary phase, based on their relative solubility.

Ion-exchange chromatography is a separation technique that is used for the separation of ions based on their charge. In this technique, stationary phase is a rigid matrix (M), the surface of which carries positive or negative charges, providing ion-exchange sites (R^+ or R^-). Counter-ions of opposite charge (Y^- or Y^+) are associated with each site in the matrix and these can exchange with similarly charged ions in the mobile phase to be held on the exchange sites. Sample ions (X^- or X^+) may thus exchange with these counter ions (Y^- or Y^+):



If the process involves the exchange of negatively charged ions, it is known as anion-exchange. The complimentary process is known as cation-exchange.

In size-exclusion chromatography (SEC), molecules are separated according to their molecular size in solution. Separation is a result of the exclusion of larger molecules from smaller pores in the column packing [4].

1.1.3 Historical development of chromatography

The science of chromatography began as early as the twentieth century [5-12], with the Russian botanist, Mikhail Tswett, who employed calcium carbonate packed glass column for the separation of plant pigments. In 1903, Tswett coined the term “chromatography”. In 1922 L. S. Palmer employed Tswett’s technique for separation of various natural products, and in 1931, Richard Kuhn employed the same to separate the isomers of ployene pigments. The chromatographic methods were developed rapidly in the years after the World War II, and found their applications in many environmental problems with the invention of various detectors. Many researchers have made substantial contribution for the development of chromatographic techniques.

Affinity chromatography was developed in the 1930s and was used to study the retention of enzymes and other proteins. This technique relies on the adsorbent bed material that has biological affinity for the substance to be separated. Arne Wilhelm Tiselius, winner of the Nobel Prize in 1948, was a main contributor to perfect the affinity chromatography through his development of many gel type resins for specific biochemical adsorption [13]. Partition chromatography was invented by A. J. P. Martin and R. L. M. Synge in 1941 [8]. They established the principles and basics of the technique of partition chromatography, and their work encouraged the rapid development of several other chromatographic methods, e.g., paper chromatography, and gas chromatography. In 1938, Russian scientists N. A. Izmailov and M. S. Shraiber developed drop chromatography on horizontal thin layers [14]. In 1945, two American chemists, J. E. Meinhard and N. F. Hall, employed this technique to separate terpenes, which was found in essential oils. Inspired by their work, Justus G. Kirchner and his co-workers in 1950 perfected Thin Layer Chromatography (TLC) using

silicic acid with starch as a binder and applied on glass plates, which acted as a stationary phase.

In 1947, the first analytical adsorption (gas-solid) chromatographic technique was developed by Fritz Prior, a graduate student under the direction of Erika Cremer at Innsbruck University. Archer John Porter Martin, who was awarded the Nobel Prize for his work in developing liquid-liquid (1941) and paper (1944) chromatography, laid the foundation for the development of gas chromatography and he later developed liquid-gas chromatography (1950). Commercially available gas chromatographs were produced in 1955 by several companies including Burrell Corp, Perkin-Elmer, and Podbelniak.

In 1959, gel filtration chromatographic technique was developed for the separation of molecules according to their molecular size. In the 1960s, in the conventional liquid chromatography, improvement was made by developing high pressure liquid chromatography also referred to high performance liquid chromatography (HPLC). Towards the end of 70's, the improvement on efficiency of HPLC technique began by the development of column packing materials and instrumentation.

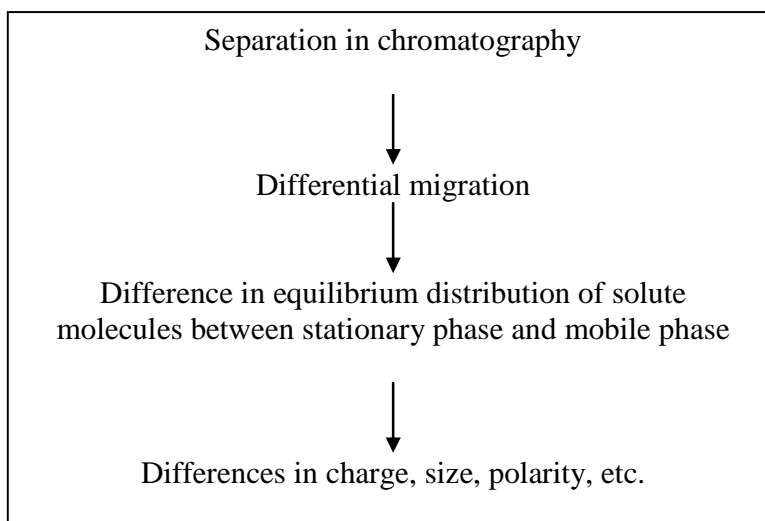
Ion-exchange methods are in use since 1850, and H. Thompson and J. T. Way, treated various clays with ammonium sulfate or carbonate solution to extract the ammonia and release calcium. In 1927, the first zeolite mineral column was employed to remove interfering calcium and magnesium ions from solution to determine the sulfate content of water. In 1940s, modern ion-exchange chromatography was developed during the Manhattan project. In 1970, Small and co-workers of Dow chemical company used this technique to determine low concentrations of ions for environmental and water quality studies [15-16].

Later development in chromatography led to the development of the micro chip based chromatographic technique due to several advantages such as rapid separations, reduced sample and solvent consumption, increased portability, and the ability to integrate pre-separation processes [17].

1.1.4 Principle of chromatography

In chromatography, main mechanism of separation of sample components is the sorption (adsorption/partition) between a stationary phase and a mobile phase. Depending upon the relative affinity of the substance for each phase, analyte is distributed between the two phases. The differential migration of the solute depends upon the interaction of the solute with the two phases. Sample molecule which has more affinity for the moving or mobile phase is carried rapidly through the column. Sample molecule which has a stronger affinity for the stationary phase, on the other hand, will spend more time in that phase, and will take a longer time to elute out of the column.

Principle of separation in chromatography



1.1.5 Retention in chromatography

In chromatography, when sample is introduced in to a column, it is distributed between mobile and stationary phase. Analytes present in the mobile phase and stationary phase are in equilibrium and this is expressed by a simple equilibrium equation,

$$k_x = \frac{[C_s]}{[C_m]} \dots\dots\dots(1.1)$$

where k_x is partition coefficient, C_s & C_m are concentration of analyte in the stationary phase & mobile phase respectively. If analyte “x” present in stationary phase and mobile phase can be written as number of moles, k_x can be expressed as k'

$$k' = \frac{(\text{moles of } x \text{ in stationary phase})}{(\text{moles of } x \text{ in mobile phase})} \dots\dots\dots(1.2)$$

Since the number of moles can be expressed as the concentration multiplied by the volume, k' (capacity factor) can be expressed as

$$k' = k_x \left(\frac{V_s}{V_m} \right) \dots\dots\dots(1.3)$$

where k_x is partition coefficient, V_s and V_m are volume of analyte in stationary phase and mobile phase respectively.

When sample molecules are completely unretained by the stationary phase, they exit the column at its void volume, which is one volume of mobile phase to pass through the column. However, the total time taken by molecules to pass through the column also includes the time spent in the stationary phase, in addition to the time it takes to run one void volume (V_m) and is expressed by $V_m k'$. Therefore, the volume of eluent that passes through the column before the sample elutes (retention volume, V_r) is expressed as:

$$V_r = V_m (1 + k') \dots\dots\dots (1.4)$$

The retention volume (V_r) is related to the flow rate (F_c), and the retention time (t_r). Likewise, the void volume of the mobile phase (V_m) is related to the flow (F_c) and the time (t_0) that void volume takes to pass through the column.

$$\begin{aligned} V_r &= t_r F_c \\ V_m &= t_0 F_c \dots\dots\dots (1.5) \end{aligned}$$

Substituting value of V_r & V_m in equation (1.4) and rearranging, the expression obtained is

$$k' = \frac{(t_r - t_0)}{t_0} \dots\dots\dots (1.6)$$

Values of variables such as t_r & t_0 are obtained from the chromatogram that is obtained experimentally. Separation between two substances is directly related to the difference in their k' values. Therefore, first step is to achieve a value of k' for a sample that is neither too small nor too large. For good separation, optimum k' falls in the range of the $1 \leq k \leq 10$ (for simple mixtures) and $1 \leq k \leq 20$ (for complex mixtures).

The selectivity (α) of a column for a particular separation, e.g., substances A and B (**Fig. 1.1**), is expressed as a ratio of their retention factors, i.e.,

$$\begin{aligned} \frac{k'_B}{k'_A} = \alpha &= \frac{\frac{t_{r_B} - t_0}{t_0}}{\frac{t_{r_A} - t_0}{t_0}} \\ &= \frac{t_{r_B} - t_0}{t_{r_A} - t_0} \end{aligned}$$

Value of selectivity (α) should be always greater than unity ($\alpha > 1$) to achieve good separation.

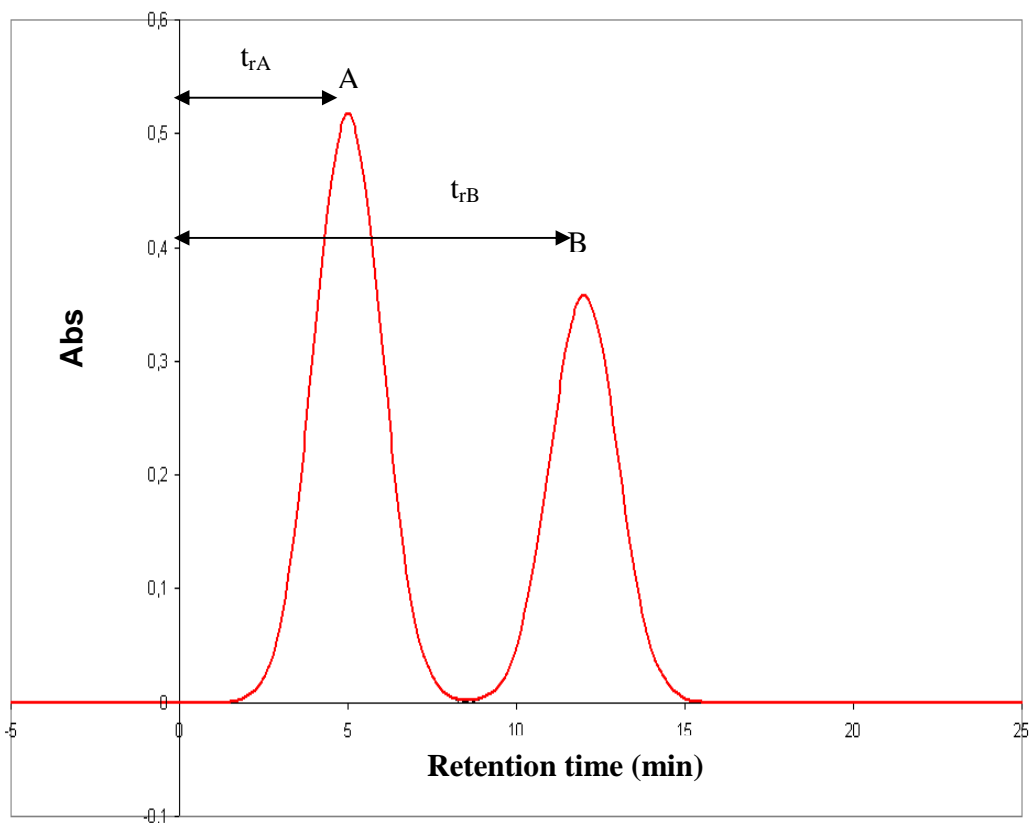


Fig.1.1. Chromatogram of substances A and B [2].

1.1.6. Efficiency of chromatographic column

In chromatographic separation, column efficiency is very important parameter and it can be defined as separation power of a column and can be defined in terms of number of theoretical plates. Number of theoretical plate provides number of separation stages and is directly proportional to the length of the column (L) in which analytes equilibrate between two phases and is inversely proportional to the thickness of the plate (H). Therefore, the number of theoretical plates (N) can be expressed as

$$N = \frac{L}{H} \dots\dots\dots(1.7)$$

Number of theoretical plates (N) can also be expressed as

$$N = 16 \left(\frac{t_r}{t_w} \right)^2 \dots\dots\dots(1.8)$$

$$\text{or } N = 5.54 \left(\frac{t_r}{t_w \frac{1}{2}} \right)^2 \dots\dots\dots(1.9)$$

where t_r , t_w , $t_{w \frac{1}{2}}$ are the retention time, peak width, and peak width at half height respectively.

The efficiency of a column varies with of several parameters such as the particle size of the packing material, uniformity of the packing, the flow rate of eluent, length of the column and the rapidity with which equilibrium is established between the two phases etc.

The number of theoretical plates (N) is inversely proportional to the diameter of packing material (d_p), i.e.,

$$N \propto \frac{1}{d_p}$$

Column efficiency can be increased by decreasing H. Plate height (H) depends on particle size of support material and mobile phase flow rate. Plate height “H” can be expressed in terms of column parameters and is written as an equation, called van Deemter equation. This equation relates the height equivalent of theoretical plate (H) of a column to the linear mobile phase velocity (u).

$$H = A + \frac{B}{u} + C u \dots\dots\dots(1.10)$$

where A, B, C, and u are eddy diffusion term, longitudinal diffusion term, mass transfer term for mobile and stationary phases and linear mobile phase velocity respectively. The column efficiency is influenced by these terms, as they are related to “H”. Hence, all terms such as A, B and C are to be minimised to reduce “H” [2]. Plot of H vs. flow rate for several columns of varied particle diameter is shown in **Fig.1.2**. It is observed from **Fig.1.2** that as the diameter (d_p) of the porous particles decreases from 10 to 3 μm , the plate height H decreases, corresponding to an increase in column efficiency per mm of column length. Therefore, for smaller particle, H is minimum and hence column efficiency is high. The type of particle and its particle-size distribution can also affect column efficiency, presumably by influencing the homogeneity of the packed bed. The effect of various terms (eddy diffusion term, longitudinal diffusion term, and mass transfer term for mobile and stationary phases) on the plot of height equivalent of theoretical plates (H) vs. flow rate (u) is shown in **Fig. 1.3**. It is observed (**Fig. 1.3**) that longitudinal diffusion term decreases and mass transfer term for mobile and stationary phases increases with increase in flow rate. Since H depends on both the terms B and C, H vs flow rate curve exhibits a minimum due to the opposing effect of longitudinal diffusion term with mass transfer term for mobile and stationary phases. Hence, chromatographic columns are to be operated at optimum flow rate to achieve maximum column efficiency.

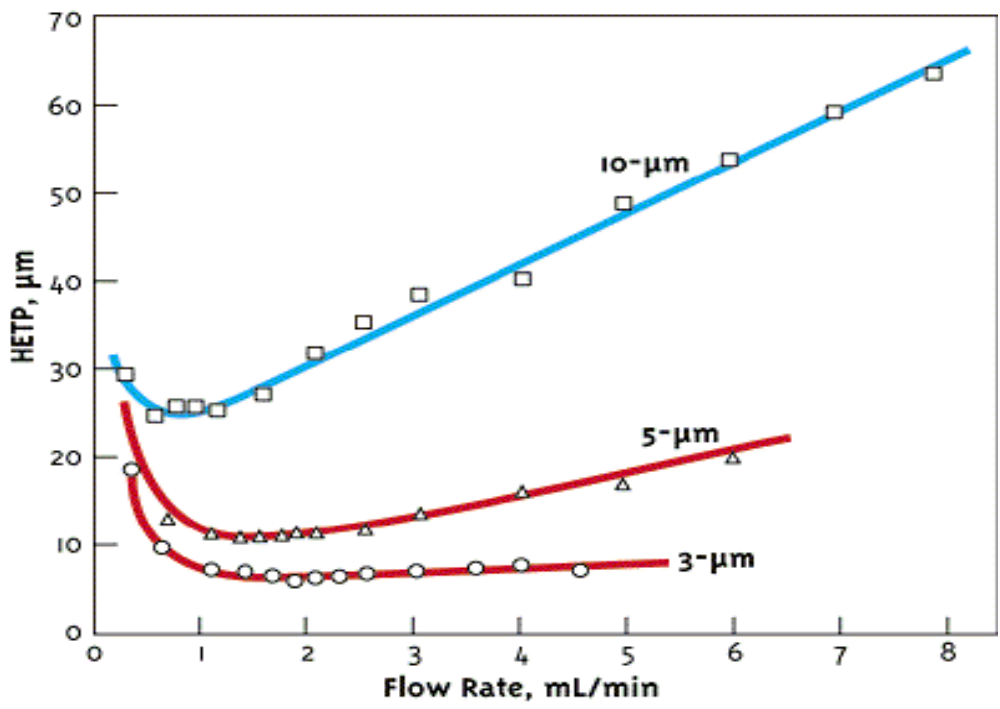


Fig.1.2. Influence of particle size on HETP [2].

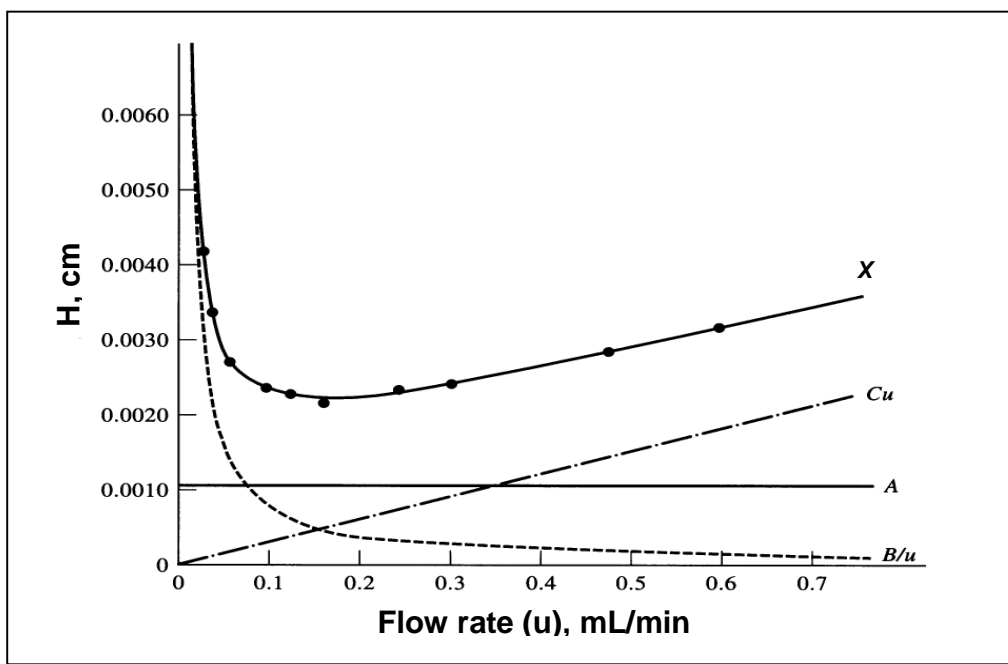


Fig.1.3. Influence of mobile phase flow rate on HETP-Contribution of eddy diffusion (A), longitudinal diffusion (B), mobile phase, stationary phase and stagnant mobile phase mass transfer (C) terms to HETP; X is resultant plot [18]

1.1.7 Resolution (R_s) in chromatography

The separation of two peaks (Fig.1.4), 1 and 2 is usually described in terms of their resolution $R_s = (\text{difference in retention times}) / (\text{average peak width})$. It can be expressed by the following equation

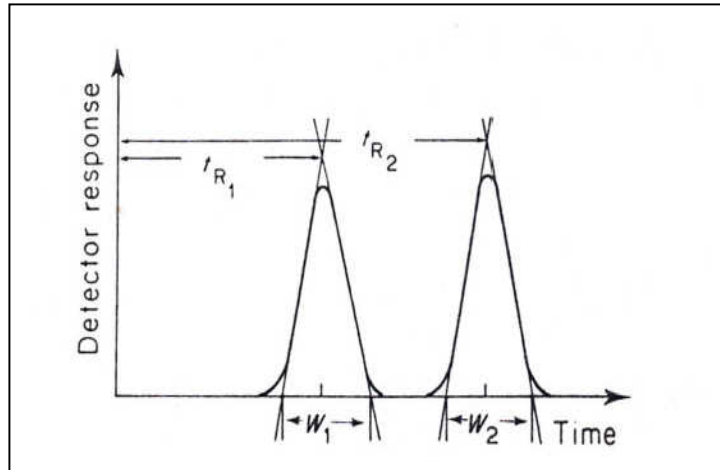


Fig.1.4. Measurement of resolution [1].

$$R_s = \frac{t_{r2} - t_{r1}}{\frac{1}{2} (t_{w1} + t_{w2})} \dots\dots\dots (1.11)$$

Where t_{r1}, t_{r2} , are retention times and t_{w1}, t_{w2} are the peak widths of the peak 1 and peak 2 respectively. If peak width t_{w1}, t_{w2} are similar, R_s is written as

$$R_s = \frac{t_{r2} - t_{r1}}{t_w} \dots\dots\dots (1.12)$$

From equation (1.6), t_{r1} and t_{r2} can be written as

$$t_{r1} = t_0 (k_1' + 1) \dots\dots\dots (1.13)$$

$$t_{r2} = t_0 (k_2' + 1) \dots\dots\dots (1.14),$$

and t_w , from equation (1.8), can be written as

$$t_w = \frac{4t_{r1}}{\sqrt{N}} \dots\dots\dots (1.15)$$

By substituting the value of t_{r1} , t_{r2} , and t_w in equation (1.12), R_s is expressed as

$$R_s = \frac{1}{4} \sqrt{N} \left(\frac{\alpha - 1}{\alpha} \right) \left(\frac{k'}{1 + k'} \right) \dots\dots\dots (1.16)$$

Resolution (R_s) depends on number of theoretical plate (N), selectivity (α) and capacity factor (k'). Necessary conditions for the good separation of two analytes are (i) very high N (ii) $\alpha \gg 1$ (iii) optimum value of k' ($1 \leq k' \leq 10$ for simple mixture and $0.5 \leq k' \leq 20$ for complex sample).

1.2 High Performance Liquid Chromatography (HPLC)

High performance liquid chromatography is a liquid chromatographic technique [2] that can separate the constituents from a mixture of compounds with very high speed and efficiency. The name HPLC was coined by the Csaba Horváth in 1970. High pressure pumps are required to force the eluent through densely packed small particle (e.g., 5 μm) to obtain high performance separation. Recently, development of HPLC in the form of ultra high pressure liquid chromatography (UPLC) has begun by the usage of small particle size based ($\leq 2 \mu\text{m}$) support. HPLC due to its high speed and efficiency of separations is employed in almost all fields of analytical chemistry. HPLC has become very useful technique to solve many separation problems in biochemistry, environmental and pharmaceutical industry, polymer and food chemistry and many other areas [19-20].

Preparative-HPLC is employed for the purification of gram to kilogram level of substances in various industries [21].

1.2.1 HPLC column packing material

Particle size for column packing refers to the average diameter of the packing particles. In conventional column chromatography, particle size of column packing materials is in the range of 100-200 μm . Hence, eluent can flow under gravity. In the case of HPLC, diameters of column packing materials are in the range of 1.8-5 μm . HPLC column has particles with narrow size distribution (e.g., in case of 1.8 μm particles, mean: 1.889 μm , SD: 0.40 μm). Number of theoretical plates (N) obtained with 5 μm particle size is usually in the range of 50,000 plates/meter for separation of organic compounds [2]. 5 μm particle size based support has been used for separation of organic as well as inorganic samples. Column lengths of 15 or 25 cm with particle size of 5 μm are generally employed in HPLC.

1.2.2 HPLC Separation modes

Depending upon the separation mechanism and the column type, HPLC can be divided into several related techniques. The most useful types for sample analysis are based on normal phase liquid chromatography (NPLC), reversed phase liquid chromatography (RPLC), and ion-pair chromatography (IC) [2].

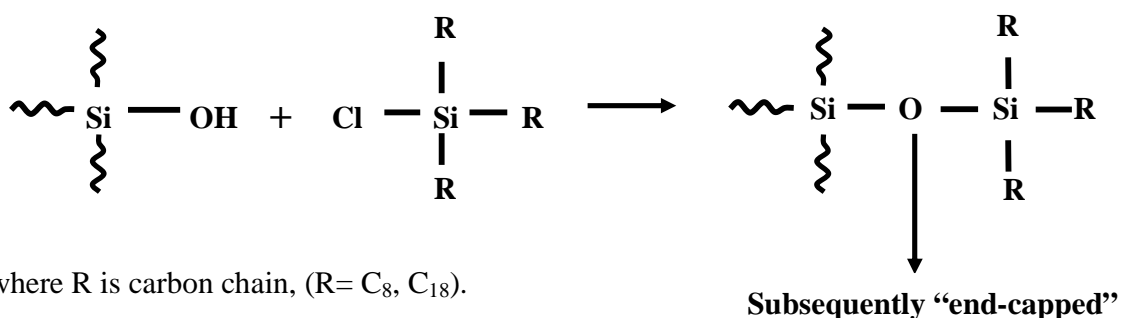
1.2.2.1 Normal Phase Liquid Chromatography (NPLC)

In normal phase liquid chromatography, the column packing materials used are polar in nature, e.g., silica and alumina; non-polar eluents such as hexane or hexane mixed with a slightly polar solvent are used as mobile phase. In this method, separation mechanism is mainly based on adsorption; the non-polar compounds elute first while the

polar molecules elute later. Retention of polar molecule increases with the proportion of nonpolar solvent in the mobile phase. In case of solvent gradient, chromatographic run is initiated with the least polar solvent (e.g. hexane), and gradually enhanced in polarity to bring out the most retained, most polar compounds. Different class of compounds can be separated on normal phase columns, e.g., polar sample molecules (mono substituted benzene), isomers, petroleum samples, lipid samples etc.

1.2.2.2 Reversed Phase Liquid Chromatography (RPLC)

In the case of reversed phase liquid chromatographic technique, nature of stationary phase material and mobile phase are just opposite to the normal phase liquid chromatography method, e.g., column packing material is non-polar (modified silica, i.e., siloxane) and mobile phase is polar in nature. Modified silica support material is prepared by reaction between an organochloro silane (R_3SiCl) with the surface -OH groups present on the silica support (Si-OH). This leaves hydrocarbon chains, which may contain two, eight, or eighteen carbons, bonded at their ends through Si-O- Si groups (siloxane) to the surface of the support. These columns are designated by the carbon number of the chains attached, with the most frequently used column being the bonded octadecyl type, called C_{18} . Surface functionalisation of silica can be performed in a monomeric or a polymeric reaction with different short-chain organosilanes to cover remaining silanol groups and this process is called “end-capping”.



Since column packing material is non-polar in nature, the main mode of retention is through dispersion forces, i.e., van der Waals forces. That is molecules are attracted through induced dipole induced dipole interaction. Separation of organic compounds using RP-HPLC is based on the difference in their hydrophobicity. In reversed phase liquid chromatography, the most polar compounds elute first while the most non-polar compounds elute latter. Reversed phase columns are employed for separation of organic molecules, protein, peptide, nucleic acid etc.

1.2.2.3 Ion chromatography

In this method, buffered aqueous solution is used as mobile phase and a resin matrix is used as stationary phase. The retention in ion chromatography is based on the ionic interaction between the charge on the stationary phase and oppositely charged sample ions. This method can be used for separation of cations (cation exchange chromatography) and anions (anion exchange chromatography). Cation exchange resins contain acidic functional groups which can be weak (e.g. COO^-) or strong (e.g. SO_3^-) and anion exchange resins contain basic functional groups which can be weak (e.g. $-\text{NH}_2$) or strong (e.g. NR_4^+). Conductivity detector is generally used in this technique for detection.

1.2.3 Chromatography with < 2 μm particle size

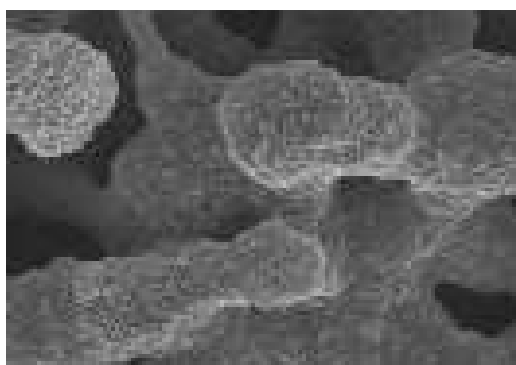
Performance of HPLC column material has been improved drastically over a period of time from irregular to spherically shaped particles and from large to small sized particles. However, over the past decades, HPLC column performance has been optimized with spherical and small sized particles.

Higher separation efficiency and faster sample analysis are two driving forces for continued improvement in HPLC column technology. Reduction in the average particle size

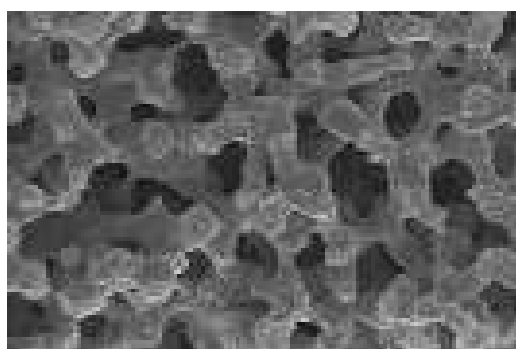
of HPLC column packing material, i.e., $< 2 \mu\text{m}$ has resulted in high speed separation of analytes. The typical number of theoretical plates obtained with small particle size based ($< 2 \mu\text{m}$) support material is $\sim 10^5$ plates per meter [2]. However, HPLC technique employing columns containing stationary phase materials of small particle size, e.g., $1.8 \mu\text{m}$ necessitates use of high operating pressures, i.e., as high as 500-1000 bar depending on the flow rate and column length. Generally, column length of 3-5 cm is employed for separation of analytes with $1.8 \mu\text{m}$ particle sized supports.

1.2.4 Separation using monolith based stationary phase

In the recent years, monolithic silica column has been widely employed for separation of analytes [22-26]. Compared to particle packed column, monolithic silica column has high permeability and separation efficiency with better resolution. Monolith column consists of a single piece of porous, rigid material (**Fig.1.5**) containing mesopores and micropores which provide faster analyte mass transfer [27, 28]. Based on the nature of support materials, monolith column can be either organic polymer or silica based. However, column efficiency offered by polymer based monolith is generally lower compared to silica based support. The higher column efficiency of silica-based monolith is due to the relatively higher surface area (typically, surface area is several hundred m^2/g) of mesoporous skeletons compared to polymer-based monolith (surface area typically lies in the range one order of magnitude smaller than silica based monolith) [29-30]. Monolith based supports are employed for various applications, e.g., separation of biomolecules, organic acids, inorganic anions, metal ions etc [31-32]. Porous monolithic silica was used for efficient separation of metal ions, e.g., alkaline-earth and transition-metal ions [31-36].



(a)



(b)

Fig.1.5 Electron micrographs of the (a) macroporous and (b) mesoporous structures in a monolithic silica rod [28].

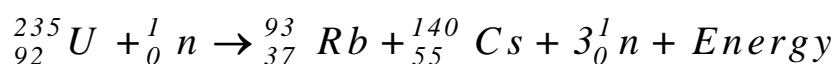
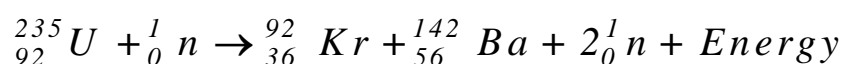
1.3 Separation chemistry in nuclear industry

1.3.1 Nuclear Power-an alternative clean source of energy

In the modern world, electricity plays a crucial role in the development of society. Natural sources of energy are fossil fuels (e.g., coal, oil, natural gas), hydro-electric energy, wind energy, solar energy etc. However, for large scale electricity generation, fossil fuels are used as primary sources of energy but the earth has limited supply of these resources. When fossil fuels are used to produce electricity, gases such as carbon dioxide and nitrogen oxide are emitted, leading to pollution in the atmosphere. Hence, nuclear power can be an alternative source of energy, which can help to preserve many of the natural resources as

well as protect environment against harmful by-products e.g., carbon dioxide and nitrogen oxide.

The main method of producing nuclear power is through nuclear fission, which is a nuclear reaction where fissile element after absorbing a neutron splits into smaller elements by releasing large amount of energy [37]. The following equations are examples of the different products that can be produced from nuclear fissions of U-235



Isotopes such as U-235, Pu-239 and U-233 are used as fuels in thermal reactors. The nuclear fission of uranium or plutonium generates a large number of fission products. The dissolver solution of spent nuclear fuel is highly radioactive due to the presence of fission products, plutonium and the minor actinides such as americium and curium. The determination of fission products and actinides such as uranium, plutonium, americium etc has great importance in nuclear waste management as well as in the determination of burn-up of spent nuclear fuel. The fission yield [38] of various fission products produced from a fast and thermal neutron fission are given in **Table.1.1**.

1.3.2 Chemistry of lanthanides

The lanthanides [39-41] consist of a unique series of metals in the periodic table. The lanthanide series is defined by the progressive filling of the 4f orbital. Electronic configuration of lanthanides is $[\text{Xe}] 4f^{1-14}5d^16s^2$. Generally, lanthanides are present in +3 oxidation state, which is more stable compared to other oxidation states. The chemical properties of lanthanides are similar due to similarity in their charge and size, which makes

it difficult to separate them from each other. Separation of lanthanides in pure form is mandatory for various applications.

The lanthanides have many applications in various fields [40, 42-46]. Lanthanides are employed in commercial applications such as alloys for aeronautical components, permanent and superconducting magnets, catalysts, phosphors, lasers, batteries, chemicals, ceramics, glass, glazes, lighting, medical imaging, technical ceramics, thermal spray powders etc. Lanthanide oxides such as europium and yttrium oxides are employed as phosphors in color television to produce red colors on television screen. Lanthanide compounds are used in streetlights, searchlight, and high-intensity light that is generally present in sports stadiums.

Table.1.1 Percentage (%) cumulative yield for some fission products

Fission Products	Isotopes of fission products	Fast fission yields for U-238	Fast fission yields for Pu-239	Thermal fission yields for U-235	Thermal fission yields for Pu-239
La	139	6.04	5.83	6.65	5.73
Ce	140, 142	10.93	10.16	12.22	10.58
Pr	141	6.76	5.62	5.81	5.34
Nd	143, 144, 145, 146, 148, 150	20.22	16.41	20.51	16.64
Sm	147, 149, 151, 152, 154	3.26	3.00	4.15	5.06
Eu	153, 155	0.55	0.72	0.19	0.61
Zr	91, 92, 93, 94, 96	25.55	18.24	30.99	19.03
Mo	95, 97, 98, 100	23.22	22.15	24.69	23.47
Ru	101, 102, 104	16.82	19.99	11.15	18.51
Rh	103	6.38	6.61	3.15	6.79

Pd	105, 106, 107, 108, 110	7.62	16.59	1.17	14.64
Rb	85, 87	2.34	1.66	3.89	1.38
Cs	133, 135, 137	19.22	21.00	19.55	20.77
Ba	138	5.96	6.04	6.91	5.82
Sr	88, 90	5.14	3.33	9.45	3.51
Y	89	3.01	1.80	4.76	1.72
Tc	99	6.20	5.77	6.14	6.19
Xe	129, 131, 132, 134, 136	22.68	24.23	21.75	24.76
Kr	83, 84, 85, 86	3.23	2.22	4.79	2.11

In ceramic industry, lanthanide oxides are employed to color the ceramic and glasses. Optical lenses are used in binoculars and cameras which are made of lanthanum oxide. Praseodymium and neodymium compounds are used in glass such as television screens. Cerium oxide is used to polish glass. Lanthanides are also employed in many emerging technologies, including hybrid cars and rechargeable batteries. Neodymium and dysprosium are used to manufacture magnets due to their high magnetic strength and low molecular weight. Hence, they are used in electric motors to produce higher power and torque with smaller size and weight. These characteristics make them very useful in the development of hybrid and electric vehicles as well as in the miniaturisation of hard disk drives used in many applications. Lanthanides also have important applications in nuclear industry. Lanthanides (La-Eu) constitute about one fourth of total fission products that are produced during nuclear fission of uranium or plutonium. Lighter lanthanides, e.g., La/Nd are used as fission monitors for atom percent burn-up determination of spent nuclear fuel

[47-49]. For e.g., Nd^{148} is used as fission monitor for the atom percent burn-up determination of PHWR spent fuel. Similarly, elemental yield of Nd was used as fission product monitor [49].

1.3.3 Actinides

Actinide [40, 50] series covers 15 elements from actinium (atomic no 89) to lawrencium (atomic no 103). As in the case of lanthanides, the ionic radius of actinides also decreases with increase in atomic number (**Fig.1.6**).

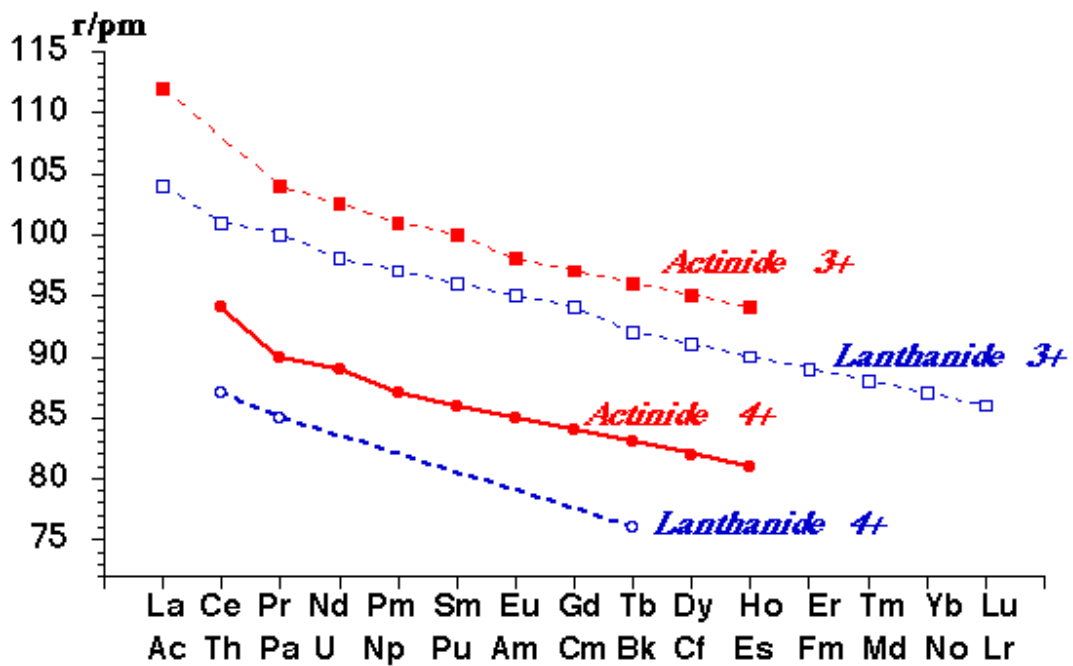
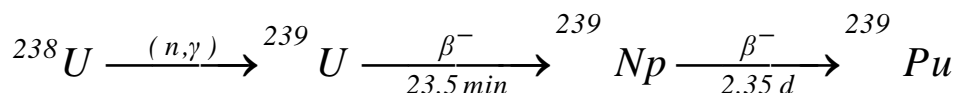


Fig.1.6. Variation of ionic radii of lanthanides and actinides with atomic number [40]

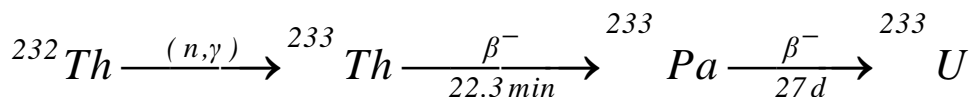
All elements in this series form a separate group within the periodic table due to the similarity in their chemical properties. The actinide series derives its name from group element actinium. Actinides with mass no ≥ 232 [38] can undergo nuclear fission and release energy upon nuclear fission. Hence, actinides are very important elements as nuclear fuel materials.

Actinides such as actinium, thorium, protactinium, and uranium are found in nature and other actinides in the series are produced artificially in nuclear reactors. Uranium and thorium have long half life and are present in the earth crust in a significant amount. Most abundant thorium ores are thorimite, thorite and monazite. Main uranium ore in the earth crust is uraninite which is also called as pitchblende. It is a mixture of its oxides in the minerals. Other uranium ores are carnotite and autunite. The actinides such as neptunium, plutonium and americium etc. are man-made and are produced in nuclear reactions. Due to the radioactivity of actinides as well as their importance in nuclear energy, the chemistry of most of these elements has been investigated thoroughly [50-52].

The main application of actinides is the production of nuclear energy and the most important isotopes are uranium-235 and plutonium-239. In nature, uranium consists primarily of two isotopes, U-238 (99.28%) and U-235 (0.72%). Other fissile isotopes are U-233 and Pu-239. U-238 is fertile isotope and through neutron capture followed by beta (β^-) decay, U-238 produces fissile isotope, Pu-239.



Thorium is three times more abundant in the earths crust than uranium. Thorium-232, which is also a fertile isotope, can be used to produce U-233. Absorption of neutron by Th-232 followed by beta (β^-) decay produces the fissile isotope U-233 which can be used as thermal reactor fuel.



Actinides also have other applications. Uranium compounds are employed in photography for toning, in leather, wood industries for stains and dyes and also as mordents

of silk [53]. Short lived isotopes are used for portable power batteries, smoke ionization detector, treatment of crayfish and neutron radiography. Thorium is employed as light-emitting material of gas mantles and as emitter in monochromatic X-ray tube. Thorium is also used in multicomponent alloys of magnesium and zinc. Th-Mg alloys are light, strong, and of high melting point and ductility. Therefore, these are employed in aviation industry and production of missiles. Thorium has good electron emission properties with long life time and low potential barrier for the emission. Uranium and thorium isotopes are used to estimate the age of various objects including stars.

Americium is employed in smoke detectors. Californium-252 has application as a strong neutron emitter [54]. Californium can be used in radiation therapy to treat certain cervical and brain cancers. It also can be used in the radiography of aircraft to detect metal fatigue, in neutron-activation detectors of explosives at airports. Pu-238 was used as the energy source in heart pacemakers [55].

1.3.4 Burn-up (Atom percent fission)

The term burn-up is employed to denote total amount of energy released by a known quantity of fuel during its life-time in a nuclear reactor. The burn-up is commonly expressed in units of atom percent fission or megawatt day/tonne (MWd/t) or gigawatt day/tonne (GWd/t). Studies on dissolver solutions of nuclear reactor fuels are essential for fuel management, waste treatment, quantification of transuranium elements etc. Measurement of atom percent fission or burn-up, an important characteristic of fuel performance is an outcome of the above studies [56-57]. Atom percent burn-up is defined as the number of fissions per 100 initial heavy element atoms, and can be expressed as

$$Atom\% \text{ fission} = \left[\frac{\left(\frac{A}{Y}\right)}{\left(H + \left(\frac{A}{Y}\right)\right)} \right] \times 100 \dots \dots \dots (1.17)$$

where “A” is the number of atoms of fission product monitor, “Y” is the effective fractional fission yield for “A” and “H” is the residual heavy element (e.g., U+Pu) atoms in the dissolver solution. The following are the main properties of fission monitors

1. They should have low capture cross-section and low formation and burn-out cross section.
2. They should be stable (or should have a very long half life).
3. They should not migrate in the fuel matrix at the operating temperature.
4. They should have large and well known fission yields. The fission yield of the fission product monitor should be similar for different fissioning nuclides.
5. Chemical separation of fission product should be feasible. Fission monitors should be available for accurate determination using chemical/radiochemical or mass spectrometric methods.

Lanthanide fission products such as Nd or La satisfy most of the requirements of fission monitors. For the thermal reactor fuels, ¹⁴⁸Nd is used as fission monitor using mass spectrometric technique; for fast reactor fuel, the monoisotopic ¹³⁹La is used as fission monitor for burn-up determination of dissolver solution of spent nuclear fuel using HPLC technique [49].

1.3.4.1 Methods for atom percent burn-up determination

Various methods have been developed for the measurement of burn-up of dissolver solutions of spent nuclear fuels and are described below [58-63].

- 1. Heavy elements isotopic ratio method:** In this method, burn-up of spent fuel is determined by measuring the isotopic ratio of heavy elements (e.g., U and Pu) on an unirradiated fuel specimen and dissolver solution of fuel after irradiation. This method is applicable generally for fuel with an appreciable burn-up.
- 2. Heavy atoms difference method:** In this method, burn-up is determined by measuring the total difference of heavy element atom contents of solution of both un-irradiated and irradiated fuel specimens. This method again is employed for relatively higher burn-up only, e.g., 5-10 atom percent burn-up
- 3. Fission product monitor method:** In this method, fission product monitor and residual heavy element contents of dissolver solution of irradiated fuel are estimated and then using fission yield data of fission product monitor, burn-up is calculated using the equation (1.17). In this method, fission product monitor is estimated using radiochemical (if it is radioactive) or instrumental technique such as spectrophotometry, X-ray, mass spectrometry [56, 64-67] and HPLC method [48-49, 68]. This technique is applicable for low as well as high burn-up.

1.3.5 Importance of separation of lanthanides and actinides

The separation of lanthanides is very important for various applications such as geological applications [45, 69] in nuclear industry [47-49] and other applications which were discussed elsewhere in this chapter. In case of geological application, lanthanides separation is very important for the investigation of rare earth mineral resources, isotopic analysis for the clarification of the geological history of the earth and analysis of living samples for the investigation of natural distribution of lanthanides in the biosphere. Efficient separation of lanthanides e.g. La and Nd is required in a shortest possible time for

the burn-up determination of dissolver solution of spent nuclear fuel to minimize radiation exposure to operator and also reduce liquid waste generation.

1.3.5.1 Methods for lanthanides and actinides separation

The classical methods for the separation of lanthanides were fractional crystallization, precipitation and redox conversion method. These methods are time consuming, laborious and not very efficient for the individual separation of lanthanides. Afterward, more efficient separation techniques such as solvent extraction and ion-exchange methods [70-76] were developed. For the assay of low level of lanthanides, an efficient separation and preconcentration techniques are required to achieve accurate and reliable results.

The classical method for actinide separation by column chromatography using Dowex-50 cation exchange resin with α -HIBA as complexing agent was crucial in discovery and identification of actinides [77-78].

Different methods are available for determination of actinides such as radiochemical method [79], flame atomic absorption [80], neutron activation analysis [81] and inductively coupled plasma mass spectrometry [82].

Several analytical techniques have been developed for the separation and determination of lanthanides and actinides [47, 69, 83-84]. Chromatographic techniques are more efficient compared to other analytical techniques and provide rapid separation of individual lanthanides as well as actinides. Amongst these techniques, HPLC with on-line detection is a well established method owing to its high speed, good sensitivity and multi-elemental analysis capability using a single injection [47-48].

1.3.5.2 High performance liquid chromatography (HPLC) for the separation of lanthanides

High performance liquid chromatography technique based on dynamic ion-exchange method was employed for the separation of lanthanides and actinides. After invention of HPLC in 1960's, separation of lanthanides was reported first by Sisson *et al* [85] and Schadel *et al* [86]. Initially, separation of lanthanides was carried out using conventional ion-exchange method [87-88]. However, these methods have certain limitations such as fixed capacity and poor mass transfer of analyte that resulted in longer analysis times and poor column efficiencies. Weak organic acids such as α -hydroxy isobutyric acid (α -HIBA), citric acid, lactic acid, tartaric acid and α -hydroxy- α -methyl butyric acid were employed as complexing agent for separation of lanthanides [77, 89-93].

Dynamic ion-exchange HPLC technique [48-49, 67-68, 94-97] was developed to improve the efficiency for individual separation of lanthanides due to several advantages compared to conventional ion-exchange technique such as variable capacity of the dynamically modified column and high column efficiency.

In dynamic ion-exchange HPLC technique, a hydrophobic stationary phase, e.g., C₁₈ was employed with a suitable ion-pairing reagent for metal ion separations. In this technique, the stationary phase is converted into an ion-exchange support with suitable modifier reagents. Some examples of ion-pairing reagents include pentane sulfonate, hexane sulfonate, octane sulfonate, and camphor sulfonate. Separation mechanisms using these techniques are explained on the basis of dynamic ion exchange, ion-pair and ion-interaction models [98-102]. The schematic of the separation models are shown in **Fig.1.7**.

In the dynamic ion exchange mode, the modifier is assumed to be sorbed onto a reversed phase C₁₈ support to create an ion-exchange surface. The adsorbed ion-pairing

reagent (IPR) imparts a charge to the stationary phase causing it to behave as an ion exchanger. A constant interchange of ion-pairing reagent (IPR) occurs between stationary phase and mobile phase, leading to formation of dynamic ion-exchange surface. The sample ions are then exchanged between stationary phase and mobile phase by an ion exchange mechanism (**Fig.1.7b**). The total concentration of the ion-pairing reagent adsorbed on a stationary phase is dependent on its concentration and its hydrophobicity.

The ion-pair model suggests formation of an ion-pair complex between an analyte ion and modifier; the ion-pair complex is subsequently partitioned between stationary phase and mobile phase (**Fig.1.7a**). Retention results mainly as a consequence of interaction taking place in the eluent between solute and ion-pairing reagent and the subsequent partition of the complex to the stationary phase. The degree of retention of ion-pair depends on the hydrophobicity of the ion-pairing reagent.

The ion-interaction model (**1.7c**) is viewed as an intermediate between the dynamic ion exchange and ion pairing models. It incorporates both the adsorptive effects which form the basis of dynamic ion exchange and the electrostatic effects, which are the basis of ion-pair model. The ion-pairing reagent is considered to be in dynamic equilibrium between the stationary phase and mobile phase, resulting in the formation of an electric double layer at the surface of stationary phase. The adsorbed ion-pairing reagent constitutes a primary layer of charge to which a diffused secondary layer of oppositely charged ions, i.e., mainly counter ions of ion-pairing reagent are attracted. The solute has to compete for a position in the secondary charged layer from which it tends to move into the primary layer as a result of electrostatic attraction.

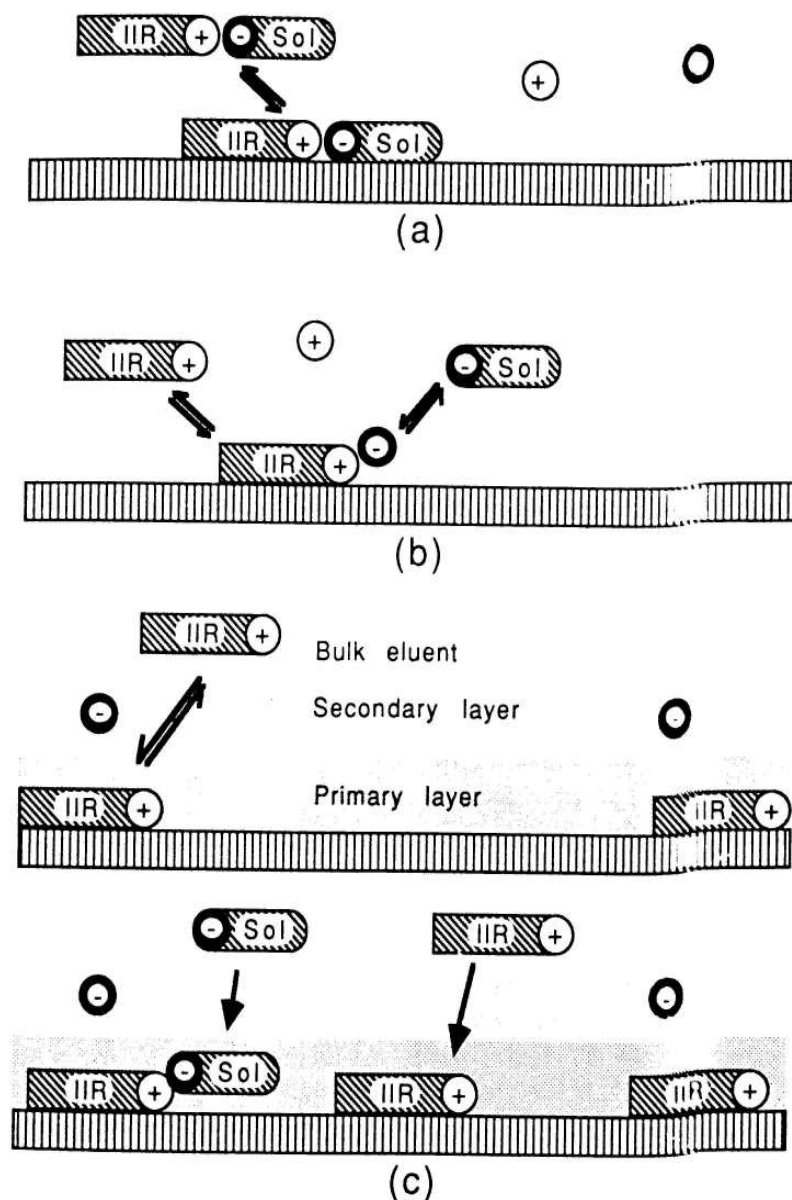


Fig.1.7. Schematic illustration of (a) the ion-pair (b) the dynamic ion-exchange and (c) the ion-interaction models for the retention of anionic solutes in the presence of a lipophilic cationic ion-interaction reagent (IIR) [98, 101].

The presence of solute in the primary layer causes a decrease in the total charge of this layer; to maintain charge balance, more ion pairing reagent ion must enter the primary layer. This indicates that the adsorption of a solute ion having opposite charge to the ion pairing reagent is accompanied by the adsorption of an ion pairing reagent ion. The overall

result is that the solute retention involves a pair of ions, i.e., solute and ion pairing reagent ions, but not necessarily an ion-pair. Though many of these models define the solute retention under certain conditions, the exact mechanism could be the combination of dynamic ion-exchange, ion-pair and ion-interaction mechanisms.

1.3.5.3 Retention of actinides

Retention behaviour of actinides such as U, Th and Pu on reversed phase support as well as modified reversed phase support was studied and reported [103-109]. Various complexing agents were employed for the separation of U and Th. Hao *et al.* [103] reported retention behaviour of U and Th on reversed phase support using α -HIBA as the mobile phase. Complexing agent such as, glycolic acid, mandelic acid, lactic acids were also employed for separation of U and Th [94-95, 110-111].

Barkley *et al* reported separation of actinides and lanthanides on dynamic ion-exchange technique using n-octane sulphonate as an ion-pairing reagent and α -HIBA as a complexing agent [112]. Separation of uranium and thorium from other metal ions in natural waters and geological materials was investigated on ion chromatography using cation-exchange resin [113-114].

Speciation of various actinides such as uranium, thorium, americium plutonium and neptunium in environmental samples, e.g., carbonate free and carbonate-rich natural water was investigated [115]. Speciation of plutonium in natural water was also reported [116]. For understanding the behaviour of actinides in biological system, speciation of actinides in biological process was investigated [117]. Speciation of actinides such as U, Th with α -HIBA was also studied [103, 106].

1.4 Methods for the determination of stability constant of lanthanides and actinides

Stability constant is a measure of the strength of the interaction between metal and ligand that form the complex. A stability constant which is also known as formation constant or binding constant is an equilibrium constant for the formation of a complex in solution. Stability constants have many applications in different branches of science such as in chemistry, biology and medicine. Methods for determination of stability constant of various metal complexes are potentiometry, conductometry, polarography, spectrophotometry, solvent extraction, ion exchange, different chromatographic methods (gel chromatography, ion chromatography, RP-HPLC etc) and capillary electrophoresis [118-121].

The individual separation of lanthanides and actinides depend on the stability constants of the lanthanide and actinide complexes. Lanthanides/actinides are hard acids and according to HSAB (hard soft acid base) principle, hard acid interacts preferentially with hard base, i.e., ligands containing oxygen and nitrogen. Lanthanides and actinides form strong complexes with oxygen containing organic acids such as α -HIBA, lactic acid, glycolic acid, mandelic acid etc. The stability constant of lanthanides with these ligands are key to identify the best complexing reagent for high performance separation. The elution pattern of lanthanides depends on the stability constants of the lanthanide complexes formed with ligands. The higher the stability constant of Ln–ligand complexes, faster will be their elution during chromatography.

1.5 Ionic liquid and its application in chromatography

Ionic liquids (ILs) are substances that are entirely comprised of ions (cation and anion). Ionic liquid with melting point below 100°C is referred to as room temperature ionic liquid (RTIL). Properties of ionic liquid are high viscosity, excellent thermal stability, low

combustibility, low vapour pressure and large electrochemical window. Due to their distinctive properties, room-temperature ionic liquids are employed in various applications such as in synthesis, catalysis [122-127], separations [128], and electrochemistry [129-131]. The physical as well as chemical properties of the room temperature ionic liquid can be tuned by careful choice of cation/anion. Therefore, they are also referred to as designer solvents. Recent advancements in ionic liquids research provide another route for achieving task-specific ionic liquids (TSILs) in which a functional group is covalently attached to the cation or anion part of the ionic liquid. Growing interest in ILs has been observed in chromatographic method such as gas chromatography (GC), capillary electrophoresis (CE) and liquid chromatography (LC). In gas chromatography ionic liquids are employed as stationary phase for separation of volatile organic compounds [132-135]. In liquid chromatography, ionic liquids are employed as mobile phase and also as modifier in stationary phase material for separation of biomolecules, natural products, amines, amino acids, nuclei compounds, drugs etc. [136-139].

1.6 Scope of Present work

In the present work, individual separation of lanthanides and actinides was investigated on reversed phase supports such as small particle (1.8 μm) support and monolith based supports. These methods were subsequently employed for the burn-up measurement on dissolver solutions of nuclear reactor fuels. A single stage double column chromatographic technique was investigated for the burn-up measurement on dissolver solution of PHWR (Pressurised Heavy Water Reactor, MAPS, Kalpakkam, India) and Fast reactor fuel (FBTR, Kalpakkam, India). An HPLC technique has been investigated for the estimation of lanthanide impurities in uranium matrix (1 in 10^6) using the dual column technique.

A method for the correlation of retention of lanthanide and some actinide complexes with the stability constant was investigated. The retention times as well as capacity factors of lanthanides and actinides were measured as a function of CSA, organic acid concentrations and mobile phase pH. From these studies, a correlation has been established between capacity factor of a metal ion, concentrations of ion-pairing reagent and complexing agent with the stability constant of lanthanide/actinide complex. Based on these studies, it has been shown that the stability constant of lanthanides and actinides can be estimated for a ligand, whose value is not reported in literature. Speciation data for plutonium in various oxidation states were obtained with α -HIBA from stability constant data. These studies were also employed to explain the elution behaviour of plutonium (various oxidation states), uranium and thorium. The elution behaviour of lanthanides and actinides was also investigated as a function of temperature using dynamic ion-exchange and reversed phase chromatographic techniques. Retention behaviour of lanthanides and actinides was examined using task specific ionic liquids as mobile phase. The individual separation of lanthanides and separation of uranium from thorium was investigated with various ionic liquids.

Organization of the thesis

This thesis is organized into the following Chapters

CHAPTER 1: Introduction

CHAPTER 2: Experimental

CHAPTER 3: Rapid Separation of Lanthanides and Actinides on Small Particle Based Chromatographic Supports.

CHAPTER 4: Liquid Chromatographic Behaviour of Lanthanides and Actinides on Monolith Based Supports

CHAPTER 5: Burn-up Measurement on Dissolver Solution of Nuclear Reactor

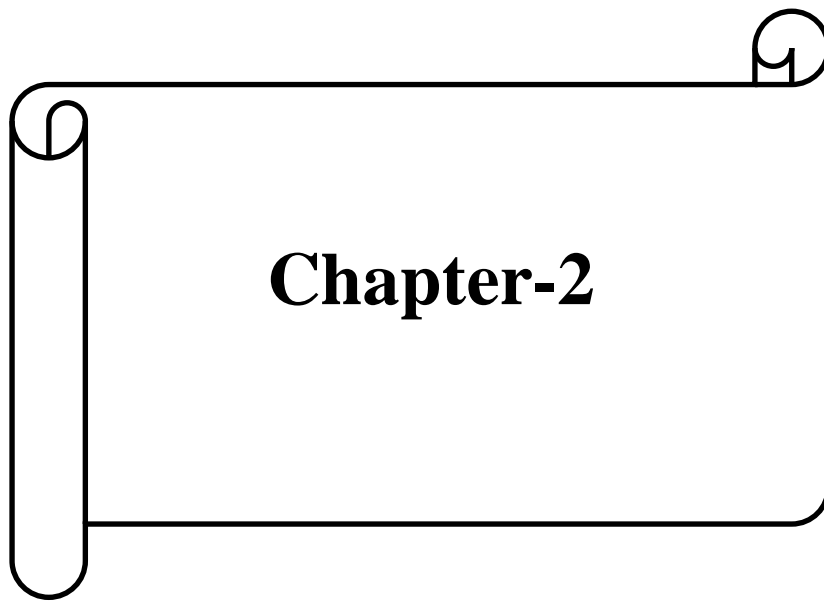
Fuels using HPLC

CHAPTER 6: Correlation of Retention of Lanthanide and Actinide Complexes with Stability Constants and their Speciation

CHAPTER 7: Influence of Temperature on the Elution Behaviour of Lanthanides and Some Actinides on Reversed Phase Supports

CHAPTER 8: Task-Specific Ionic Liquids in Liquid Chromatography-Studies on the Retention Behaviour of Lanthanides and Some Actinides

CHAPTER 9: Summary and Conclusion



Chapter-2

Chapter-2

Experimental

2.1 HPLC Instrumentation

The components of HPLC system employed in the present work consisted of the following

- (1) Mobile phase reservoir
- (2) Solvent delivery pumps (Jasco PU-1580)
- (3) Gradient mixer
- (4) Sample injector (Rheodyne 7725).
- (5) Reversed phase C₁₈ columns
- (6) Post-column delivery system (Jasco PU-1580)
- (7) UV-VIS Spectrophotometric detector (190-900 nm) (Jasco UV-1570)
- (8) Data acquisition system

Each component of HPLC system is described below. The schematic diagram and photograph of HPLC system are shown in **Fig.2.1** and **Fig.2.2** respectively.

The HPLC system was set-up in fumehood for studies involving radioactive materials. High pressure pumps used for the delivery of mobile phase and post-column reagent were placed outside the fumehood. However, the Rheodyne sample injector, columns, and detector were kept inside the fumehood. The eluate from the chromatographic experiments was collected inside the fumehood. The data acquisition (Borwin Software) from the UV-Vis detector was done through cables, connected to a computer through a Borwin interface, which was kept outside the fumehood. The schematic of the radioactive HPLC system is shown in **Fig.2.3**.

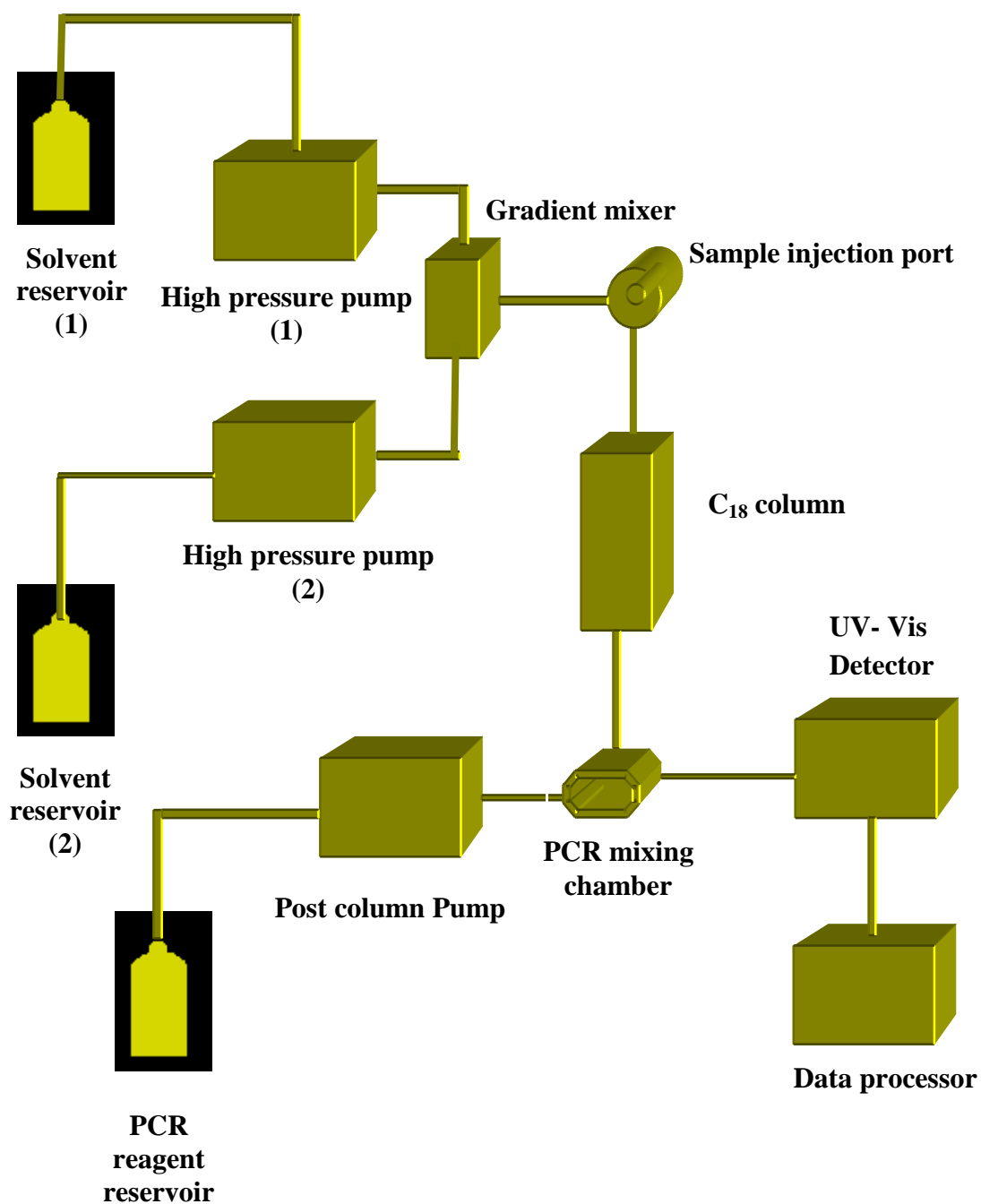


Fig.2.1. Schematic diagram of High Performance Liquid Chromatography (HPLC)

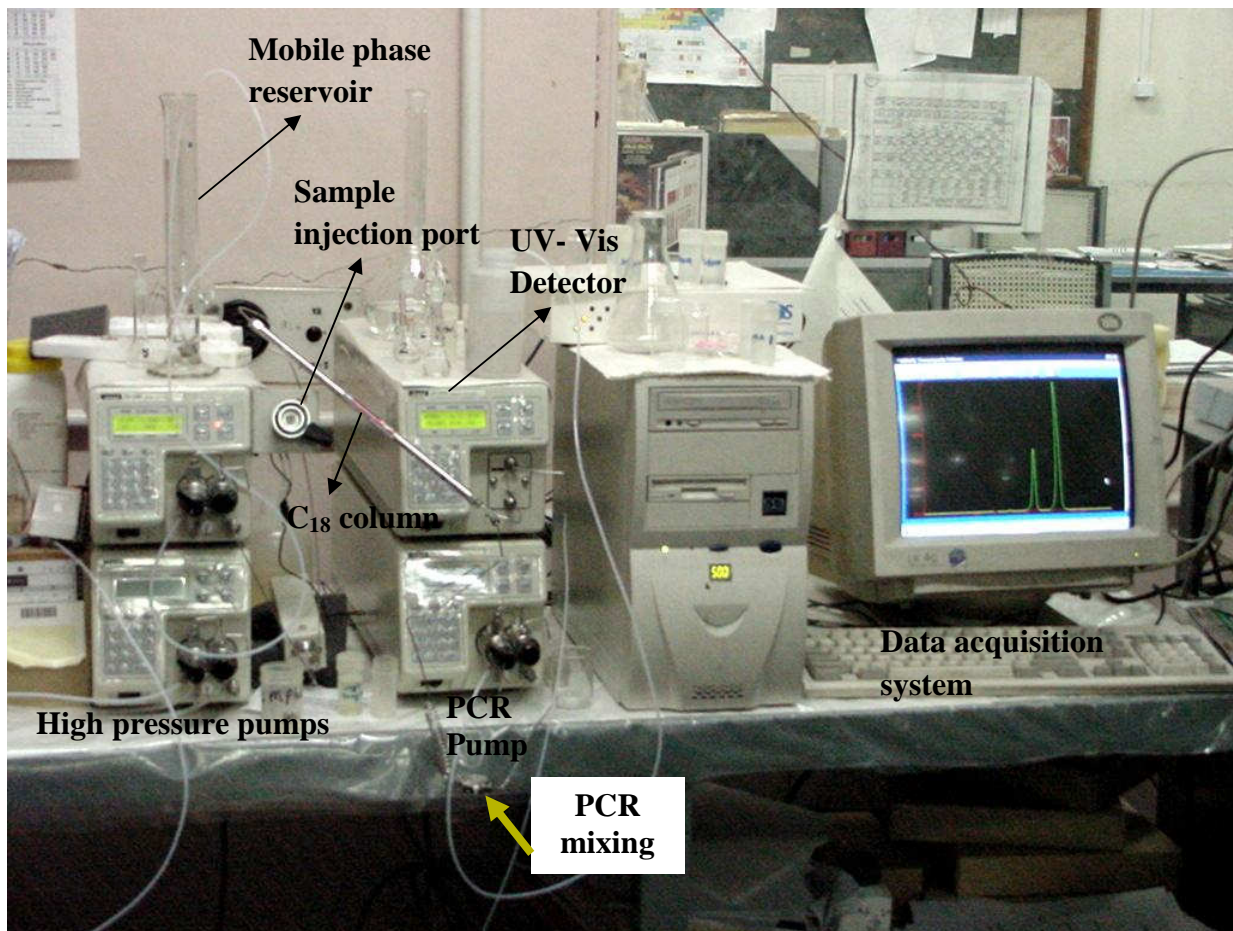


Fig.2.2. Photograph of HPLC system used in present study

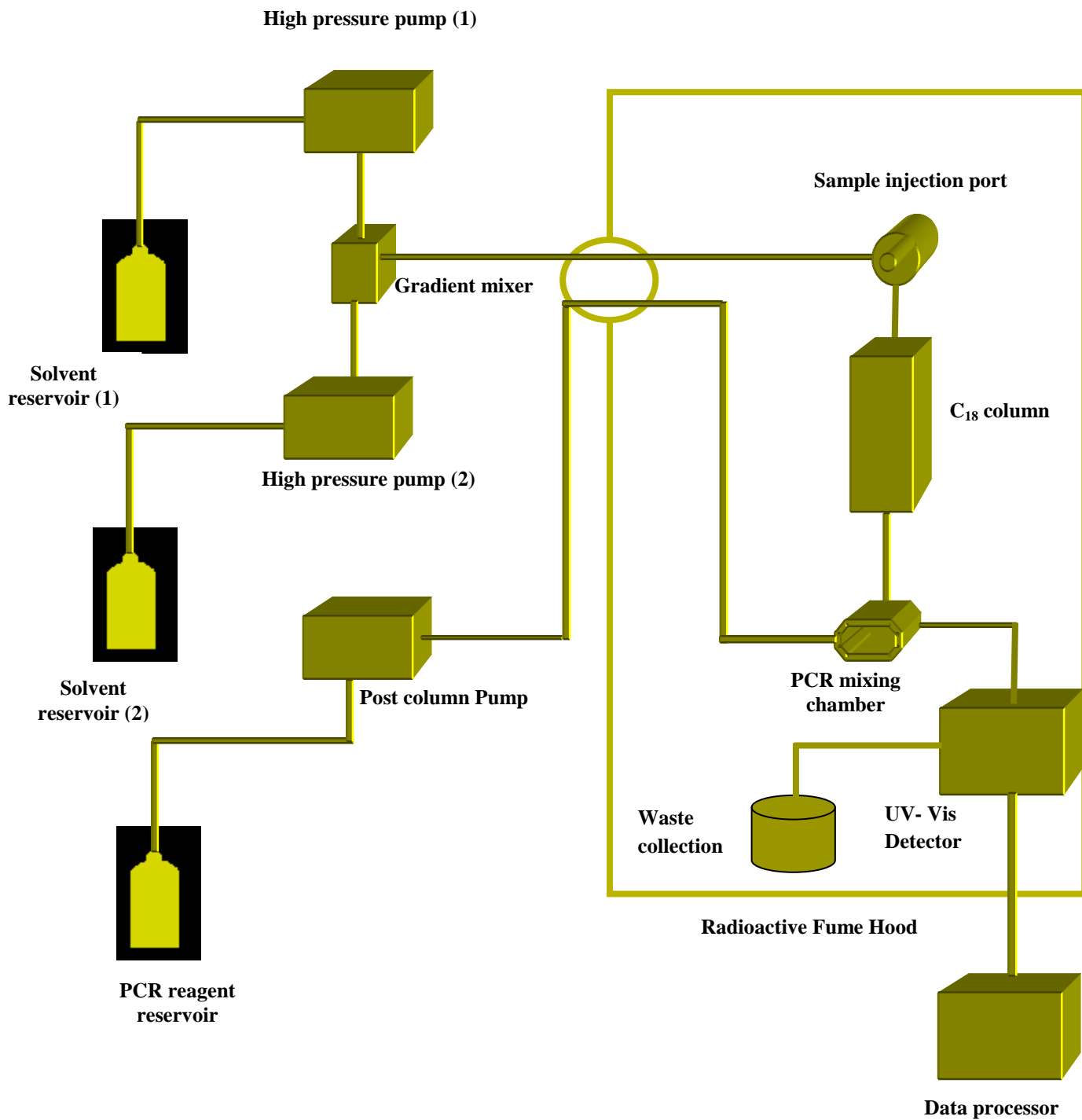


Fig.2.3. Schematic diagram of HPLC system for radioactive sample analysis

2.1.1 Solvent (mobile phase) reservoir

Mobile phase reservoir is an essential part of the HPLC system. Glass reagent bottles were employed as solvent reservoir. For isocratic applications using premixed mobile phase, only a single reservoir was employed whereas two reservoirs were employed for gradient applications. Mobile phases should be free from particulate matters which otherwise may damage the pumps by accumulating at the top of the column and cause plugging; mobile phase was hence degassed using sonication to remove the dissolved gases. After sonication, mobile-phase was filtered through 0.2 μm filter prior to delivering solvent through a column.

2.1.2 High pressure pump

The solvent delivery pumps are very important part for delivering mobile phase that carries the sample component through stationary phase support. The most important characteristic of the HPLC pump is its ability to deliver pulse-free flow of a solvent at constant rate. A pressure up to 500 bar can be generated by the solvent delivery systems employed in the present work. In the present study, reciprocating dual piston (Fig.2.4) pumping systems were employed for the delivery of solvents [2].

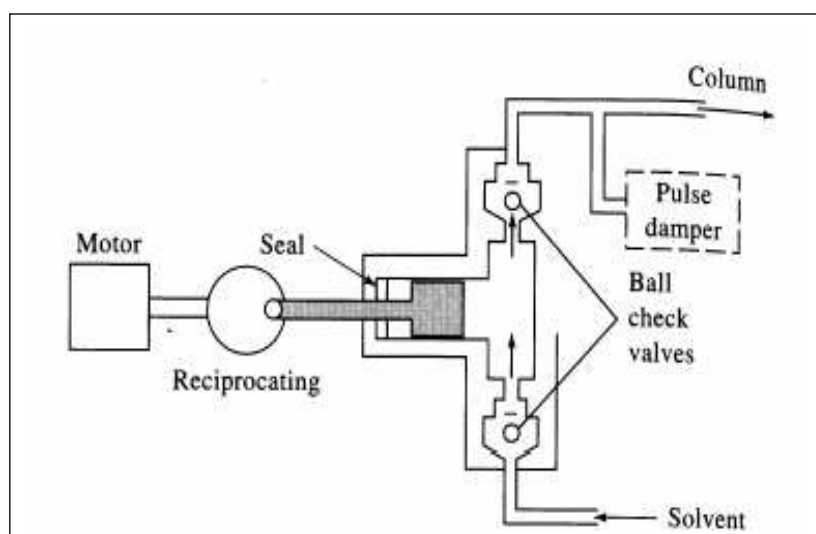


Fig.2.4 Schematic diagram of HPLC reciprocating pump [2]

2.1.3 Tubing and fittings

Tubing and the fittings are required to connect various components of HPLC system for transporting the mobile phase and sample. Narrow bore stainless steel tubings (outer dia ~ 1/16 inch; Inner dia ~ 0.1-0.3 mm) were employed for the connections between solvent containers, pumps, columns and detectors.

2.1.4 Gradient mixer

In case of gradient elution, the mobile-phase composition was altered during the chromatographic run and hence on-line mixing of solvents from two separate reservoirs was employed. High-pressure gradient mixing system was employed in the study for gradient elution. Two pumps were employed for high pressure gradient mixing.

2.1.5 Sample Injector

In the present study, a Rheodyne sample injector (7725/7125) (**Fig.2.5**) was used with 20/100/200 μL sample loop. This sample injector contained a six-port injection valve with a sampling loop. Sample solutions were injected into the column through a 20/100/200 μL sample loop injector.

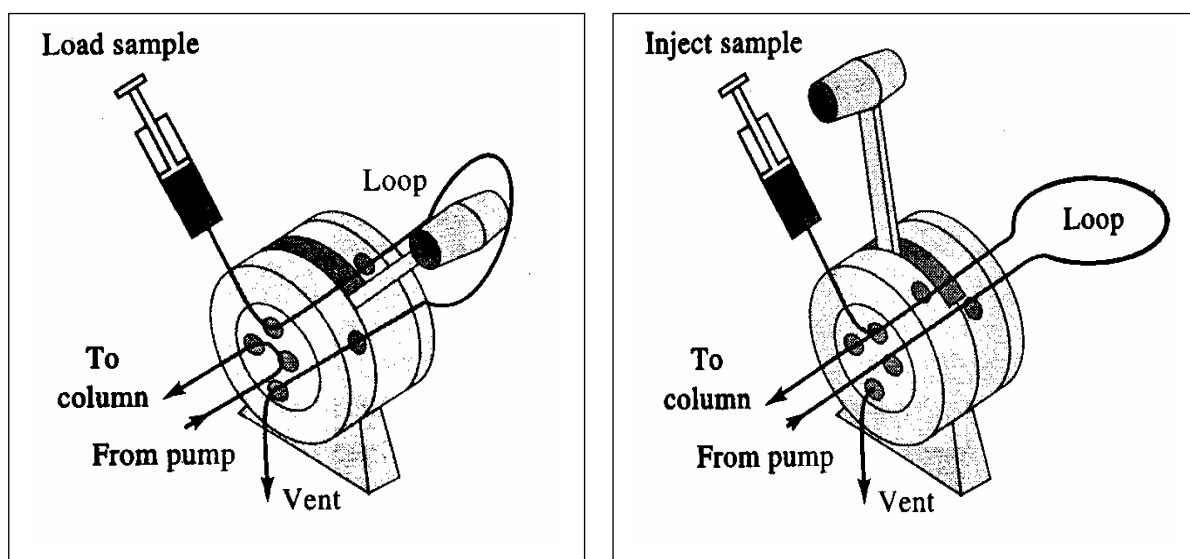


Fig.2.5. HPLC Rheodyne sample injector [2]

2.1.6 HPLC Columns

Column is the heart of the HPLC system. In the present study, the following reversed phase columns were employed [(a). C₁₈, 250 mm x 4.6 mm, 5 μm (Hypersil); (b). C₁₈, 50 mm x 4.6 mm, 1.8 μm (Peerless); (c). C₁₈, 30 mm x 4.6 mm, 1.8 μm (Peerless); (d). Reverse phase monolith columns with dimensions, surface area, macroporous and mesoporous structure of {(i). 100 mm x 4.6 mm, chromolith (Merck), 300 m²g⁻¹, 2 μm, and 13 nm. (ii). 50 mm x 2 mm (Merck); 300-360 m²g⁻¹, 1.5 μm, and 10 nm respectively}]

To enhance the life time of the reversed phase column, a guard column was placed before the column. The guard columns pick up any particulates that are present at the exit of the pump.

2.1.7 HPLC Detector

Detector is the eye of HPLC system [140]. In the present work, it was positioned after the column and detects sample molecules after elution from the chromatographic column. The main characteristics of liquid chromatographic detector used in the present work are high sensitivity (measurable minimum absorbance: 0.0005 ABU; Noise < ±0.000005 ABU; Drift: < 0.0002 ABU/h), ability to remain unaffected by changes in the temperature and mobile phase flow rate, reliability, the convenience for usage, linear response with the amount of solute, and wide dynamic range. Detection limits of some lanthanides (La, Ce, Pr, Nd and Sm) and actinides (U and Th) under typical experimental conditions were measured and results are given in **Table.2.1**.

The UV-Vis detector works on principle of Lambert-Beers law which is written as

$$A = \log \left(\frac{I}{I_0} \right) = \epsilon b c$$

where A , I_0 , I , ϵ , b , c are absorbance, intensity of incident light, intensity of the transmitted light, molar absorptivity (or molar extinction coefficient) of the sample, cell path-length in cm, and sample concentration in mole/lit respectively.

Table.2.1. Detection limits of some lanthanides (La, Ce, Pr, Nd and Sm) and some actinides (U and Th)

25 cm length reversed phase support				
Experimental conditions	Elements		Detection limits	
			(μg)	(ng)
0.01 M CSA + 0.1 M α -HIBA; pH:3; Flow rate: 2 mL/min;	Lanthanides	La	0.011	11
		Ce	0.013	13
		Pr	0.013	13
		Nd	0.014	14
		Sm	0.014	14
0.15 M α -HIBA; pH:3; Flow rate: 2 mL/min	Actinides	U	0.027	27
		Th	0.025	25

**Precision of the measurement: ± 1 to 2 %*

** Detection was carried out using post-column derivatisation method with arsenazo(III) at 655 nm.*

Due to the high sensitivity of this detector, tens of ng levels of analyte, e.g., lanthanide ions can be detected. The flow cells used for absorption detectors are designed to expose the maximum length of sample for the light to pass through, while keeping the volume as small as possible, to ensure that the resolution is not compromised. The cell has a “Z” shape to provide the maximum path length with a cell volume as low as 8 μL .

2.2 Post-column derivatisation method for detection

In the present study, post-column derivatisation technique was employed for the detection of lanthanides and actinides. In this technique, the effluent from the column was mixed with the colouring reagent, Arsenazo(III) (2,2'-(1,8-dihydroxy-3,6-disulfonaphthalene-2,7-bisazo)bis(benzene-arsenic acid)) after the column using a “T” connector and the complex was sent to a UV-Vis detector. The lanthanide (La-Lu) and actinide (U, Th, Am and Pu) complexes were detected at 655 nm. The rapid and efficient mixing of colour-producing reagent with eluent is essential and dead volume must be minimised for achieving better resolution and sensitivity. Colouring reagent, 4-(2-pyridylazo)-resorcinol (PAR) was also employed in the present work for detection of transition metal ions at 530 nm. The molar absorption coefficient of lanthanide-arsenazo complex, e.g., La-arsenazo and uranium-arsenazo complexes were found to be ~ 64,000 and 49, 000 $\text{lit}\cdot\text{mol}^{-1}\cdot\text{cm}^{-1}$ respectively under typical experimental conditions (0.01 M CSA + 0.1 M α -HIBA solution with pH: 3.5).

2.3 Preparation of standard solution of lanthanides, U, Th, Pu and Am

Lanthanide standards were prepared from their respective oxides by dissolving them in concentrated nitric acid medium, evaporating to near dryness, re-dissolving in 0.01 N HNO_3 and standardising with EDTA. In this standardisation procedure, initially, standard solutions of EDTA were prepared by dissolving solid di-sodium di-hydrogen ethylenediaminetetraacetic acid dihydrate with a few crystals of sodium hydroxide in deionised water. The EDTA solution was standardized by titrating with standard magnesium solution at pH 10 using ammonium chloride-ammonia ($\text{NH}_4\text{Cl-NH}_3$) buffer using Eriochrome Black T as the indicator. Aliquots of lanthanides solutions were standardised at a pH 6 with standard EDTA solution, using hexamethylene tetramine (HMTA) as buffer and methylthymol blue as indicator [141-142].

Uranium standards were prepared from U_3O_8 by heating at $600^{\circ}C$ for 6 hrs followed by dissolution in concentrated nitric acid medium. The uranium solution was evaporated to near dryness and re-dissolved in 1 N HNO_3 . Thorium standards were prepared by dissolving thorium nitrate in 1 N HNO_3 medium. The solutions of thorium and uranium were standardized by complexometric titration with diethylenetriamine pentaacetic acid (DTPA) [143] and gravimetry [144] (as U_3O_8) respectively. Generally, standard solution of lanthanides, U and Th in 0.01N HNO_3 medium were injected into HPLC system.

The plutonium solution was standardized by potentiometric titration. In this method, plutonium was oxidised to +6 state with an oxidising reagent, e.g., silver oxide in nitric acid medium and the excess oxidising reagent was destroyed by treatment with sulphamic acid. Subsequently, 0.1 M ferrous ammonium sulphate was added to convert plutonium from +6 to +3 state. Plutonium solution was titrated with standard potassium dichromate solution using calomel as reference electrode and platinum as working electrode.

Plutonium(IV) nitrate solution was reduced to Pu(III) using hydroxylamine hydrochloride. PuO_2^{+2} was prepared by the addition of AgO to solution of plutonium. Similarly, $NaNO_2$ was added to a solution of plutonium for the preparation of Pu(IV) sample.

Americium solution was standardised by counting method. In this method, Am stock solution was diluted with 1 M HNO_3 medium. The diluted americium solution was planchatted in stainless steel disk and its activity was counted in alpha scintillation detector. From the efficiency of the counter, activity of standard americium was calculated. Am solutions were also assayed by counting its 60 KeV gamma ray using NaI (Tl) detector.

Pu(III), Pu(IV), PuO₂⁺² and Am(III) in 0.01 N HNO₃ medium were injected into the HPLC system.

2.4 Calibration studies

For preparing calibration plots, lanthanide samples (La-Eu) over the concentration range of 2-50 ppm, U(2-150 ppm) and Pu(III) (4-25) (injected amount, 20 μL) were introduced into the HPLC system using dynamically modified (with ion-pairing reagent, CSA) 3 cm length support of 1.8 μm particle size and 10 cm length monolith support.

In the reversed phase chromatographic study, U (2-100 ppm), Pu(IV) (2-20 ppm) and Pu(III) (4-25 ppm) nitrate solutions were injected into the HPLC system for the calibration studies. Sodium nitrite was added to ensure plutonium in its Pu(IV) oxidation state. Pu(III) was prepared from Pu(IV) nitrate solutions by the addition of hydroxylamine hydrochloride. The correlation coefficients were found to be 0.999-0.996 for lanthanides and 0.999 and 0.997 for uranium and plutonium respectively.

2.5 Mobile phase preparation

Mobile phase solutions were prepared using Milli-Q water. In the dynamic ion-exchange chromatographic experiments, ion-pairing reagent, camphor-10-sulfonic acid (CSA) was mixed with complexing agent, e.g., α-HIBA and employed as the eluent. Appropriate amounts of CSA with α-HIBA were dissolved in water and the pH was adjusted with dilute ammonia. In reversed phase chromatographic experiments, mobile phase was prepared by dissolving appropriate amounts of complexing agent (e.g., α-HIBA) in HPLC grade water and its pH was adjusted with ammonia. The post-column reagent, Arsenazo(III) (Tokyo Kasei) was prepared in water (0.15 mM) and used as such

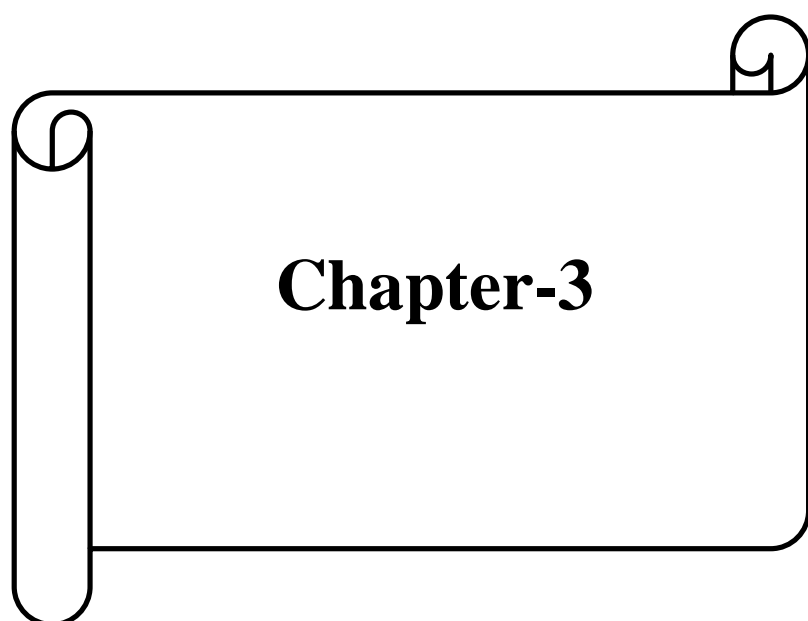
throughout the study. The mobile phase and post-column reagent solutions were degassed and filtered through 0.2 μm filter prior to use.

2.6 Preparation of “dynamically” coated columns

The reversed phase columns (3 cm length (1.8 μm), 5 cm length (1.8 μm), 25 cm length (5 μm), and 10 cm length monolith) were modified into a dynamic ion-exchange support using water soluble modifier, e.g., ion-pairing reagent, CSA. A mobile phase solution (CSA+ α -HIBA) was passed through the reverse phase support to establish a dynamic ion-exchange surface. About 25 mL of mobile phase was passed through 3/5 cm length columns to establish a dynamic ion-exchange surface. In the case of 25 cm length column, about 50 mL of mobile phase was passed prior to sample injection.

2.7 Preparation of “Permanently” coated columns

In the present study, permanently coated columns were prepared by passing a solution of an extractant, e.g., TOPO through a reversed phase supports (5 cm and 25 cm) at a typical flow rate of 0.2 mL/min. TOPO solutions were prepared in a methanol-water mixtures (typically, 75:25 v/v methanol to water). Higher methanol content was employed in some studies to ensure complete dissolution of TOPO. When the coating was completed, the column was washed with about 20 mL water. Appropriate mobile phase was employed for separation of sample molecules.



Chapter-3

Chapter-3

Rapid Separation of Lanthanides and Actinides on Small Particle Based Chromatographic Supports

3.1 Introduction

Advances and developments in the chemistry of lanthanide separation by liquid chromatographic techniques have been reviewed in literature [145-146, 84]. The procedures for isolation of lanthanides from dissolver solutions of nuclear reactor fuels for burn-up measurements were discussed [48-49, 147]. Lighter lanthanides (La, Ce, Pr, Nd, Sm and Eu) constitute about one fourth of the total fission products produced in nuclear fission of uranium or plutonium [38]. Thus accurate estimation of Nd or La in the dissolver solution can be used to determine number of fissions taken place in the spent nuclear reactor fuel [48-49, 147-148].

Separation of lanthanides in about 9 min using C₁₈ support with sodium octanesulfonate as the ion-pairing reagent and α -HIBA as the complexing reagent for elution was reported [48]. In these studies, a 15 cm length reversed phase column was employed with 0.01 M sodium octanesulfonate as modifier. The α -HIBA concentration was varied from 0.05 to 0.4 M in a gradient elution mode. In another study, a mixture of α -HIBA and sodium *n*-octanesulfonate was employed for the separation of individual lanthanides, the total separation time of lanthanides, U and Th was found to be 11 min [95]; lanthanides were mutually separated from each other in about 8 min. In one of the studies, mandelic acid was employed as the complexing reagent for elution with octanesulfonate as the ion-pairing reagent for the separation of lanthanides [94]; using a gradient delivery of mandelic acid, lanthanides were separated from each other in about 20 minutes. A

separation procedure for the isolation of individual lanthanides using camphor-10-sulfonic acid (CSA) as the ion-pairing reagent was reported [49, 148]. In all these studies, the separation of lanthanides using gradient elution was achieved in not less than 8 minutes using 15 or 25 cm length supports of 5 μm particle size.

The separation of lanthanides from uranium matrix, uranium from thorium etc in various studies related to nuclear fuel cycle, demands rapid and high-resolution separation. Reversed phase HPLC has become a powerful technique for separation of uranium and thorium [94, 103, 110]. Retention behaviour of uranium and thorium on polystyrene substrates modified with metal chelating reagents such as dipicolinic acid, calmagite and “PAR” was reported [113, 149]. In all these studies, retention of uranium and thorium was investigated using 5 μm particle sized supports.

3.1.1 Need for development of ultra-fast separations

The development of HPLC based methods for rapid separation of individual lanthanides and actinides is important to reduce the radiation exposure to the analyst during the course of determination of burn-up of a dissolver solution of nuclear reactor fuel; similarly, assay of lanthanides and actinides in various streams of nuclear fuel cycle e.g. high level liquid waste demands rapid separation procedures to minimize radiation exposure and also helps in minimization of secondary waste generation. The selection of appropriate column length with suitable particle size is an important factor for achieving rapid and high resolution separations. The best possible way to decrease plate height and analysis time is to decrease the particle size of the column packing material. The efficiency of a chromatographic column as a function of mobile phase flow velocity can be described by the van Deemter equation [2]; decreasing the particle size causes an improvement in separation efficiency per unit column length. Thus the major motivation in the present study

towards use of small particle size (1.8 micron support material) column is to enhance separation efficiency with faster analysis for the isolation of individual lanthanides as well as actinides from highly radioactive solutions for burn-up measurements on nuclear reactor fuels and that could enable reduction in the radiation exposure to the operator

However, the use of small particle size i.e. 1.8 micron results in a high back pressure and results in the need for systems to deliver solvents at high pressures, typically in the range of 500 bar with precise flow rates. Thus UPLC (ultra high pressure liquid chromatography) technique employing columns containing stationary phase materials of small particle size e.g. 1.8 μm necessitates use of high operating pressures, i.e., 400-1000 bar depending on the flow rate and column length. In this chapter, results on the use of small particle (1.8 μm) based reversed phase support for the development of rapid separation of lanthanides and actinides were discussed. Columns with 1.8 μm based supports were employed in the present work to obtain high column efficiencies for the development of rapid separation procedures by using the traditional HPLC pumping system itself, i.e. with a solvent delivery system that delivers mobile phase up to 500 bar. In these studies, efforts were made to investigate the retention behaviour of lanthanides under various experimental conditions on 1.8 μm columns with 3 cm as well as 5 cm length to effectively achieve the shorter separation time, leading to the development of rapid separation methods. The results obtained were compared with the traditionally employed 25 cm length column of 5 μm particle size. Based on the investigations with 1.8 μm particle sized 3 cm length support, a reversed phase HPLC method has also been developed for the rapid and accurate analysis of lanthanide elements in uranium matrix.

3.2 EXPERIMENTAL

In dynamic ion-exchange experiments, about 25 mL, 25 mL and 50 mL of mobile phase was passed through 3 cm, 5 cm and 25 cm length columns respectively prior to sample injection. Similarly, in reversed phase chromatographic separation of uranium and thorium, α -HIBA was employed as complexing agent and about 20 mL was passed through the 3 and 5 cm length columns, while 30 mL was passed through 25 cm length column for equilibration prior to sample injection. Linear calibration plots for lanthanides (1-25 ppm), U (2-200 ppm) and Th (2-50 ppm) were obtained in the chromatographic experiments.

3.3 RESULTS AND DISCUSSION

3.3.1 Lanthanide separations – gradient elution

In the present study, a 25 cm length reversed phase column with a 5 μ m particle size was initially employed for individual separation of lanthanides. A CSA solution of 0.01 M was employed as modifier. The concentration of HIBA was altered from 0.05 to 0.15 M (pH: 3.7). The lanthanides could be separated from each other in about 7.8 min, on par with some of the studies reported earlier (**Fig.3.1**).

To reduce the separation time further, 1.8 μ m particle size based reversed phase supports were investigated in the present work for the isolation of individual lanthanides. Various gradient profiles were employed by varying the concentrations of CSA (0.01, 0.02, and 0.025 M), α -HIBA and mobile phase pH (3.3-4). However, the concentration of CSA as well as pH was generally kept constant during the course of gradient run; only, α -HIBA concentration was varied (0.05 to 0.15 M) in a gradient mode to effect the separation. For the 5 cm column length and 1.8 μ m particle size support, under suitable experimental conditions (**Table.3.1**), a rapid separation of the individual lanthanides was achieved, the typical separation time being 4.9 min (**Fig.3.2**).

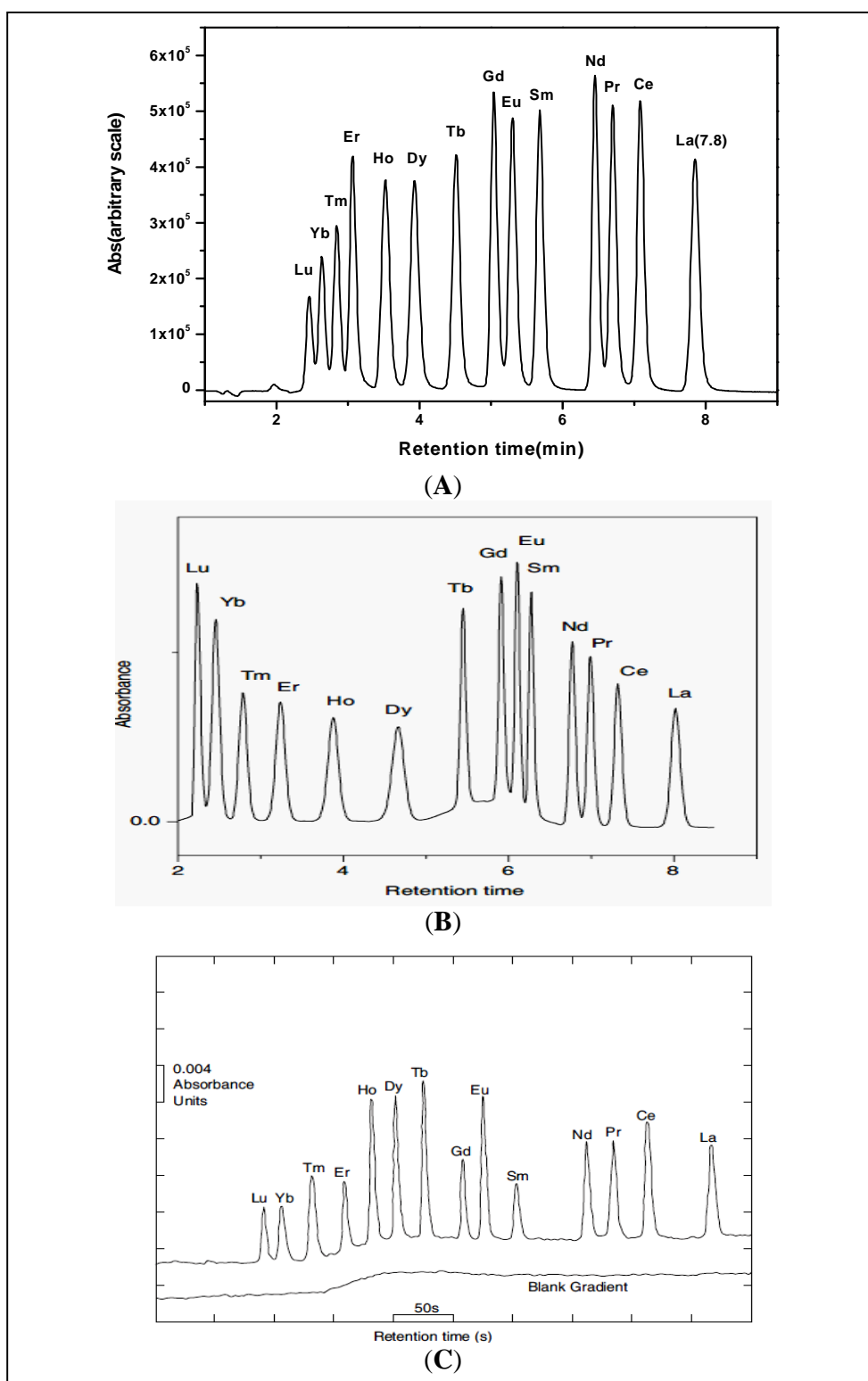


Fig.3.1. Separation of lanthanides using gradient elution. (A) Present work: Mobile phase: 0.01 M CSA; α -HIBA varied from 0.05 M to 0.15 M; pH: 3.7; Flow rate: 2 mL/min. Detection: PCR with arsenazo(III) at 655 nm; PCR flow rate: 1 mL/min. Sample:

lanthanides (20 ppm) in 0.01N HNO₃. **(B) Vasudeva Rao *et al*, 2005 work:** Column: Reverse phase C₁₈ (25 cm length with particle size of 5 μm); Mobile phase: 0.05 M CSA; α-HIBA varied from 0.07 M to 0.3 M; pH: 3.8; Flow rate: 2 mL/min. Detection: PCR with arsenazo(III) at 655 nm; PCR flow rate: 1.5 mL/min [147]. **(C) Cassidy *et al*, 1984 work:** Column: Supelco LC₁₈; Mobile phase: 0.01 M 1-octanesulfonate; α-HIBA varied from 0.05 M to 0.4 M; pH: 4.6; Flow rate: 2 mL/min. Detection: PCR with arsenazo(III) at 653 nm; PCR flow rate: 1.5 mL/min. Sample: lanthanides (10 ppm) [48].

Table.3.1 Gradient elution for separation of lanthanides- a comparison

Column type		Experimental conditions			Results
Length (cm)	Particle size (μm)	CSA (M)	α-HIBA (M)	pH	
25	5	0.01	0.05-0.15	3.7	a good separation of all 14 lanthanides; Separation time ~ 7.8 min.
5	1.8	0.01	0.05-0.1	3.7	a good separation of all 14 lanthanides; Separation time ~ 4.9 min.
3	1.8	0.0225	0.05-0.25	3.4	Rapid separation of all 14 lanthanides; Separation time ~ 3.6 min.
		0.01	0.05-0.15	3.7	Good separation of all 14 lanthanides; Separation time ~ 4.2 min.

The above studies indicated the advantage of reduction in the particle size in achieving faster separation. Further studies were continued with shorter column length, i.e., 3 cm length reversed phase support for the development of gradient elution method. CSA solutions of 0.01 to 0.025 M were employed in independent experiments. In all these experiments, α-HIBA concentration was varied from 0.05 to 0.25 M. The pH of the mobile phase was altered in the range, 3.5-3.8, though it was kept constant in a particular gradient run. Using a binary gradient, various gradient elution profiles were generated and employed for isolation of lanthanides under various mobile phase compositions. Under various

experimental conditions, about 200 gradients were generated and employed for the fast separation of lanthanides on 3 cm length reversed phase support. Some gradient profiles are listed in **Table.3.2**. In one of these studies, individual separation of lanthanides was achieved in about 3.6 min; the optimum conditions of CSA, α -HIBA and pH being 0.0225 M, 0.05 to 0.25 M and 3.4 respectively (**Fig.3.3**). These results are summarized in **Table.3.1 & Table.3.2**. Reduction of the particle size and column length resulted in a faster separation of individual lanthanides; in general rapid separations were achieved with 3 cm length 1.8 μ m support compared to the other supports. Thus both particle size and column length play a key role in the development of faster and efficient separation procedures.

The capacity factor for lanthanides decreases with increase in α -HIBA concentration and mobile phase pH and mobile phase flow rate. However, capacity factor of lanthanides increases with in concentration of modifier, CSA. Variation of capacity factor with concentrations of α -HIBA, CSA, mobile phase pH and mobile phase flow rate are shown in **Fig.3.4, Fig.3.5, Fig.3.6** and **Fig.3.7** respectively.

Table.3.2 Gradient programming for separation of lanthanides on 3 cm length reversed phase support

No	Gradients		Experimental conditions			Total separation time of lanthanides (min)
	Input time (min)	Solvent composition (A)	Solvent composition (A)	Solvent composition (B)	Flow rate (mL/min)	
1	0-1.9 2-3.6 3.7-8 8.1	100% 40% 0% 100%	0.02 M CSA + 0.05 M α -HIBA; pH: 3.5	0.02 M CSA + 0.15 M α -HIBA; pH: 3.5	1	A good separation of all 14 lanthanides; separation time~ 8.62 min

2	0-1 1.3 1.4 1.7 2.4 2.6 2.8 3 3.2 3.3 3.5-7.0 7.1	100% 95% 90% 75% 70% 60% 40% 30% 20% 10% 0% 100%	0.02 M CSA + 0.05 M α -HIBA; pH: 3.5	0.02 M CSA + 0.15 M α -HIBA; pH: 3.5	1	A good separation of all 14 lanthanides; separation time ~ 6.38 min
3	0-1 1.1-2.2 2.3-3.1 3.2-4.2 4.3-5.5 5.6	100% 50% 30% 20% 0% 100%	0.02 M CSA + 0.05 M α -HIBA; pH: 3.5	0.02 M CSA + 0.2 M α -HIBA; pH: 3.5	1	A good separation of all lanthanides; separation time ~ 5.01 min
4	0-0.5 0.6-1.3 1.4-2.5 2.6-3.2 3.3	100% 65% 35% 0% 100%	0.02 M CSA + 0.05 M α -HIBA; pH: 3.5	0.02 M CSA + 0.2 M α -HIBA; pH: 3.5	2	A good separation of all lanthanides; separation time ~ 5.90 min
5	0-1.4 1.5-2.9 3-4.8 4.9-6 6.1	100% 70% 25% 0% 100%	0.02 M CSA + 0.05 M α -HIBA; pH: 3.5	0.02 M CSA + 0.2 M α -HIBA; pH: 3.5	2	A good separation of all lanthanides; separation time ~ 5.80 min
6	0-0.5 0.6-1.4 1.5-2.5 2.6-3.2 3.5	100% 65% 35% 0% 100%	0.0225 M CSA + 0.05 M α - HIBA; pH: 3.5	0.0225 M CSA + 0.2 M α -HIBA; pH: 3.5	2	A good separation of all lanthanides; separation time ~ 3.77 min
7	0-0.5 0.6-1.0 1.1-1.6 1.7-2.6	90% 75% 70% 50%	0.0225 M CSA + 0.05 M α -HIBA;	0.025 M CSA + 0.2 M α -HIBA; pH: 3.5	2	A good separation of all lanthanides; separation time

	2.7-3.3 3.4	0% 100%	pH: 3.5			~ 3.83 min
8	0-0.5 0.6-1.0 1.1-1.6 1.7-2.3 2.4-3.4 3.5	95% 75% 70% 45% 10% 100%	0.0225 M CSA + 0.05 M α -HIBA; pH: 3.4	0.025 M CSA + 0.2 M α -HIBA; pH: 3.4	2	A good separation of all lanthanides; separation time ~ 3.63 min

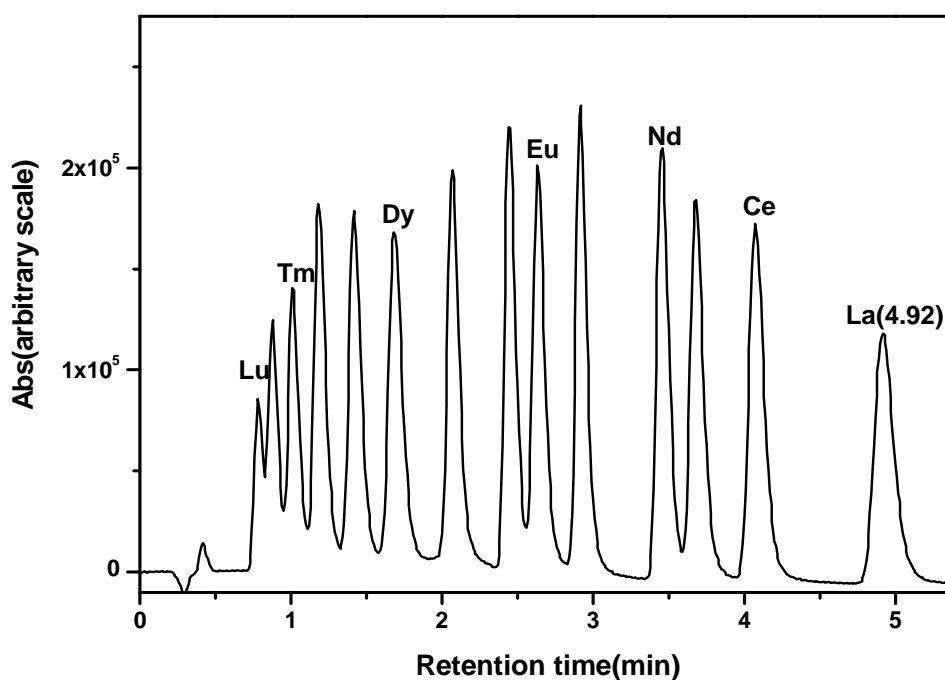


Fig.3.2. Separation of lanthanides on a 1.8 μm particle size of 5 cm length column using gradient elution. Mobile phase: 0.01 M CSA; α -HIBA varied from 0.05 to 0.1 M; pH: 3.7; Flow rate: 2 mL/min; PCR flow rate: 1 mL/min; Detection: 655 nm; Sample: lanthanides (~ 5 ppm) in 0.001 N HNO₃

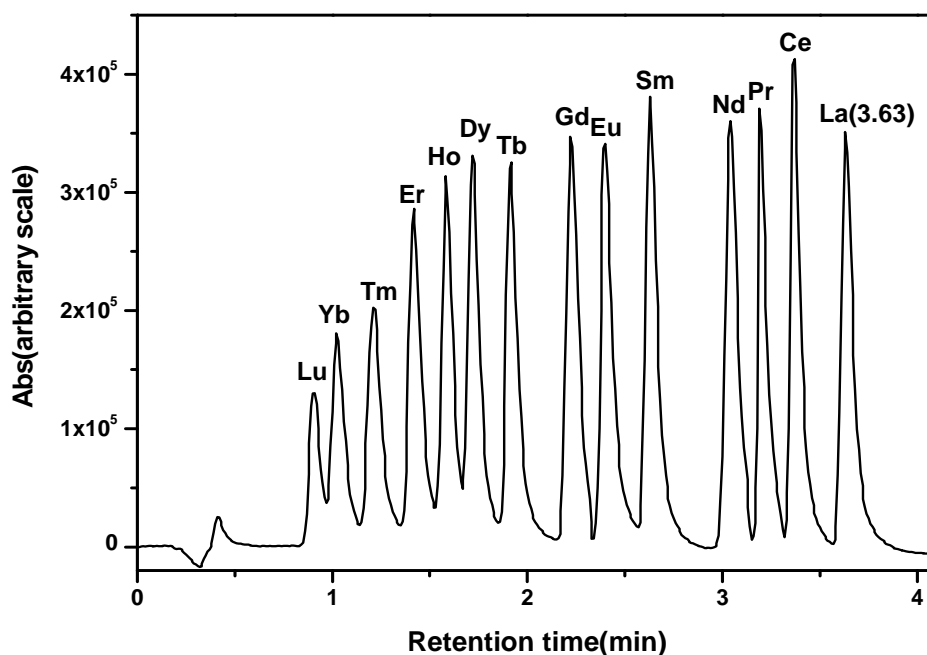


Fig.3.3. Separation of lanthanides on a 1.8 μm particle size of 3 cm length column using gradient elution. Mobile phase: 0.0225 M CSA; α -HIBA varied from 0.05 to 0.25 M; pH: 3.4; Flow rate: 2 mL/min; PCR flow rate: 1 mL/min; Detection 655 nm; Sample: lanthanides (10 ppm) in 0.001 N HNO₃.

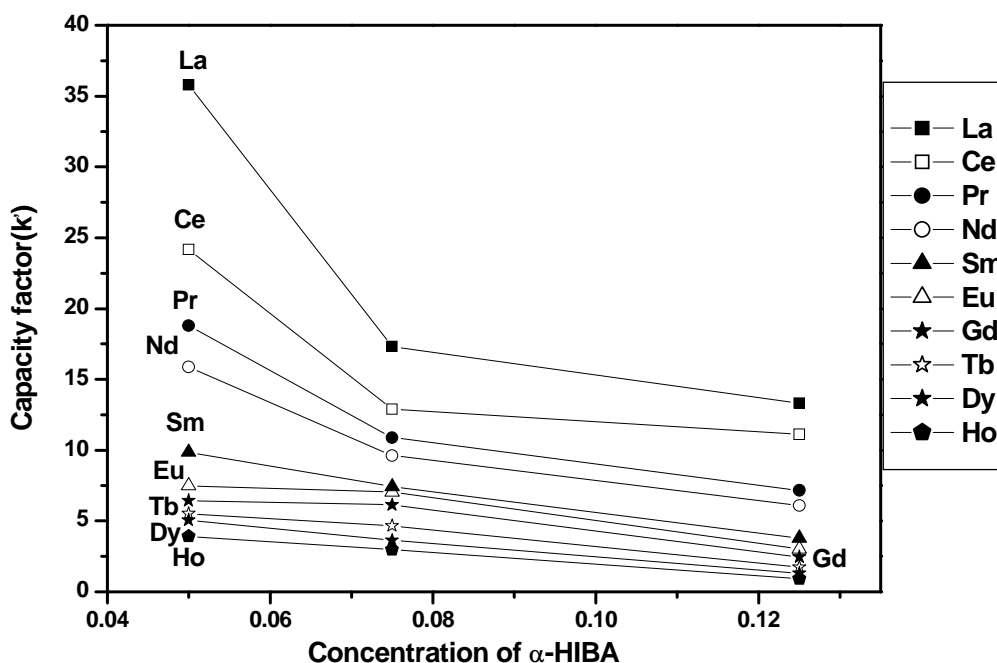


Fig.3.4. Variation of capacity factor of some lanthanides as a function of α -HIBA concentration on 1.8 μm based support. Column: 3 cm length (1.8 μm) column; Mobile phase: 0.01 M CSA + α -HIBA; pH: 3.5; Flow rate: 2 mL/min; PCR flow rate: 1 mL/min; Detection 655 nm; Sample: lanthanides (10 ppm) in 0.001 N HNO₃.

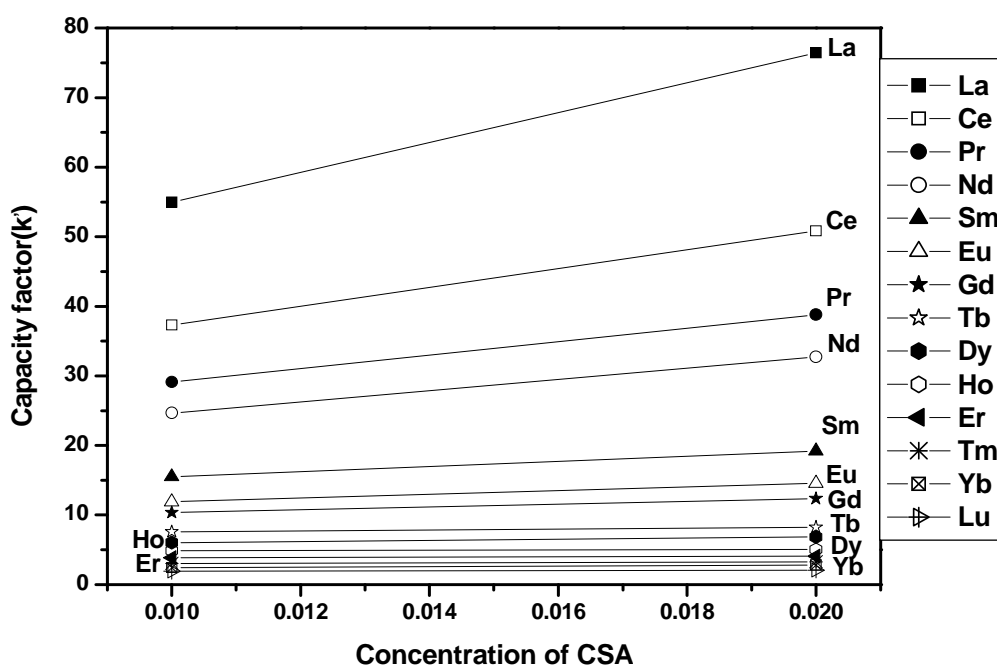


Fig.3.5. Variation of capacity factor of some lanthanides as a function of CSA concentration on 1.8 μm based support. Column: 3 cm length (1.8 μm) column; Mobile phase: CSA + 0.05 α -HIBA; pH: 3.5; Flow rate: 0.5 mL/min; PCR flow rate: 1 mL/min; Detection 655 nm; Sample: lanthanides (10 ppm) in 0.001 N HNO_3 .

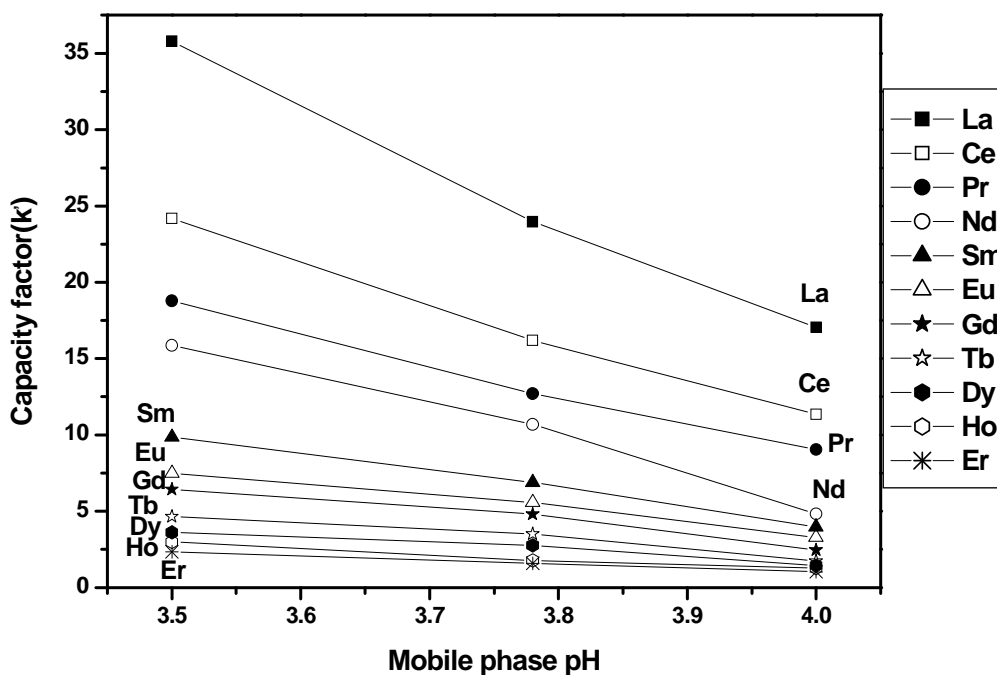


Fig.3.6. Variation of capacity factor of some lanthanides as a function of mobile phase pH on 1.8 μm based support. Column: 3 cm length (1.8 μm) column; Mobile phase: 0.01 M CSA + 0.05 M α -HIBA; pH: 3.5; Flow rate: 2 mL/min; PCR flow rate: 1 mL/min; Detection 655 nm; Sample: lanthanides (10 ppm) in 0.001 N HNO_3 .

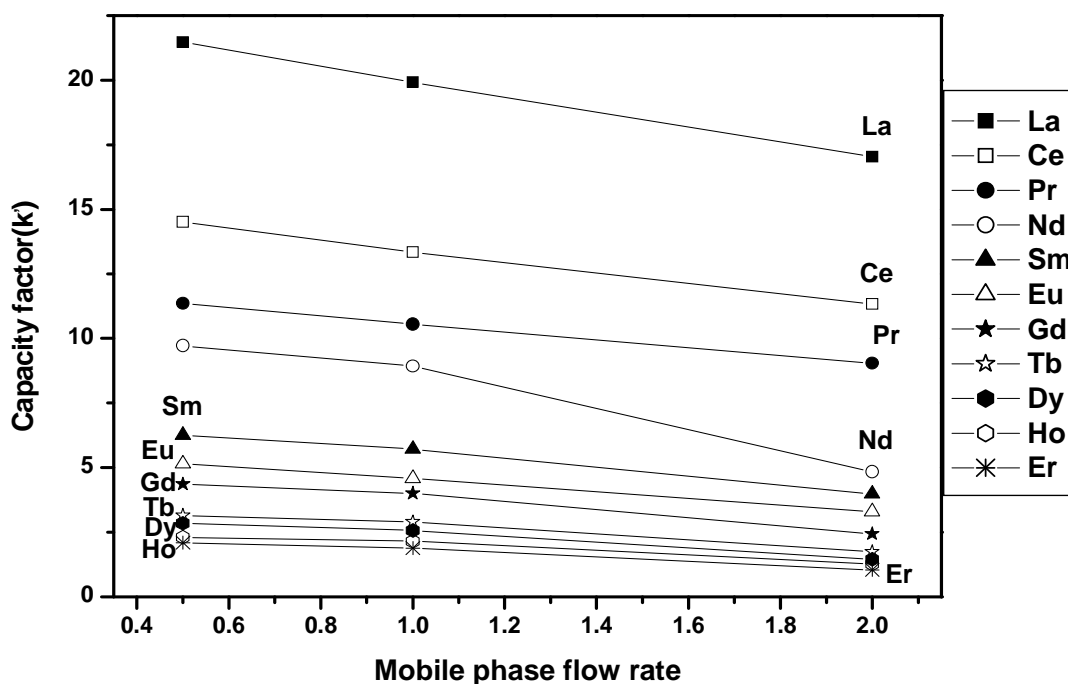


Fig.3.7. Variation of capacity factor of some lanthanides as a function of mobile phase flow rate on 1.8 μm based support. Column: 3 cm length (1.8 μm); Mobile phase: 0.01CSA + 0.05 α -HIBA; pH: 4; PCR flow rate: 1 mL/min; Detection 655 nm; Sample: lanthanides (10 ppm) in 0.001 N HNO_3 .

The decrease in solute retention with increase in mobile phase pH or α -HIBA concentration is attributed to the better complexing ability of α -HIBA with lanthanides. The increase in solute retention with increase in CSA concentration was due to enhanced retention of lanthanides as there are more $\text{RSO}_3^- \text{H}^+$ moieties sorbed on to the reversed phase support. Separation factor (α) of adjacent lanthanides was also calculated under various experimental conditions and the results are shown in **Table.3.3**.

Table.3.3 Separation factors for adjacent lanthanides on 3 cm length (1.8 μm) column under various experimental conditions

Lanthanides	Separation factor (α)			
	0.05 M α -HIBA +0.01 M CSA, pH :3.5, Flow rate : 2 mL/min	0.05 M α -HIBA +0.02 M CSA, pH :3.5, Flow rate : 2 mL/min	0.05 M α -HIBA +0.01 M CSA, pH :3.5, Flow rate : 0.5 mL/min	0.075 M α - HIBA +0.01 M CSA, pH :4, Flow rate : 0.5 mL/min
La:Ce	1.48	1.50	1.47	1.48
Ce:Pr	1.28	1.31	1.28	1.28
Pr:Nd	1.18	1.18	1.19	1.17
Nd:Sm	1.61	1.70	1.59	1.55
Sm:Eu	1.21	1.22	1.20	1.21
Eu:Gd	1.16	1.18	1.15	1.18
Gd:Tb	1.38	1.40	1.36	1.38
Tb:Dy	1.28	1.30	1.26	1.27
Dy:Ho	1.21	1.25	1.24	1.23
Ho:Er	1.27	1.24	1.23	1.25
Er:Tm	1.28	1.23	1.26	1.24
Tm:Yb	1.22	1.28	1.23	1.26
Yb-Lu	1.20	1.16	1.18	1.15

3.3.2. Lanthanide separations – isocratic elution

The results on the isocratic elution of lanthanides from different supports are compared in **Table 3.4**. The retention time and capacity factor obtained with 3 cm length (1.8 μm) support was found to be less than the one obtained with 5 cm (1.8 μm) and 25 cm (5 μm) length columns under similar experimental conditions, with more or less similar resolution between adjacent lanthanides. The results on isocratic elution obtained with 3 and 5 cm length supports are also shown in **Fig.3.8** and **Fig.3.9** respectively. The column efficiency of small particle (1.8 μm) supports in terms of number of theoretical plates for separation of lanthanides was computed and the results are compared with the efficiency of the 5 μm based reversed phase support (**Table.3.5**).

Table.3.4 Isocratic elution for separation of lanthanides – a comparison

Column type		Experimental conditions			Results
Length (cm)	Particle size (µm)	CSA (M)	α-HIBA (M)	pH	
25	5	0.01	0.1	3.28	All lanthanides separated; Separation time ~ 51 min.
		0.01	0.1	3.55	All lanthanides well separated in ~ 19min.
5	1.8	0.01	0.05	3.5	All lanthanides well separated ~ 45min.
		0.01	0.05	3.78	All lanthanides well separated in ~ 16min.
		0.01	0.1	3.5	La-Tb well separated in ~ 8min.
		0.01	0.1	3.75	La separated from other 13 lanthanides in ~ 3.5min
3	1.8	0.01	0.05	3.5	All lanthanides well separated in ~ 12min.
		0.01	0.05	3.78	La-Ho were well resolved in 6min. Er-Lu were not base-line separated.
		0.02	0.1	3.8	La-Gd could be well resolved in ~ 2.5min; La could be very well separated from Ce and other La fission products.

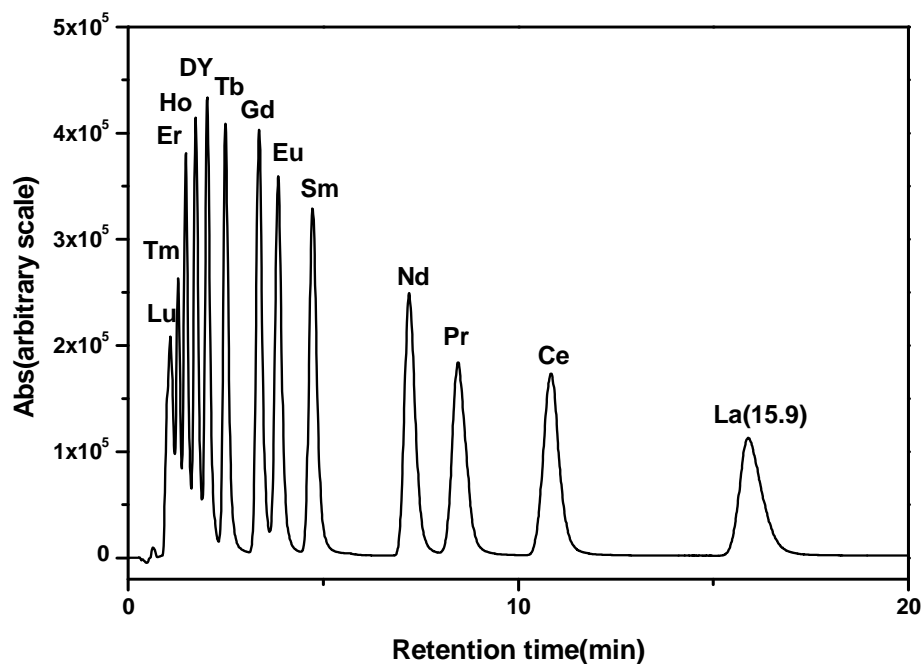


Fig.3.8. Separation of lanthanides by isocratic elution from 1.8 μm , 5 cm length reversed phase column. Mobile phase: 0.05 M α -HIBA + 0.01 M CSA; pH: 3.78; Flow rate: 1.5 mL/min; PCR flow rate: 1 mL/min; Detection: 655 nm; Sample: Lanthanides (20 ppm) in 0.001 N HNO_3 .

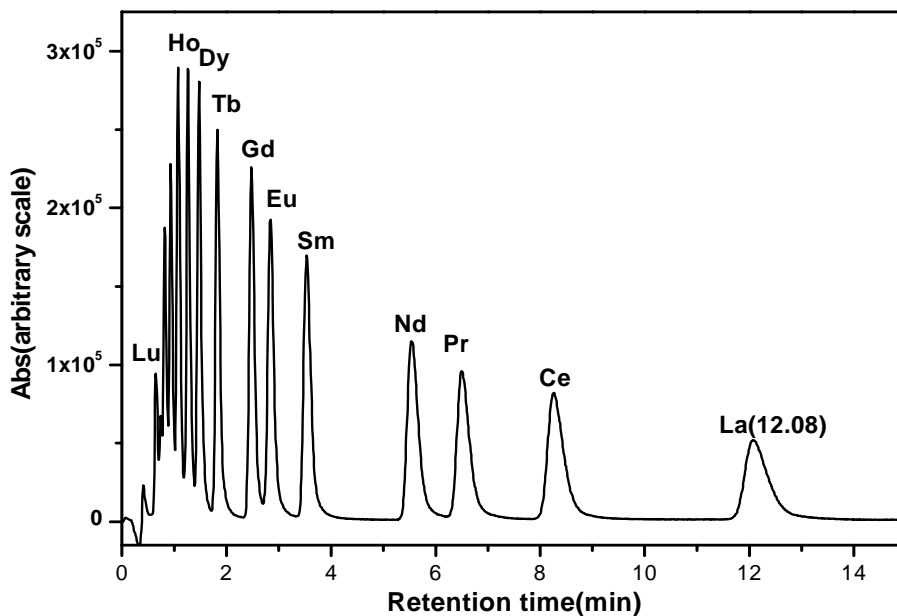


Fig.3.9. Separation of lanthanides by isocratic elution from 1.8 μm , 3 cm length reversed phase column. Mobile phase: 0.01 M CSA + 0.05 M α -HIBA; pH: 3.5; Flow rate: 2 mL/min; PCR flow rate: 1 mL/min; Detection: 655 nm; Sample: lanthanides (20 ppm) in 0.001 N HNO_3 .

Table.3.5 Column efficiency of lanthanides-a comparison

Columns with various particle size	Experimental conditions	Number of theoretical plates (plates per meter)				
		La	Ce	Pr	Nd	Sm
3 cm length (1.8 μm)	0.05 M α -HIBA + 0.01 M CSA; pH: 3.50; Flow rate: 2 mL/min	94512	96286	102517	86516	86873
5 cm length (1.8 μm)	0.05 M α -HIBA + 0.01 M CSA; pH: 3.78; Flow rate: 1.5 mL/min	70680	67702	65598	65680	62362
25 cm length (5 μm)	0.1 M α -HIBA + 0.015 M CSA; pH: 2.90; Flow rate: 3 mL/min	37854	36480	36736	33642	29607

Interesting consequences of these studies are the development of an isocratic elution procedure for the separation of lighter lanthanides (La-Gd). They could be resolved from each other in about 2.55 min using 1.8 μm support (**Fig.3.10**). Lanthanum could be very well separated from cerium and other lanthanides using a mobile phase consisting of 0.02 M CSA and 0.1 M α -HIBA with pH adjusted to 3.8. Since the assay of lanthanum is essential in the experiments involving burn-up measurements of nuclear reactor fuels, where it is employed as the fission product monitor, these experimental conditions can be employed for its determination. The results on the separation of lanthanide fission products from dissolver solution of fast reactor fuel are discussed in Chapter 5. Detection limits (3sigma) for lanthanides were found to be ~ 10-20 ng in these experiments.

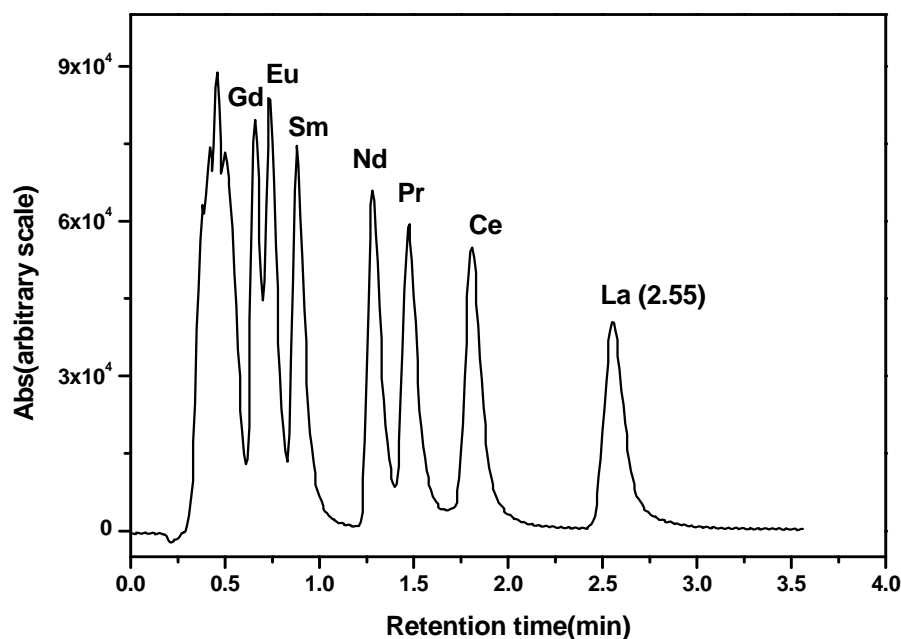


Fig.3.10. Separation of lanthanum from other lanthanides on 1.8 μm , 3 cm length reversed phase column in about 2.55 min. Mobile phase: 0.02 M CSA + 0.1 M α -HIBA; pH: 3.8; Flow rate: 2 mL/min; PCR flow rate: 1 mL/min; Detection: 655 nm; Sample: lanthanides (20 ppm) in 0.001 N HNO_3 .

3.3.3. Retention behaviour of uranium and thorium

3.3.3.1. Retention behaviour without modifier

The results on the retention behavior of uranium and thorium on a 3 cm length column of 1.8 μm particle size are shown in **Fig.3.11** and **Fig.3.12** with 0.1 M and 0.15 M α -HIBA as a function of pH. The capacity factors for both uranium and thorium decreases with increase in α -HIBA concentration, but increase with increase in mobile phase pH. Speciation of uranium and thorium at 0.05 M and 0.15 M α -HIBA were computed from stability constant data and results are shown in **Fig.3.13** and **Fig.3.14**. The complexation of uranyl ion by α -HIBA can result in the formation of species, e.g., $[\text{UO}_2(\text{IBA})]^+$, $[\text{UO}_2(\text{IBA})_2]$ and $[\text{UO}_2(\text{IBA})_3]^-$. Similarly, Th(IV) with α -HIBA forms species such as $\text{Th}(\text{IBA})^{+3}$, $\text{Th}(\text{IBA})_2^{+2}$, $\text{Th}(\text{IBA})_3^+$, and $\text{Th}(\text{IBA})_4$. The fraction of each species is

dependent on pH and α -HIBA concentration [103, 106]. Higher retention for uranyl ion at pH: 4 is due to the species, $[\text{UO}_2(\text{IBA})_3]^-$, which has 3 HIBA moieties and hence results in strong hydrophobic interaction with C_{18} support through induced dipole induced dipole interaction. The species, $[\text{UO}_2(\text{IBA})]^+$ has the lowest retention on the reversed phase support. The lower retention of Th(IV) compared to U(VI) is due to the possible formation of anionic species e.g. $[\text{Th}(\text{IBA})_4(\text{OH})_2]^{2-}$, which is expected to have a lower retention on a hydrophobic support. Thorium which is in +4 oxidation state is prone to hydrolysis at $\text{pH} > 3$. Similar separation studies were performed on 5 cm length reversed phase support of $1.8 \mu\text{m}$ particle size with 0.1 M, 0.15 M α -HIBA as a function of pH and results are shown in Fig.3.15, and Fig.3.16.

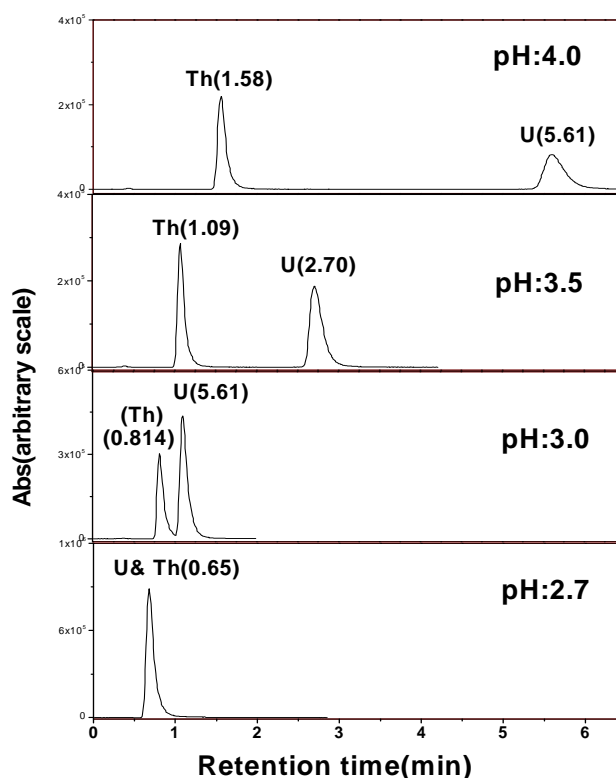


Fig.3.11. Retention behaviour of U and Th on $1.8 \mu\text{m}$, 3 cm length reversed phase column with 0.1 M α -HIBA as a function of pH. Mobile phase: 0.1 M α -HIBA; Flow rate: 2 mL/min; PCR flow rate: 1 mL/min; Detection: 655 nm; Sample: U (33 ppm), Th (25 ppm) in 0.01 N HNO_3 .

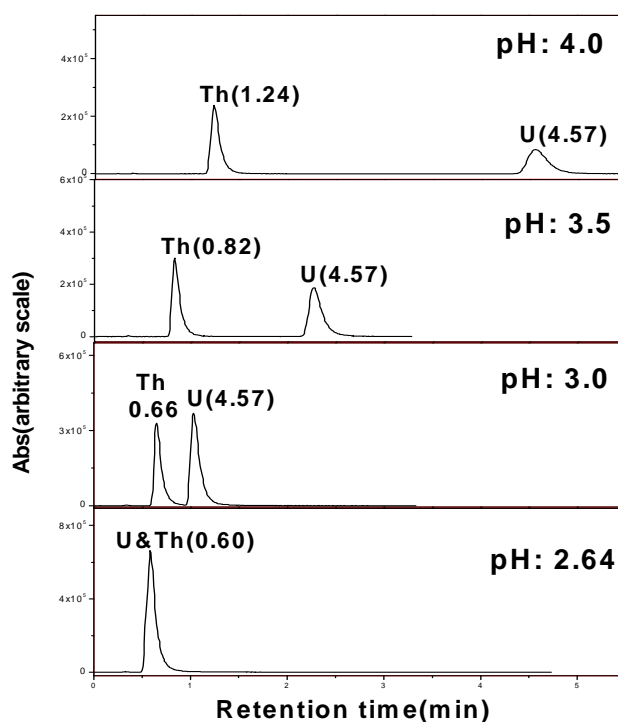


Fig.3.12. Retention behaviour of U and Th on 1.8 μm , 3 cm length reversed phase column with 0.15 M α -HIBA as a function of pH. Mobile phase: 0.15 M α -HIBA; Flow rate: 2 mL/min; PCR flow rate: 1 mL/min; Detection: 655 nm; Sample: U (33 ppm), Th (25 ppm) in 0.01 N HNO_3 .

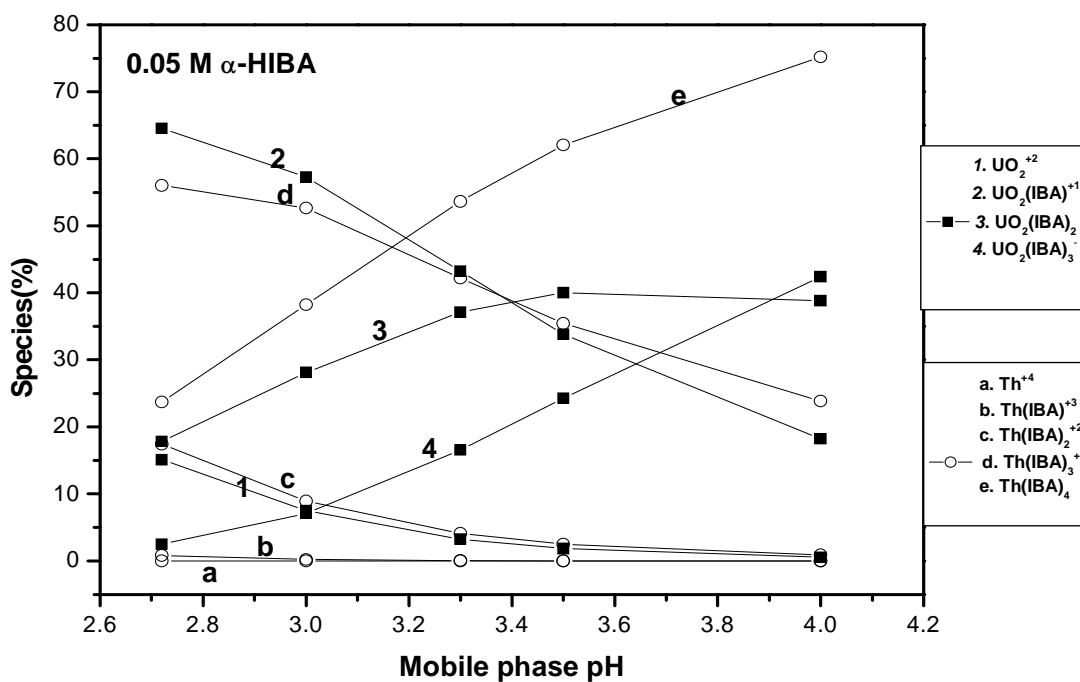


Fig.3.13. Speciation of (a) uranium-HIBA and (b) thorium-HIBA complexes as a function of mobile phase pH. Mobile phase: 0.05 M α -HIBA

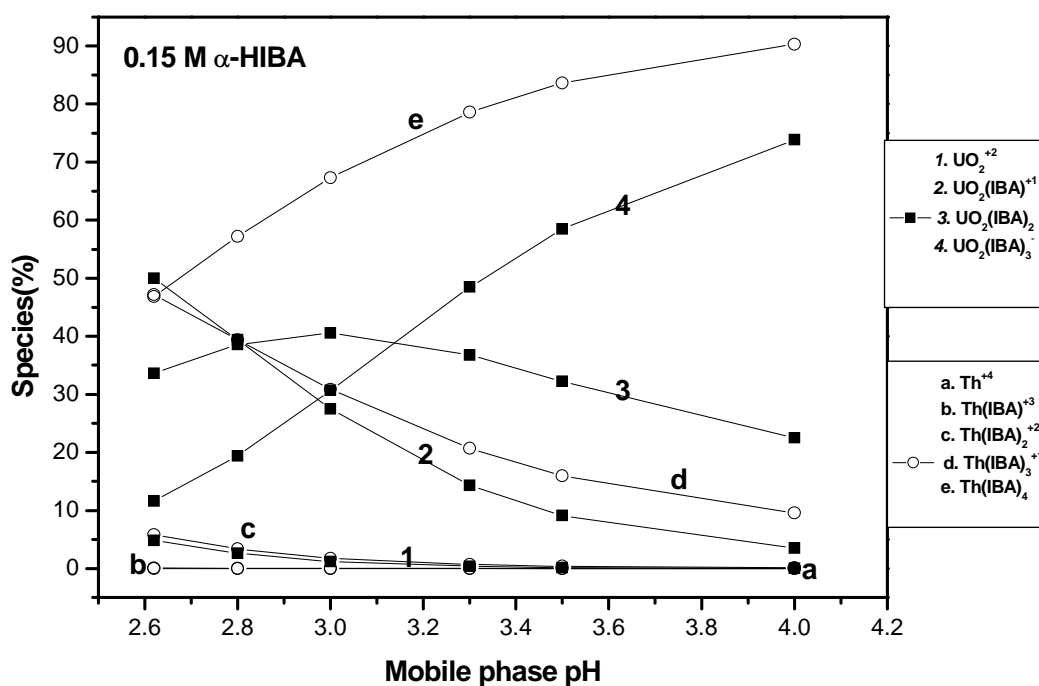


Fig.3.14. Speciation of (a) uranium-HIBA and (b) thorium-HIBA complexes as a function of mobile phase pH. Mobile phase: 0.15 M α -HIBA

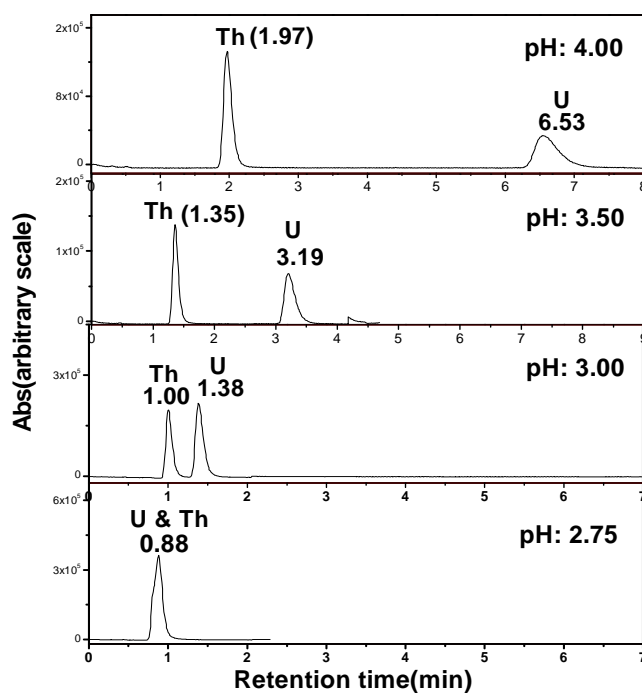


Fig.3.15. Retention behaviour of U and Th on 1.8 μm , 5 cm length reversed phase column with 0.1 M α -HIBA as function of pH. Mobile phase: 0.1 M α -HIBA; Flow rate: 2 mL/min; PCR flow rate: 1 mL/min; Detection: 655 nm; Sample: U (33 ppm), Th (25 ppm) in 0.01N HNO_3 .

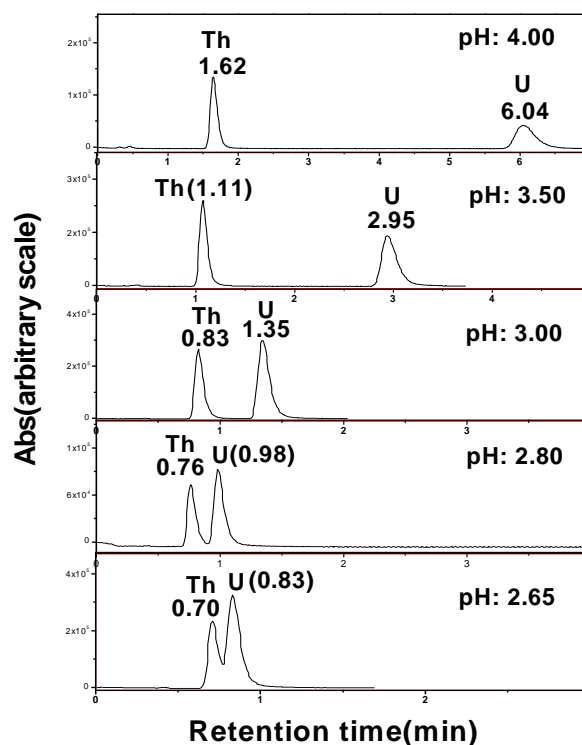


Fig.3.16. Retention behaviour of U and Th on 1.8 μm , 5 cm length reversed phase column with 0.15 M α -HIBA as a function of pH. Mobile phase: 0.15 M α -HIBA; Flow rate: 2 mL/min; PCR flow rate: 1 mL/min; Detection: 655 nm; Sample: U (33 ppm), Th (25 ppm) in 0.01N HNO_3 .

Lanthanides as a group can be isolated from uranium and thorium in a minute, enabling the development of a rapid separation procedure for determination of these elements in samples such as lanthanides in uranium matrix, monazite sand etc. However, under these conditions, all 14 lanthanides elute together. A typical study involving isolation of Nd from U and Th is shown in **Fig. 3.17**.

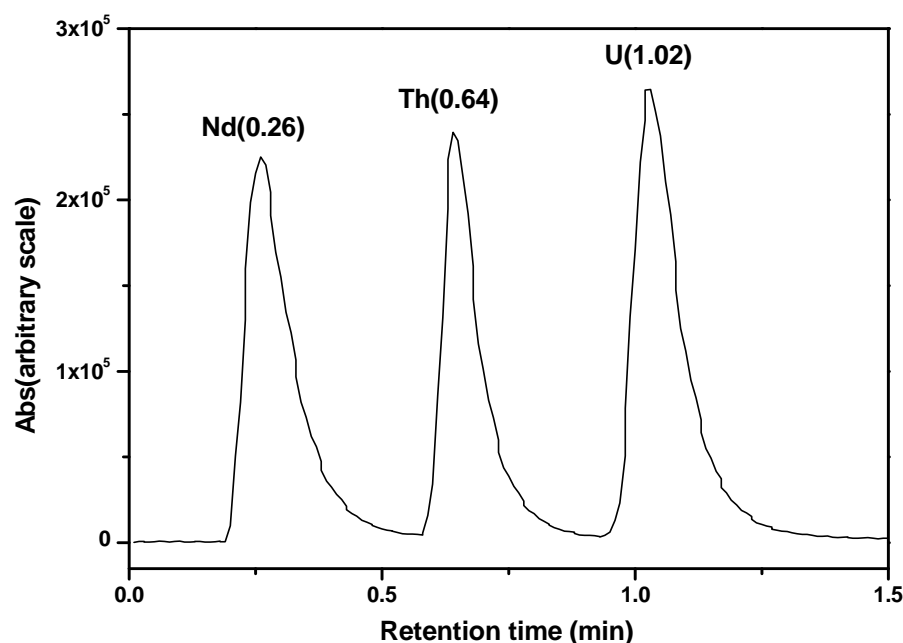


Fig.3.17. Retention behaviour of Nd, Th and U on 1.8 μm , 3 cm length reversed phase column at pH 3. Mobile phase: 0.15 M α -HIBA; Flow rate: 2 mL/min; PCR flow rate: 1 mL/min; Detection: 655 nm; Sample: U (33 ppm), Th (25 ppm) and Nd (25 ppm) in 0.01N HNO_3 .

The separation factors for U/Th obtained using 3, 5 and 25 cm length columns are shown in **Fig.3.18**. Separation factor (α) is the ratio of capacity factor of U to Th; “ α ” is obtained from k'_U / k'_{Th} . Capacity factor of uranium is obtained from following expression: $k'_U = (t_r - t_0) / t_0$, where k'_U is capacity factor for uranium, t_r is retention time of uranium; t_0 is time taken by a “non-retained solute. Similarly, k' of thorium was measured. The highest retention for uranium and thorium was observed with the of 25 cm length column. The 25 cm length column relatively offers more number of hydrophobic sites for interactions compared to the 3 and 5 cm length supports. However, the separation factors for U/Th obtained from these columns are found to be more or less similar. A marginal increase in separation factor was observed with 3 cm length column, when a solution of α -HIBA with pH: 4 was employed. The number of active sites of the reversed phase support increases

with increase of column length. Hence, the relative retention of both U and Th increase with column length and hence similar separation factors are obtained in all these cases.

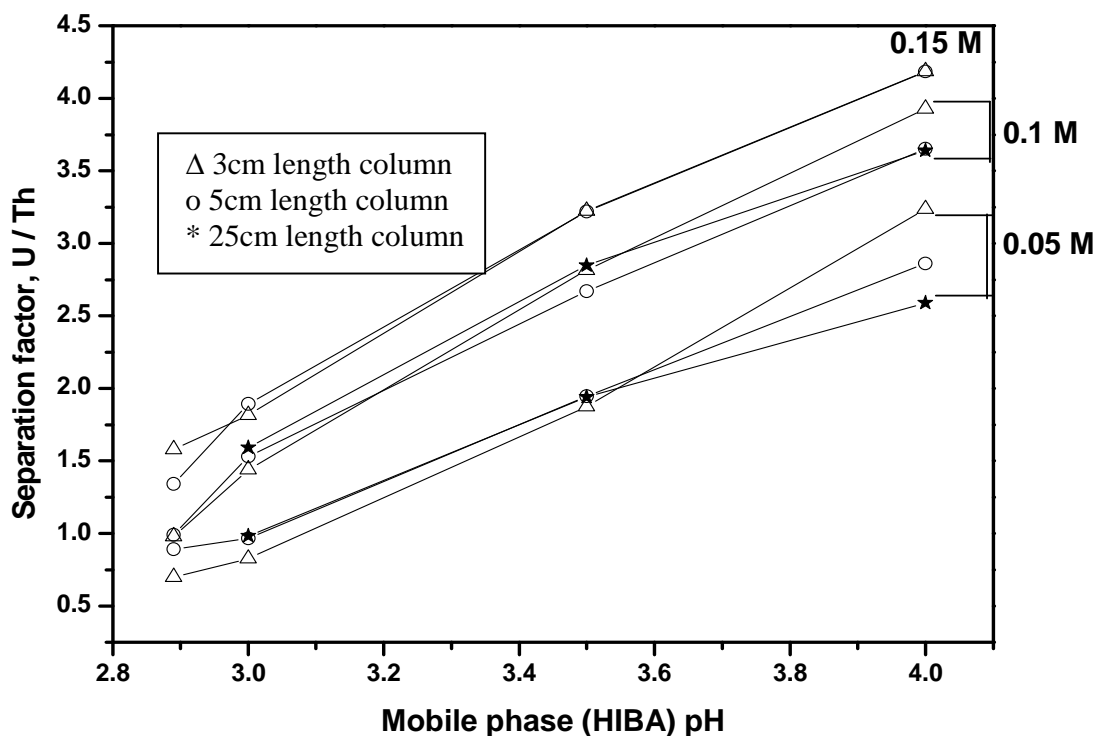


Fig.3.18. Separation factor of U/Th. Separation factors as a function of mobile phase (α -HIBA) pH and its concentration for 3 (1.8 μ m), 5 (1.8 μ m) and 25 cm (5 μ m) length reversed phase columns.

A good reduction in separation time was achieved with 3 cm length support compared to 5 and 25 cm length columns without compromising the separation factor for U/Th and these experimental conditions are crucial for designing ultra-fast separation procedures. For e.g. when U and Th are present in comparable quantities, an excellent base line separation is obtained in one minute with 3 cm length support and these conditions can be used for analyzing solutions of uranium and thorium in samples of nuclear fuel cycle. However, analysis of uranium in thorium matrix can be better carried out under the experimental conditions, 0.15 M α -HIBA at pH: 4, because under these conditions, the

separation period is long enough to enable the complete elution of matrix thorium followed by the elution of uranium.

3.3.3.2 Separation of U from Th using dynamic ion-exchange technique

Fig.3.19 and **Fig.3.20** shows the separation of uranium from thorium using 1.8 μm reversed phase supports of 3 and 5 cm length respectively in the presence of camphor-10-sulfonic acid (CSA) as modifier; a good base-line separation was achieved in these studies. Interesting separation behaviour was observed when α -HIBA concentration was reduced to 0.05 M, where uranium eluted ahead of thorium (**Fig.3.20b**), contrary to the earlier observation. The retention for both uranium and thorium decreases with increase in mobile phase pH. The influence of mobile phase composition on the retention behaviour of U and Th is shown in **Fig.3.21**. The retention for uranium decreases with increase in α -HIBA concentration and mobile phase pH, as observed in an ion-exchange mechanism. However, a very marginal increase in retention was observed with 0.1 and 0.15 M α -HIBA solutions of pH above 3.5. The marginal change is possibly due to uranium sorption by hydrophobic interaction, i.e., van der waals interaction on a reversed phase support as the CSA concentration of only 0.01 M was employed in these studies. Thus beside an ion-exchange mechanism, a hydrophobic interaction can also play a role in enhancing the retention of uranium. Retention for Th(IV) was higher than that of uranium (UO_2^{+2}) because of its charge and hence strong interaction with CSA leading to higher retention. Th(IV) was not eluted from 0.05 as well as 0.1 M α -HIBA solutions when the mobile phase pH was less than 3. The retention for thorium decreases with increase in α -HIBA concentration; the reduction in Th retention became significant when the mobile phase pH was raised above 3 because of the strong complexation of Th with α -HIBA. Under these conditions, a good fraction of α -HIBA dissociates to form stronger complexes with Th(IV). The reversed phase

HPLC technique also showed promising features for the assay of plutonium in its various oxidation states and these results are discussed in Chapter 6.

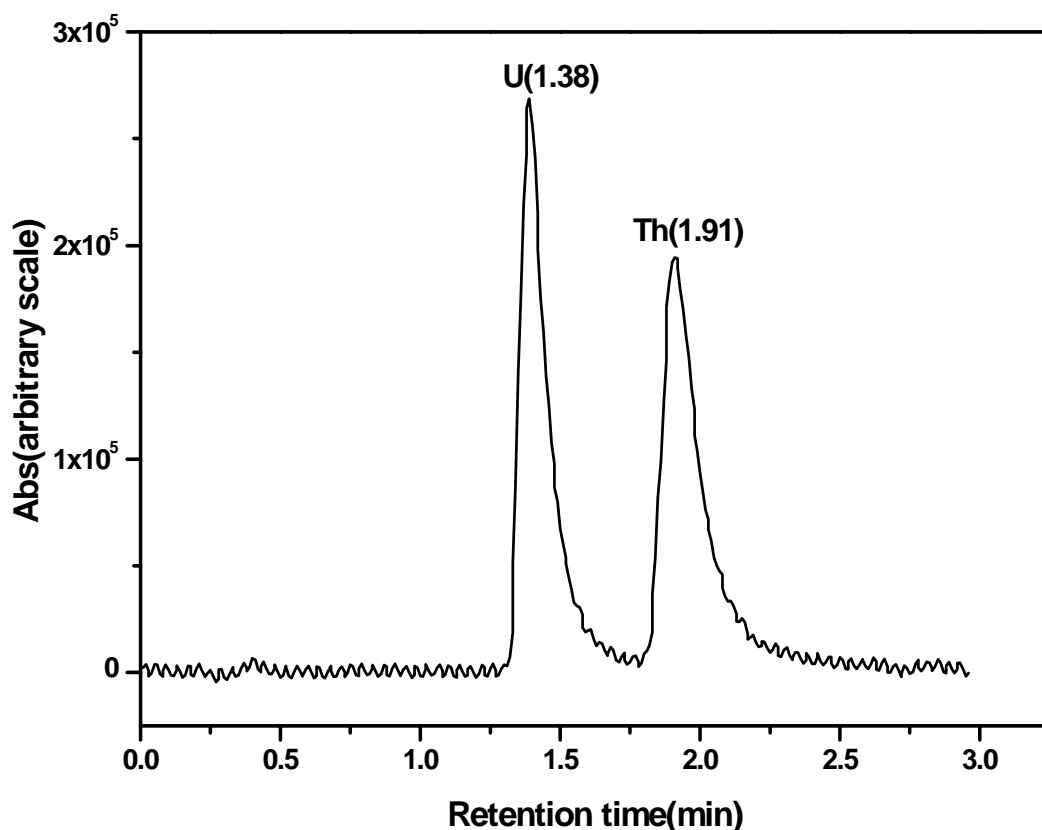


Fig.3.19. Separation of U and Th on 1.8 μm , 3 cm length support using dynamic ion-exchange chromatography.

Column: 1.8 μm , 3 cm length reversed phase support; Mobile phase: 0.05 M α -HIBA + 0.01 M CSA; pH: 3.64; Flow rate: 2 mL/min; PCR flow rate: 1 mL/min; Detection: 655 nm; Sample: U (33 ppm) and Th (25 ppm) in 0.01 N HNO₃.

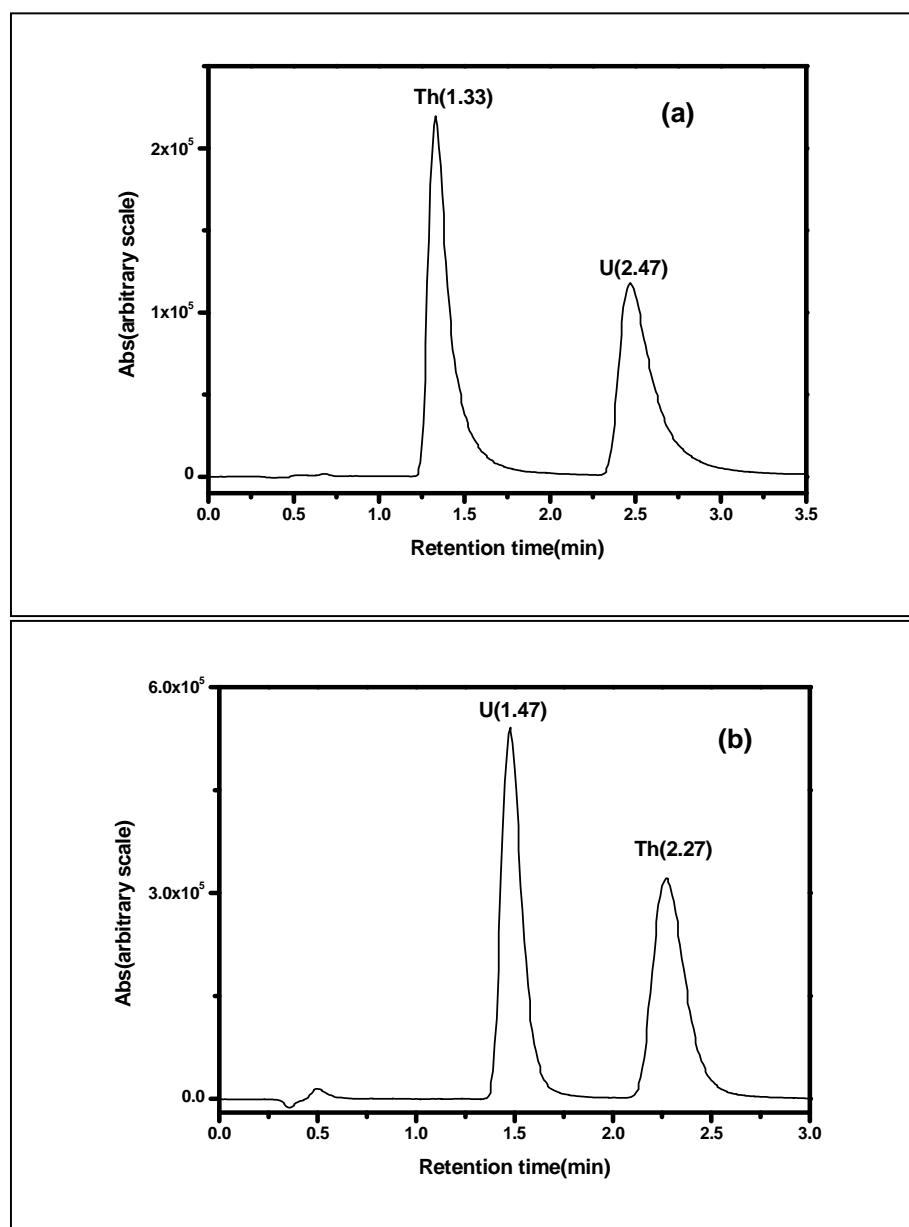


Fig.3.20. Separation of U from Th on a 1.8 μm , 5 cm length reversed phase column using dynamic ion-exchange chromatography. Mobile phase: (a) 0.1 M α -HIBA+0.01 M CSA, pH: 3.75; (b) 0.05 M α -HIBA+0.01 M CSA; pH: 3.42, Flow rate: 1.5 mL/min. PCR flow rate: 1 mL/min; Detection: 655 nm.

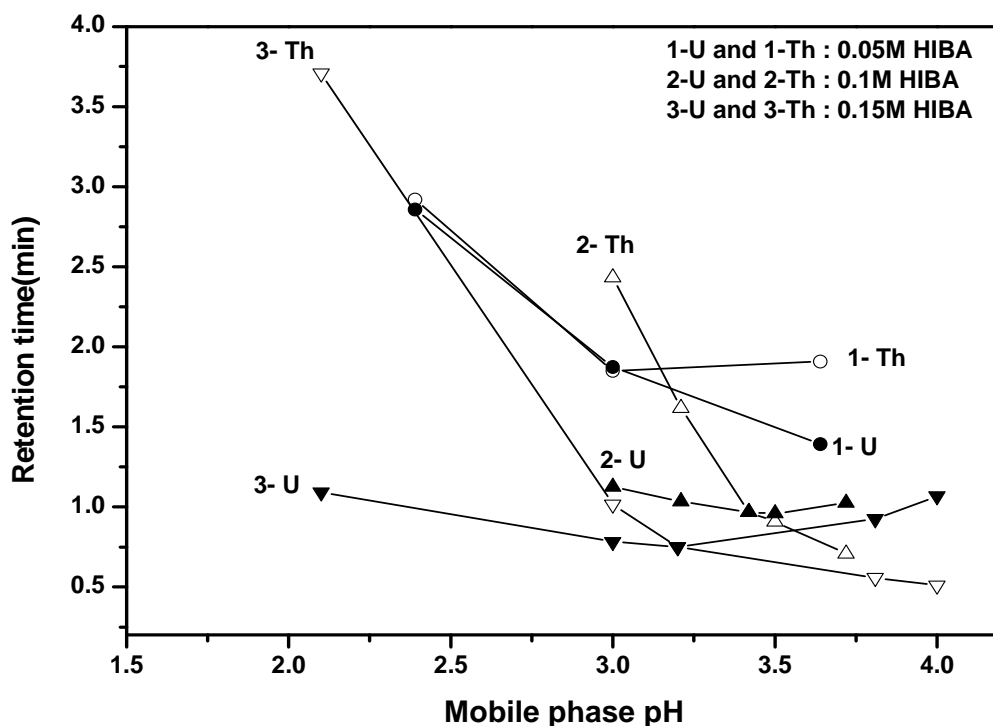


Fig.3.21. Influence of α -HIBA concentration and pH on the retention behaviour of U and Th in the presence of CSA. Column: 3 cm length, 1.8 μ m support; Mobile phase: 0.01 M CSA + 0.05 - 0.15 M α -HIBA; flow rate: 2 mL/min.

3.4 Application of small particle based support (3 cm length with particle size of 1.8 μ m)

3.4.1 Determination of lanthanides in uranium matrix

The efficiency of the pyrochemical process is evaluated by the analysis of cathode deposit, which requires the determination of lanthanides in low levels in uranium matrix [150]. Based on the studies with 3 cm length 1.8 μ m support, an analytical characterization method has been developed for the rapid and accurate analysis of lanthanide elements in uranium matrix, i.e. typical ratios (La:U) being, 1: 2,000.

Several samples were analysed for lanthanides in salt matrix. The salt matrix composition was $MgCl_2 + NaCl + KCl + UO_2Cl_2 +$ lanthanides. The salts were dissolved in HNO_3 medium prior to HPLC analysis. Uranium contents of these samples were also

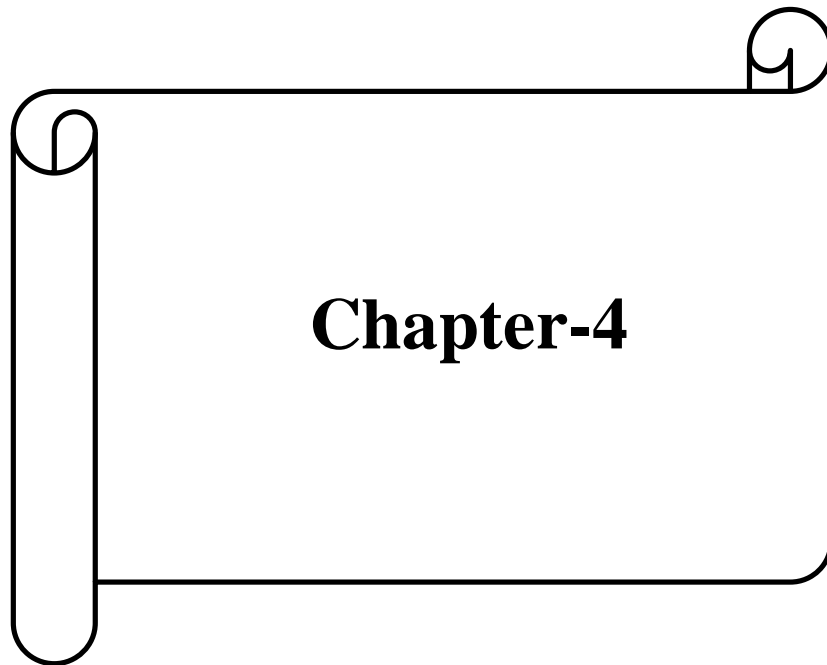
determined directly or with suitable dilution. For e.g. Nd (1-3 ppm) as well as La (1-3 ppm) were separated from U matrix (e.g. 5 mg/mL) and determined by HPLC. The results of these investigations were compared with standard analytical methods. For e.g. in one study, the lanthanide contents were measured using ICP-OES after removing uranium matrix with solvent extraction. The lanthanide values measured with HPLC technique were found to be in good agreement ($\pm 3\%$). The concentration of uranium was also measured by the titration method, Davies and Gray [151] and compared with data obtained by HPLC. For example, in typical experiment, the uranium content measured using Davies and Gray method was found to be 5.22 mg/mL and the result was compared with the uranium values measured with HPLC technique, which was 5.20 mg/mL, results of 5 runs (5.28, 5.17, 5.19, 5.23, 5.12 mg/mL). In another experiment, uranium value estimated using Davies and Gray was found to be 3.42 mg/mL and uranium value estimated using HPLC method was 3.41 mg/mL, results of five runs (3.44, 3.39, 3.47, 3.36, 3.38 mg/mL). These studies established that the rapid separation method developed with 1.8 μm support is found to be fast, reliable and provide accuracy required for a typical regular analysis. An added advantage is that the HPLC technique does not require pre-separation of matrix uranium for the assay of lanthanides unlike other analytical techniques, where it becomes a pre-requisite.

Rapid separation methods were also employed for the estimation of uranium, plutonium and lanthanides fission products from dissolver solution of spent fuel and these results are discussed in Chapter-5 in detail.

3.5. Conclusion

A dynamic ion-exchange HPLC based technique has been developed and demonstrated for the rapid separation of individual lanthanides using 1.8 μm supports. The

selection of appropriate column with suitable particle size with gradient elution technique has been identified as an important factor for achieving rapid and high resolution separation. Lanthanides could be separated from each other in about 3.6 min. Uranium could be rapidly isolated from thorium in one minute. Similarly, lanthanides can be isolated from uranium and thorium in about a minute.



Chapter-4

Chapter-4

Liquid Chromatographic Behavior of Lanthanides and Actinides on Monolith Based Supports

4.1. Introduction

In the recent past, chromatographic support material using monolith material has been studied extensively. A monolith column consists of a single piece of porous, rigid material containing mesopores and macropores, which provide fast analyte mass transfer [27]. Macropores form a dense network of pores while the mesopores form the fine porous structure of the column. Major chromatographic features of monolithic column arise from this mesopore/macropore structure. A monolith column can be an organic polymer or silica based. Hjerten *et al* [152] introduced polyacrylamides based support for protein separation. Preparation of polyacrylates or poly(styrene-co-divinylbenzene) based support material in the presence of porogen was reported in literature [153]. Monolith based supports are employed for various applications, e.g., separation of biomolecules, organic acids, inorganic anions, metal ions etc. Porous monolithic silica support was used for efficient separation of alkaline earth and transition metal cations [31]. Due to several advantages such as high mechanical strength, high stability and inertness, silica based monolith material can be used as the column material for conventional applications, similar to microparticle packed HPLC column. Tanaka *et al* developed silica based monolith support materials [154]. Minakuchi *et al* [155] reported the preparation of a monolith silica column using a sol-gel process. This process involved hydrolysis and polycondensation of alkoxy silans in the presence of water soluble polymer. The mechanism of formation of monolithic silica gel column with bimodal pore structure was reported in literature [156]. Preparation of monolithic support column

with high column efficiency and low back pressure was demonstrated [29, 157]. It is evident from the van Deemter plot that monolith silica provides significantly higher separation efficiency than particle-packed columns (**Fig.4.1**) [158-161].

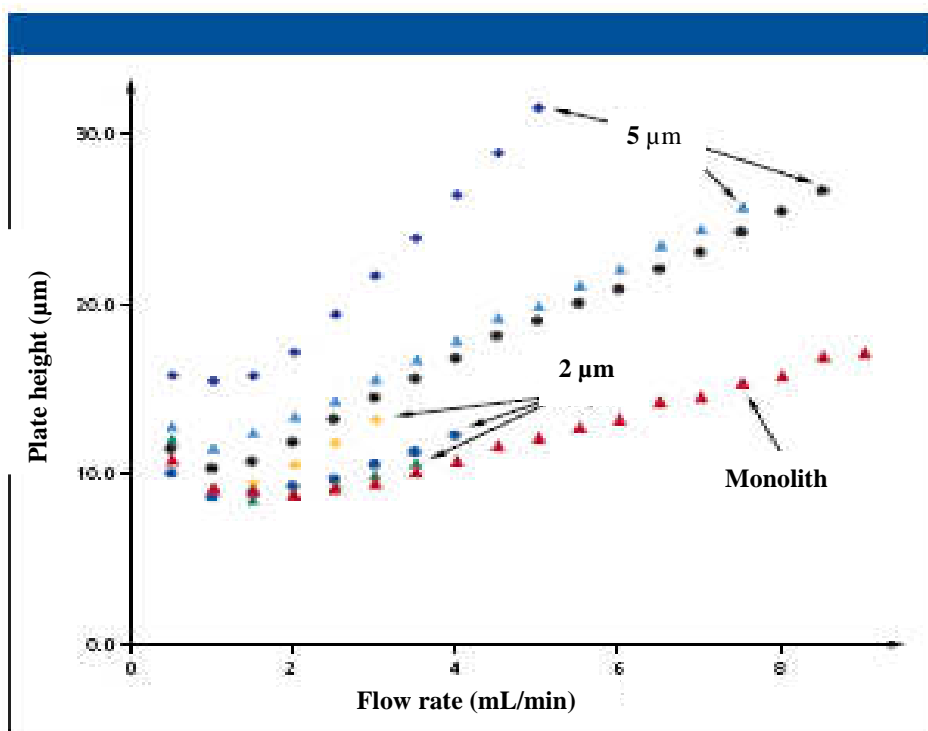


Fig.4.1. Plate height (H) vs flow rate (u) for monolith and particle packed HPLC columns [28]

A clear advantage of monolith material is that it can be operated at higher flow rates but with lower back pressure. Higher column permeability results in higher operating flow rate, which drastically reduces analysis time and provides high separation efficiency [162].

N, N-dialkyl amides have shown promising properties for actinide recovery due to presence of acidic as well as amide functional moieties, [163-165] and their solubility in the aqueous phase is also very low. In the present work, bis-2-ethylhexyl succinamic acid (BEHSA), which possesses both acidic as well as amide functional moieties, was investigated on monolith support in the extraction chromatography mode for its potential towards actinides separation. Use of HNO₃ as the mobile phase was also investigated for the

isolation of U and Th from BEHSA modified monolithic supports. In these studies, the retention of lanthanides and actinides was investigated on monolith supports under dynamic ion-exchange as well as reversed phase experimental conditions. These techniques were employed to determine lanthanides such as Nd and La, uranium, as well as plutonium in the dissolver solution for the determination of atom percent fission and results are discussed in Chapter-5 in detail.

4.2. EXPERIMENTAL

4.2.1 Modification of monolith column

The compound, BEHSA (**Fig.4.2**) was synthesised and characterized as reported [106, 166]. The required amount of BEHSA was dissolved in 100 mL methanol-water mixture (e.g. 60:40) and passed through the 10 cm as well as 5 cm length monolith column at a flow rate of 0.5 mL/min. When the coating was completed, the columns were washed with 25 mL water. After the completion of studies with a particular coating, the BEHSA was washed and removed completely with 50 mL methanol. The same 10 and 5 length monolith columns were reused for all studies carried out in the present work.

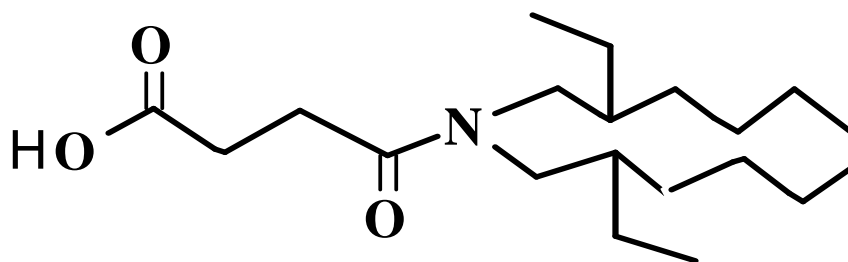


Fig.4.2. Structure of bis-2-ethylhexyl succinamic acid (BEHSA)

4.2.2 Determination of the BEHSA content on monolithic column

The exact contents of BEHSA in the modified support were determined using the HPLC technique (**Table.4.1**). A separate monolithic column (10 cm length) with methanol as the mobile phase was employed. Standard solutions of BEHSA (10-1000 ppm) were prepared and injected into HPLC system and detected at 215 nm (**Fig.4.3**). The amount of BEHSA coated on to the 10 and 5 cm length monolith columns was determined using the calibration plot.

Table.4.1 Modifier content on 10 cm and 5 cm length monolith coated support

Monolith column	BEHSA Passed (mmol)	Actual amount coated (mmol)
10 cm length	0.38	0.36
	1.19	0.716
	3.41	1.47
	5.14	1.93
5 cm length	1.34	0.143
	5.35	0.218
	10.99	0.477
	11.92	0.544

BEHSA dissolved in 60% methanol - 40% H₂O mixture, coating was carried out at a flow rate of 0.5 mL/min. 100 mL of solution employed for coating the column.

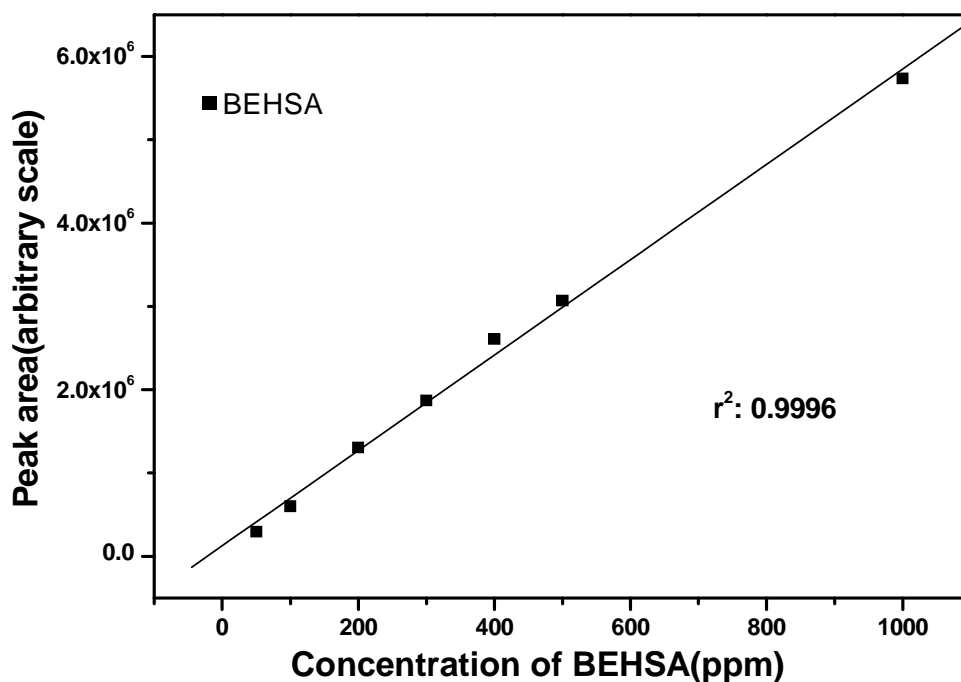


Fig.4.3. Calibration plot for bis-2-ethylhexyl succinamic acid (BEHSA) using HPLC with UV-Vis detection (Det: 215 nm).

4.3. RESULTS AND DISCUSSION

4.3.1 Separation of lanthanides using a monolith column of 10 cm length

4.3.1.1 Gradient elution

A gradient elution procedure for isolation of individual lanthanides was studied extensively using monolith support under dynamic ion-exchange conditions. Large number of gradient profiles were generated by varying the concentrations of CSA (0.01, 0.02, and 0.03 M), α -HIBA (0.05 – 0.2 M), mobile phase pH (3.3-3.9) and mobile phase flow rates (2-7 mL/min). In a typical gradient run, the concentration of CSA and mobile phase flow rate were kept constant and only the α -HIBA concentration was varied (0.05 to 0.2 M). Some gradient profiles employed are listed in **Table.4.2**. Based on these studies, a binary gradient elution method has been developed for the rapid separation of lanthanides from La

to Lu in about 2.8 min, wherein the mobile phase was CSA, α -HIBA and pH being 0.03 M, 0.05 to 0.15 M and 3.5-3.8, respectively (Fig.4.4).

Table.4.2 Gradient programming for separation of lanthanides on 10 cm length monolith support

No	Gradients		Experimental conditions			Total separation time of lanthanides (min)
	Input time (min)	Solvent composition (A)	Solvent composition (A)	Solvent composition (B)	Flow rate (mL/min)	
1	0-1.0 1.1-1.4 1.5-1.8 1.9-2.2 2.3-2.6 2.7-10.0 10.1	100% 70% 50% 30% 10% 0% 100%	0.01 M CSA + 0.05 M α -HIBA; pH: 3.3	0.01 M CSA + 0.1 M α -HIBA; pH: 3.3	2	A good separation of all 14 lanthanides; separation time~7.39 min
2	0-1.0 1.1-1.4 1.5-1.8 1.9-2.2 2.3-2.6 2.7-9.0	100% 80% 60% 40% 20% 0%	0.01 M CSA + 0.05 M α -HIBA; pH: 3.54	0.01 M CSA + 0.1 M α -HIBA; pH: 3.7	2	A good separation of all 14 lanthanides; separation time~5.90 min
3	0-1.0 1.4-1.7 1.8-2.1 2.2-2.6 2.7-3.0 3.1-6.0 6.1	100% 80% 60% 40% 20% 0% 100%	0.01 M CSA + 0.05 M α -HIBA; pH: 3.7	0.01 M CSA + 0.1 M α -HIBA; pH: 3.7	2	A good separation of all 14 lanthanides; separation time ~ 5.64
4	0 0.5 1.0 2.5 3.0 3.6-5.0 5.1	100% 80% 70% 30% 20% 0% 100%	0.02 M CSA + 0.05 M α -HIBA; pH: 3.40	0.02 M CSA + 0.15 M α -HIBA; pH: 3.52	4	A good separation of all 14 lanthanides; separation time ~ 4.42

5	0 1.2 2.0 2.5 2.7 3.0 3.6-4.5 4.7	100% 90% 80% 60% 40% 30% 0% 100%	0.02 M CSA + 0.05 M α -HIBA; pH: 3.45	0.02 M CSA + 0.15 M α -HIBA; pH: 3.52	6	A good separation of all 14 lanthanides; separation time ~ 4.17
6	0 1.0 1.7 2.1 2.3 3-3.8 4.0	100% 90% 80% 60% 40% 0% 100%	0.02 M CSA + 0.05 M α -HIBA; pH: 3.45	0.02 M CSA + 0.15 M α -HIBA; pH: 3.5	7	A good separation of all 14 lanthanides; separation time ~ 3.40
7	0 1.0 1.2 1.6 2.1 2.3 2.9-3.8 4.0	100% 70% 90% 50% 30% 35% 0% 100%	0.02 M CSA + 0.05 M α -HIBA; pH: 3.51	0.02 M CSA + 0.15 M α -HIBA; pH: 3.51	7	A good separation of all 14 lanthanides; separation time ~ 3.12
8	0 1.0 1.2 1.6 2.1 2.3 2.5-3.8 4.0	100% 70% 90% 50% 30% 35% 0% 100%	0.02 M CSA + 0.05 M α -HIBA; pH: 3.51	0.02 M CSA + 0.15 M α -HIBA; pH: 3.51	7	A good separation of all 14 lanthanides; separation time ~ 3.01
9	0 0.4 0.8 1.0 1.6 2.0 2.5-3.2 3.3	100% 90% 70% 80% 50% 40% 0% 100%	0.03 M CSA + 0.05 M α -HIBA; pH: 3.5	0.03 M CSA + 0.15 M α -HIBA; pH: 3.8	7	A good separation of all 14 lanthanides; separation time ~ 2.8

These studies have established that monolith supports could be operated at higher flow rates with lower back pressure resulting in a higher column permeability, which drastically

reduced separation time and at the same time also provided higher separation efficiency. HPLC separation procedure developed for isolation of individual lanthanides using 1.8 μm support resulted in a separation time of about 3.63 min (Chapter-3) and the use of monolith support has resulted in a further reduction of the separation time, i.e. 2.8 min. The efficiency of monolith based support was studied under various experimental conditions for separation of lanthanides and the results are shown in **Table.4.3**.

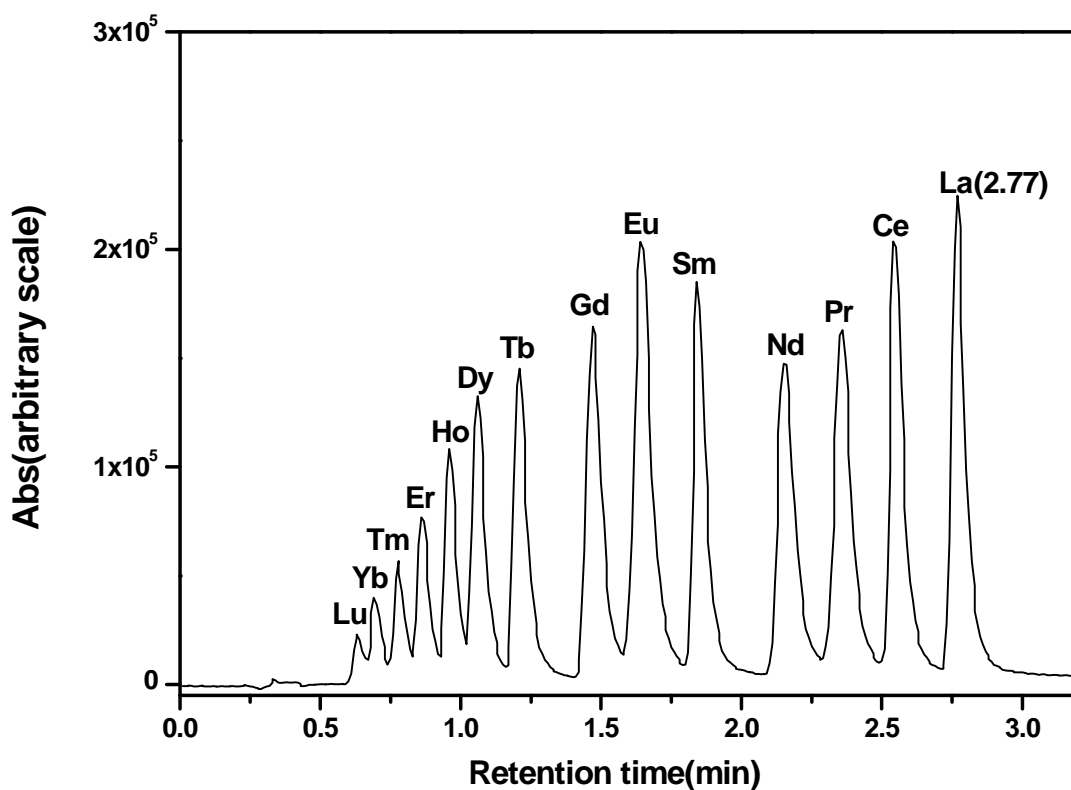


Fig.4.4. Separation of lanthanides on a monolith column using dynamic ion exchange chromatography. Column: 10 cm length monolith; Mobile Phase: (A) 0.03 M CSA, 0.05 M α -HIBA (pH: 3.5) + (B) 0.03 M CSA, 0.15 M α -HIBA (pH: 3.8); flow rate: 7 mL/min; Post-column reagent (PCR) flow rate: 1 mL/min; Detection: 655 nm; Sample: lanthanides (16 ppm) in 0.01 N HNO_3 ; 20 μL injected.

The capacity factor for lanthanides decreases with increase in α -HIBA concentration and mobile phase pH (**Fig.4.5** and **Fig.4.6**) which is attributed to the better complexing ability of α -HIBA with lanthanides under these conditions. However, capacity factor increases with increase in concentration of CSA (**Fig.4.7**). Separation factors of adjacent lanthanides were calculated under various experimental conditions and results were shown in **Table.4.4-4.6**.

Table.4.3 Efficiency of 10 cm length monolith column for separation of lanthanides

Experimental conditions	Number of theoretical plates (plates/m)				
	La	Ce	Pr	Nd	Sm
0.05 M α -HIBA+ 0.01 M CSA; pH: 3.5; Flow rate: 2 mL/min	41443	40529	43719	41225	44417
0.075 M α -HIBA+ 0.01 M CSA; pH: 3.2; Flow rate: 7 mL/min	39333	40960	38302	38729	35286
0.1 M α -HIBA+ 0.01 M CSA; pH: 3.3; Flow rate: 2 mL/min	42725	39705	43916	42087	44501

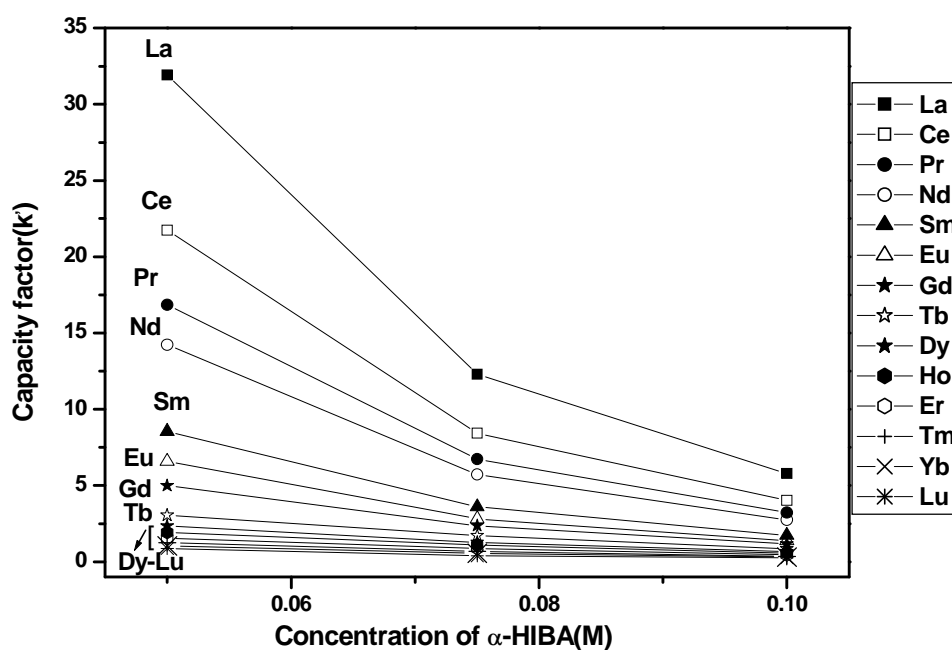


Fig.4.5. Variation of capacity factor of lanthanides as a function of α -HIBA concentration on a monolith column. Column: 10 cm length monolith column; Mobile phase: 0.01 M CSA + α -HIBA; pH: 3.5; Flow rate: 2 mL/min; PCR flow rate: 0.5 mL/min; Detection 655 nm; Sample: lanthanides (10 ppm) in 0.001 N HNO₃.

Table.4.4. Separation factor of adjacent lanthanides as a function of α -HIBA concentration from 10 cm length monolith support.

Experimental condition: 0.01 M CSA + α -HIBA, pH: 3.5, Flow rate: 2 mL/min

Lanthanides	0.05 M α -HIBA	0.075 M α -HIBA	0.1 M α -HIBA
	Separation factor (α)	Separation factor (α)	Separation factor (α)
La :Ce	1.47	1.45	1.44
Ce :Pr	1.29	1.25	1.24
Pr :Nd	1.18	1.17	1.16
Nd :Sm	1.66	1.59	1.58
Sm :Eu	1.29	1.28	1.25
Eu :Gd	1.23	1.18	1.18
Gd :Tb	1.46	1.38	1.38
Tb :Dy	1.29	1.33	1.30
Dy :Ho	1.21	1.17	1.19
Ho :Er	1.25	1.27	1.21
Er :Tm	1.22	1.27	1.31
Tm :Yb	1.19	1.21	1.17
Yb :Lu	1.20	1.18	1.12

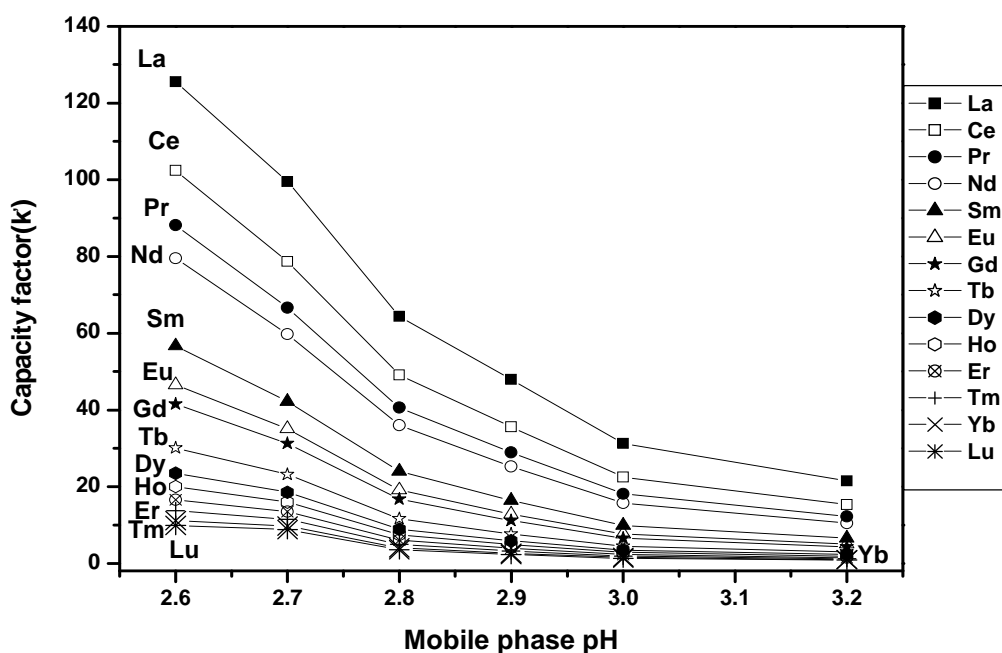


Fig.4.6. Variation of capacity factor of lanthanides as a function of mobile phase pH on a monolith column. Column: 10 cm length monolith column; Mobile phase: 0.01 M CSA + 0.1 M α -HIBA; Flow rate: 2 mL/min; PCR flow rate: 0.5 mL/min; Detection 655 nm; Sample: lanthanides (10 ppm) in 0.001 N HNO₃.

Table.4.5. Separation factor of adjacent lanthanides as a function of mobile phase pH from 10 cm length monolith support.

Experimental condition: 0.01 M CSA + 0.1 M α -HIBA, Flow rate: 2 mL/min

Lanthanides	Separation factor (α)					
	pH :2.6	pH :2.7	pH :2.8	pH :2.9	pH :3	pH :3.2
La :Ce	1.22	1.26	1.31	1.35	1.39	1.41
Ce :Pr	1.16	1.18	1.21	1.23	1.24	1.25
Pr :Nd	1.11	1.11	1.13	1.14	1.15	1.16
Nd :Sm	1.40	1.41	1.49	1.54	1.58	1.60
Sm :Eu	1.22	1.20	1.26	1.28	1.28	1.29
Eu :Gd	1.12	1.12	1.14	1.15	1.16	1.17
Gd :Tb	1.38	1.34	1.44	1.44	1.45	1.45
Tb :Dy	1.28	1.25	1.30	1.31	1.30	1.30
Dy :Ho	1.17	1.16	1.20	1.20	1.21	1.22
Ho :Er	1.21	1.18	1.22	1.23	1.23	1.23
Er :Tm	1.20	1.17	1.21	1.22	1.22	1.23
Tm :Yb	1.23	1.18	1.22	1.23	1.22	1.22
Yb :Lu	1.13	1.11	1.14	1.14	1.16	1.17

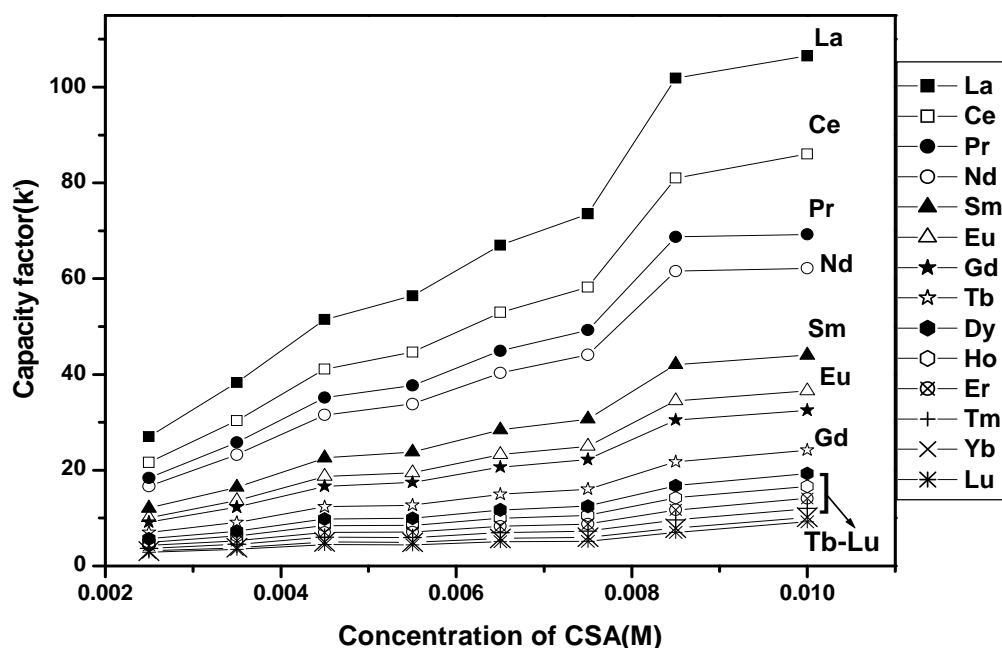


Fig.4.7. Variation of capacity factor of lanthanides as a function of CSA concentration on a monolith column. Column: 10 cm length monolith column; Mobile phase: CSA + 0.1 M α -HIBA; pH: 2.7; Flow rate: 2 mL/min; PCR flow rate: 0.5 mL/min; Detection 655 nm; Sample: lanthanides (10 ppm) in 0.001 N HNO₃.

Table.4.6. Separation factor of adjacent lanthanides as a function of CSA concentration from 10 cm length monolith support.

Experimental condition: CSA + 0.1 M α -HIBA, pH: 2.7, Flow rate: 2 mL/min

Lanthanides	Separation factor (α)							
	0.0025 M CSA	0.0035 M CSA	0.0045 M CSA	0.0055 M CSA	0.0065 M CSA	0.0075 M CSA	0.0085 M CSA	0.01 M CSA
La :Ce	1.25	1.26	1.25	1.26	1.26	1.26	1.26	1.26
Ce :Pr	1.17	1.17	1.17	1.18	1.18	1.18	1.17	1.18
Pr :Nd	1.10	1.11	1.11	1.11	1.11	1.12	1.1	1.11
Nd :Sm	1.38	1.41	1.40	1.42	1.42	1.43	1.46	1.41
Sm :Eu	1.19	1.21	1.20	1.22	1.22	1.23	1.22	1.20
Eu :Gd	1.09	1.11	1.12	1.11	1.12	1.12	1.13	1.12
Gd :Tb	1.31	1.34	1.35	1.38	1.38	1.38	1.40	1.35
Tb :Dy	1.23	1.25	1.26	1.27	1.27	1.28	1.29	1.25
Dy :Ho	1.15	1.16	1.16	1.17	1.17	1.18	1.18	1.16
Ho :Er	1.17	1.19	1.201	1.20	1.21	1.21	1.21	1.18
Er :Tm	1.16	1.17	1.18	1.19	1.19	1.20	1.21	1.17
Tm :Yb	1.17	1.19	1.20	1.20	1.21	1.21	1.22	1.18
Yb :Lu	1.11	1.10	1.11	1.12	1.12	1.17	1.13	1.10

4.3.1.2. Isocratic elution

In an isocratic elution method, individual lanthanides were separated from each other on a 10 cm length monolith support and the results are summarized in **Table 4.7**. In a typical experiment, the separation time was very well reduced to about 5 min (**Fig.4.8**) with good resolution between adjacent lanthanides and this could be achieved with the use of higher operating flow rates as the pressure drop across the column was found to be lower compared to 5 μm based columns. In another study, lanthanum was separated from other lanthanides in about 1.77 min (**Table 4.7**). Hence, experiments were also carried out with dissolver solution to determine lanthanum concentration under these experimental conditions and the results are discussed later, i.e., in Chapter-5.

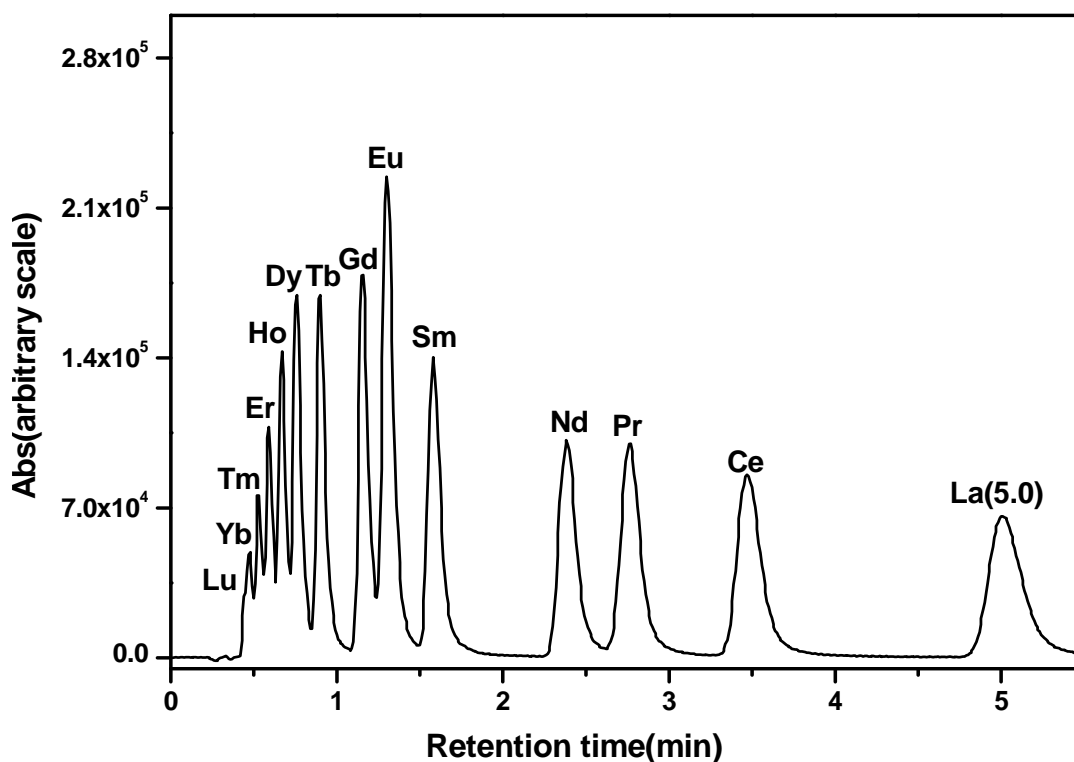


Fig.4.8. Separation of lanthanides by isocratic elution from 10 cm length monolith column.

Column: 10 cm monolith; Mobile phase: 0.01 M CSA + 0.05 M α -HIBA; pH: 3.7; flow rate: 7 mL/min; PCR flow rate: 1 mL/min; Detection: 655 nm; Sample: lanthanides (16 ppm) in 0.01 N HNO_3 ; 20 μL injected.

Table.4.7 Gradient and isocratic elution for separation of lanthanides using monolith column

S. No.	Monolith column length (cm)	Elution profile	Experimental conditions				Results
			CSA (M)	α -HIBA (M)	pH	Flow rate (mL/min)	
1.	10	Gradient elution	0.03	0.05 -0.15	3.5 - 3.8	7	Fast separation of all 14 lanthanides; separation time ~ 2.8 min.
2.		Isocratic elution	0.01	0.1	3.2	2	All lanthanides separated; separation time ~ 15 min.
			0.01	0.1	3.2	6	Most of the lanthanides well resolved from each other; separation time ~ 5 min.
			0.01	0.05	3.7	7	All lanthanides are well separated from each other; separation time ~ 5 min.
			0.01	0.1	3.6	5	“La” well resolved from other lanthanides; heavier lanthanides not resolved; separation time ~ 1.8 min.
3.	5	Gradient elution	0.05	0.01- 0.1	4	2	Separation of all 14 lanthanides; separation time ~ 4.8 min.
4.	5	Isocratic elution	0.03	0.05	3.2	2	All lanthanides separated; separation time ~ 8.9 min.
			0.03	0.05	3.5	2	La-Sm fractions resolved; heavier lanthanides not resolved completely; separation time ~ 2.4 min.

4.3.2 Lanthanide separations using monolith support of 5 cm length

4.3.2.1 Gradient elution

The separation of lanthanides was also investigated from a 5 cm length monolith support with a surface area of 300-310 m²g⁻¹ with 1.5 μ m macroporous and 10 nm mesoporous structure. These studies were carried out to compare the performance with the 10 cm length monolith support described above. **Fig.4.9.** shows gradient elution separation

of lanthanides from the 5 cm length support; Lanthanides could be isolated from each other in about 4.77 min. Under the experimental conditions of the present work, faster separation was achieved with 10 cm length support (surface area of $360 \text{ m}^2\text{g}^{-1}$ with $2 \mu\text{m}$ macroporous and 13 nm mesopore) (Fig.4.4) over a 5 cm length support (surface area of $300 \text{ m}^2\text{g}^{-1}$ with $1.5 \mu\text{m}$ macroporous and 10 nm mesopore) (Fig.4.9).

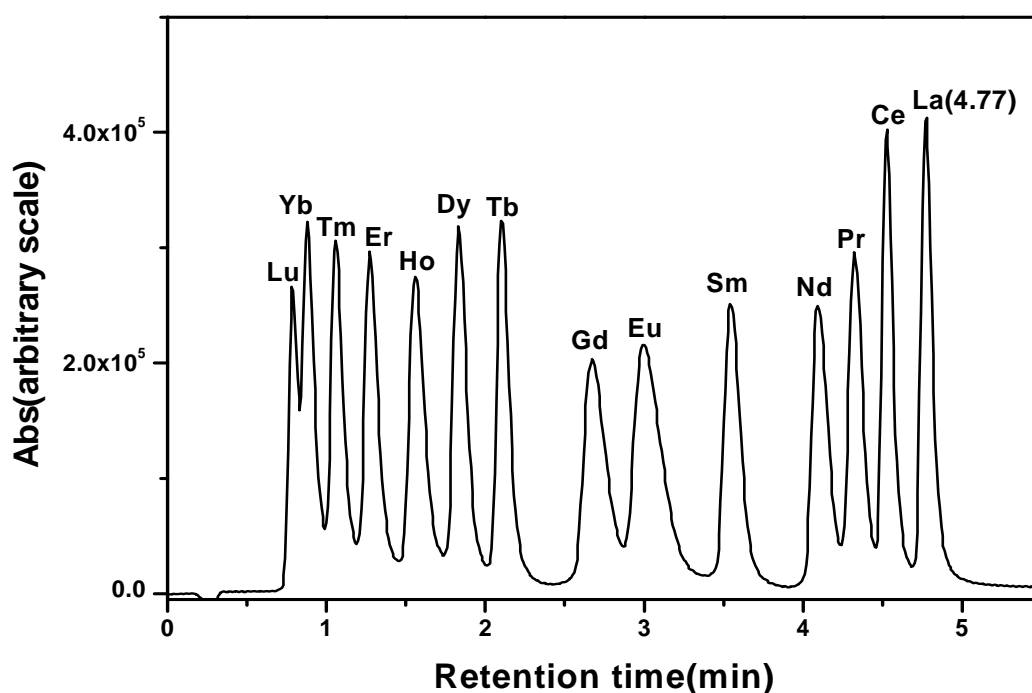


Fig.4.9. Separation of lanthanides on a 5 cm length monolith column using dynamic ion-exchange chromatography. Column: 5 cm length monolith; Mobile Phase: (A) 0.05 M CSA, 0.01 M α -HIBA + (B) 0.05 M CSA, 0.1 M α -HIBA; pH: 4; flow rate: 2 mL/min; PCR flow rate: 1 mL/min; detection 655 nm, sample: lanthanides (16 ppm) in 0.01 N HNO_3 ; 20 μL injected.

4.3.2.2 Isocratic elution from 5 cm length support

The results of the isocratic elution are shown in **Table 4.7**. The back pressure with 5 cm length ($1.5 \mu\text{m}$ macroporous and 10 nm mesoporous structure) monolith was much higher (back pressure: 67 bar with mobile phase flow rate: 1 mL/min) compared to 10 cm length support ($2 \mu\text{m}$ macroporous and 13 nm mesoporous structure) (back pressure: 19 bar

with mobile phase flow rate: 1 mL/min); hence the 5 cm length support could not be operated at higher flow rates compared to the 10 cm length support. The 10 cm length monolith support provided a faster and more efficient separation under the experimental conditions of the present study compared to the 5 cm length support. For example, the separation factors obtained with 10 cm length support for adjacent lanthanides e.g. Pr-Nd, Ce-Pr and La-Ce (**Table.4.8**) were similar or marginally higher compared to the one obtained with 5 cm length support. Typical chromatogram for isocratic elution of lanthanides using 5 cm length support is shown in **Fig.4.10**. Faster separations were achieved with 10 cm length monolith support (**Fig.4.8**) over the 5 cm length column (**Fig.4.10**).

Table.4.8. Separation factor of adjacent lanthanides from 5 and 10 cm length monolith support.

Lanthanides	10 cm length monolith support	5 cm length monolith support
	Separation factor (α)	Separation factor (α)
La :Ce	1.48	1.40
Ce :Pr	1.28	1.28
Pr :Nd	1.19	1.17
Nd :Sm	1.62	1.61
Sm :Eu	1.25	1.24
Eu :Gd	1.17	1.17

* e.g., Separation factor (α) for La:Ce = k'_{La}/k'_{Ce} ; k' = Capacity factor

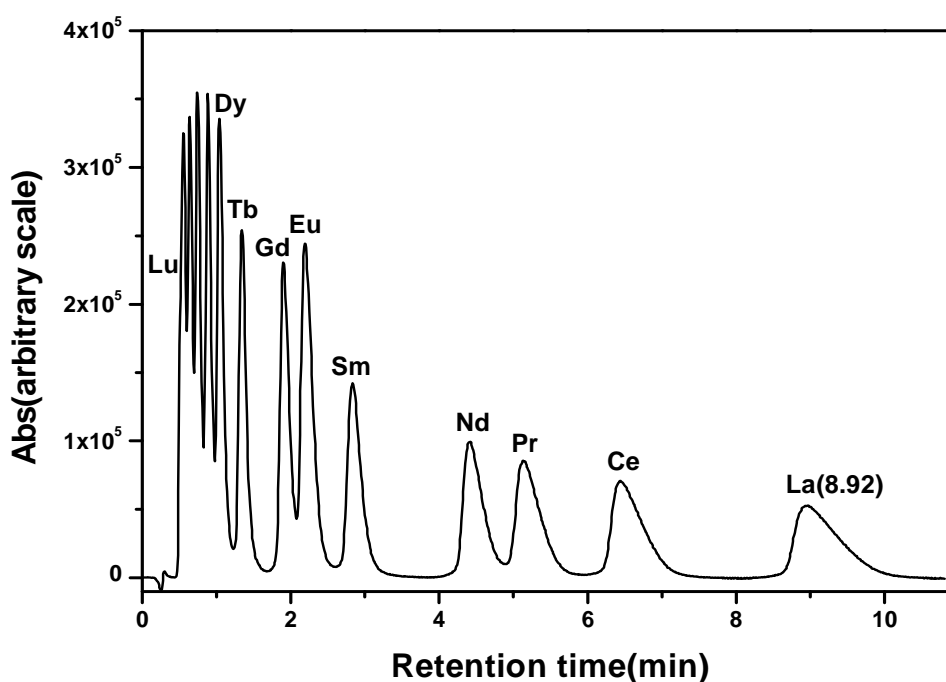


Fig.4.10. Separation of lanthanides by isocratic elution from 5 cm length fast gradient monolith column. Column: 5 cm monolith; Mobile Phase: (A) 0.03 M CSA, 0.05 M α -HIBA; pH: 3.2; flow rate: 2 mL/min; PCR flow rate: 1 mL/min; detection 655 nm, sample: lanthanides (16 ppm) in 0.01 N HNO₃; 20 μ L injected.

4.3.3. Retention studies on uranium and thorium from 10 cm length monolith column

4.3.3.1. Retention behaviour under dynamic ion-exchange condition

The separation of uranium from thorium using dynamic ion-exchange chromatography is shown in **Fig.4.11**. At lower pH (pH: 2.3), higher retention of thorium is observed compared to uranium due to the higher charge of Th (Th in +4 state) compared to uranium (UO_2^{+2}), indicating cation exchange mechanism. As pH is raised, complexation of U and Th with HIBA is enhanced, leading to the early elution of both U and Th. However, at higher pH (pH:4), most of the uranium exists predominantly as $[\text{UO}_2(\text{IBA})_3]^-$ complex, which has higher reversed phase affinity (through van der waals interaction) compared to thorium complex, $[\text{Th}(\text{IBA})_4(\text{OH})_2]^{2-}$, which has lower affinity on the support. This is

because, the concentration of modifier, CSA employed was only 0.01 M and hence uranium complex can be sorbed on the support through van der waal interaction as well.

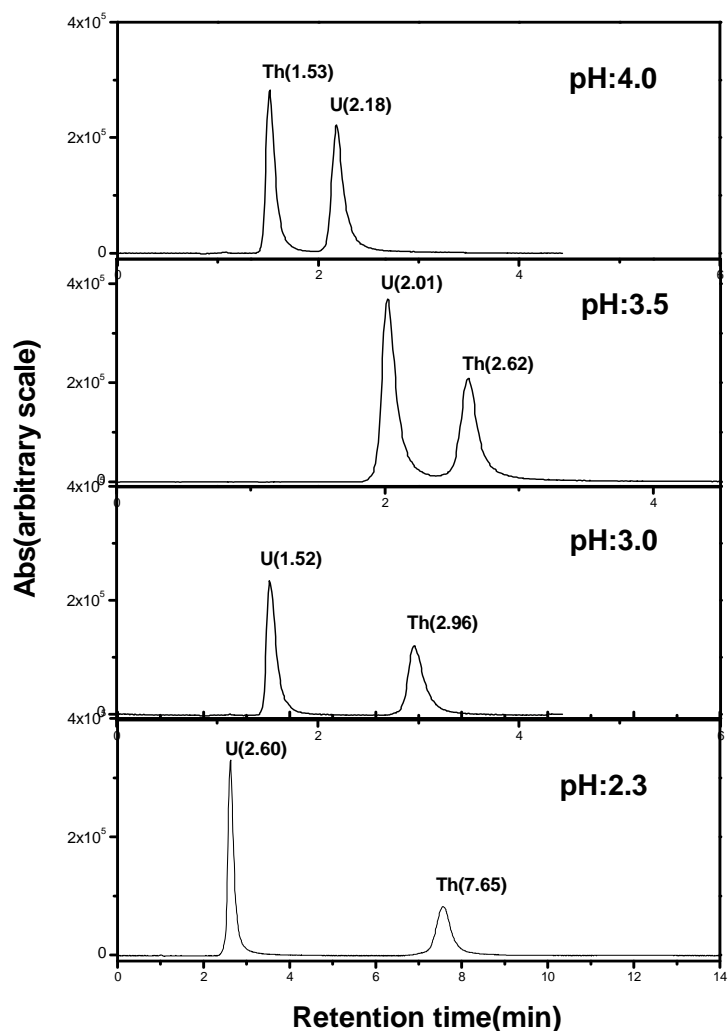


Fig.4.11. Retention behaviour of U and Th on dynamically modified 10 cm length reversed phase monolith column as a function of mobile phase pH. Column: 10 cm length monolith; Mobile phase: 0.01 M CSA + 0.15 M α -HIBA; Flow rate: 2 mL/min; PCR flow rate: 1 mL/min; Detection: 655 nm; Sample: U and Th in 0.01 N HNO₃; 20 μ L injected.

The separation factor (k'_{Th} / k'_U) accordingly decreases with increase in α -HIBA concentration and mobile phase pH (Fig.4.12). Retention of Th (IV) is higher than that of

uranium (UO_2^{+2}) because of its strong interaction with CSA due to its higher charge. The retention of thorium decrease with increase in α -HIBA concentration; the reduction in Th retention becomes significant when the mobile phase pH is above “3” because of the strong complexation of Th with α -HIBA. Under these conditions, a good fraction of α -HIBA dissociates to form stronger complexes with Th (IV). Thorium is eluted prior to uranium when the pH of α -HIBA solution is at 4, possibly indicating strong retention of uranyl ion with the support through reversed phase interaction, i.e., induced dipole-dipole interaction.

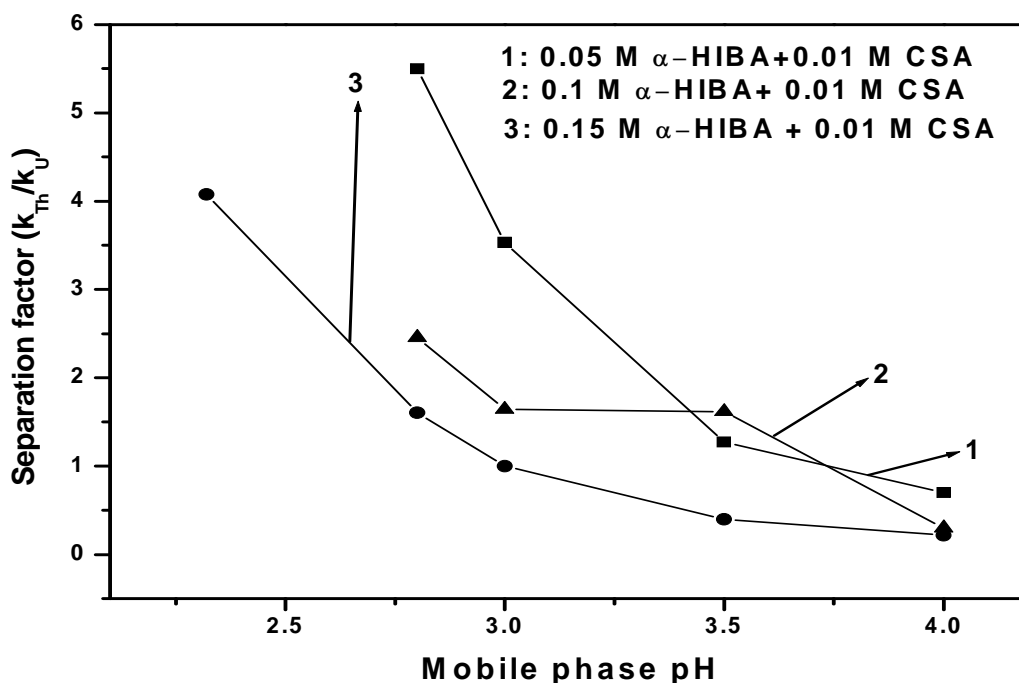


Fig.4.12. Separation factor for Th/U as a function of mobile phase pH and concentration from 10 cm length monolith support.

4.3.3.2. Retention of U and Th without CSA modifier – reversed phase condition

Elution of uranium and thorium from 10 cm length bare monolith support was also studied using α -HIBA solutions of 0.05, 0.1, and 0.15 M (pH: 2.6 to 4). In these studies, mobile phase pH was chosen in the range between pH: 2.6 and 4 for the following reasons.

The as- prepared solution of 0.1 M α -HIBA in water has a pH of 2.6 and hence this pH was the lowest studied in the present work; pH > 4 was also not used due to large retention time at higher pH. The retention for both uranium and thorium increase with increase in mobile phase pH. Typical results are shown in Fig.4.13.

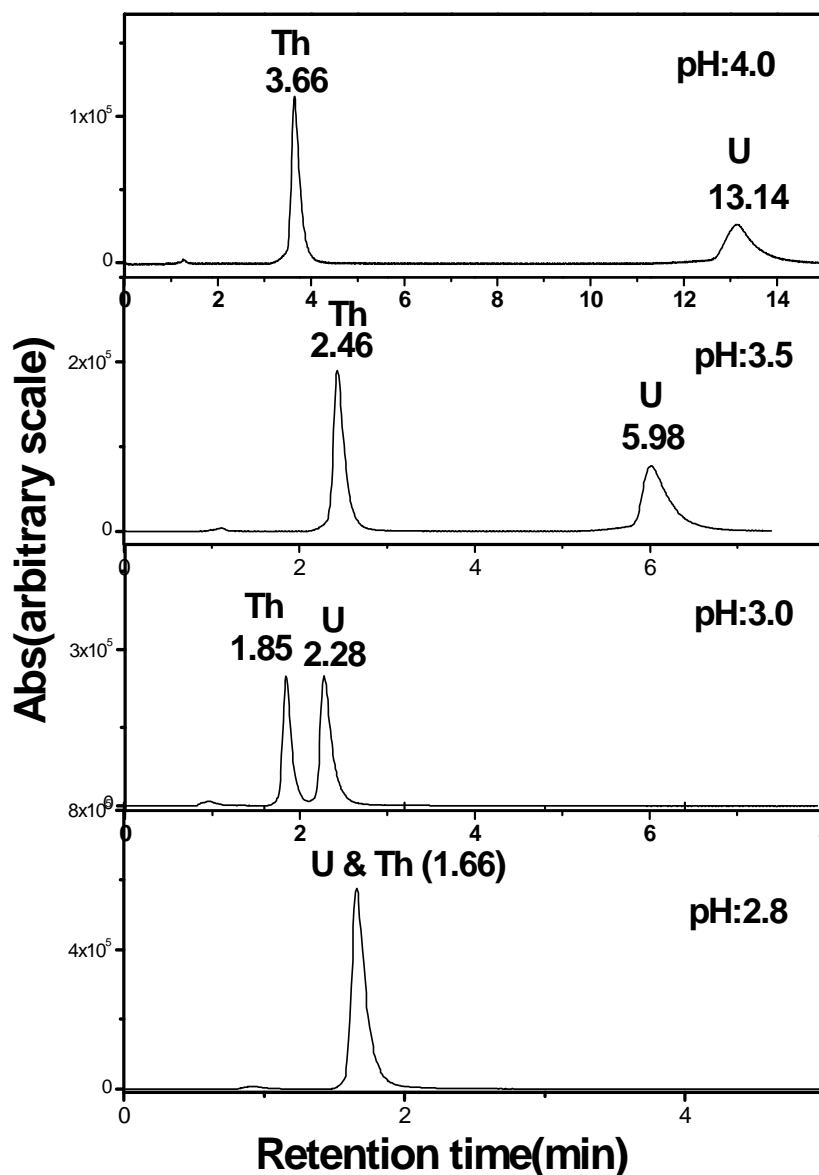


Fig.4.13. Retention behaviour of U and Th on 10 cm length reversed phase monolith column as a function of mobile phase pH. Column: 10 cm length monolith; Mobile phase: 0.1 M α -HIBA; PCR flow rate: 1 mL/min; Detection: 655 nm; Sample: U and Th (25 ppm) in 0.01 N HNO₃; 20 μ L injected.

The capacity factor and separation factor of uranium and thorium were calculated under various experimental conditions and results are summarised in **Table 4.9**. Highest separation factors were obtained with 0.15 M α -HIBA. The separation of U and Th as function of mobile phase flow rate under typical experimental conditions are shown in **Fig.4.14**. In this study, mobile phase flow rate was varied from 2 to 6 mL/min using 0.15 M α -HIBA solution of pH: 3. Uranium and thorium could be separated in about 50 sec in these studies.

Table.4.9. Separation factor for U and Th as a function of mobile phase pH and concentration from 10 cm length monolith support.

pH	Mobile phase (α -HIBA)								
	0.05 M			0.1 M			0.15 M		
	Capacity factor		Separation factor(k'_U/k'_{Th}) (α)	Capacity factor		Separation factor(k'_U/k'_{Th}) (α)	Capacity factor		Separation factor(k'_U/k'_{Th}) (α)
	(k'_U)	(k'_{Th})		(k'_U)	(k'_{Th})		(k'_U)	(k'_{Th})	
As it is pH	0.91	1.18	0.77	0.82	0.82	1	0.56	0.56	1
3	1.45	1.45	1	1.40	0.95	1.48	1.15	0.63	1.82
3.5	4.59	1.92	2.40	4.48	1.26	3.57	3.96	1.07	3.68
4	10.14	2.71	3.74	9.68	1.97	4.90	7.68	1.47	5.23

- *As it is pH of 0.15 M α -HIBA solution: 2.63, as it is pH of 0.1 M α -HIBA solution: 2.72, as it is pH of 0.05 M α -HIBA solution: 2.81,*

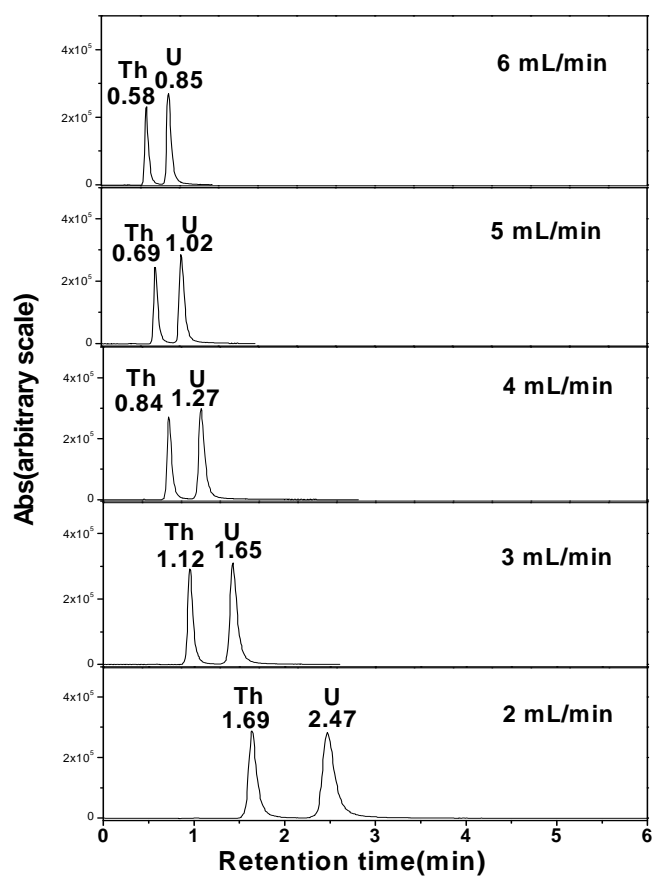


Fig.4.14. Retention behaviour of U and Th on 10 cm length reversed phase monolith column as a function of mobile phase flow rate. Column: 10 cm length monolith; Mobile phase: 0.15 M α -HIBA; pH: 3; PCR flow rate: 1 mL/min; Detection: 655 nm; Sample: U and Th (25 ppm) in 0.01 N HNO₃; 20 μ L injected.

4.3.3.3. Retention of U and Th on modified monolith support: Studies on BEHSA coated monolithic column

The retention of U and Th was investigated from BEHSA modified monolith reversed phase support to investigate its preferential retention of U over Th. The separation of U from Th as a function of mobile phase flow rate from 1.19 mM BEHSA coated monolith is shown in **Fig.4.15**. Rapid separation of U from Th was demonstrated, i.e. under 30 sec with good base line separation.

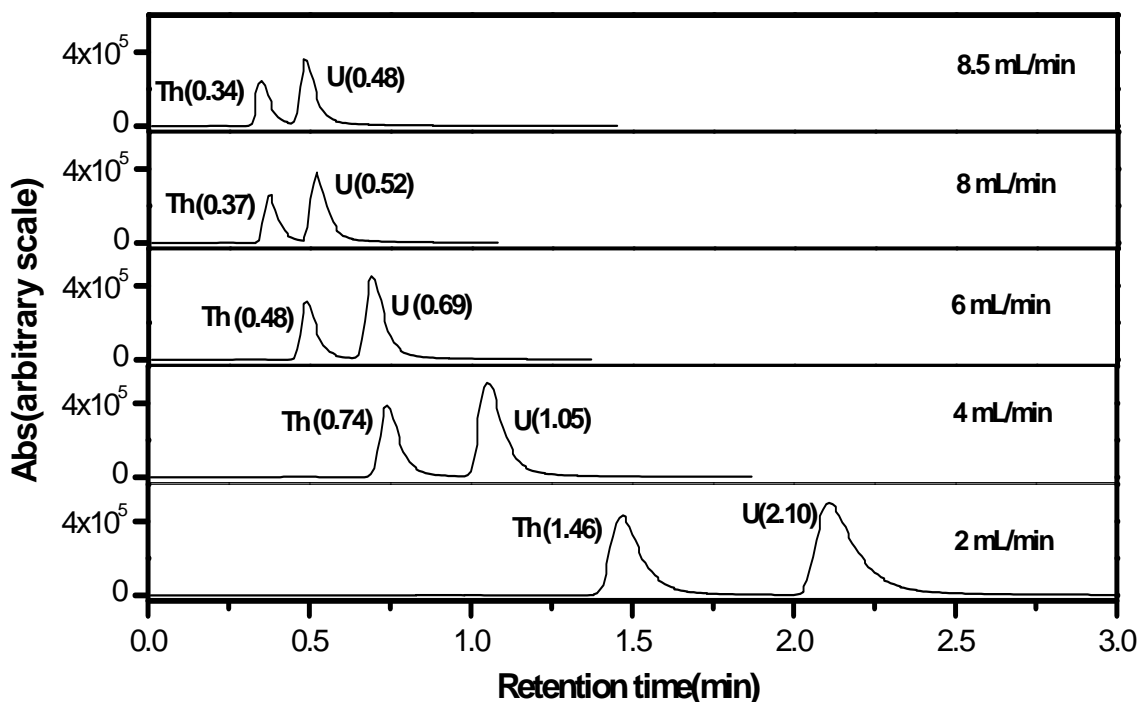


Fig.4.15. Retention behaviour of U and Th on BEHSA modified reversed phase column as a function of mobile phase flow rate. Column: 10 cm length monolith coated with 1.19 mM BEHSA; Mobile phase: 0.15 M α -HIBA; pH: 2.8; PCR flow rate: 1 mL/min; Detection: 655 nm; Sample: U and Th (25 ppm) in 0.01 N HNO₃; 20 μ L injected.

4.3.3.3.1 Influence of BEHSA concentration

The capacity factors (**Fig.4.16**) and separation factors (**Fig.4.17**) for U/Th from bare and BEHSA modified monolith supports are shown. The highest separation factor was obtained at 5.14 mM BEHSA coatings for 0.15 M α -HIBA solution. The retention or capacity factor of Th (IV) was lower compared to U (VI) from BEHSA support when α -HIBA was used as eluent. Thorium would form mainly anionic species with α -HIBA, e.g., $[\text{Th}(\text{IBA})_4(\text{OH})_2]^{2-}$, especially at pH > 3, which has a lower affinity compared to that of uranium species, $[\text{UO}_2(\text{IBA})_3]^-$.

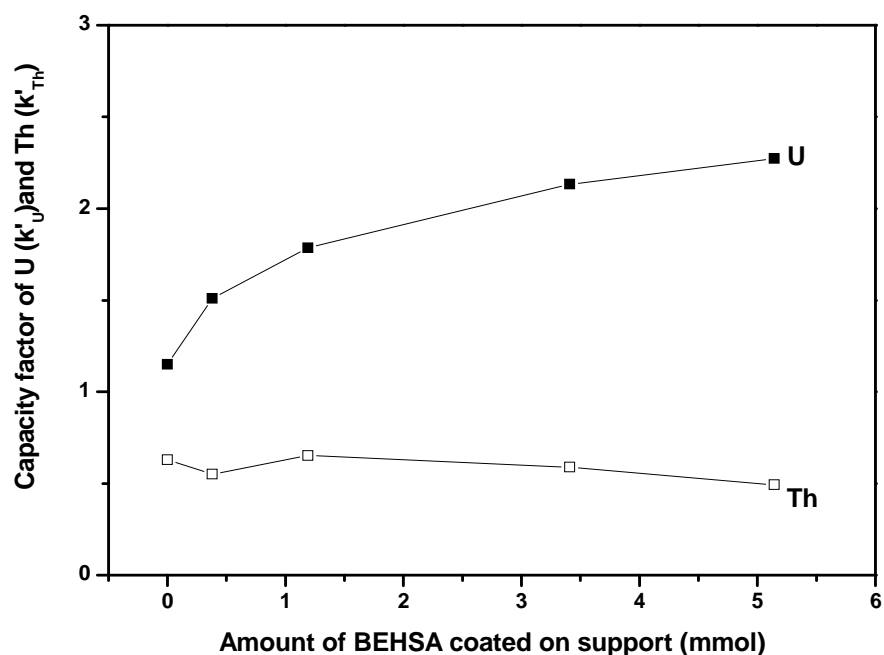


Fig.4.16 Capacity factor (k') of U and Th on BEHSA modified support. Column: BEHSA modified 10 cm length monolith support; Mobile phase: 0.15 M α -HIBA; pH: 3, flow rate: 2 mL/min

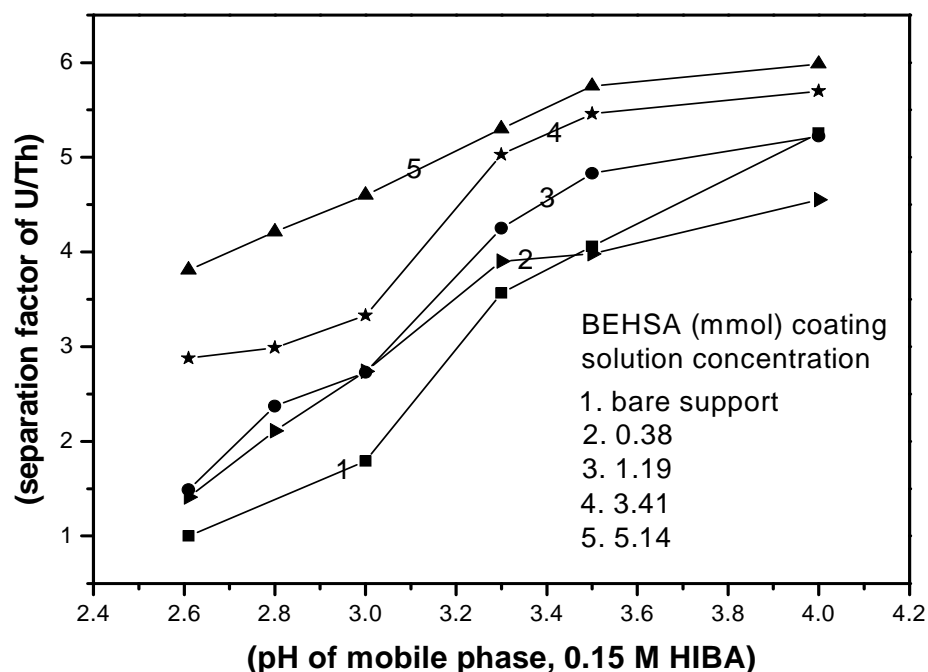


Fig.4.17. Influence of BEHSA concentration on the separation factor of U/Th. Column: BEHSA modified 10 cm length monolith support; Mobile phase: 0.15 M α -HIBA; flow rate: 2 mL/min.

These complexes are mainly sorbed on C₁₈ column through van der waals interaction. The highest separation factor was obtained when the BEHSA content on the coated support was high, clearly indicating the influence of the amide moiety in selectively complexing and retaining uranium over thorium.

4.3.3.3.2 Uranium and Thorium separation with HNO₃ as mobile phase

The retention of U and Th on the BEHSA coated monolith support with HNO₃ as eluent was also investigated. The absence of a complexing agent, e.g., α -HIBA in the mobile phase will be of great use for collecting the pure fractions of metal ions especially when the system is scaled up for preparative separations. Thorium did not elute with 0.001 N HNO₃, whereas “U” eluted with severe tailing. Employing HNO₃ as mobile phase (pH: 2.4), U (t_r: 0.88 min) and Th (t_r: 9.3 min) were separated from each other. However with HNO₃ (pH: 2), the separation was achieved in about 0.38 min (**Fig.4.18A**).

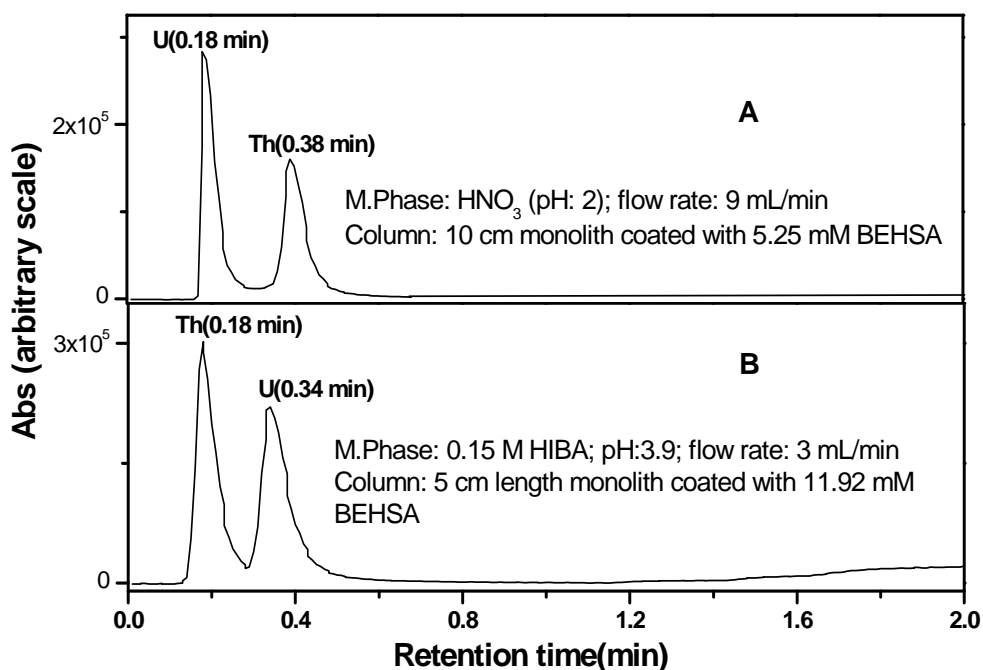


Fig.4.18. Retention behavior of U & Th on a BEHSA modified 10 cm and 5 cm length monolith support

With HNO_3 as mobile phase, uranium elutes prior to thorium, indicating the dominance of cation-exchanging ability of BEHSA. In another study, the elution behavior of uranium and thorium was investigated on 5 cm length monolith support modified with BEHSA. In these studies, BEHSA solutions of 1.34 to 11.92 mM were employed for column modification. The separation of “U” from “Th” was demonstrated in 0.34 min with the modified monolith (**Fig.4.18B**) support. The use of HNO_3 (pH: 2.18) from 5 cm length BEHSA modified monolith resulted in a separation time of 0.41 min.

4.3.4. Comparison of performance of monolithic column with 1.8 micron particle based column during dynamic ion exchange chromatographic studies

The column efficiency (N) of monolithic column employed in the present work is about 1,10,000 plates per meter for the separation of organic compounds. However, when monolithic column was modified with ion-pairing reagent, CSA, the column efficiency in a typical experiment reduced to about 44,000 (maximum observed in the present study). Similarly, the column efficiency of 1.8 micron based support is 1,80,000 plates per meter for isolation of organic compounds. This column when operated under dynamic ion exchange mode has provided in a typical experiment, about 1,00,000 plates per meter. Thus modification of both monolith as well as 1.8 micron based supports with ion-pairing reagent has resulted in only about 40-50% of the total number of original plates / column efficiency. Still the total number of plates available are sufficiently large enough for significant reduction in separation times of individual lanthanides/ actinides. Though the number of plates observed with monolith column in dynamic ion exchange experiments is less compared to 1.8 micron support, the fact that the monoliths can be operated at much higher flow rates with lower back pressure has resulted in overall reduced separation time. Under typical experimental condition, various parameters such as capacity factor (k'), separation

factor (α), number of theoretical plates (plates/meter) etc for separation of lanthanides on different supports (25 cm length (5 μm), 5 cm length (1.8 μm), 3 cm length (1.8 μm) and 10 cm length monolith reversed phase supports) are compared (**Table.4.10**).

Table.4.10. Comparison of column parameters for separation of lanthanides

Experimental conditions: Mobile phase: 0.1 M α -HIBA + 0.01 M CSA, pH: 3.5, Flow rate: 2 mL/min

Lanthanides	Capacity factor (k')				Lanthanide pairs	Separation factor (α)			
	25 cm length (5 μm)	5 cm length (1.8 μm)	3 cm length (1.8 μm)	10 cm length monolith		25 cm (5 μm)	5 cm (1.8 μm)	3 cm (1.8 μm)	10 cm monolith
La	9.81	28.32	15.27	7.33	La:Ce	1.39	1.46	1.41	1.44
Ce	7.04	19.36	10.80	5.10	Ce:Pr	1.22	1.27	1.23	1.24
Pr	5.75	15.19	8.75	4.10	Pr:Nd	1.14	1.18	1.17	1.16
Nd	5.03	12.88	7.48	3.54	Nd:Sm	1.49	1.59	1.51	1.54
Sm	3.37	8.07	4.93	2.29	Sm:Eu	1.23	1.26	1.21	1.25
Eu	2.74	6.40	4.09	1.83	Eu:Gd	1.14	1.16	1.12	1.18
Gd	2.41	5.50	3.56	1.55	Gd:Tb	1.33	1.44	1.44	1.36
Tb	1.81	3.80	2.48	1.14	Tb:Dy	1.27	1.26	1.11	1.17
Dy	1.42	3.00	2.23	0.97	Dy:Ho	1.16	1.21	1.20	1.35

Capacity factor, k' ($k' = t_r - t_0 / t_0$); t_0 observed with 25 cm, 5 cm, 3 cm and 10 cm length columns are 1.31, 0.41, 0.32 and 0.80 respectively.

* Maximum pressure tolerance of monolithic columns: 200 bar

* Pressure for the delivery of mobile phase at a flow rate of 2 mL/min:

- 210 bar for 25 cm length (5 μm),
- 290 bar for 5 cm length (1.8 μm),
- 180 bar for 3 cm length (1.8 μm) and
- 38 bar for 10 cm length monolith reversed phase supports.

* Approximate number of theoretical plates (**plates/meter**):

- 37,000 for 25 cm length (5 μm),
- 70,000 for 5 cm length (1.8 μm),
- 1,00,000 for 3 cm length (1.8 μm) and
- 44,000 for 10 cm length monolith supports.

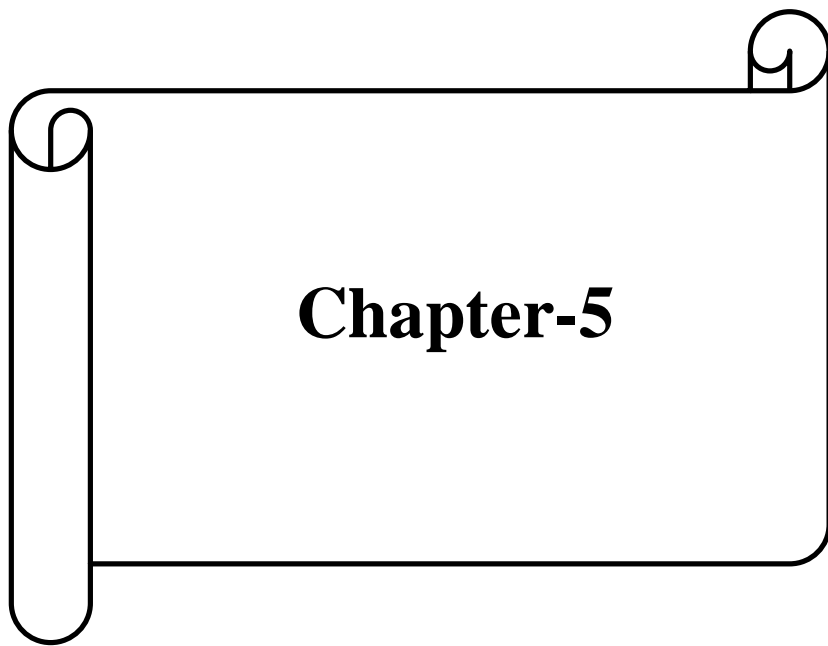
Based on the total number of plates that are available, the 25 cm length column is expected to give marginally better separation factor compared to the other two columns. This is because, the total number of separation stages / plates computed from a 25 cm length column (~ 9250 plates in total) are higher than one observed with monolith (~ 4400 in total) as well as with one obtained on a 1.8 micron based 3 cm length column (~ 3000 in total). However, it has been observed that the separation factors observed with both monolithic and 1.8 micron based 3 cm length columns are in general, marginally higher compared to the one observed with the 25 cm length 5 micron based support (**Table 4.10**). Further studies are required to understand this surprising trend, i.e. column behaviour during dynamic ion-exchange chromatographic experiments. The separations with 3 cm length (1.8 μm) as well as 10 cm length monolith columns are generally faster compared to 25 cm length (5 μm) column; this is because the separation factor achieved with 25 cm length could be achieved with use of only 3 cm in column length by the reduction in particle size to 1.8 micron.

The capacity factor, of lanthanides observed from 3 cm as well as 5 cm length (1.8 μm) columns is higher compared to the one observed with the 25 cm length (5 μm) column (**Table.4.10**). This is due to the lower void volume (t_0) observed with both 3 and 5 cm length (1.8 μm) columns compared to the 25 cm length (5 μm) column.

4.4 Conclusion

Monolithic columns were employed in a dynamic ion-exchange mode for the development of rapid separation of individual lanthanides using a monolith support in about 2.8 min, possibly the fastest liquid chromatographic procedure developed till date in literature. The BEHSA modified monolith supports offered rapid separation, excellent baseline resolution and higher separation factor for U and Th, compared to the bare monolithic

support. The development of rapid separation procedures using monolith based supports offer new avenues for detection and estimation of lanthanides and actinides in various stages of the nuclear fuel cycle.



Chapter-5

Chapter-5

Burn-up Measurement on Dissolver Solution of Nuclear Reactor Fuels using HPLC

5.1 Atom percent determination of burn-up on dissolver solution of a fast reactor fuel

5.1.1 Introduction

Estimation of burn-up is an important parameter for the study of fuel performance, an indication of energy production from unit mass of fuel [57, 63, 167-169]. The measurement of burn-up on dissolver solution of fast reactor fuel subjected to high burn-up is challenging due to the high levels of radioactivity associated with the fuel. Various methods have been developed to measure the burn-up of dissolver solution of spent nuclear fuels. Among these, isotope dilution mass spectrometric technique (IDMS) is a well established technique and is a classical method for the measurement of burn-up on nuclear reactor fuels [56, 64-66]. The schematic diagram indicating various steps of the IDMS technique is shown in **Fig. 5.1**. HPLC based technique has also been developed for rapid and accurate determination of burn-up of nuclear reactor fuels [47-48, 68, 170].

In this chapter, results on burn-up determination of Fast Breeder Test Reactor (FBTR) spent fuel using HPLC based rapid separation methods are discussed. The dynamic ion-exchange HPLC technique using small particle based support (1.8 μm) as well as monolith based support was employed for the first time for the determination of lanthanides and actinides and hence burn-up of FBTR spent fuel discharged at a burn-up of a ~ 155 GWd/t.

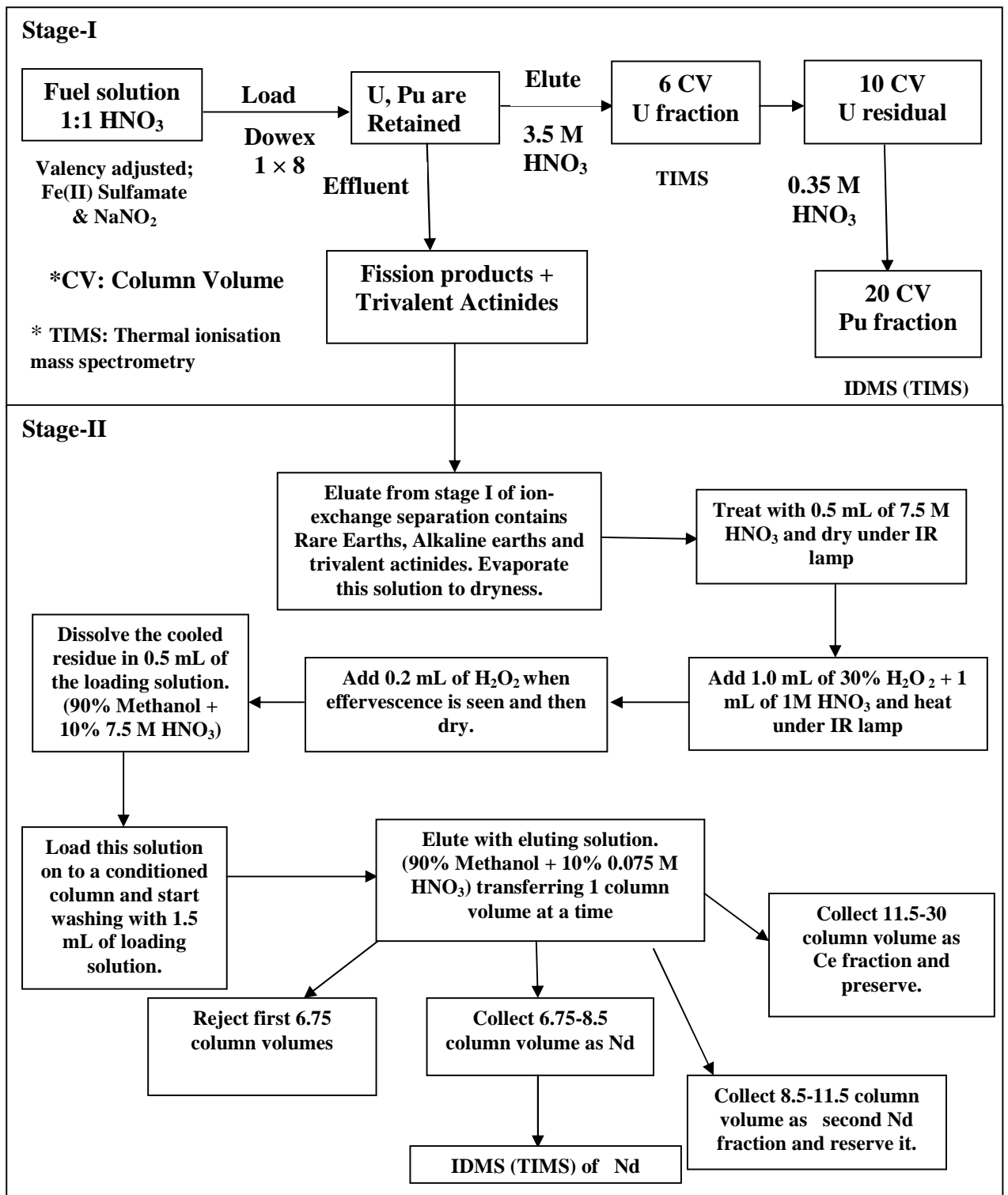


Fig.5.1. Schematic of mass spectrometric technique for burn-up determination on nuclear reactor fuels

In the initial studies, U and Pu present in the dissolver solution of FBTR fuel were removed by an ion-exchange chromatography. The fission product fraction after removal of U and Pu was subsequently injected into HPLC system for the assay of burn-up monitors i.e. La and Nd. Reversed phase chromatographic technique was employed for the determination of uranium and plutonium in the dissolver solution. Subsequently, HPLC technique using monolith support was demonstrated for the first time for the direct injection of dissolver solution from FBTR without any pre-separation of matrix uranium and plutonium. The atom percent fission was determined based on these measurements and the results are discussed.

5.1.2 EXPERIMENTAL

5.1.2.1 Studies involving dissolver solution of spent fuel (FBTR)

The U-Pu mixed carbide pellets from the fuel pin irradiated in FBTR with a nominal burn-up of about 1,55,000 MWd/t were dissolved in 12 M HNO₃ medium [48]. In some experiments, U and Pu present in dissolver solution were separated from fission products on an anion exchange column (Dowex Anion exchange, 100-200 mesh, 1×8 mm) using 1:1 HNO₃ medium. Uranium and plutonium were eluted from the column subsequently using 3 N HNO₃ and 0.5 N HNO₃ respectively. Lanthanide fission products, uranium, and plutonium fractions were brought into 0.01 N HNO₃ medium as a feed for their individual separation using HPLC. In a few experiments, the dissolver solution containing U, Pu, and lanthanides and other fission products in HNO₃ medium was evaporated to near dryness, re-dissolved in 0.01 N HNO₃ (or α -HIBA medium) and directly injected into the HPLC system for the assay of lanthanides, uranium and plutonium with appropriate dilutions.

5.1.3 RESULTS AND DISCUSSION

5.1.3.1 Estimation of lanthanides in dissolver solution of fast reactor fuel using small particle (1.8 μm) based support

The lanthanides present in dissolver solution of the spent fuel were mutually separated using dynamic ion-exchange with 3 cm length column (1.8 μm) and the resultant chromatogram is shown in **Fig.5.2**. All lanthanides were eluted in about 4.2 min.

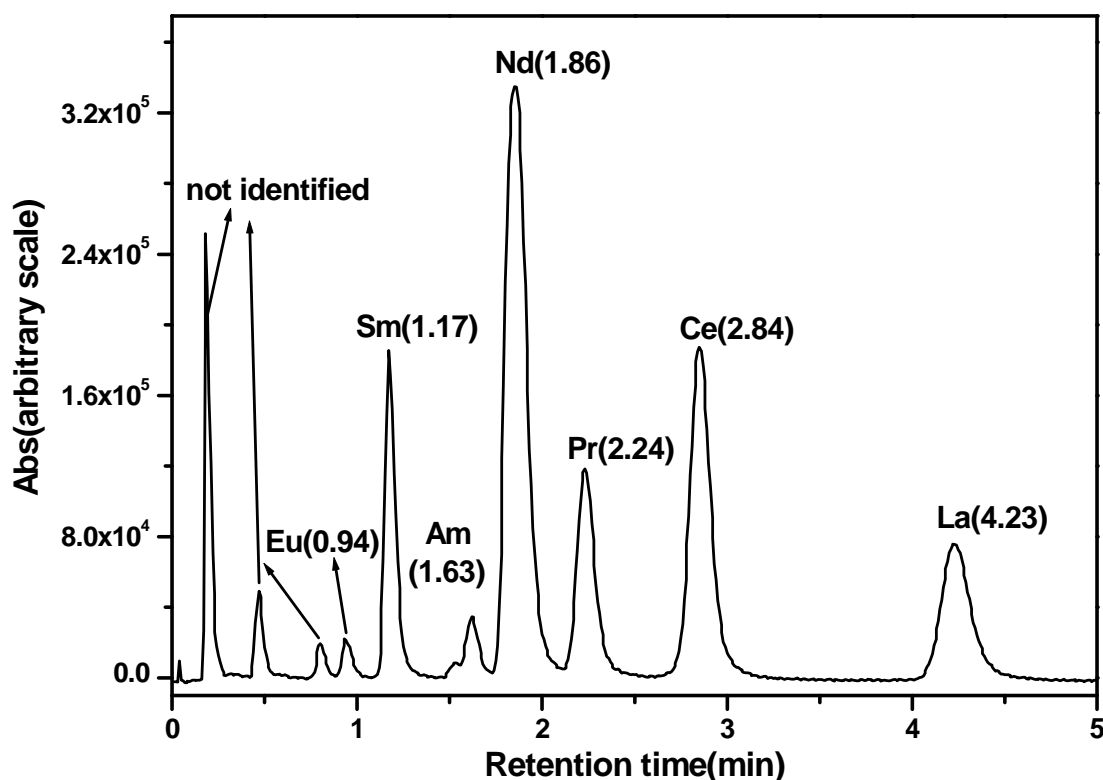


Fig.5.2. Separation of individual lanthanide fission products from dissolver solution using 1.8 μm based support. Column: 3 cm length 1.8 μm reversed phase. Mobile phase: 0.1 M α -HIBA and 0.02 M CSA; pH: 3.6; Flow rate: 4 mL/min. Detection: PCR with arsenazo(III) at 655 nm.

5.1.3.2 Separation and determination of lanthanides in dissolver solution of fast reactor fuel using monolith support

In the initial studies, the lanthanide fraction after the removal of U and Pu by anion exchange chromatography was employed for the determination of Nd or La concentration in

the dissolver solutions. However to reduce the overall separation time, direct injection of dissolver solution was also investigated and the results are shown in **Fig.5.3**.

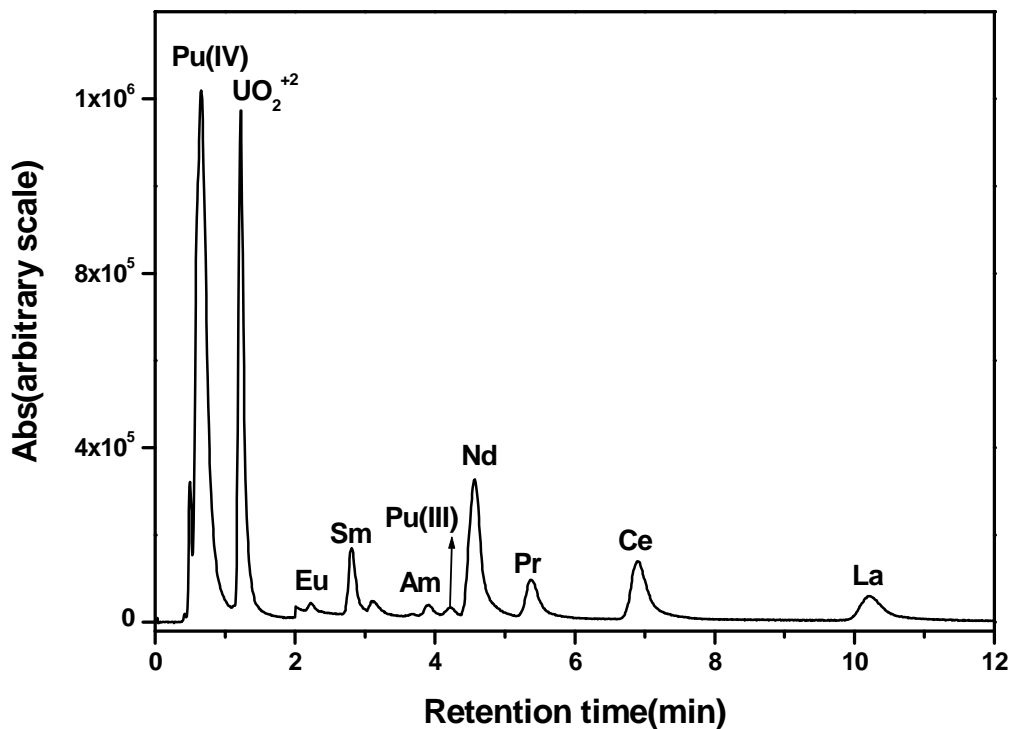


Fig.5.3. Direct injection of dissolver solution (burn-up~ 155 Gwd/ton) using monolith support. Column: 10 cm length monolith; Mobile Phase: 0.03 M CSA + 0.06 M α -HIBA; pH: 3.61; flow rate: 4 mL/min; PCR flow rate: 1 mL/min; Detection: 655 nm; Sample: dissolver solution evaporated and re-dissolved in α -HIBA medium.

The lanthanides present in the dissolver solution were mutually separated as well as resolved from uranium and plutonium under dynamic ion-exchange conditions from monolithic column. The concentration of La, Ce, Pr, Nd, and Sm were determined in the dissolver solution using a calibration plot. The fission product monitor, lanthanum present in dissolver solution was well separated from uranium and Pu(IV) in about 1.8 min under the experimental condition with 0.01 M CSA + 0.1 M α -HIBA; pH: 3.6 and flow rate: 5 mL/min (**Fig.5.4**). The concentration of lanthanum measured under these conditions agreed well with the results of the experimental conditions used in **Fig.5.3**.

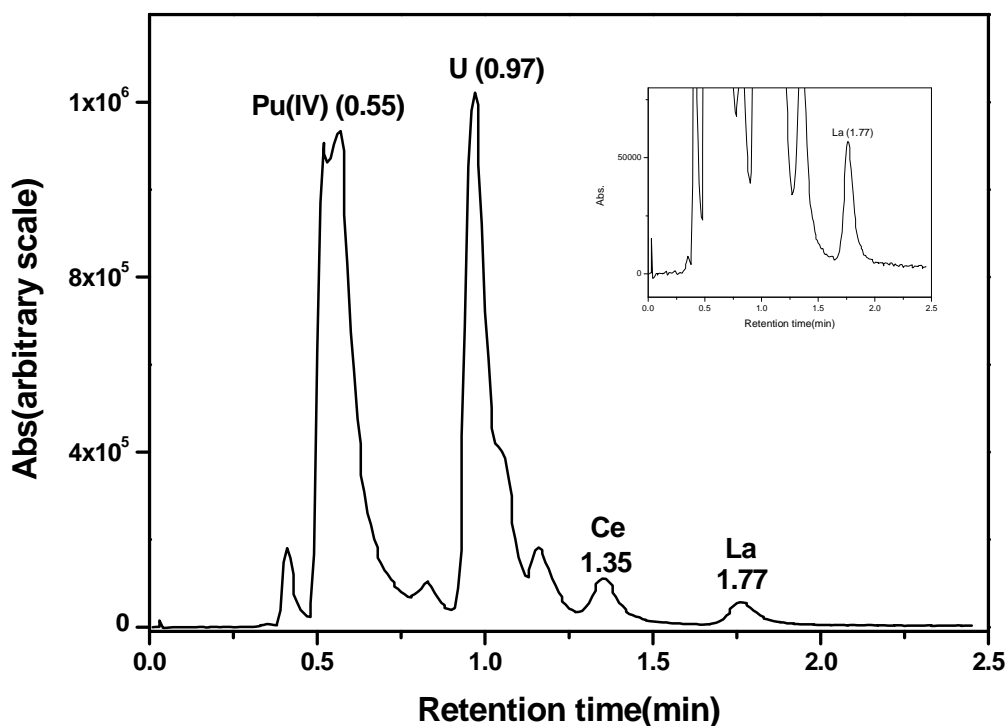


Fig.5.4. Separation and estimation of lanthanum from uranium and plutonium present in dissolver solution in 1.8 min using monolith support. Column: 10 cm length monolith; Mobile Phase: 0.01 M CSA + 0.1 M α -HIBA; pH: 3.6; flow rate: 5 mL/min; PCR flow rate: 1 mL/min; Detection: 655 nm; Sample: Dissolver solution in 0.1 M α -HIBA. Inset: La (t_r : 1.77 min) isolated from U, Pu and other fission products in the dissolver solution.

The concentrations of lanthanides (La, Ce, Pr, Nd and Sm) and actinides (U and Pu) in the dissolver solution of fast reactor fuel were estimated using (A) small particle based and (B) monolith supports and the results are shown in **Table.5.1**. Data on the atom percent burn-up determined using La and Nd as fission monitors are also included. These studies established that the dynamic ion exchange HPLC technique using reversed phase supports can be used for direct assay of lanthanides present in the dissolver solution without the need for pre-separation of the matrix component, U and Pu.

Table.5.1. Estimation of lanthanides, uranium and plutonium in dissolver solution using (A) small particle and (B) monolith supports for measurement of atom percent burn-up

Element	(A)		(B)	
	Estimation on small particle (3 cm length with particle size 1.8 µm) based support		Estimation on monolith (10 cm length) based support	
	Concentration (per gram of dissolver solution)	Atom percent burn-up	Concentration (per gram of dissolver solution)	Atom percent burn-up
La	144 µg/g	15.7	166.6 µg	16
Ce	251 µg/g		283.1 µg	
Pr	139 µg/g		152.4 µg	
Nd	410 µg/g	15.4	474.5 µg	15.7
Sm	122 µg/g		133.7 µg	
U	8.0 mg/g		9.05 mg	
Pu	14.7 mg/g		16.7 mg	

** A and B: Two different aliquots of dissolver solution*

Lanthanide fission products such as Nd and La satisfy the major requirements of a fission monitor, as they are stable, do not migrate appreciably in the fuel and have large and well known fission yields [38]. The fission yield of La for Pu-239 and U-238 fast fission differs by about 3.53% (^{139}La yield for the fast fission of Pu-239 and U-238 is 5.83 and 6.04 respectively; the yields are expressed as the number of fission product atoms formed in one hundred fissions). Thus neglecting the contribution by U-238 in the formation of La would result in only a maximum error of about 3–4 % in the fission yield calculation. Hence, La is

an ideal fission monitor despite of its yield being one third of that of Nd. Moreover, the fission product “La” is essentially monoisotopic, (^{139}La) and thus allows use of chemical techniques for its assay. The use of Nd as fission monitor demands calculation of the individual yields both from U-238 and Pu-239 as they differ by about 23 % i.e. total Nd yield for Pu-239 and U-238 fast fission is 16.41 and 20.22 respectively. As the fuel employed in the FBTR is plutonium rich (70 % PuC and 30 % UC), the La and Nd yields corresponding to Pu-239 were employed to compute the burn-up. The atom percent fission obtained for fast reactor fuel using total La, i.e. essentially ^{139}La as fission monitor showed good agreement with the use of total Nd (^{143}Nd , ^{144}Nd , ^{145}Nd , ^{146}Nd , ^{148}Nd and ^{150}Nd) as fission monitor.

5.1.3.3 Separation and determination of U and Pu in dissolver solution of fast reactor fuel using small particle (1.8 μm) based support

The uranium present in dissolver solution of the spent fuel was separated from plutonium using reversed phase HPLC with 3 cm length column (1.8 μm) and the resultant chromatogram is shown in **Fig.5.5 and Fig.5.6**. U(VI) is well separated from Pu(III) as well as Pu(IV). The concentrations of total uranium in the dissolver solution (**Table.5.1**) were determined using calibration plots. The retention times for Pu(III) as well as Pu(IV) were identified by individually injecting these samples (pure Pu(III) and Pu(IV)) in reversed phase HPLC system. The retention of Pu(III) is almost comparable to that of lanthanides. These studies indicated that Pu(IV)-hydroxy isobutyrate complexes are more hydrophobic compared to Pu(III) complexes and hence Pu(IV) is eluted later. However for the quantitative analysis, Pu was reduced to Pu(III) and its concentration in dissolver solution was obtained using a calibration plot, which was prepared using plutonium standards.

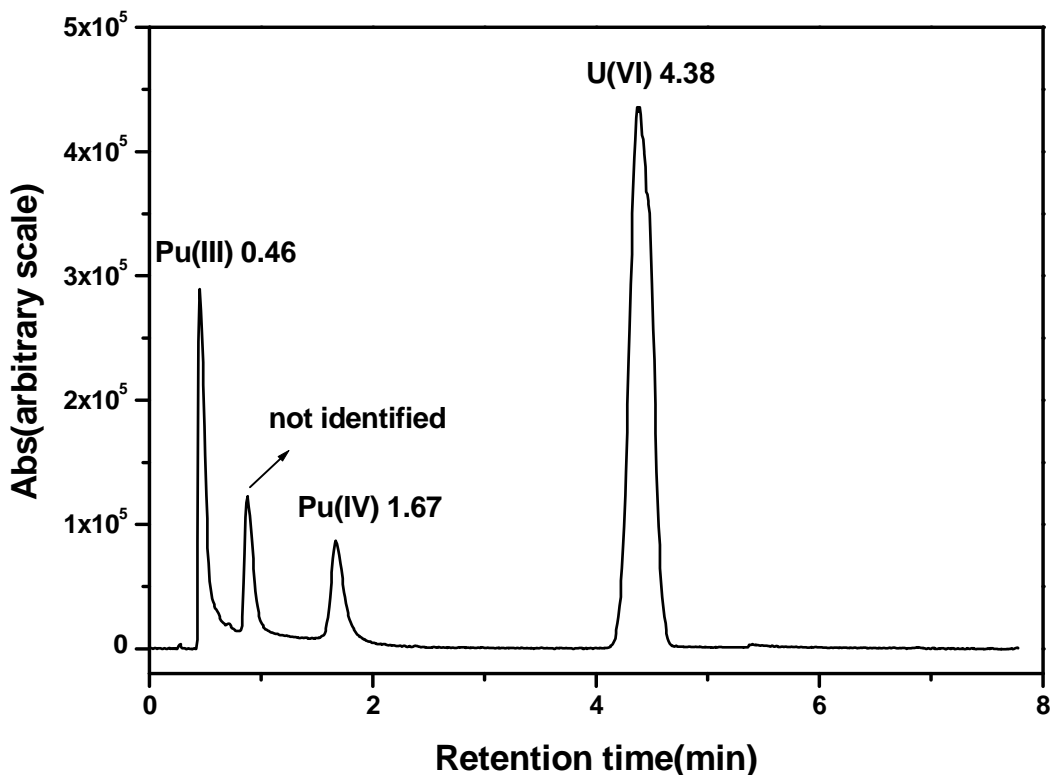


Fig.5.5. Injection of dissolver solution into small particle (1.8 μm) based reversed phase support after separation from fission products by anion exchange. Column: 3 cm length 1.8 μm reversed phase; Mobile phase: 0.1 M α -HIBA, pH: 3.5, flow rate: 2 mL/min; Detection: PCR with arsenazo(III) at 655 nm (fraction collected, redissolved in 0.01 N HNO_3).

However, the retention or capacity factors of Pu(IV) are lower compared to U(VI) which is possibly due to the formation of anionic species e.g. $[\text{Pu}(\text{IBA})_4(\text{OH})_2]^{2-}$, similar to thorium, which is expected to have a lower retention on a hydrophobic support. These studies indicated that uranium-hydroxy isobutyrate complexes are more hydrophobic compared to Pu(III) as well as Pu(IV) complexes. The concentration of uranium in the dissolver solution was also estimated by the Davis-Gray technique [151]. The HPLC results were found to be within $\pm 1\%$ with Davis-Gray method. The reversed phase HPLC technique also showed promising features for the assay of plutonium in its various oxidation states.

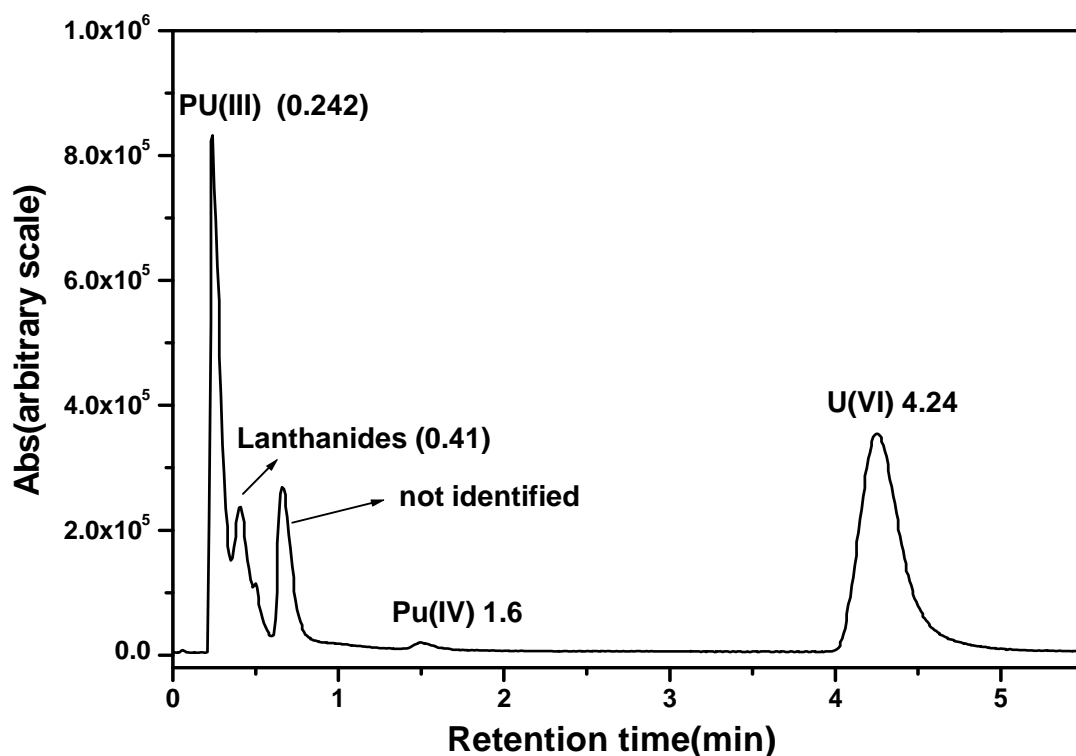


Fig.5.6. Direct injection of dissolver solution into small particle (1.8 μm) based without any pre-separation. Column: 3 cm length 1.8 μm reversed phase support; Mobile phase: 0.1 M α -HIBA, pH: 3.5, flow rate: 2 mL/min; Detection: PCR with arsenazo(III) at 655 nm (dissolver solution was diluted in 0.01 N HNO_3).

5.1.3.4 Separation and determination of uranium and plutonium using monolithic column

Uranium and plutonium present in dissolver solution were determined by both dynamic ion-exchange and reversed phase chromatographic techniques. Uranium as well as plutonium were not determined in the same run along with lanthanides since the U and Pu peaks showed near saturation during the assay of the lanthanide fraction. Hence, the dissolver solution was directly injected after appropriate dilution for the determination of uranium or plutonium. Experimental conditions, nearly similar to one employed in **Fig.5.3** were used for the assay of uranium, Pu(IV) and Pu(III) (**Fig.5.7**).

The reversed phase HPLC technique using monolith support was also employed in the present study for the determination of uranium (**Fig.5.8**) and Pu(III) (**Fig.5.9**). The results are found to be in good agreement ($\pm 2\%$) with the one obtained using the dynamic ion-exchange technique.

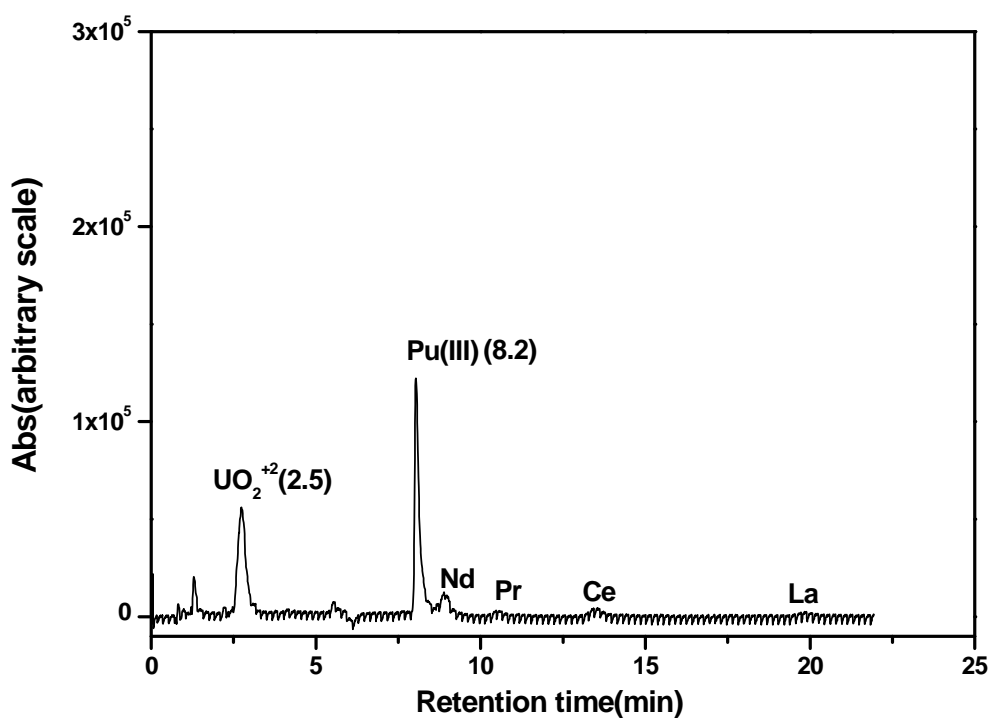


Fig.5.7. Direct injection of dissolver solution for uranium and plutonium assay by dynamic ion exchange. Column: 10 cm length monolith; Mobile Phase: 0.03 M CSA + 0.06 M α -HIBA; pH: 3.61; flow rate: 2 mL/min; PCR flow rate: 1 mL/min; Detection: 655 nm; Sample: dissolver solution (in 0.01 N HNO_3) + hydroxylamine hydrochloride (Pu reduced to Pu(III)).

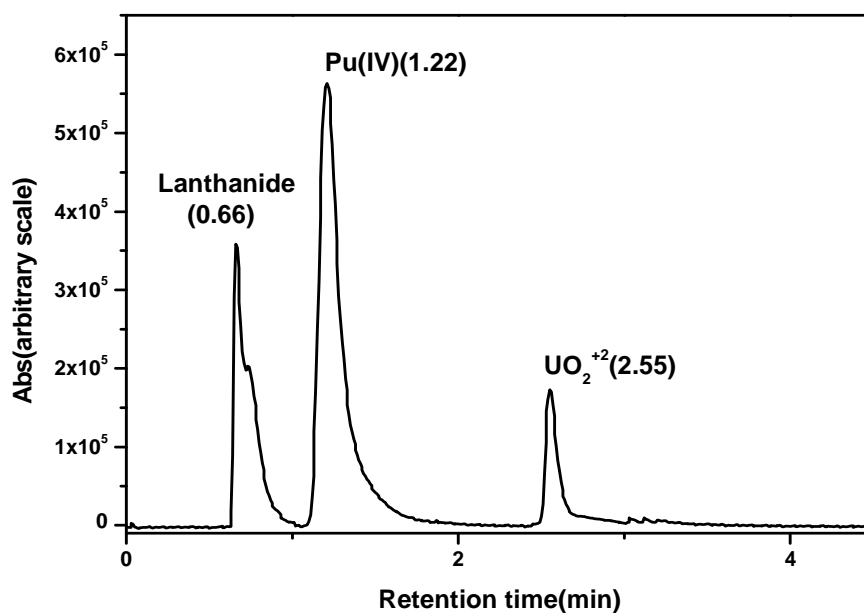


Fig.5.8. Direct assay of uranium present in dissolver solution using reversed phase monolith support. Column: 10 cm length monolith; Mobile Phase: 0.1 M α -HIBA; pH: 3.2; flow rate: 2.5 mL/min; PCR flow rate 1 mL/min; Detection: 655 nm; Sample: Dissolver solution in 0.01 N HNO₃ medium; 20 μ L injected. (NaNO₂ was added to keep Pu in Pu(IV) state)

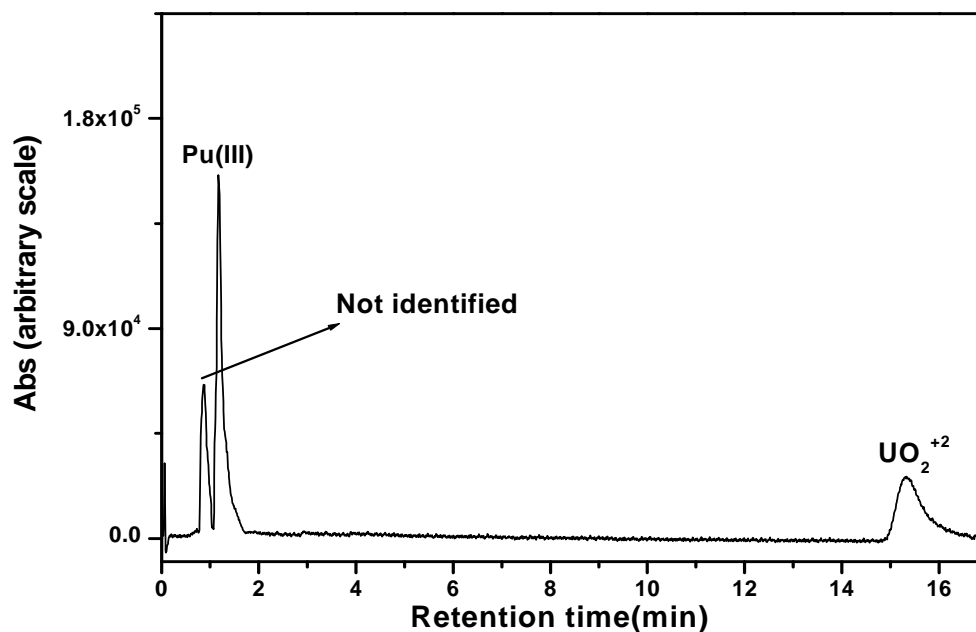


Fig.5.9. Direct plutonium assay from dissolver solution using reversed phase monolith support. Column: 10 cm length monolith; Mobile Phase: 0.1 M α -HIBA; pH: 4.2; flow rate: 2 mL/min; PCR flow rate: 1 mL/min; Detection: 655 nm; Sample: dissolver solution in 0.01 N HNO₃ + hydroxylamine hydrochloride (Pu in Pu (III)).

5.1.3.5 Identification of americium in dissolver solution

Americium, the minor actinide, present in the dissolver solution was identified by injecting pure Am(III) and measuring its retention time (**Fig.5.10**). The “Am” fraction was also collected and analysed using a HP Ge detector. These studies established the potential application of the LC technique for “Am fraction collection” as well as its assay in dissolver solutions, HLW etc.

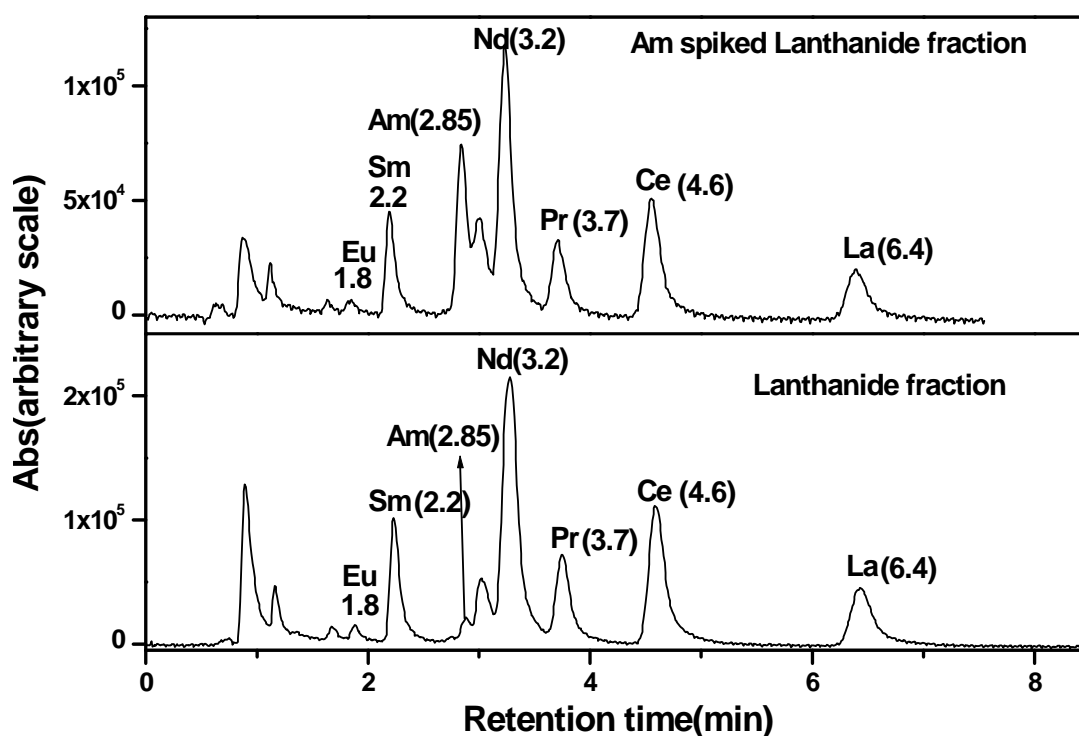


Fig.5.10. Identification of Am from dissolver solution. Column: 10 cm length monolith; Mobile Phase: 0.015 M CSA + 0.1 M α -HIBA; pH: 3.4; flow rate: 3 mL/min; PCR flow rate: 1 mL/min; Detection: 655 nm. (In these experiments major amount of U and Pu was removed prior to identification of Am)

5.1.3.6 Minimisation of radiation exposure and waste

The contact radiation dose for about 0.1 g diluted dissolver solution was found to be ~ 0.3 mSv (0.1 g of the dissolver solution was containing 17 μ g La, 47 μ g Nd, 900 μ g of U and 1670 μ g of Pu). In this part of work, typically 0.1 g of the dissolver solution was diluted

with HNO₃ / HIBA medium and directly injected into the HPLC for the determination of lanthanide fission products, uranium, and plutonium. The development of the rapid separation technique using monolith, which resulted in isolation of “La” from the dissolver solution in about 1.8 min, Pu(III) from other actinides and fission products in 1.18 min, and that of UO₂⁺² from other actinides and fission products in about 1.35 min resulted in the minimization of radiation exposure to the personnel. Though it is difficult to quantify at this stage, the reduction in separation times of U, Pu, and La’s achieved in the present work, would probably reduce the overall exposure easily by about 10 times. The overall reduction in separation time also reduces the waste that is generated during the course of the campaign.

5.1.4 Conclusion

The rapid separation techniques using small particle based (1.8 µm) as well as monolith based supports were demonstrated for the assay of uranium, plutonium, and lanthanides present in the dissolver solution of a fast reactor fuel discharged at about 155 GWd/ton. The dynamic ion-exchange technique was employed for measuring the concentrations of fission product lanthanides such as La, Ce, Pr, Nd and Sm in the dissolver solution of fast reactor fuel.

Uranium and plutonium concentrations were measured accurately in the dissolver solution of fast reactor fuel using reversed phase as well as dynamic ion-exchange based HPLC techniques. A dynamic ion exchange chromatographic technique was also developed for the identification of the minor actinide, americium.

5.2 Determination of lanthanides in uranium matrix using single stage double column chromatography and its application to burn-up measurement of nuclear reactor fuels

5.2.1 Introduction

The most common method for the determination of lanthanides in uranium matrix involves removal of uranium by a suitable technique such as solvent extraction [171-172], extraction chromatography [100] and anion-exchange followed by determination of lanthanides using liquid chromatography, ICP-AES etc. In one of the studies [100], lanthanide fission products present in dissolver solution of nuclear reactor fuel were separated from uranium matrix using a di-(2-ethylhexyl phosphoric acid) (HDEHP) coated column. In some studies, lanthanides and uranium present in comparable levels was separated and determined [68, 112, 173]. Separation of lanthanides as group i.e. total lanthanides in uranium matrix of salts from pyrochemical studies using extraction chromatographic technique was also reported [105-106].

In the determination of lanthanides in uranium matrix, e.g. lanthanide impurity in the pellets of UO_2 demands development of HPLC technique where uranium to lanthanides ratio could be $10^5:1$ to as high as $10^6:1$. Moreover, loading analytical column with large amounts of uranium during HPLC run results in long regeneration times for subsequent analysis. In one of the technique reported in literature [174], uranium matrix was removed on a semi-preparative reversed phase column (21.2×100 mm, reversed phase C_{18}) and lanthanides were separated subsequently on a cation exchange column using single stage chromatographic method. In these studies, uranium containing solution with a concentration as high as 5 mg/mL was injected into the liquid chromatographic system; using 20 mg uranium loading onto the column, lanthanide impurities in uranium matrix were

determined. To avoid use of expensive preparative columns and also for the multiple analysis of lanthanide fission products such as Sm, Pr and Nd in uranium matrix, a single stage dual column chromatographic technique has been developed in the present work to overcome the difficulties associated with uranium interference.

Organophosphorous compounds are attractive candidates for the extraction of actinides [175-182] and their extraction efficiency in ascending order is phosphates, phosphonates, phosphinites and phosphine oxides. The most widely used neutral extractants are tri-n-butylphosphate (TBP) and tri-n-octyl phosphine oxide (TOPO). TOPO offers a very high distribution ratio for uranium and lower distribution ratio for lanthanides and other fission products [183] and hence a promising candidate for pre-concentration of uranium by extraction chromatographic technique. Since its aqueous phase solubility is very low, it is an attractive candidate for holding uranium during extraction chromatographic technique. Extraction of uranium with TOPO can be represented as



This chapter also deals with the separation and determination of lanthanides in uranium matrix using single stage dual column HPLC technique. In these studies, two columns were connected in a series, first column (5 cm length reversed phase support) modified with TOPO for holding uranium and the second one, an analytical column (10 cm length monolithic reversed phase support, modified into a cation exchange column by ion-interaction chromatography, with an ion pairing reagent, CSA) for individual separation of lanthanides. During a chromatographic run, uranium is retained in the first column by complex formation with TOPO and lanthanides are passed on to the second column, where they get isolated from each other. Samples of lanthanides in uranium matrix of various proportions were injected into the coupled dual column for separation and determination of

lanthanides in uranium matrix. Studies were carried out to study the factors affecting the retention of uranium, lanthanides and other fission products such as Zr, Mo, Cs, Ba, Sr, Ru, Rh, and Pd on the TOPO modified column. Based on these studies, a single stage coupled column chromatographic method has been developed for the rapid and accurate determination of lanthanides in uranium matrix. The technique was demonstrated for the determination of atom percent burn-up on the dissolver solution from a PHWR nuclear reactor fuel (MAPS, Kalpakkam, India) and the results are discussed. The retention behavior of Pu(III), Pu(IV), and Am(III) was also investigated on the coupled column. Subsequently, the lanthanide fission products were separated and determined from a dissolver solution of a fast reactor fuel (FBTR) and these results are discussed.

5.2.2 EXPERIMENTAL

5.2.2.1 Column-1:

5.2.2.1.1 Preparation of TOPO modified reversed phase (5 cm length) support

TOPO modified support was prepared by passing a solution of TOPO (100 mL) through a reversed phase support at a typical flow rate of 0.2 mL/min. TOPO solutions were prepared in a methanol-water mixtures (typically, 75:25 v/v methanol to water). Higher methanol content was employed in some studies to ensure complete dissolution of TOPO. Acetone-water mixture was also employed in one of these studies to prepare TOPO modified support. When the coating was completed, the column was washed with about 20 mL water. After the completion of studies with a particular TOPO sorbed support, the same was washed and removed completely with ~ 25 mL of methanol. The same 5 cm length column was reused for all studies carried out in the present work. All the experiments were carried out at 25°C. The amount of TOPO sorbed / coated onto the support was determined by gravimetry (**Table.5.2**).

5.2.2.1.2 Preparation of TOPO modified 25 cm (4.6 mm dia) length reversed phase support

TOPO coated 25 cm length reversed phase support was prepared by passing 3.91 mmol TOPO (TOPO dissolved in 500 mL of methanol (71%)–water (29%) mixture) through a 25 cm length reversed phase support at a flow rate of 0.25 mL/min. Actual amount of TOPO coated on to the column was estimated by gravimetry (**Table.5.2**).

Table.5.2. Preparation of TOPO modified 5 cm and 25 cm length support: coating solutions and % sorption

Reversed phase supports	Coating solution (%)	Amount of TOPO passed (mmol)	Amount of TOPO coated (mmol)	% TOPO sorbed on column
5 cm	MeOH-Water (84: 16)	1.33	0.16	12.2 %
	MeOH-Water (75 : 25)	1.13	0.21	18.6 %
	MeOH-Water (75 : 25)	1.44	0.28	19.4 %
	MeOH-Water (70 : 30)	1.85	0.43	23.2 %
	MeOH-Water (70 : 30)	2.20	0.54	24.6 %
	Acetone-Water (65 : 35)	2.20	0.12	5.5 %
25 cm	MeOH-Water (71 : 29)	3.91	1.60	40.92%

5.2.2.2 Column-2: Modification of 10 cm length reversed phase monolithic support into a dynamic ion-exchange column

The reversed phase monolith support was modified into a dynamic ion-exchange column using water soluble ion-pairing reagent, CSA. A mobile phase solution (CSA+ α -HIBA) was passed through the reversed phase support (typically 30 mL) to establish a dynamic ion-exchange surface, after which samples were introduced into the HPLC system for separation.

5.2.2.3 Dissolution of spent fuel (PHWR)

The fuel pellets (UO_2) from the PHWR fuel pin were dissolved in boiling 8 M HNO_3 medium [49]. The dissolver solutions containing U, Pu, and fission products in HNO_3 medium were evaporated to near dryness, re-dissolved in 1 N HNO_3 medium. The dissolver solution was directly injected into the HPLC system with appropriate dilutions using 0.01 N HNO_3 medium for assay of lanthanides, uranium and plutonium.

5.2.3 RESULTS AND DISCUSSION

5.2.3.1 Separation of lanthanides in U matrix on analytical column

In dynamic ion-exchange chromatographic technique, lanthanides such as Sm and Nd could be well separated from uranium, only if lanthanide to uranium ratio does not exceed 1:500. When lanthanide to uranium ratio was raised to 1:1000, lanthanides such as Sm, Nd and Pr could not be resolved from matrix uranium (**Fig.5.11**). Thus for samples with higher uranium to lanthanide ratio, e.g. 2000:1, individual lanthanides could not be separated from each other and determined in a single chromatographic run because of uranium interference. This will be the case for dissolver solutions from PHWR subjected to a burn-up of around 5000 MWd/ton, where uranium to neodymium ratio could be \sim 2000:1. Considering these aspects, a coupled dual column chromatographic technique has been

developed in the present study to overcome the difficulties associated with uranium interference during the quantitative determination of lanthanide fission products such as Sm, Pr, and Nd in the uranium matrix.

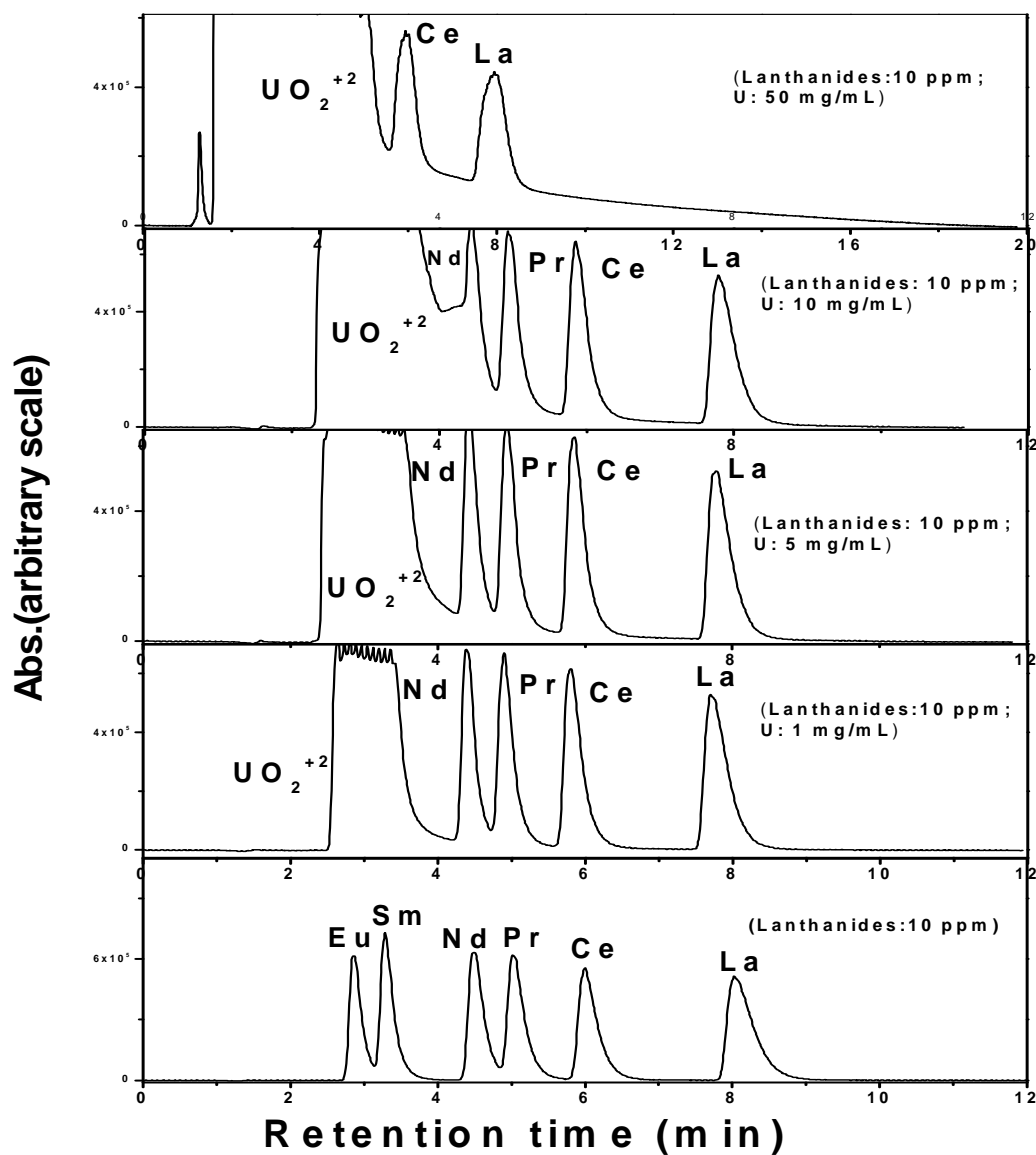


Fig.5.11. Separation of individual lighter lanthanides on a monolithic column in the presence of uranium. Column: 10 cm length reversed phase monolithic column; Mobile phase: 0.1 M α -HIBA + 0.015 M CSA; pH: 3.52; Flow rate: 2 mL/min; PCR flow rate: 0.5 mL/min; Detection: 655 nm; Sample: Lanthanides (La, Ce Pr, Nd, Sm and Eu; 10 ppm each) and U (up to 50 mg/mL) in 0.01 N HNO_3 ; 100 μ L sample injected.

5.2.3.2 Separation of lanthanides from uranium matrix using single stage double column chromatographic method

Individual separation of lanthanides from each other as well as from uranium matrix was studied using single stage double column chromatographic technique. In this technique, TOPO coated 5 cm length reversed phase support was connected in a series ahead of an analytical column, which was dynamically modified into a cation exchanger using CSA.

In this method, uranium & lanthanides solutions were injected directly into the HPLC system containing the dual (coupled) column in series. The schematic of double column chromatography for separation of lanthanides from uranium matrix is shown in Fig.5.12.

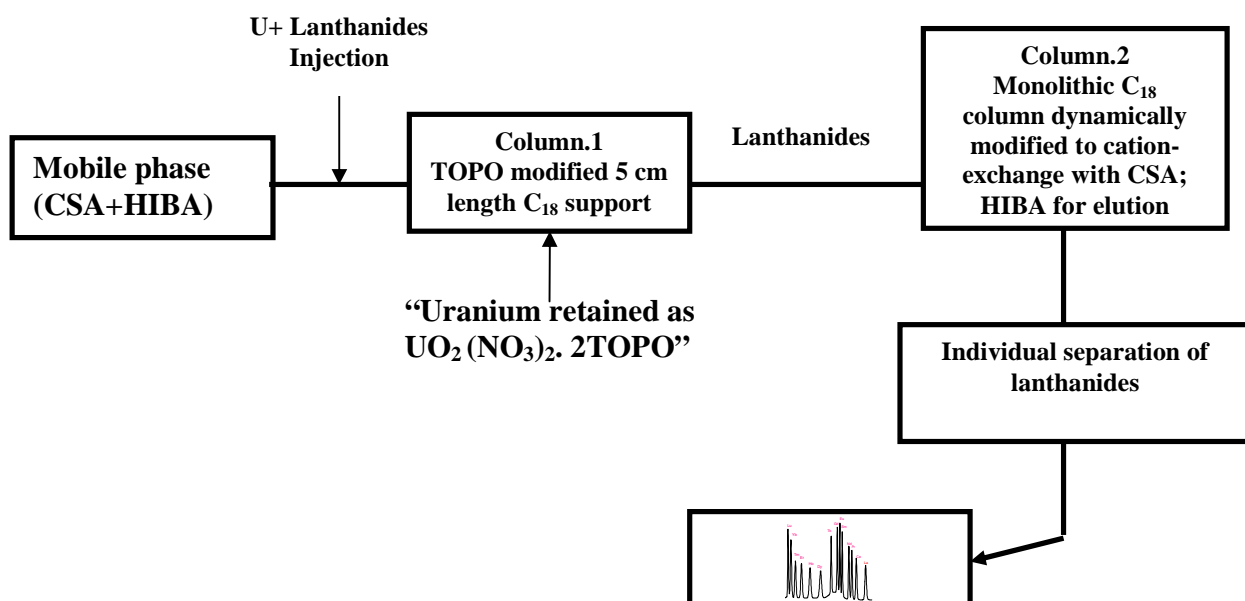


Fig.5.12. Schematic of single stage dual column chromatographic technique for separation of lanthanides in uranium matrix

Separation of individual lanthanides on a monolithic column using dynamic ion-exchange chromatographic technique was studied with and without use of TOPO coated column (Fig.5.13). A mobile phase consisting of CSA (0.015 M) and α -HIBA (0.1M) was

employed for isolation of individual lanthanides. Initially lanthanide separation was carried out on dynamically modified monolithic column (without TOPO coated column) and total separation time was 8.63 min. Under similar experimental conditions, separation of lanthanides was studied by connecting two columns in series, i.e. TOPO sorbed support was the first, followed by dynamically modified analytical column. The total separation time of lanthanides was marginally enhanced and was found to be 9.02 min. The separation factor of some adjacent lanthanides was calculated and the results are given in **Table.5.3**. These studies have established that TOPO coated support did not affect the performance of analytical column and hence TOPO coated column was connected ahead of a monolithic analytical column for the separation and determination of lanthanides in uranium matrix.

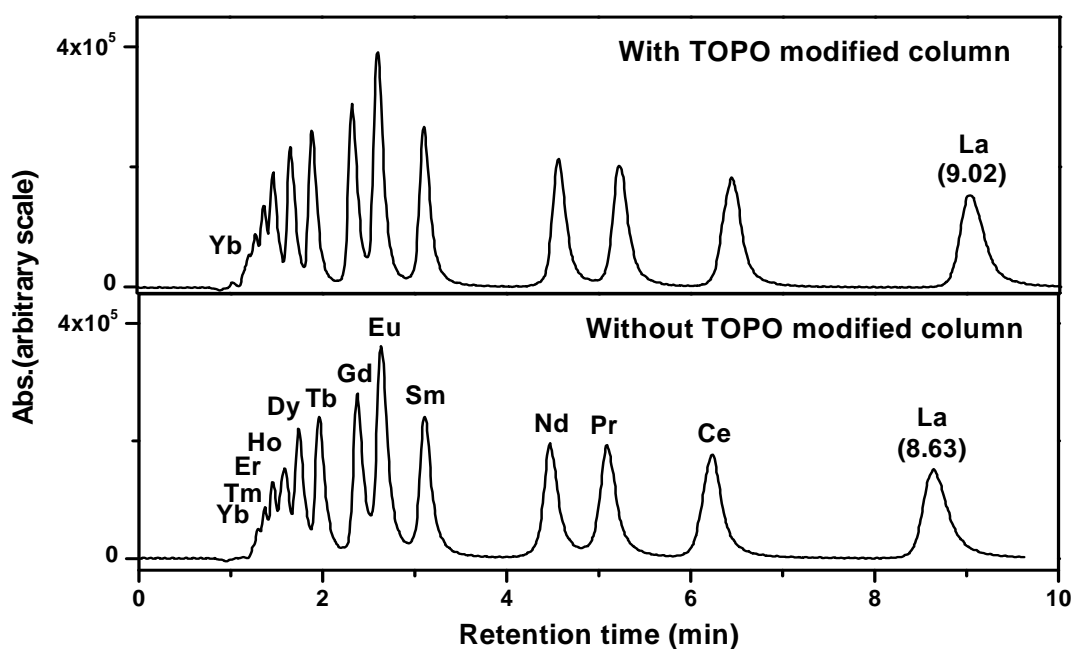


Fig.5.13. Separation of lanthanides using dynamic ion-exchange chromatography with and without connecting TOPO coated column. Columns: 5 cm length TOPO coated column (0.21 mmol sorbed); Analytical column: 10 cm length reversed phase monolith support; Mobile phase: 0.1 M α -HIBA + 0.015 M CSA; pH: 3.5; Flow rate: 2 mL/min; PCR flow rate: 0.5 mL/min; Detection: 655 nm; Sample: Lanthanides (~ 10 ppm) in 0.01 N HNO₃; 20 μ L injected.

Table.5.3. Separation factors for some adjacent lanthanides on a monolithic column with and without TOPO coated column

Lanthanides	Separation factor(α)	
	Monolithic column only	Dual column (TOPO coated column + monolithic column)
La:Ce	1.44	1.45
Ce:Pr	1.26	1.27
Pr:Nd	1.17	1.16
Nd:Sm	1.59	1.60
Sm:Eu	1.26	1.27
Eu:Gd	1.14	1.15
Gd-Tb	1.37	1.37
Tb-Dy	1.29	1.29

Columns used. **Study.1.** 10 cm monolith support only; **Study.2:** Column.1: 0.21 mmol TOPO sorbed 5 cm length support+Column.2: 10 cm length monolith; Mobile phase: 0.1 M α -HIBA + 0.015 M CSA; pH: 3.5; Flow rate: 2 mL/min.

5.2.3.3 Breakthrough studies on TOPO coated column

Initially uranium loading capacity on the TOPO coated column was investigated. Breakthrough studies were carried out on a 0.21mmol TOPO loaded support and a profile under typical experimental condition is shown in **Fig.5.14**. In this study, a uranium solution of 25 μ g/mL in 0.01 N HNO₃ medium was passed through the column at a flow rate of 0.5 mL/min. 100% breakthrough was observed after passing about 260 mL of solution. About 6.3 mg of uranium could be loaded on to the column during these studies. These studies have established that lanthanides in uranium matrix can be directly injected for selective sorption of uranium during chromatographic runs. Similar studies were also carried out with 0.54 mmol TOPO sorbed support and the uranium loading capacity was found to be ~15 mg under the above experimental conditions.

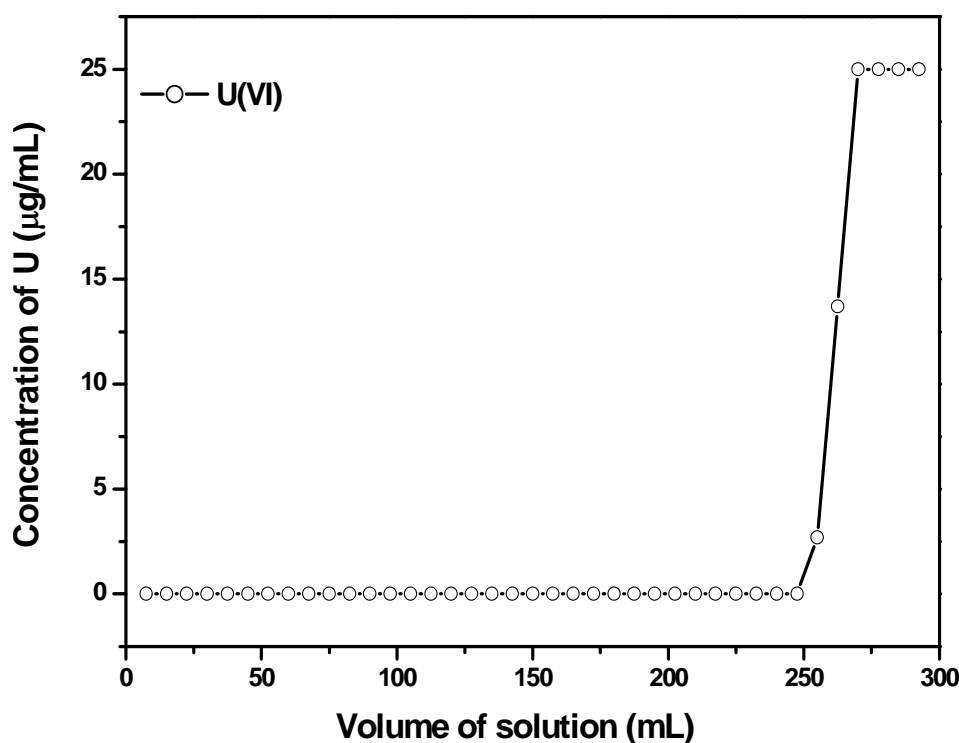


Fig.5.14. Breakthrough profile of uranium on TOPO coated support. U(VI) solution (25 ppm in 0.01 N HNO₃) was passed through a TOPO sorbed 5 cm length reversed phase support. Flow rate: 0.5 mL/min; Actual amount of TOPO sorbed on the reversed phase support was 0.21 mmol.

5.2.3.4 Separation of lanthanides from uranium matrix: Influence of TOPO content on the separation

The separation of individual lanthanides from uranium matrix was studied using coupled column method. In these studies, the uranium loading capacity of 0.12, 0.16, 0.21, 0.39, 0.44 and 0.54 mmol TOPO sorbed columns were investigated. Samples of lanthanide (e.g. 4 µg/mL) in uranium matrix were injected (20 µL) consecutively into the HPLC system, i.e. after the elution of last lanthanide, lanthanum, the next sample was injected and so on. The results of these studies are shown in **Table.5.4**. For example, when sample solutions containing lanthanides (4 µg/mL) with uranium (10 mg/mL) were injected into the HPLC with coupled column consisting of 0.54 mmol sorbed TOPO support and a

monolithic column, 27 consecutive injections could be performed for separation and determination of lanthanides in uranium matrix (**Fig.5.15**). Uranium elution was observed during the 28th injection of the sample, i.e. the overloaded uranium from the first column (TOPO sorbed support) was transferred to the analytical column (second column), from where it was eluted. Thus, 7, 15, 16, 24, 25 and 27 successive injection of samples (lanthanides 4 µg/mL and uranium 10 mg/mL) could be carried out with 0.12, 0.16, 0.21, 0.39, 0.44 and 0.54 mmol TOPO sorbed supports respectively. As expected, uranium was retained on the modified reversed phase support and eluted at different time intervals depending upon the amount of TOPO sorbed onto the reversed phase support.

In a typical experiment, 45 successive injections of sample (lanthanide to uranium ratio 1000, where lanthanide concentration was 4 µg/mL and that of uranium was 4 mg/mL) were carried out prior to matrix uranium elution in the determination of lanthanides (**Fig.5.16**). The following results were observed from coupled column method containing 0.21mmol TOPO sorbed support. When the ratio of lanthanide to uranium was 1:2500 (lanthanides: 4 µg/mL, U:10 mg/mL), 16 successive chromatographic runs could be carried out; similarly, when the ratio was 1:7500 (Las: 4 µg/mL, U: 30 mg/mL), five consecutive samples could be separated and determined; when the ratio was raised to 1:12,500 (lanthanides: 4 µg/mL, U:50 mg/mL), three chromatographic runs were carried out; when La to U ratio was further raised to 1:15,000 (lanthanides: 4 µg/mL, U: 60 mg/mL), two chromatographic runs could be successively carried out prior to uranium elution. Samples with lanthanide to uranium ratio, as high as 1: 25,000 (lanthanides: 4 µg/mL, U: 100 mg/mL) were also successfully determined for the lanthanides and uranium interference was observed from the second run onwards. The 10 % breakthrough data for uranium loading on the TOPO sorbed column can be employed for prediction on the

number of samples that can be injected prior to uranium elution during dual column chromatographic studies on the determination of lanthanides in uranium matrix. Uranium elution from experiments involving “successive injection method” is mainly influenced by amount of TOPO sorbed on the support and volume and concentration of HIBA that has been passed through the column. It has been established that the prediction of uranium elution from dual column is close to the experimentally observed results (**Fig.5.17 and Table.5.5**).

Table.5.4. Separation of lanthanides in the presence of uranium matrix. Influence of uranium and TOPO contents on separation behaviour

Experimental: Column-1: 5 cm length TOPO coated column; Column-2: 10 cm length monolithic support; Mobile phase: 0.015 M CSA + 0.1 M HIBA; pH: 3.5, flow rate: 2 mL/min; Lanthanides: 4 ppm each

TOPO sorbed on 5 cm length column (mmol)	Concentration of U injected (mg/mL) into HPLC	Results
0.12	10 mg/mL	Lanthanides resolved from each other up to 7 injections; U elution begins at 8 th injection.
0.16	10 mg/mL	Lanthanides resolved from each other up to 15 injections; U elution begins at 16 th injection.
0.21	4 mg/mL	Lanthanides resolved from each other up to 44 injections; U elution begins at 45 th injection.
	10 mg/mL	Lanthanides resolved from each other up to 16 injections; U elution begins at 17 th injection
	30 mg/mL	Lanthanides resolved from each other up to 5 injections; U elution begins at 6 th injection
	50 mg/mL	Lanthanides resolved from each other up to 3 injections; U elution begins at

		4 th injection
	60 mg/mL	Lanthanides resolved from each other up to 2 injections; U elution begins at 3 rd injection
	100 mg/mL	Lanthanides resolved from each other for the first run; U elution begins at 2 nd injection
0.39	10 mg/mL	Lanthanides resolved from each other up to 24 injections; U elution begins at 25 th injection
0.44	10 mg/mL	Lanthanides resolved from each other up to 25 injections; U elution begins at 26 th injection
0.54	10 mg/mL	Lanthanides resolved from each other up to 27 injections; U elution begins at 28 th injection

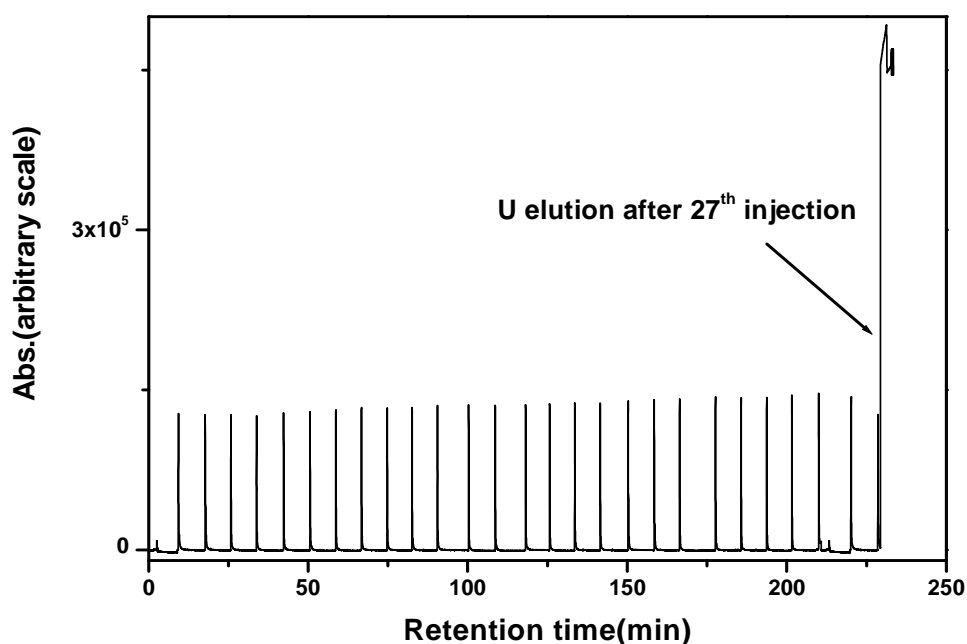


Fig.5.15. Elution behaviour of lanthanum in the presence of matrix uranium in a dual coupled column chromatography. Column.1.: 5 cm length TOPO coated reversed phase support (0.54 mmol TOPO sorption); Column.2: 10 cm monolithic column. Mobile phase: 0.015 M CSA+ 0.1 M α -HIBA; pH: 3.5; Flow rate: 2 mL/min; PCR flow rate: 0.5 mL/min; Detection: 655 nm; Sample: Mixture of U (10 mg/mL) and La (4 μ g/mL) in 0.01 N HNO₃; 20 μ L injected.

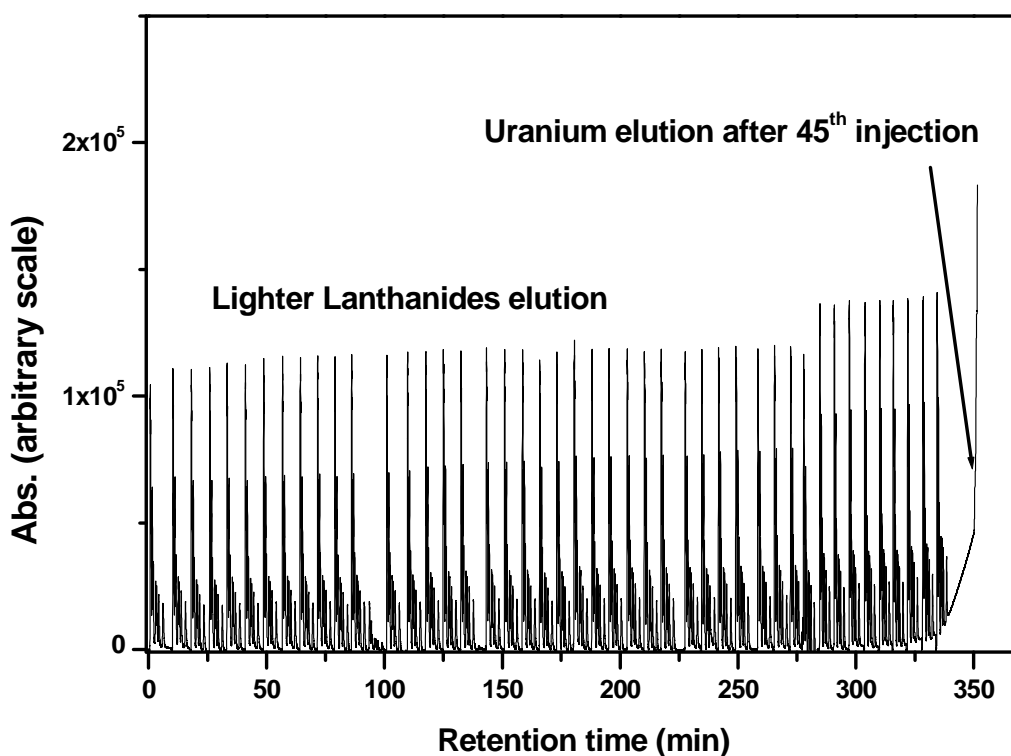


Fig.5.16. Separation of lanthanides from uranium matrix using single stage double column chromatographic technique. Column.1: TOPO coated reversed phase support of 5 cm length (0.21 mmol TOPO sorption); Column.2. Monolithic column modified to cation exchange. Mobile phase: 0.1 M α -HIBA + 0.01 M CSA; pH: 3.3; Flow rate: 2 mL/min; PCR flow rate: 0.5 mL/min; Detection: 655 nm; Sample: Mixture of U (4 mg/mL) and lighter lanthanides (4 μ g/mL) in 0.01 N HNO₃ acid; 20 μ L injected.

The uranium sorption capacity in the dynamic mode i.e. chromatographic run mode was studied on column-1 in the presence and absence of CSA using HIBA as the complexing reagent for elution. Though the ion-pairing reagent, CSA is expected mainly to modify the column-2 i.e. reversed phase monolithic column into a cation exchange type, it is expected that CSA may also sorb on to the TOPO coated column-1 by dispersion forces. The results observed in the present study indicated that uranium sorption capacity of the column-1 has not been significantly altered in the presence of CSA.

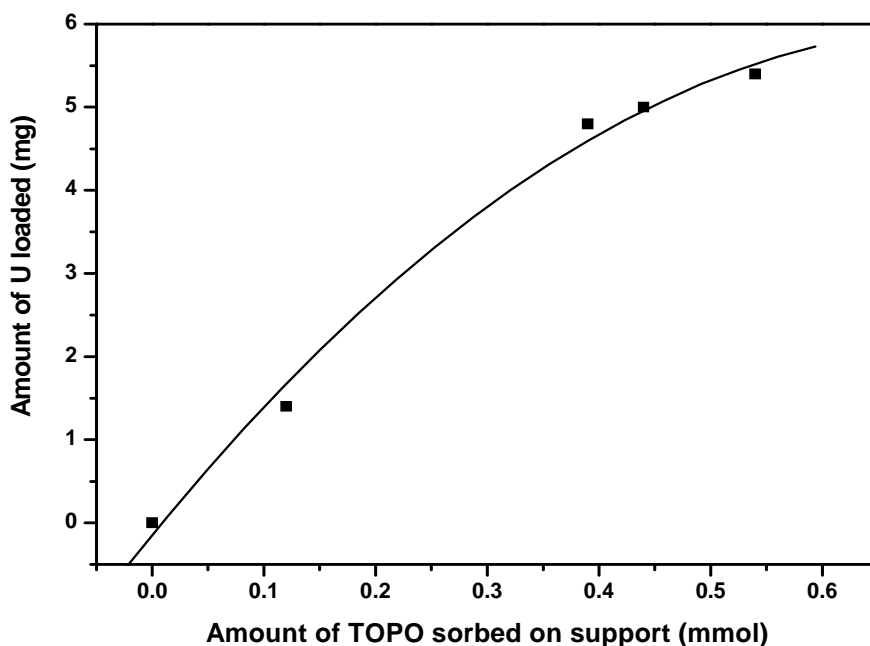


Fig.5.17. Uranium loading on TOPO coated supports. Column.1: 5 cm length TOPO sorbed reversed phase support + Column.2: dynamically modified 10 cm length reversed phase monolith support

Table.5.5 Predicted and experimentally observed number of injections on the TOPO coated support

TOPO sorbed on 5 cm length column (mmol)	Concentration of U injected (mg/mL) into HPLC	Number of injections	
		Predicted from plot	Experimentally obtained
0.16	10 mg/mL	12	15
0.21	4 mg/mL	39	44
	10 mg/mL	15	16
	30 mg/mL	6	5
	50 mg/mL	3	3

5.2.3.4.1 Lanthanides in uranium matrix (1:10⁶)

In some studies, a solution of lighter lanthanides (La-Eu; 0.1 µg/mL) in uranium matrix (100 mg/mL) was directly injected (100 µL) into the dual column HPLC system. In these studies, a 25 cm length reversed phase column sorbed with 1.60 mmol TOPO was connected in series with a 10 cm length monolith column (dynamically modified into cation exchange) for the separation and determination of lanthanides. Eleven sample solutions of lanthanides in uranium matrix (1 in 10⁶) were consecutively injected for the determination of lanthanides (**Fig.5.18**). These studies have demonstrated that lanthanide impurities in uranium matrix can be determined without matrix removal. Regeneration of TOPO sorbed 25 cm length column was carried out using 100 mL of 0.2 M EDTA (pH: 6).

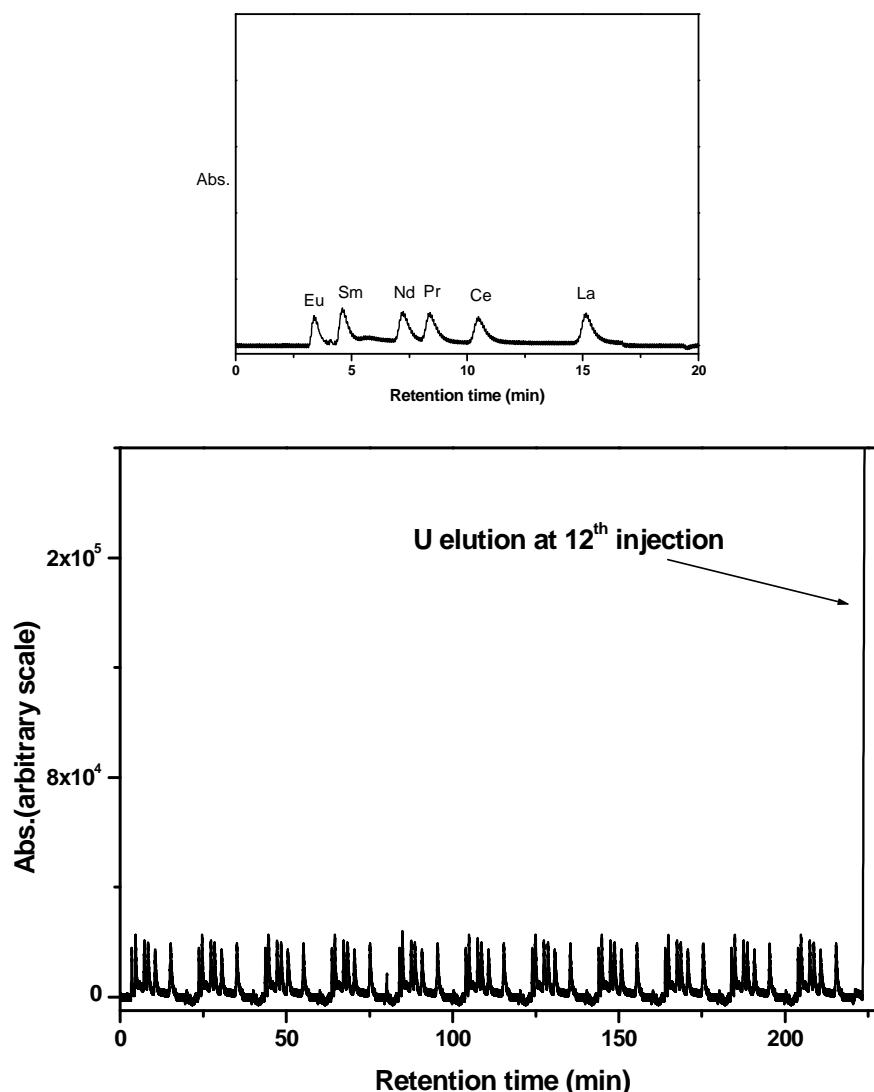


Fig.5.18. Separation of lanthanide impurities in uranium matrix (~ 1 part lanthanide in 10^6 part uranium) using dual column technique. Column.1.: 25 cm length reversed phase support (1.60 mmol TOPO sorbed) + Column.2: dynamically modified 10 cm length reversed phase monolithic column; Mobile phase: 0.1 M α -HIBA + 0.02 M CSA; pH: 3.48; Flow rate: 1.5 mL/min; PCR flow rate: 0.5 mL/min; Detection: 655 nm; Sample: U (100 mg/g) and lanthanides (0.1 μ g/g of La, Ce, Pr, Nd, Sm and Eu) in 0.01 N HNO₃; 20 μ L injected. (Top figure shows individual lanthanide separation in one particular run)

5.2.3.5 Significance of use of 5 cm length TOPO coated column

In the present study, 5 cm length TOPO coated column was mainly employed for the following reasons:

(1) To maintain near similar total separation time of lanthanides from (A) an analytical monolithic column of 10 cm length and (B) dual column, 5 cm length TOPO coated column connected in series with an analytical monolithic 10 cm length column under given experimental condition. Use of longer TOPO coated column, e.g. 25 cm length may lead to longer separation time of lanthanides from dual columns compared to the use of 5 cm length column (higher void volume with 25 cm over 5 cm length column).

(2) Use of longer TOPO coated columns i.e. 25 cm length over 5 cm one during dual column chromatographic method should result in higher uranium loading as relatively larger quantities of TOPO can be coated on a 25 cm over 5 cm length support due to additional availability of sites for TOPO sorption (through dispersion forces).

3. However, in a particular study, we have also employed a 25 cm length TOPO coated column in series with a monolithic column for assay of lanthanides in uranium matrix. In these studies, uranium contents were far higher, i.e. 1 part lanthanide in 10^6 parts of uranium. Thus to accommodate larger quantity of uranium, a longer TOPO coated column (25 cm length) was employed over a smaller column length (5 cm length).

5.2.3.6 Regeneration of “uranium sorbed TOPO coated column”

After completion of set of chromatographic experiments, regeneration of TOPO sorbed column was carried out using α -HIBA or EDTA as the complexing agent to remove the sorbed uranium from the support. In the initial studies, uranium from the support was eluted with 0.15 M α -HIBA solution (pH: 2.8). Uranium was eluted with severe tailing from the TOPO coated support. Subsequently, 0.2 M solution of EDTA (pH: 6) (50 mL) was employed as the complexing reagent for the elution of uranium. A severe tailing, which was observed with HIBA, was not observed when EDTA was employed as a complexing

reagent. The column was subsequently washed with water followed by methanol and the same was recoated for different TOPO loading studies.

5.2.3.7. Retention behavior of fission products, Pu(III), Pu(IV) and Am(III) on TOPO coated reversed phase support

The elution behaviour of various fission products was investigated on a TOPO coated reversed phase support. In the initial studies, a simulated fission product solution containing 250 $\mu\text{g/mL}$ of each of these metal ions, i.e. Mo, Sr, Ba, Ru, Zr, Pd, Rh, Nd and Cs were injected (injected amount $\sim 40\text{-}50 \mu\text{g}$) in to the HPLC system containing TOPO coated column. A mobile phase solution of 0.01 N HNO_3 was used for elution. In total, ten eluted fractions of 2 mL each were collected and the elements such as Sr, Ba, Cs, Rh Zr, Mo, Ru, and Pd were analysed using ICP-AES technique for the fission products.

The elution of fission products from TOPO coated column from HNO_3 medium is shown in **Fig.5.19a**. Fission products such as Nd, Sr, Ba, Ru, Rh, and Cs were eluted in the first fraction; the metal ions, Mo and Pd were eluted under six fractions; however Zr could not be eluted with 0.01 N HNO_3 medium. The elution behaviour was subsequently investigated using 0.1 M $\alpha\text{-HIBA}$ (pH: 3.5) as the mobile phase and the results are shown in **Fig.5.19b**. It was observed that most of the fission products such as Mo, Sr, Ba, Ru, Zr, Rh, Nd and Cs were eluted in the first fraction (i.e. 2 mL) and Pd elution was observed till four fractions. The experiment was also carried out in the presence of matrix uranium and similar elution behaviour was observed for the above fission products. Uranium however did not elute from the TOPO coated column under these experimental conditions.

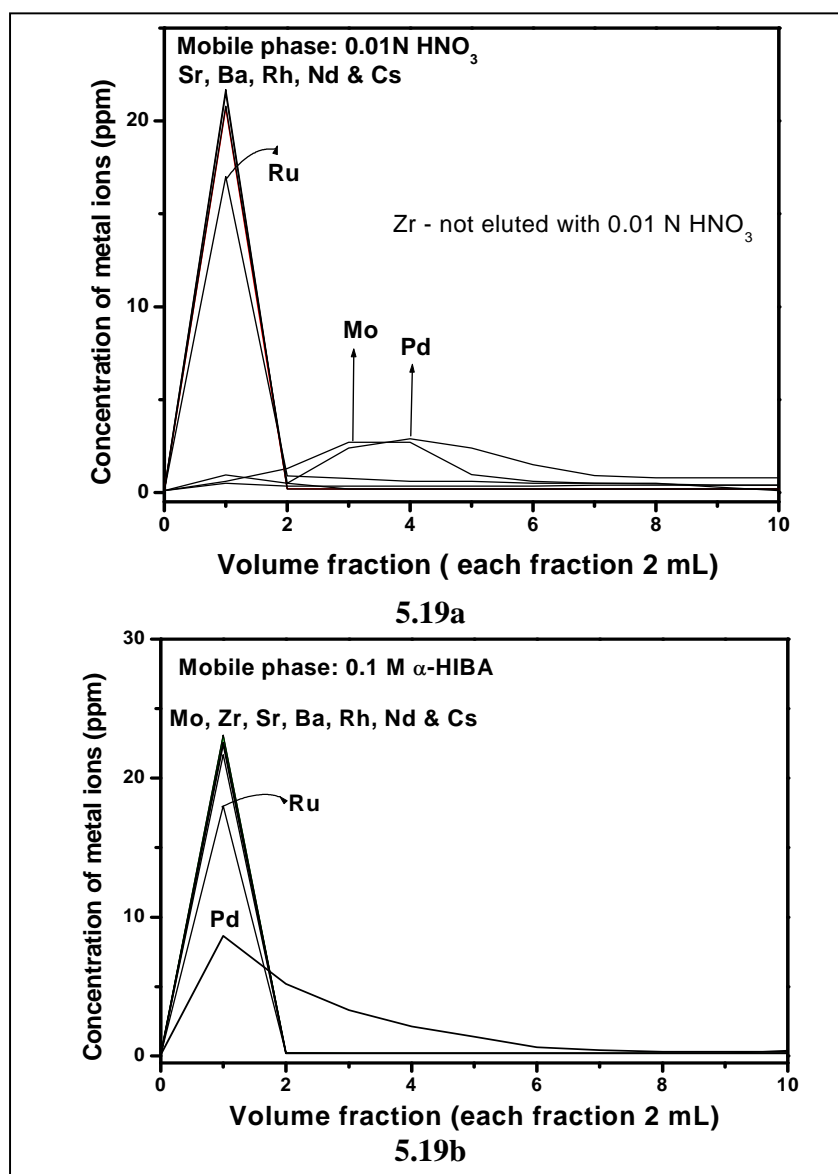


Fig.5.19. Elution behaviour of fission products on TOPO coated reversed phase support. Column: 5 cm length reversed phase support modified with 0.21 mmol TOPO; 5.19a. Mobile phase: 0.01 N HNO₃; 5.19b. Mobile phase: 0.1 M α -HIBA; pH: 3.5; Flow rate: 2 mL/min; PCR flow rate: 0.5 mL/min; Detection: 655 nm; Sample: simulated fission products (each metal ion ~ 200-250 μ g/mL; 200 μ L injection; injected amount 40-50 μ g of each element) in 0.01 N HNO₃.

The retention of actinides species such as Pu(III), Am(III) and Pu(IV) was also investigated on TOPO coated reversed phase column using 0.1 M α -HIBA (pH 3.5) as the mobile phase. The ions, Pu(III) / Am(III) (0.42 min) and Pu(IV) (0.50 min) were eluted

close to dead volume, i.e. t_0 indicating their poor affinity on TOPO coated column (Fig.5.20). However, uranium was strongly complexed and retained on the TOPO coated support.

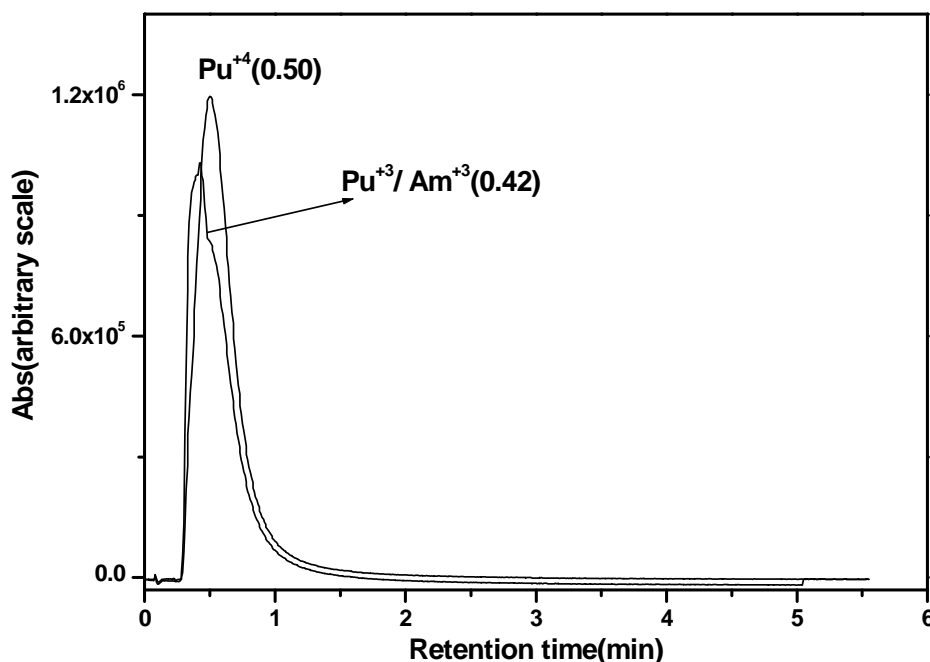


Fig.5.20. Retention behaviour of Pu(III), Pu(IV) and Am(III) on TOPO coated reversed phase support: Column: 5 cm length reversed phase support (0.21 mmol TOPO sorbed); Mobile phase: 0.1 M α -HIBA; pH: 3.5; Flow rate: 2 mL/min; PCR flow rate: 0.5 mL/min; Detection: 655 nm; Sample: Am(\sim 4ppm), Pu(III) and Pu(IV) \sim 20 ppm in 0.1 M HIBA; 20 μ L injected.

5.2.3.8 Burn-up determination of PHWR fuel by single stage double column chromatography

Lanthanide fission products such as La, Ce, Pr, Nd and Sm in the dissolver solution of PHWR fuel were separated and estimated without removal of “matrix uranium” using single stage dual column chromatographic technique. The initial studies were carried out with a simulated dissolver solution. A mobile phase made of 0.015 M CSA with 0.1 M α -HIBA (pH: 3.4) was employed for individual separation of lanthanide fission products. In these studies, 30 consecutive injections were carried out and lanthanides (\sim 3 μ g/mL) were

separated and determined prior to elution of matrix uranium (5 mg/mL) (**Fig.5.21**). Thus the support has been qualified for 30 successive analysis of sample of dissolver solution. Subsequently, dissolver solution from PHWR fuel was injected into HPLC system for individual separation of lanthanides fission products (**Fig.5.22**). Plutonium present in the dissolver solution was converted to Pu(IV) by adding NaNO_2 prior to sample injection. The concentration of La, Ce, Pr, Nd and Sm were estimated in the dissolver solution using calibration plots and the results are shown in **Table.5.6**. Reversed phase HPLC technique was employed for the estimation of uranium and plutonium using monolithic column with 0.1 M α -HIBA (pH of 3.5) as the mobile phase. Americium, the minor actinide present in the dissolver solution was identified by injecting pure Am(III) as well as spiking with dissolver solution (**Fig.5.23**). The atom percent burn-up of the dissolver solution was determined using La, Pr and Nd as fission monitors [38]. The atom percent burn-up of dissolver solution of PHWR fuel was found to be 0.943 with La as fission monitor; 0.967 with Pr as fission monitor and 0.961 with Nd as fission monitor. These studies established that the TOPO coated single stage dual column chromatographic technique can be used for direct assay of lanthanide fission products present in dissolver without pre-separation of “matrix” uranium. These studies also can be applied to estimate the lanthanide fission products in dissolver solution of nuclear reactor fuel subjected to a very low burn-up (when Nd to U ratio as low as $\sim 1:10,000$).

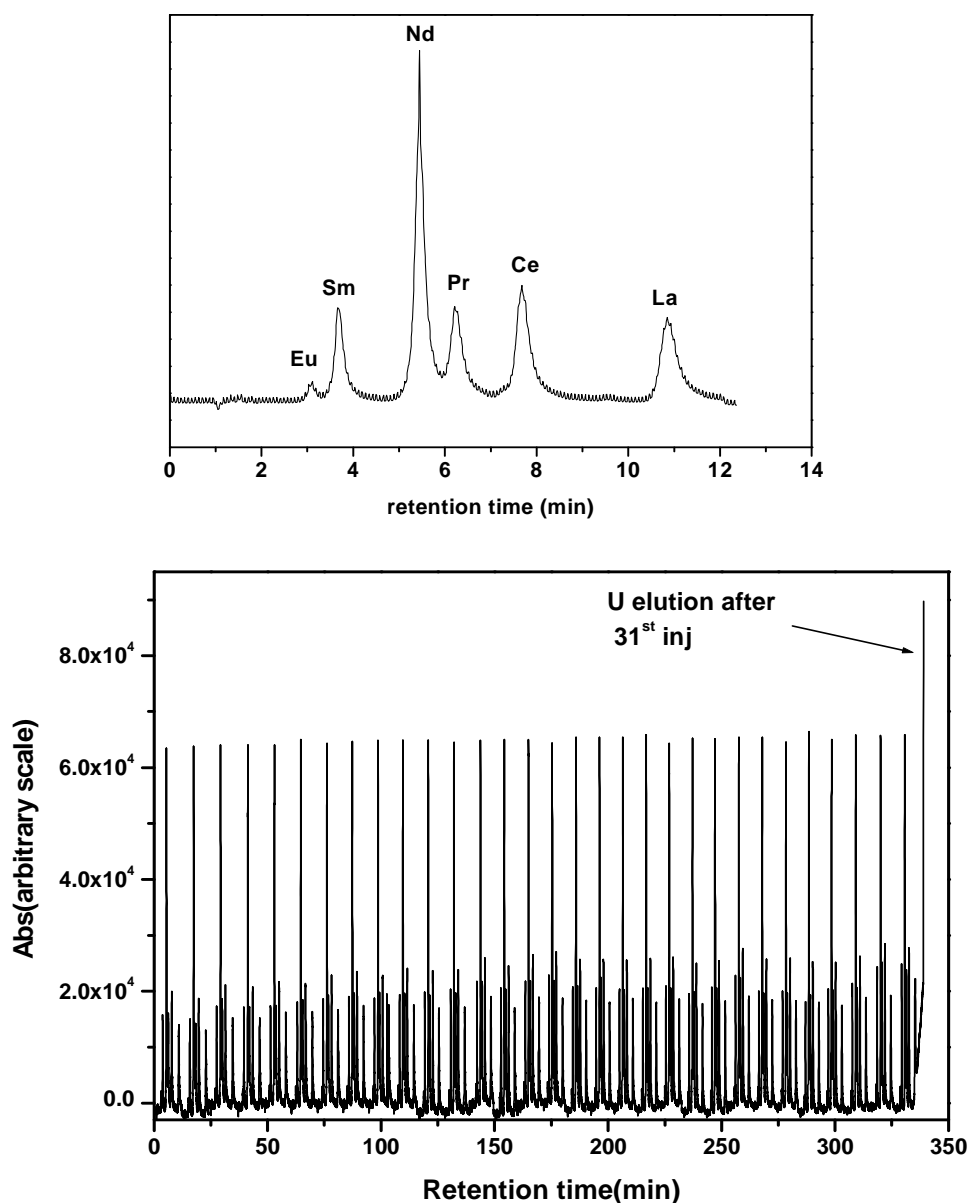


Fig.5.21. Separation of simulated dissolver solution containing lanthanides from uranium matrix using single stage double column chromatographic support. Column.1.: 5 cm length reversed phase support (0.21 mmol TOPO sorbed)+ Column.2: dynamically modified 10 cm length reversed phase monolith support; Mobile phase: 0.1 M α -HIBA + 0.015 M CSA; pH: 3.4; Flow rate: 2 mL/min; PCR flow rate: 0.5 mL/min; Detection: 655 nm; Sample: Mixture of U (5 mg/g) and lanthanide fission products (3 μ g/g) in 0.01 N HNO₃; 20 μ L injected.

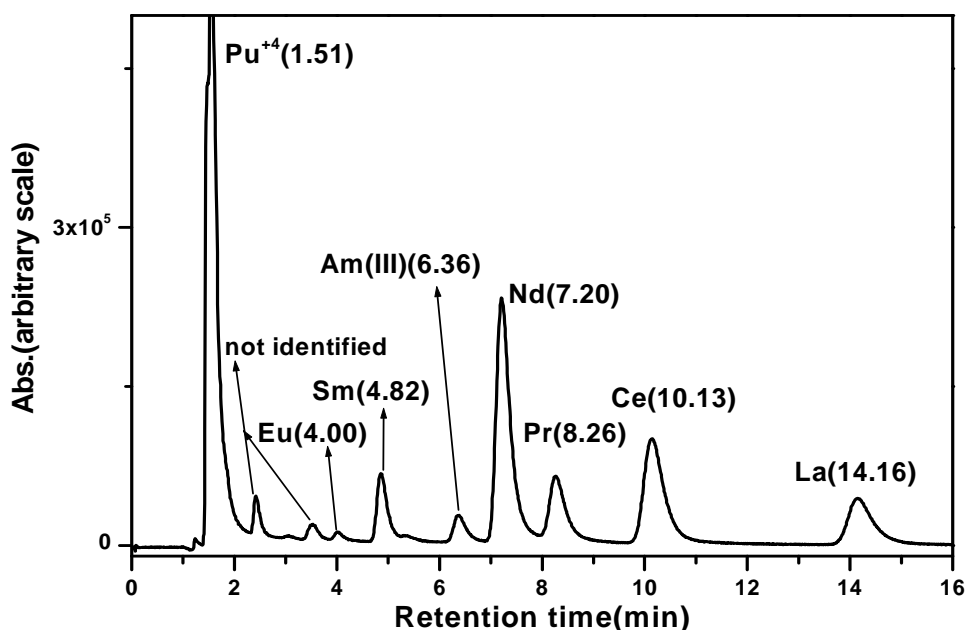


Fig.5.22. Direct assay of lanthanide fission products present in the dissolver solution of PHWR spent fuel using single stage double column chromatographic technique. Columns: (1). 5 cm length reversed phase with 0.21 mmol TOPO sorption + (2). dynamically modified 10 cm length reversed phase monolith support; Mobile phase: 0.1 M α -HIBA + 0.015 M CSA; pH: 3.35; Flow rate: 2 mL/min; PCR flow rate: 0.5 mL/min; Detection: 655 nm; Sample: dissolver solution of PHWR spent nuclear fuel; 20 μ L injected.

Table.5.6 Estimation of lanthanides and actinides in dissolver solution of PHWR spent fuel - determination of atom percent burn-up

Element	Concentration (per gram of dissolver solution)	Burn-up (atom percent)
La	10.0 μ g	0.943
Ce	19.2 μ g	
Pr	9.3 μ g	0.967
Nd	32.0 μ g	0.961
Sm	7.9 μ g	
Eu	0.6 μ g	
U	29.2 mg	
Pu	116 μ g	

- Approximately 50% fissions were from U-235 and 50% from Pu-239 towards the total fission; the same was arrived by measuring Nd/Sm ratio from HPLC experiments. The value of fractional fission yield (Y) employed in the determination of atom% fission was Nd (18.58/100); La (6.19/100) and Pr(5.57/100) [38]

Uncertainties in the measurement \pm 2-3 %

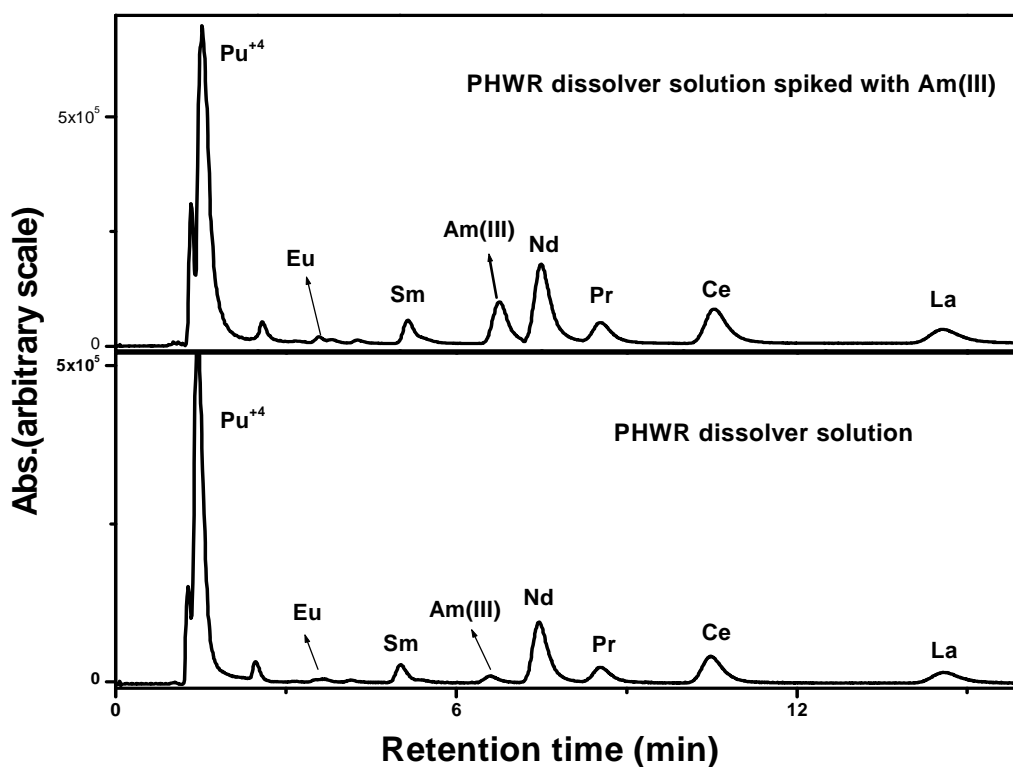


Fig.5.23. Identification of Am(III)/Pu(III) from dissolver solution of PHWR spent fuel using single stage double column chromatographic support. Columns: 5 cm length reversed phase support coated with 0.21 mmol TOPO + dynamically modified 10 cm length reversed phase monolith support; Mobile phase: 0.1 M α -HIBA + 0.015 M CSA; pH: 3.35; Flow rate: 2 mL/min; PCR flow rate: 0.5 mL/min; Detection: 655 nm; Sample: dissolver solution of PHWR spent nuclear fuel in 0.01 N HNO₃ acid; 20 μ L injected.

5.2.3.9 Elution behaviour of U, Pu, Am and lanthanide fission products present in the dissolver solution of fast reactor fuel

The coupled column chromatographic technique was also employed to separate and estimate lanthanide fission products from dissolver solution of a fast reactor fuel subjected to a burn-up of ~ 155 GWd/t (Fig.5.24).

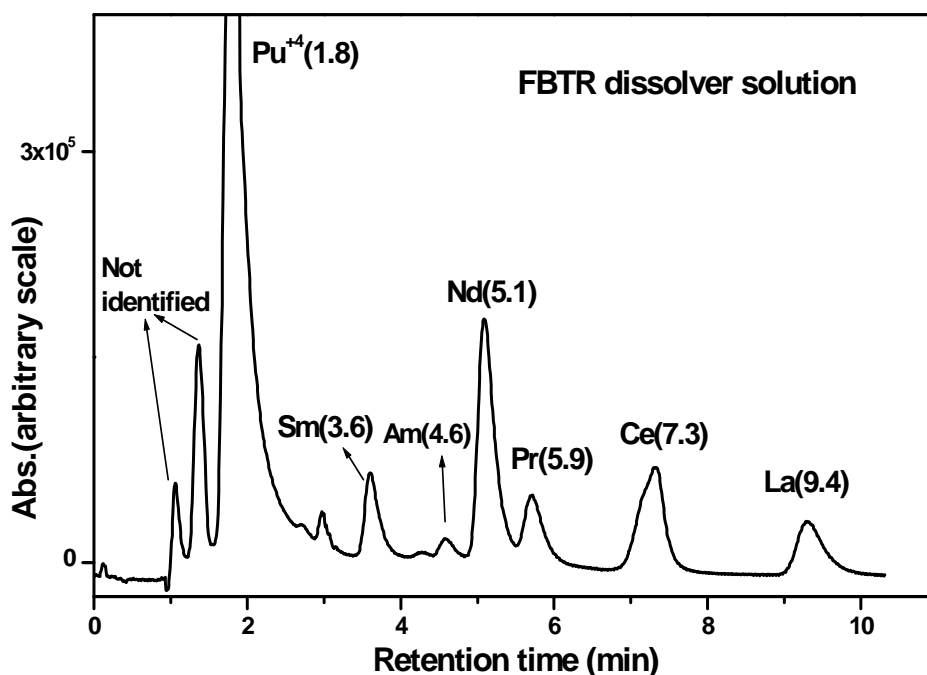


Fig.5.24. Elution behaviour of plutonium and lanthanide fission products present in the dissolver solution of fast reactor fuel by single stage double column chromatography: Columns: 5 cm length reversed phase support coated with 0.21 mmol TOPO + dynamically modified 10 cm length reversed phase monolith column; Mobile phase: 0.1 M α -HIBA + 0.015 M CSA; pH: 3.45; Flow rate: 2 mL/min; PCR flow rate: 0.5 mL/min; Detection: 655 nm; 20 μ L injected.

Plutonium present in the dissolver solution was adjusted to +4 oxidation state prior to sample injection. The dissolver solution from fast reactor was directly injected into the HPLC system, containing TOPO coated column connected in a series with dynamically modified reversed phase monolith support. Uranium was sorbed on first column, whereas plutonium, americium and lanthanide fission products were transferred to the second column, where lanthanide fission products were separated from each other. The concentrations of lanthanide fission products in the dissolver solution were estimated and the results are shown in **Table.5.7**. In the measurement of lanthanides fission products,

interference of Pu (in +4 oxidation state) was not observed due to early elution of Pu(IV) (1.8 min) compared to lanthanide fission products.

Table.5.7. Estimation of lanthanide fission products, U and Pu in dissolver solution of Fast Reactor Fuel

Element	Concentration (per gram of dissolver solution)	Burn-up (atom percent)
La	33 µg	15.9
Ce	56 µg	
Pr	30 µg	
Nd	95 µg	15.7
Sm	27 µg	
U	1800 µg	
Pu	3350 µg	

- Uncertainties in the measurement $\pm 2-3$ %

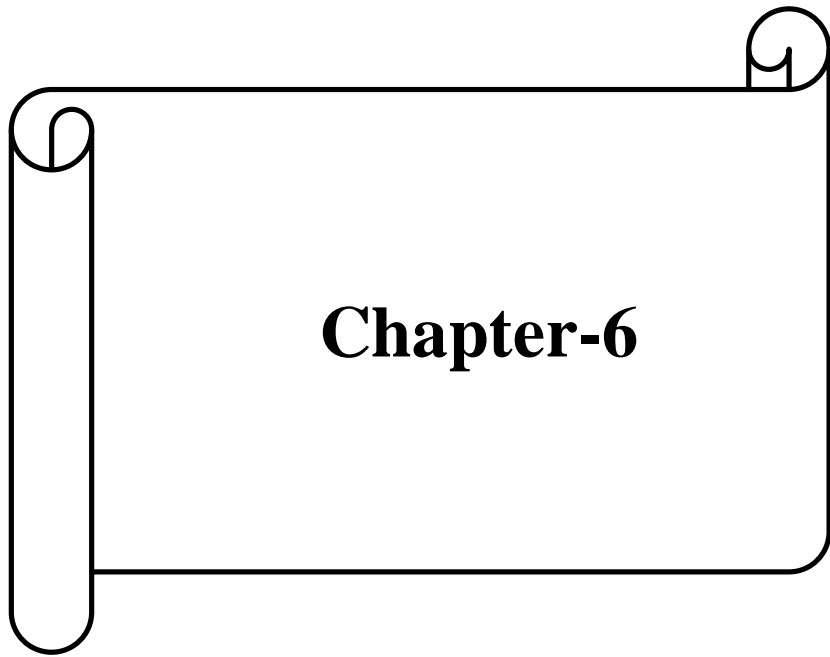
5.2.3.10 Advantages of burn-up measurements with HPLC technique

The determination of atom percent burn-up has been generally carried out using a well established Isotope Dilution Mass Spectrometric (IDMS) technique [65]. Estimation of lanthanide fission products as well as uranium and plutonium for the determination of atom percent burn-up using HPLC technique is less time consuming compared to the steps involved in the method using IDMS technique. For the IDMS method, fission monitor (Nd-148 is generally used as burn-up monitor) and heavier elements (U and Pu) are purified and obtained in multiple separation stages. Initially uranium and plutonium will be isolated from fission products from 1:1 HNO₃ medium using an anion exchange column. Uranium is later eluted using 3 N HNO₃ and plutonium is subsequently eluted using 1 N HNO₃. The fission products containing lanthanide fraction will be isolated from each other in a second

stage using an anion exchange column using methanol-HNO₃ medium for the isolation of pure neodymium fraction. Thus the isolation of U, Pu and fission product monitor demands multiple separation steps. However, in the present HPLC method of study, separation and determination of uranium, plutonium and lanthanide fission products was carried out in a single step. The precision and accuracy of the chromatographic technique with post-column derivatisation technique employed in the present study is generally found to be $\pm 2-3\%$. Earlier studies from our laboratory [49] have established that atom percent results obtained by HPLC are $\pm 2-3\%$ of mass spectrometry results.

5.2.4 Conclusion

A single stage dual column chromatographic technique was developed and demonstrated for the separation and determination of lanthanides in uranium matrix. The uranium loading capacity on the TOPO coated column was studied in detail and it was established that the use of supports with higher "TOPO load" resulted in higher uranium loading. Successive injection of lanthanide samples in uranium matrix was demonstrated and lanthanides were separated and quantitatively determined. Lanthanide fission products such as La, Ce, Pr, Nd and Sm in the dissolver solution of PHWR fuel were separated and determined without removal of matrix uranium for the burn-up measurements. The retention behaviour of Am(III), Pu(III), Pu(IV) and fission products such as Zr, Mo, Cs, Ba, Sr, Ru, Rh, Pd was also investigated on the dual column. Samples with lanthanide to uranium ratio, as high as 1 in 10⁶ were directly injected into the HPLC system for the quantitative separation and determination of lanthanides. The single stage chromatographic technique can also be extended for the determination of lanthanide impurities in samples of UO₂ pellet without removal of uranium matrix.



Chapter-6

Correlation of Retention of Lanthanide and Actinide Complexes with Stability Constants and their Speciation

6.1 Introduction

One of the important factors governing the separation efficiency of individual lanthanides/actinides is the stability constant of the metal–ligand complex. Therefore, stability constant data of lanthanide/actinide complexes are important in the development of high performance separation procedures. A wide variety of techniques are available for the determination of stability constant. However, these are in most cases amenable for measurements of a single metal ion only. Chromatographic methods on the other hand provide the interesting possibility of computing the stability constant of several metal ions in one single experiment or set of experiments. Chromatographic and electrophoretic methods have been studied for the estimation of stability constant of metal complexes from the retention data [120, 184-188]. Retention model of metal ions using ion chromatography were reported in literature [189-190]. In chromatographic techniques, stability constants of metal complexes were determined through the measurement of changes in either capacity factor (chromatography) or the distribution ratio (ion-exchange) of the analyte upon a change in complexing agent concentration. In most systems investigated in literature, the dependence of reciprocal values of capacity factors ($1/k'$) on the ligand concentration $[L]$ was carried out and a linear plot of $1/k'$ vs ligand concentration was obtained. The assumption involved in these studies is the presence of a single predominant complex. Typically six different ligand concentrations were used to obtain the plot in these studies [189-190]. A gel chromatographic method was also reported for the determination of stability constant of metal complexes [191]. The metal complex was eluted prior to free

metal ion and stability constants were determined from concentrations of free metal ion and metal complex. The stability constant of metal complexes has been traditionally determined experimentally, using methods such as potentiometry [192-194], polarography [195], conductometry [196-197], spectrophotometry [198], solvent extraction [199] and ion exchange [200-201].

In the present work, the correlation of retention of lanthanide and some actinide complexes with their respective stability constant is attempted. A large set of data on the capacity factor of lanthanides and some actinides generated under various experimental conditions of mobile phase composition was investigated in detail. From these studies, a correlation has been established between the retention of the complexes of lanthanides (e.g. lanthanides with HIBA) and the concentrations of each of the individual species, i.e. free metal ion $[M^{3+}]$, dipositive $[ML]^{2+}$, monopositive $[ML_2]^+$, neutral $[ML_3]$ and anionic species $[ML_4]^-$. From these correlations, the stability constant of other lanthanides and actinides were estimated.

Based on these studies, a correlation has been developed, which recognizes the competition for the metal ion between the organic acid, e.g., α -HIBA and an ion-pairing reagent, RSO_3H (CSA) with that of stability constant. The chromatographic runs were carried out at two different pH at lower ligand $[A^-]$ concentrations, and these results were employed to correlate capacity factor with stability constant i.e. the capacity factors obtained in two different runs were correlated with $[A^-]$ and β_1 and β_2 were estimated by solving two simultaneous equations. β_3 was subsequently estimated by carrying out the chromatographic run at relatively higher pH. Studies were also taken up to employ a single chromatogram for the estimation of stability constant at various ionic strengths.

After validation of the correlations, studies were carried out to develop a procedure for the estimation of stability constant of lanthanides / actinides with a ligand, whose value is not reported. A reversed phase chromatographic technique was investigated for individual separation of some of the actinides. The speciation data obtained from stability constant determination was employed to explain the retention behaviour of actinide complexes.

6.2. EXPERIMENTAL

The dynamic ion-exchange separation of lanthanides and some actinides was investigated by varying the concentration of ion-pairing reagent (CSA), complexing agent (e.g., α -HIBA), mobile phase pH and mobile phase flow rate. All chromatographic studies were carried out at 25°C. Experiments were performed with α -HIBA, mandelic acid, lactic acid and tartaric acid as the complexing agents for separation of individual lanthanides and some actinides.

6.3. RESULTS AND DISCUSSION

6.3.1. Estimation of capacity factor of lanthanides and actinides based on their species

The retention of lanthanides and actinides was studied as function of CSA and α -HIBA concentrations; similarly, retention was also studied as a function of mobile phase pH. In a typical study, the pH of the mobile phase (0.1 M α -HIBA and 0.01 M CSA) was increased from 2.5 to 3.5. The capacity factor for lanthanides, Pu(III) and Am(III) was found to decrease with increase in pH (**Fig.6.1**). In another study, the CSA concentration was varied from 0.0025 to 0.01 M at a mobile phase pH 2.7. The capacity factor for lanthanides and actinides increases with the increase in CSA concentration (**Fig.6.2**).

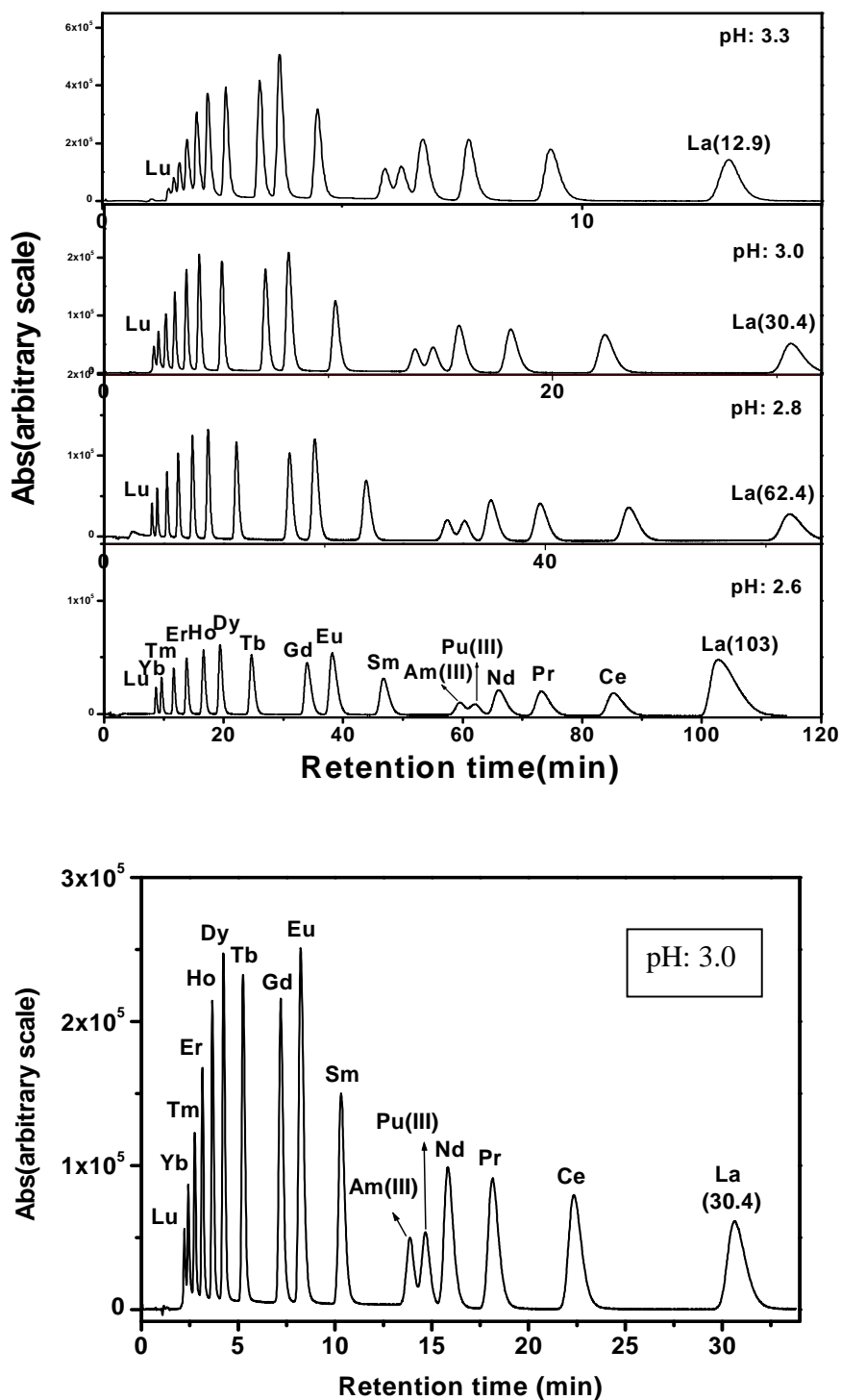


Fig.6.1. Retention of lanthanides, Am(III) and Pu(III) as a function of mobile phase pH. Mobile phase: 0.1 M HIBA + 0.01 M CSA; Flow rate: 2 mL/min; PCR flow rate: 0.5 mL/min; Detection: 655 nm; Sample: lanthanides (12 ppm), Pu(III) (~10ppm) and Am(III) (~4 ppm) in 0.01 N HNO₃

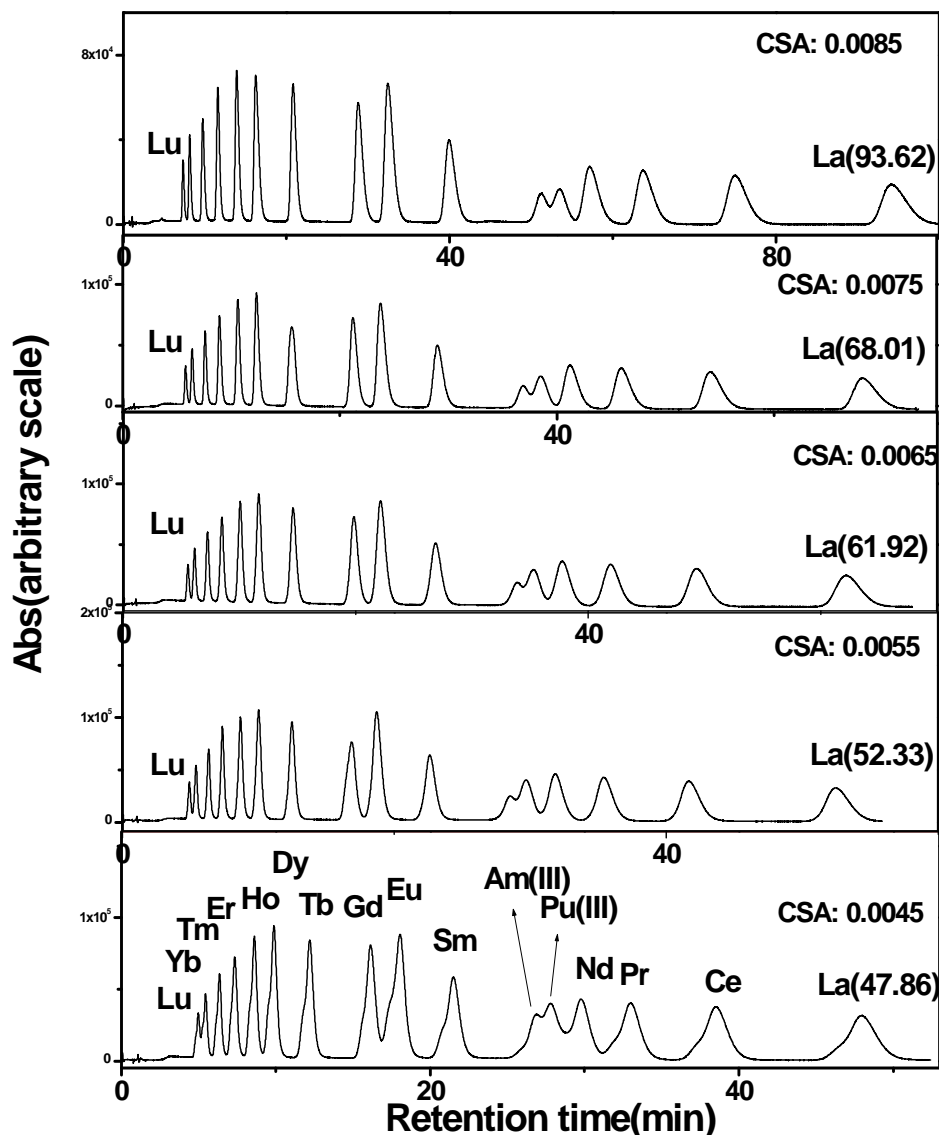


Fig.6.2. Retention of lanthanides, Am(III) and Pu(III) as a function of CSA concentration. Mobile phase: 0.1 M HIBA + CSA (0.0045M-0.0085M); pH: 2.7; Flow rate: 2 mL/min; PCR flow rate: 0.5 mL/min; Detection: 655 nm; Sample: lanthanides (12 ppm), Pu(III) (~ 10ppm) and Am(III) (~ 4 ppm) in 0.01 N HNO₃.

The capacity factor for metal ions decreases with increase in α -HIBA concentration. For a fixed concentration of CSA, the capacity factor of an analyte decreases with an increase in the concentration of α -HIBA and pH. Under a given set of conditions, such as pH and concentration of the eluent (e.g. α -HIBA), the analytes can be present in mobile

phase in the form of various species. Each of these complex stoichiometries does not yield separate peak in the chromatogram, but all of the complexes together produce a single peak. However, as the relative proportions of these complexes change, for example, by changes in pH, the capacity factors are altered. For lanthanides, fractions of various species were calculated using stability constant data from corresponding metal-ligand equilibrium equations (6.1-6.8). It was seen from the calculated fraction of species that at one particular pH, fraction of uncomplexed species is more for “La” whereas, fraction of anionic species is more for “Lu”. Hence for each lanthanide, distribution of relative proportion of the species will mainly decide the retention time.

The concentration of each of the species is given by the corresponding metal-ligand equilibrium, which is summarized as follows:

$$[LnA^{+2}] = K_1 [Ln^{+3}] [A^-] \dots\dots\dots (6.1)$$

$$[LnA_2^{+1}] = K_1 K_2 [Ln^{+3}] [A^-]^2 \dots\dots\dots(6.2)$$

$$[LnA_3] = K_1 K_2 K_3 [Ln^{+3}] [A^-]^3 \dots\dots\dots(6.3)$$

$$[LnA_4^{-1}] = K_1 K_2 K_3 K_4 [Ln^{+3}] [A^-]^4 \dots\dots(6.4)$$

where $[Ln^{+3}]$ and $[A^-]$ are the concentrations of the uncomplexed metal and ligand anion respectively. K_1, K_2, K_3, K_4 are the stepwise stability constants. The overall stability constants, β_i are defined as follows:

$$\beta_1 = K_1; \beta_2 = K_1 K_2; \beta_3 = K_1 K_2 K_3; \text{ and } \beta_4 = K_1 K_2 K_3 K_4 \dots\dots\dots(6.5)$$

The total metal ion concentration (T_m), can be written as

$$T_m = [Ln^{+3}] + [LnA^{+2}] + [LnA_2^{+1}] + [LnA_3] + [LnA_4^{-1}] \dots\dots\dots(6.6)$$

which can be expressed in terms of the stability constant as

$$T_m = [Ln^{+3}] \left\{ 1 + K_1[A^-] + K_1K_2[A^-]^2 + K_1K_2K_3[A^-]^3 + K_1K_2K_3K_4[A^-]^4 \right\} \dots\dots\dots(6.7)$$

From a knowledge of $[A^-]$, K_1 , K_2 , K_3 and K_4 , the free metal ion concentration $[Ln^{+3}]$ can be calculated from equation 6.7. $F_{Ln^{+3}}$, $F_{LnA^{+2}}$, $F_{LnA_2^{+1}}$, F_{LnA_3} and $F_{LnA_4^{-1}}$ were calculated by using equations (6.8), with the use of literature value of stability constant, ligand concentration $[A^-]$, and total metal ion concentration (T_m) for each pH. $[A^-]$ was calculated from the knowledge of the pKa [103, 202-203] of the acid eluent and pH of the solution.

$$F_{Ln^{+3}} = Ln^{+3} * 100 / T_m; \dots\dots\dots(6.8)$$

$$F_{LnA^{+2}} = LnA^{+2} * 100 / T_m;$$

$$F_{LnA_2^{+1}} = LnA_2^{+1} * 100 / T_m;$$

$$F_{LnA_3} = LnA_3 * 100 / T_m;$$

$$F_{LnA_4^{-1}} = LnA_4^{-1} * 100 / T_m$$

From these studies, a correlation was established between capacity factor and metal-ligand species, which was derived from stability constant data and is shown in equation - 6.9

$$k' = x_1 F_{Ln^{+3}} + x_2 F_{LnA^{+2}} + x_3 F_{LnA_2^{+1}} + x_4 F_{LnA_3} + x_5 F_{LnA_4^{-1}} \dots\dots\dots (6.9)$$

$$x_{i (1-5)} = A_i + B_i pH$$

Species, $F_{Ln^{+3}}$, $F_{LnA^{+2}}$, $F_{LnA_2^{+1}}$, F_{LnA_3} and $F_{LnA_4^{-1}}$ are fractions of uncomplexed, dipositive, monopositive, neutral and anionic species respectively of lanthanides with α -HIBA. x_1 , x_2 , x_3 , x_4 , and x_5 correspond to coefficients representing uncomplexed, dipositive, monopositive, neutral and anionic species respectively.

Capacity factor, k' were different for different lanthanides. Five lanthanides were chosen to solve the equation (6.9). For each lanthanide we have one equation, hence for five lanthanides, five equations were obtained. Solving five simultaneous equations by matrix

method, the values of x_1 to x_5 were obtained. These coefficients / constants depend on pH, hence x_1 to x_5 were plotted against pH and fitted linear plots. Parameters A_i and B_i were obtained from these plots. Subsequently, the term, $(A_i + B_i \text{ pH})$ was calculated, which is same for all lanthanides but vary as a function of pH. By substituting the values of $(A_i + B_i \text{ pH})$ and $F_{Ln^{+3}}$, $F_{LnA^{+2}}$, $F_{LnA_2^{+1}}$, F_{LnA_3} , $F_{LnA_4^{-1}}$ at particular pH for various lanthanides, the capacity factors were estimated (**Table.6.1**). The estimated retention (k') data for all lanthanides with the exception of La (especially at pH 2.6) agreed very well with the experimental one.

The following expression was developed in the present study for the prediction of retention i.e. capacity factor (k') of metal ion:

$$k' = (A_1 + B_1 \text{ pH}) F_{Ln^{+3}} + (A_2 + B_2 \text{ pH}) F_{LnA^{+2}} + (A_3 + B_3 \text{ pH}) F_{LnA_2^{+1}} + (A_4 + B_4 \text{ pH}) F_{LnA_3} + (A_5 + B_5 \text{ pH}) F_{LnA_4^{-1}} \dots \dots \dots (6.10)$$

$A_1 = 10.722$	$B_1 = -3.305$
$A_2 = -0.498$	$B_2 = 0.236$
$A_3 = -0.015$	$B_3 = -0.016$
$A_4 = 1.871$	$B_4 = -0.596$
$A_5 = -2.605$	$B_5 = 0.868$

* pH employed : 2.6, 2.7, 2.8, 2.9 and 3

* Stability constant data for **Pr, Sm, Gd, Dy, and Yb** were used to obtain coefficients in the equation 6.10 by matrix method.

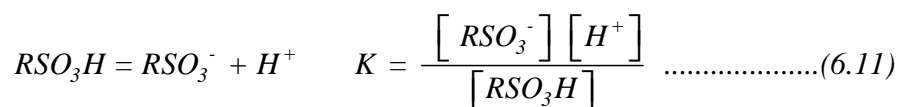
Table.6.1. Comparison of experimentally measured capacity factor (k') of lanthanides and some actinides with the predicted one

Lanthanides	pH: 2.6		pH:2.7		pH:2.8		pH 2.9		pH:3.0	
	Exp. k'	Pred. k'								
La	73.30	83.65	61.28	61.12	42.69	43.86	33.70	30.42	23.95	20.54
Ce	59.46	62.99	48.36	46.67	32.51	34.79	25.31	25.65	17.74	18.81
Pr	51.40	53.35	40.87	38.37	27.04	27.75	21.00	19.72	14.58	13.84
Nd	46.60	44.29	36.64	32.67	23.99	24.53	18.45	18.30	12.83	13.51
Sm	33.91	34.49	25.78	24.00	16.34	16.89	12.55	11.63	8.59	7.80
Eu	28.31	30.74	21.35	21.28	13.30	14.93	10.15	10.23	6.96	6.79
Gd	25.67	27.21	18.95	18.49	11.80	12.57	8.97	8.47	6.13	5.32
Tb	19.18	18.89	13.97	12.95	8.61	9.01	6.54	6.02	4.52	3.61
Dy	15.40	15.29	11.10	10.86	6.83	7.77	5.21	5.27	3.64	3.17
Ho	13.31	13.88	9.52	10.02	5.85	7.25	4.46	4.97	3.13	3.09
Er	11.21	10.00	7.96	7.80	4.95	5.53	3.75	3.72	2.65	2.39
Tm	9.50	9.29	6.75	6.51	4.22	4.52	3.19	3.07	2.28	2.32
Yb	7.90	8.07	5.64	5.38	3.58	3.58	2.71	2.52	1.97	2.49
Lu	7.14	4.79	5.07	2.60	3.20	1.35	2.42	1.02	1.76	1.86
Am	41.33	42.41	32.86	30.20	21.29	21.20	16.38	14.65	11.31	9.89
Pu	43.94	42.88	34.20	30.33	22.28	21.32	17.12	14.91	11.93	10.26

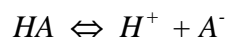
6.3.2 Estimation of stability constant and its validation (method-1)

The above studies have established a correlation between retention of lanthanides/some actinides and stability constant on a chromatographic support. Hence an attempt was made in the present study to relate stability constant directly with capacity factor of lanthanide / actinide, concentration of ion-pairing reagent, [RSO₃⁻] and [A⁻]. In this study, equations were derived for the capacity factor based on a model, describing a competition for lanthanide complexation between the ion pairing reagent, RSO₃H, namely CSA and the hydroxyacid ligand. These equations were then used for estimating the stability constants of the lanthanide-hydroxyacid complexes.

Acid dissociation constant of the ion pairing reagent, CSA is given as:.



Similarly, the dissociation of the weak hydroxy acids e.g. HIBA is given as:



The equation depicting the equilibrium constant of the metal complexes with ion pairing reagent can be written as:

$$RSO_3^- + M \rightleftharpoons RSO_3M \quad K_s = \frac{[RSO_3M]}{[RSO_3^-][M]} \dots\dots\dots(6.12)$$

The equilibrium for the first stepwise stability constant (K_1) for the lanthanide complexes with the hydroxyacid is written as follows

$$M + A^- \rightleftharpoons MA_1 \quad K_1 = \frac{[MA_1]}{[M][A^-]}$$

which yields

$$[MA_1] = K_1 [M] [A^-] \dots\dots\dots (6.13)$$

It is thus asserted that the capacity factor of the analyte is inversely proportional to the concentration of the analyte complex with the hydroxy acid (MA_1) and directly proportional to the concentration of the complex with the ion pairing reagent, RSO_3^- . This is based on the fact that the larger the concentration of metal complex with the ion-pairing reagent, the more strongly bound the lanthanide ion onto the stationary phase resulting in a higher capacity factor. Conversely, a higher concentration of the analyte complex with the hydroxyacid implies a larger fraction of the analyte in the mobile phase resulting in a shorter retention. The capacity factor actually observed therefore results from a competition between these two factors and is expressed as:

$$k' \propto \frac{[RSO_3M]}{[MA_1]}$$

or, $k' = \frac{X [RSO_3M]}{[MA_1]}, \dots\dots\dots(6.14)$

where X is a proportionality constant that depends on instrumental factors such as length of the column, flow rate, etc.

Substituting for the concentration of [RSO₃M] and [MA₁] from Eq. 6.12 and 6.13, we can write k' as

$$k' = \frac{X \{K_s [RSO_3^-] [M]\}}{\{K_1 [M][A^-]\}}$$

or, $k' = \frac{Y [RSO_3^-]}{K_1 [A^-]} \dots\dots\dots (6.14a),$

where the constants, X (from Eq. 6.14) and K_s (from Eq. 6.12) have been replaced by a single constant, “Y” where $Y = X.K_s$.

It must be recognized that in equation 6.14a for the capacity factor, only the first stability constant, K₁, of the metal complex with the hydroxyacid, has been considered. Equation 6.14a is therefore applicable only under experimental conditions where the equilibrium involving the first stability constant is exclusively operative or dominant. This is the case when the concentration of [A⁻] is very small at lower pH or lower concentrations of the hydroxyacids. As the [A⁻] is increased, there is a progressive involvement of higher order equilibria. Under conditions where both K₁ and K₂ are important, Eq. 6.14a must be expanded as follows:

$$k' = \frac{Y [RSO_3^-]}{\left\{ K_1 [A^-] + K_1 K_2 [A^-]^2 \right\}} \dots\dots\dots (6.15),$$

It can be seen that k' is inversely proportional to the concentrations of both MA_1 and MA_2 , and the sum of MA_1 and MA_2 concentrations together yield the amount of the analyte present in the mobile phase. Equation 6.15 can be rewritten to yield an equation where $(k')^{-1}$ is expressed as a polynomial in $[A^-]$, where the coefficients of the polynomial involve the overall stability constants.

$$\frac{Y [RSO_3^-]}{k'} = \beta_1 [A^-] + \beta_2 [A^-]^2 + \beta_3 [A^-]^3 + \beta_4 [A^-]^4 \dots\dots\dots (6.16)$$

In the execution of the fitting procedure for the determination of the stability constants, first consider experimental conditions, where only $[MA_1]$ and $[MA_2]$ are dominant and hence only the terms involving β_1 and β_2 in equation 6.16 need to be retained. With α -HIBA, this condition is achieved by maintaining the pH of the eluent solution to values below 2.8. Chromatograms were recorded for various values of pH over the range 2.5 to 3.2 for the reasons explained in the estimation of β_3 . In a chromatographic run at a given pH of the eluent, the capacity factor, k' was determined for each of the lanthanides. The value of $[RSO_3^-]$ at a given pH is determined from the pKa value of the ion-pairing reagent. A fit of the terms of the left hand side of the truncated Eq. 6.16, against $[A^-]$ yields both β_1 and β_2 for a given analyte.

$$\frac{Y [RSO_3^-]}{k'} = \beta_1 [A^-] + \beta_2 [A^-]^2 \dots\dots\dots(6.17)$$

However, in order to perform the fit, knowledge of the value of “Y” is necessary and its determination is discussed below.

“Y” is given as

$$Y = X.K_s$$

where X is an instrumental parameter and K_s is the stability constant of the analyte complex with the ion pairing reagent, CSA. The values of K_s for the different analytes with CSA are not available in the literature and hence “Y” has to be determined experimentally, for which the following method was devised. A lanthanide, which we shall refer to as the “calibrant analyte”, was chosen, for which the stability constant, K_1 and K_2 for the complexes with the hydroxyacid is known. At a given pH, $[RSO_3^-]$ can be calculated from its pKa value. From the experimentally determined capacity factor for this lanthanide, the constant “Y”, the only unknown, was determined. Using this value for the constant Y, fit to Eq. 6.17 was performed to determine the stability constants for the other lanthanides and actinides.

6.3.2.1 Estimation of β_3

The higher order stability constants become significant as the concentrations of $[A^-]$ increases, which in effect was achieved as the pH was increased. Chromatograms recorded at pH greater than 3.0 therefore allow for the determination of β_3 and even β_4 . Using experiments performed at low pH values (e.g. 2.5-2.8), β_1 and β_2 were first determined. The values for lower order stability constants were then fixed at these values during the determination of β_3 .

The method was validated by the estimation of stability constant of lanthanides and actinides with α -HIBA using a single calibrant, Sm and the results are shown in **Table.6.2**.

Table.6.2. Stability constant of lanthanides with α -HIBA estimated for 0.2 M ionic strength at 25⁰C (method-I)

Chromatographic exp. conditions: α -HIBA: 0.1 M; CSA: 0.005 M, pH: 2.6 & 2.7 used for $\log\beta_1$ & $\log\beta_2$, pH: 3 for $\log\beta_3$.

*Lit.data (R. Portanova *et al*, 2003, [192]): for 0.2 M ionic strength at 25⁰C.

Calibrant: Sm.

Lanthanides & Actinides	$\log(\beta_1)$		$\log(\beta_2)$		$\log(\beta_3)$	
	*Lit. Data	Present study	Lit. Data	Present study	Lit.Data	Present study
La	2.3	2.55(10.8)	4.04	4.03(0.25)	**	#
Ce	2.55	2.58(1.17)	4.08	4.35(6.61)	5.49	5.91(7.65)
Pr	2.59	2.60(0.38)	4.37	4.54(3.89)	5.60	5.53(1.25)
Nd	2.74	2.64(3.65)	4.42	4.58(3.62)	5.98	6.26(4.68)
Sm	2.75	2.70(1.82)	4.77	4.85(1.68)	6.17	6.37(3.24)
Eu	2.79	2.76(1.07)	4.86	5.00(2.88)	6.34	6.67(5.20)
Gd	2.79	2.81(0.72)	4.98	5.01(0.60)	6.50	6.71(3.23)
Tb	2.92	2.89(1.03)	5.24	5.15(1.72)	6.86	7.05(2.7)
Dy	2.94	3.04(3.4)	5.45	5.20(4.59)	7.29	7.13(2.19)
Ho	2.98	3.06(2.68)	5.54	5.30(4.33)	7.44	7.10(4.56)
Er	3.01	3.08(2.32)	5.70	5.41(5.09)	7.58	7.35(3.03)
Tm	3.1	3.12(0.64)	5.79	5.51(4.83)	7.71	7.37(4.41)
Yb	3.13	3.14(0.32)	5.87	5.63(4.09)	7.94	7.66(3.52)
Lu	3.18	3.16(0.63)	6.05	5.69(5.95)	8.07	7.75(3.96)
Pu	**	2.66	**	4.60	**	#
Am	**	2.7	**	4.61	**	#

** Not available in literature.

unable to estimate from fit.

Parenthesis: % Deviation from literature data.

The percentage deviation in the estimates of $\log \beta_1$, $\log \beta_2$ and $\log \beta_3$ using the single calibrant is generally found to be $\pm 5\%$ with few exceptions. It is clear from this study that this method is not restrictive and use of single calibrant yield good estimates of the stability constants of entire lanthanides and some actinides such as Pu(III) and Am(III). The method was also validated by estimation of stability constants of lanthanides with lactic acid (**Table.6.3**) and mandelic acid (**Table.6.4**). The results are again in good agreement with the literature data. The approach was employed to estimate stability constant of lanthanides with tartaric acid for which most of the data is not available in literature (**Table.6.5**).

Table.6.3. Stability constant of lanthanides with lactic acid estimated for 2 M ionic strength at 25⁰C (method-1)

Chromatographic Exp: 0.008 M CSA + 0.05 M Lactic acid, pH 2.6 & 2.7 for $\log \beta_1$ & $\log \beta_2$, pH: 2.8 for $\log \beta_3$.

Lit.data(R. Portanova *et al*, 2003 [192]): for 2 M ionic strength at 25⁰C.

Calibrant: Sm.

Lanthanides (III)	$\log \beta_1$		$\log \beta_2$		$\log \beta_3$	
	Lit.data	Present study	Lit.data	Present study	Lit.data	Present study
La	2.27	2.29(0.88)	3.95	3.89(1.52)	5.06	5.35(5.73)
Ce	2.33	2.31(0.86)	4.10	4.09(0.24)	5.21	5.96(14.39)
Pr	**	2.49	**	4.01	**	6.01
Nd	2.47	2.43(1.62)	4.37	4.51(3.20)	5.60	6.07(8.39)
Sm	2.56	2.50(2.34)	4.58	4.65(1.53)	5.90	#
Eu	2.53	2.56(1.18)	4.6	4.63(0.65)	5.88	#
Gd	2.53	2.55(0.80)	4.63	4.66(0.65)	5.91	5.97(1.01)
Tb	**	2.70	**	4.74	**	5.77
Dy	2.72	2.71(0.37)	4.77	4.88(2.31)	6.77	6.72(0.74)
Ho	2.71	2.73(0.74)	4.97	4.87(2.01)	6.55	6.63(1.22)
Er	2.77	2.83(2.16)	5.11	5.06(0.98)	6.70	6.82(1.79)
Tm	**	2.82	**	5.19	**	#
Yb	2.85	2.79(2.10)	5.27	5.3(0.57)	6.9	6.85(0.72)
Lu	**	2.81	**	5.7	**	7.45

** Data not available in literature.

unable to estimate.

Parenthesis: % Deviation from literature data.

Table.6.4. Stability constant of lanthanides with mandelic acid estimated for 0.1 M ionic strength at 25⁰C

Chromatographic exp. conditions: mandelic acid: 0.05 M; CSA: 0.006 M, pH: 2.52.

Lit.data(R. Portanova *et al*, 2003[192]) in parenthesis: 0.1 M ionic strength at 25⁰C

Calibrants: Eu (method-I); La, Nd, Ho, Yb (method-II)

Lanthanide (III)	A		Lanthanide	B	
	log(β_1)	log(β_2)		log(β_1)	log(β_2)
La	2.57(2.55)	4.74(4.14)	La	2.53(2.55)	4.13(4.14)
Ce	2.68(**)	4.90(**)	Ce	2.63(**)	4.40(**)
Pr	2.79(2.76)	5.09(4.65)	Pr	2.70(2.76)	4.56(4.65)
Nd	2.80(2.83)	5.11(4.77)	Nd	2.75(2.83)	4.66(4.77)
Sm	2.84(2.90)	5.15(4.75)	Sm	2.86(2.90)	4.88(4.75)
Eu	2.88(2.95)	5.17(5.07)	Eu	2.93(2.95)	5.01(5.07)
Gd	2.90(2.88)	5.18(5.01)	Gd	2.98(2.88)	5.10(5.01)
Tb	2.96(3.01)	5.21(5.25)	Tb	3.06(3.01)	5.27(5.25)
Dy	3.01(3.03)	5.23(5.29)	Dy	3.10(3.03)	5.37(5.29)
Ho	3.03(3.05)	5.26(5.35)	Ho	3.11(3.05)	5.44(5.35)
Er	3.07(3.15)	5.27(5.41)	Er	3.16(3.15)	5.53(5.41)
Tm	3.08(3.20)	5.30(5.56)	Tm	3.19(3.20)	5.60(5.56)
Yb	3.13(3.29)	5.30(5.76)	Yb	3.30(3.29)	5.75(5.76)
Lu	3.15(3.25)	5.31(5.83)	Lu	3.32(3.25)	5.80(5.83)

A: Estimation of stability constant (method-1)

B: Estimation based on Speciation data (method-2)

** data not available in literature.

% Deviations are found to be 0.32% to 8.92% from lit.data.

Table.6.5. Stability constant of lanthanides with tartaric acid estimated for 0.015 M ionic strength at 25⁰C (method-1)

Chromatographic exp. conditions: tartaric acid: 0.05 M; CSA: 0.003 M, pH: 2.5 & 2.7 for logβ₁ & logβ₂, Chromatographic temp: 25⁰C

Lit.data (V. V. Nikonorov *et al*, 2010 [186]): for 0.015 M ionic strength at 25⁰C

Calibrant: Pr

Lanthanides (III)	log β ₁		log β ₂	
	Lit.data	Present study	Lit.data	Present study
La	3.89	4.19	7.31	7.33
Ce	3.96	4.25	7.45	7.47
Pr	4.04	4.38	7.6	7.58
Nd	4.02	4.48	7.56	7.64
Sm	4.05	4.50	7.63	7.73
Eu	**	4.50	**	7.73
Gd	**	4.56	**	7.67
Tb	**	4.53	**	7.64
Dy	**	4.52	**	7.64
Ho	**	4.53	**	7.64
Er	**	4.62	**	7.67
Tm	**	4.64	**	7.71
Yb	**	4.78	**	7.78
Lu	**	4.89	**	7.80

** data not available in literature.

6.3.2.2 Influence of column length, mobile phase flow rate, RSO₃⁻, [A⁻] on Y

$$\text{Capacity factor, } k' = \frac{Y \left[\text{RSO}_3^- \right]}{\left\{ K_I \left[\text{A}^- \right] + K_I K_2 \left[\text{A}^- \right]^2 \right\}} \dots\dots\dots (6.15)$$

The constant in equation 6.14a, Y, is composed of two terms, “K_s”, the stability constant of the analyte CSA complex and “X”, which is an instrument dependent parameter. For a fixed concentration of A⁻ and RSO₃⁻ concentration, X can be expected to increase with increase in the length of the column. The value of the constant, X, was found to be ~2 times larger when experiments were run using 25 cm length reversed phase column compared

with that observed with a 10 cm length monolith column. At fixed A^- concentration and fixed column length, X (instrument parameter constant) should not vary with increase of RSO_3^- concentration; hence Y which is the product of $K_s \cdot X$ (K_s is constant) will not vary as well. However, capacity factor increases with increase of RSO_3^- concentration, keeping the ratio of $[RSO_3^-]/k'$ constant, Y remaining unchanged. This was examined by carrying out an experiment with varying concentrations of CSA and the capacity factor was proportional to RSO_3^- concentration, keeping the Y constant. Similarly, concentration of A^- was varied in some experiments, and Y remained constant with changes in A^- concentration (changes in A^- was altering the capacity factor, e.g., increase in A^- reducing the capacity factor and vice versa). In some studies, Y value was also measured under various mobile phase flow rates (1-5 mL/min) and exponential variation of Y value from 1 mL/min to 5 mL/min was observed (**Table.6.6**).

Table.6.6. Variation of $Y (K_s \cdot X)$ as a function of mobile phase flow rates for calibrant, S_m

Chromatographic exp. conditions: α -HIBA: 0.1 M; CSA: 0.005 M, pH: 2.6; Chromatographic temp: 25⁰C

Flow rate (mL/min)	$Y (K_s \cdot X)$ value of calibrant, S_m
1	52367
2	26183
3	17455
4	13094
5	10512

Thus Y, product of instrument factor, X and K_s remains constant and can only be altered by varying the mobile phase flow rate, altering the column length, type of column i.e., relative hydrophobicity etc.

6.3.3 Estimation of stability constant of unknown complexing agent with metal ion

Equation 6.14a for two different complexing agents can be written as

$$k'_{(acid1)} = \frac{Y [RSO_3^-]}{K_{1(acid1)} [A^-]} \dots\dots\dots (6.18)$$

$$k'_{(acid2)} = \frac{Y [RSO_3^-]}{K_{1(acid2)} [A^-]} \dots\dots\dots (6.19),$$

On rearrangement of equation 6.18 and 6.19 results (at a lower pH e. g. pH: 2.6) the following:

$$K_{1(acid2)} = \frac{k'_{(acid1)} \cdot K_{1(acid1)}}{k'_{(acid2)}} \dots\dots\dots(6.20)$$

where $k'_{(acid1)}$ & $k'_{(acid2)}$ are capacity factors of metal ions with acid1 and acid2 respectively; $K_{1(acid1)}$ & $K_{1(acid2)}$: are stepwise stability constants of metal ions with acid1 & acid2 respectively. From relative retention data and $\log\beta_1$ with known system, stability constants of metal ions with unknown ligands can be estimated. The validity of the method was tested using HIBA as well as lactic acid and the results are given in **Table.6.7**. This method can be applied to estimate stability constant of actinides with ligands, which are of importance in the chelation therapy, e.g., in the treatment of internal contamination of actinides. Similarly, successful design of new ligands for individual separation of actinides / lanthanides, demands knowledge of stability constant and the chromatographic technique developed in the present study offers an alternate method of quick estimation.

Table.6.7. Estimation of stability constant of lanthanides with a ligand (method-1) whose data is not reported: Validation of the method

Lanthanides (III)	Chromatographic data with HIBA used to estimate $\log\beta_1$ with lactic acid and mandelic acid (A)			Chromatographic data with lactic acid used to estimate $\log\beta_1$ with HIBA and mandelic acid (B)		
	$\log\beta_1$ with α -HIBA at 2M ionic strength	Estimated data with lactic acid at 2M ionic strength	Estimated data with mandelic acid at 2M ionic strength	$\log\beta_1$ with lactic acid at 0.1M ionic strength	Estimated data with HIBA at 0.1 M ionic strength	Estimated data with mandelic acid at 0.1 M ionic strength
	$\log\beta_1$	$\log\beta_1$ **	$\log\beta_1$ ***	$\log\beta_1$	$\log\beta_1$ **	$\log\beta_1$ ***
La	2.31#	2.6 (2.27)	2.20 (1.93)	2.44*	2.04 (2.3)	1.83 (2.55)
Ce	2.43*	2.69 (2.33)	2.24 (2.17)	2.23#	2.17 (2.55)	1.78 (NA)
Pr	2.51#	2.74 (NA)	2.27 (2.30)	2.69*	2.19 (2.59)	1.85 (2.76)
Nd	2.62*	2.84 (2.47)	2.34 (2.43)	2.38#	2.26(2.74)	1.88 (2.83)
Sm	2.75*	2.88 (2.56)	2.37 (2.47)	2.49#	2.45 (2.75)	1.97 (2.90)
Eu	2.70*	2.78 (2.53)	2.24 (2.25)	2.90#	2.82 (2.79)	2.37 (2.95)
Gd	2.82*	2.86 (2.53)	2.35 (2.42)	2.96*	2.86 (2.79)	2.39 (2.88)
Tb	2.83*	2.81 (NA)	2.30 (2.52)	2.96#	2.98 (2.92)	2.45 (3.01)
Dy	2.94#	2.89 (2.72)	2.35 (2.57)	3.09*	3.08 (2.94)	2.49 (3.03)
Ho	3.05*	2.97 (2.71)	2.43 (2.54)	3.09#	3.17 (2.98)	2.55 (3.05)
Er	3.07*	2.97 (2.77)	2.40 (2.68)	3.21*	3.27 (3.01)	2.60 (3.15)
Tm	3.05*	2.94 (NA)	2.34 (NA)	3.26#	3.36 (3.1)	2.65 (3.20)
Yb	3.07#	2.97 (2.85)	2.32 (2.72)	3.41#	3.51 (3.13)	2.76 (3.29)
Lu	3.12#	3.01 (NA)	2.35 (2.77)	3.40*	3.62 (3.18)	2.85 (3.25)

(A):

Lit.data (R. Portanova *et al*, 2003 [192]) in parenthesis.

* Literature data available only for Ce, Nd, Sm, Eu, Gd, Tb, Ho, Er, and Tm at 25°C

Estimated using method-I at 25°C; lit.data not available for La, Pr, Dy, Yb and Lu

** Estimated stability constant compared with lit.data at 2 M ionic strength and 25°C;

*** Estimated stability constant compared with lit.data at 2 M ionic strength at 25°C;

NA- lit. data not available.

(B):

Literature data (R. Portanova *et al*, 2003 [192]) in parenthesis.

* Lit.data available only for La, Pr, Gd, Dy, Er and Lu at 25°C

estimated by method-I, present study at 25°C

** Estimated stability constant data at 0.1 M ionic strength compared with lit.data at 0.2 M ionic strength and 25°C as lit.data at 0.1 M ionic strength is not available.

*** Estimated stability constant at 0.1 M ionic strength compared with stability constant of lit. data at 0.1 M ionic strength at 25°C.

6.3.4 Estimation of stability constant from speciation data (method-2)

The well known lanthanide contraction can be used for the prediction of stability constants of metal complexes, for a given ionic strength. The precision of the method depends on the use of 4 or 5 or 6 calibrants for the estimation of stability constant of other lanthanides. A study was also taken up in the present work for the estimation of stability constant with use of three or four lanthanide calibrants for any given ionic strength. In this method, it is recognized that for a given set of conditions, such as pH and concentration of the eluents, a lanthanide has a characteristic capacity factor. It has been established that, a given capacity factor uniquely fixes the relative concentration of the various stoichiometries, e.g., Ln^{+3} , LnA^{+2} etc. which in turn can be used to determine the stability constants.

In order to establish a correlation between the fraction of various species and the capacity factors, four representative lanthanides (e.g., Lu, Ho, Gd and Pr) are chosen for a given concentration of the eluents and pH. For the experimental conditions adopted in this study, each of the lanthanides manifest different fraction of each of the stoichiometries, due to their differences in the stability constants. **Fig.6.3a** shows the plot of $[\text{Ln}^{+3}]$ vs. capacity factor (k') for the lanthanides, while each of the **Fig.6.3b-e**, show the plot of the fractions of the complexed species for each of the lanthanides. Each of the plots demanded a different functional form to provide the best fit. While in **Fig.6.3a**, the data fits into a straight line fit, **Fig.6.3b and c** sought a polynomial of order 2, while **Figs.6.3d and 6.3e** were best fit using an exponential. It is reiterated that all the five figures constitute a single experiment. These plots provide the fractions of each of the stoichiometries of the complexes of other lanthanides, once their capacity factors are known. From a knowledge of the fractions of each stoichiometric species, the calculations of Eqs. 6.2-6.5 can be reversed to obtain the

stability constants. Likewise, from the observed capacity factors of Pu^{3+} and Am^{3+} , the corresponding stability constants were also determined. In the fitting process, the linear fit incorporates two fit parameters, while the second order polynomial and the exponential fit required three fit parameters, which demands the use of at least four data points. Hence four lanthanides, e.g. Pr, Gd, Ho and Lu spanning the range of entire lanthanide series were chosen for the purpose of the fit. The validation of the method was tested by the estimation of stability constant of entire lanthanides, Pu^{3+} and Am^{3+} with α -HIBA (**Table.6.8**). Similarly, the method was validated by estimation of stability constant of lanthanides with mandelic acid (**Table.6.4**). The method was also validated by estimation of stability constant of lanthanides with lactic acid (**Table.6.9**). It is established that the $\log\beta$ values estimated from this method are generally in very good agreement with the literature data ($\pm 5\%$).

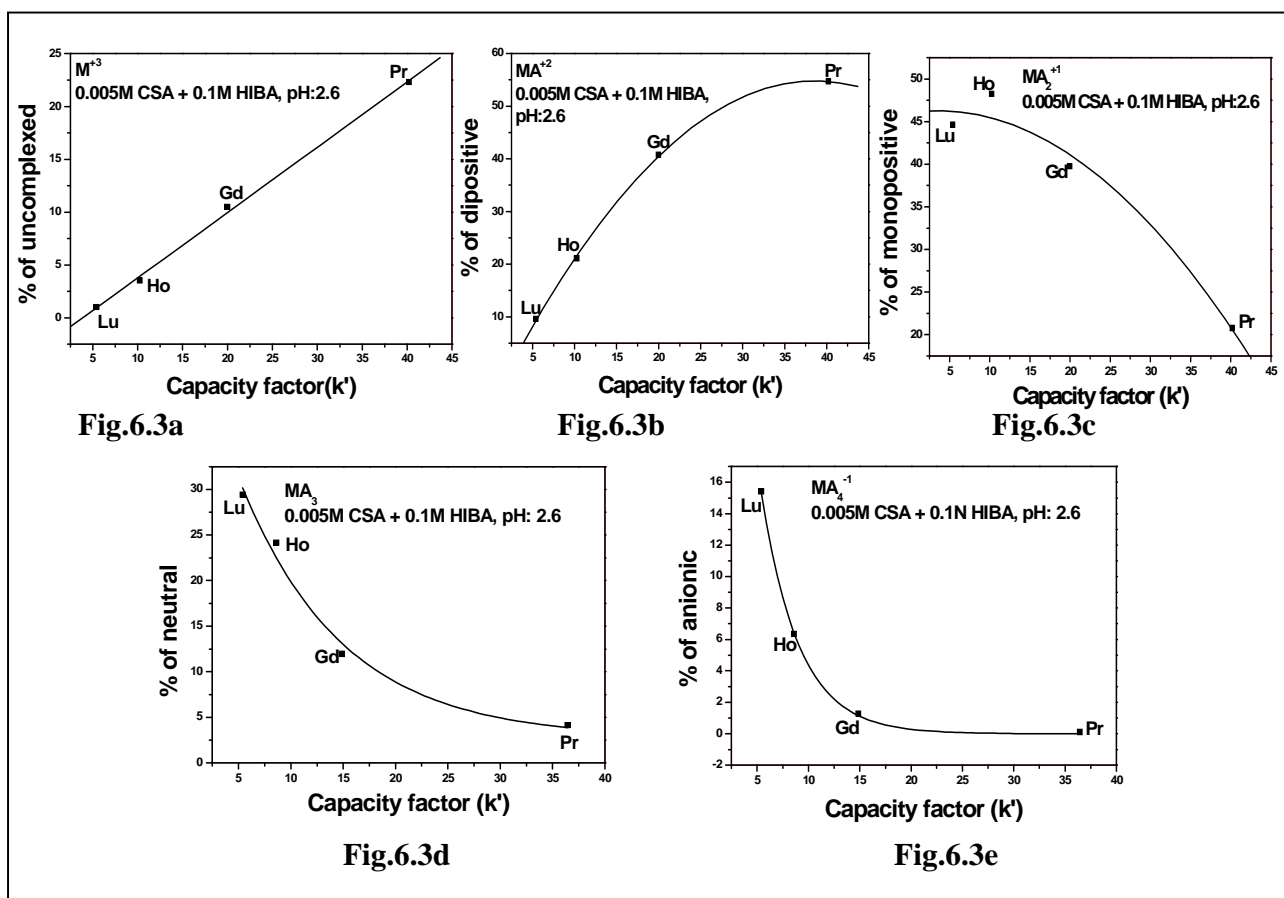


Fig.6.3. Plot of uncomplexed (M^{+3}), dipositive (MA^{+2}), monopositive (MA_2^{+1}), neutral (MA_3) & anionic (MA_4^{-1}) species of lanthanides (Pr, Gd, Ho, Lu)-HIBA complexes against capacity factor (k').

Table.6.8. Stability constant of lanthanides with α -HIBA (method-2), estimated for 0.2 M ionic strength at 25⁰C

Chromatographic exp. conditions: HIBA: 0.1 M; CSA: 0.005 M, pH: 2.6.

*Lit.data(R. Portanova *et al*, 2003 [192]): for 0.2 M ionic strength at 25⁰C.

Calibrants: Pr, Gd, Ho and Lu.

Lanthanides & Actinides	log(β_1)		log(β_2)		log(β_3)		log(β_4)	
	*Lit. Data	Present study	Lit. Data	Present study	Lit. Data	Present study	Lit. Data	Present study
La	2.3	2.32(0.87)	4.04	4.08(0.99)	**	5.23	**	#
Ce	2.55	2.50(1.96)	4.08	4.15(1.71)	5.49	5.63(2.55)	**	#
Pr	2.59	2.58(0.38)	4.37	4.35(0.46)	5.60	5.67(1.25)	6.38	#
Nd	2.74	2.63(4.01)	4.42	4.50(1.81)	5.98	5.76(3.68)	6.58	6.22(5.47)
Sm	2.75	2.74(0.36)	4.77	4.81(0.84)	6.17	6.22(0.81)	7.38	6.33(14.2)
Eu	2.79	2.78(0.36)	4.86	4.94(1.64)	6.34	6.43(1.42)	7.59	6.95(8.43)
Gd	2.79	2.81(0.72)	4.98	5.01(0.60)	6.50	6.54(0.61)	7.65	7.25(5.23)
Tb	2.92	2.86(2.05)	5.24	5.20(0.76)	6.86	6.88(0.29)	8.09	8.02(0.86)
Dy	2.94	2.91(1.02)	5.45	5.35(1.83)	7.29	7.12(2.33)	8.5	8.51(0.12)
Ho	2.98	2.94(1.34)	5.54	5.45(1.62)	7.44	7.29(2.01)	8.74	8.81(0.80)
Er	3.01	2.97(1.33)	5.70	5.59(1.93)	7.58	7.48(1.32)	9.03	9.13(1.11)
Tm	3.1	3.02(2.58)	5.79	5.73(1.03)	7.71	7.68(0.39)	9.33	9.44(1.18)
Yb	3.13	3.11(0.64)	5.87	5.97(1.70)	7.94	7.93(0.13)	9.72	9.79(0.71)
Lu	3.18	3.19(0.31)	6.05	6.09(0.66)	8.07	8.10(0.37)	9.99	10.01(0.20)
Pu	**	2.65	**	4.61	**	5.94	**	#
Am	**	2.67	**	4.60	**	6.00	**	#

** Not available in literature.

unable to estimate from fit.

Parenthesis: % Deviation from literature data.

Table.6.9. Stability constant of lanthanides with lactic acid (method-2), estimated for 2 M ionic strength & 0.1 M ionic strength at 25⁰C

Chromatographic Exp: 0.008M CSA+0.05M lactic acid; pH: 2.6

Lit.data: for 2 M & 0.1 M ionic strength at 25⁰C;

La, Sm, Ho and Yb- calibrants (2 M ionic strength) & La, Gd, Lu - calibrants (0.1 M ionic strength)

lanthanides	2 M ionic strength			lanthanides	0.1 M ionic strength	
	log(β_1)	log(β_2)	log(β_3)		log(β_1)	log(β_2)
La	2.26(2.27)	3.92(3.95)	5.09(5.06)	La	2.23(2.44)	3.60(4.32)
Ce	2.38(2.33)	4.18(4.10)	5.41(5.21)	Ce	2.23(**)	3.95(**)
Pr	2.46(**)	4.35(**)	5.64 (**)	Pr	2.33(2.69)	4.08(4.96)
Nd	2.50(2.47)	4.44(4.37)	5.78(5.60)	Nd	2.38(**)	4.10(**)
Sm	2.58(2.56)	4.63(4.58)	6.04(5.90)	Sm	2.49(**)	4.57(**)
Eu	2.59(2.53)	4.67(4.60)	6.10(5.88)	Eu	2.90(**)	4.86(**)
Gd	2.59(2.53)	4.67(4.63)	6.10(5.91)	Gd	2.90(2.96)	4.86(5.09)
Tb	2.63(**)	4.76(**)	6.24(**)	Tb	2.96(**)	4.98(**)
Dy	2.68(2.72)	4.87(4.77)	6.40(6.77)	Dy	3.03(3.09)	5.32(5.38)
Ho	2.71(2.71)	4.95(4.97)	6.50(6.55)	Ho	3.09(**)	5.37(**)
Er	2.75(2.77)	5.05(5.11)	6.64(6.70)	Er	3.17(3.21)	5.49(5.57)
Tm	2.78(**)	5.14(**)	6.78(**)	Tm	3.26(**)	5.61(**)
Yb	2.83(2.85)	5.26(5.27)	6.95(6.90)	Yb	3.41(**)	5.79(**)
Lu	2.86(**)	5.32(**)	7.03(**)	Lu	3.51(3.40)	5.91(5.82)

Literature data (R. Portanova et al, 2003 [192] in parenthesis.

*** literature data not available.*

% deviations from lit.data: 0.44 to 6.48%.

6.3.4.1 Influence of RSO₃H on retention

Increase in the proportion of uncomplexed species [M⁺³] of a metal ion increases capacity factor while, formation of complexed species, e.g., with organic acid α -HIBA, reduces the capacity factor in general for a given RSO₃⁻ concentration (**Fig.6.4**). These studies clearly established that K_S (lanthanide stability constant with RSO₃H, e.g. CSA)

increases from La to Lu. However for a given metal ion and $[A^-]$, capacity factor increases proportionally with increase in RSO_3^- concentration.

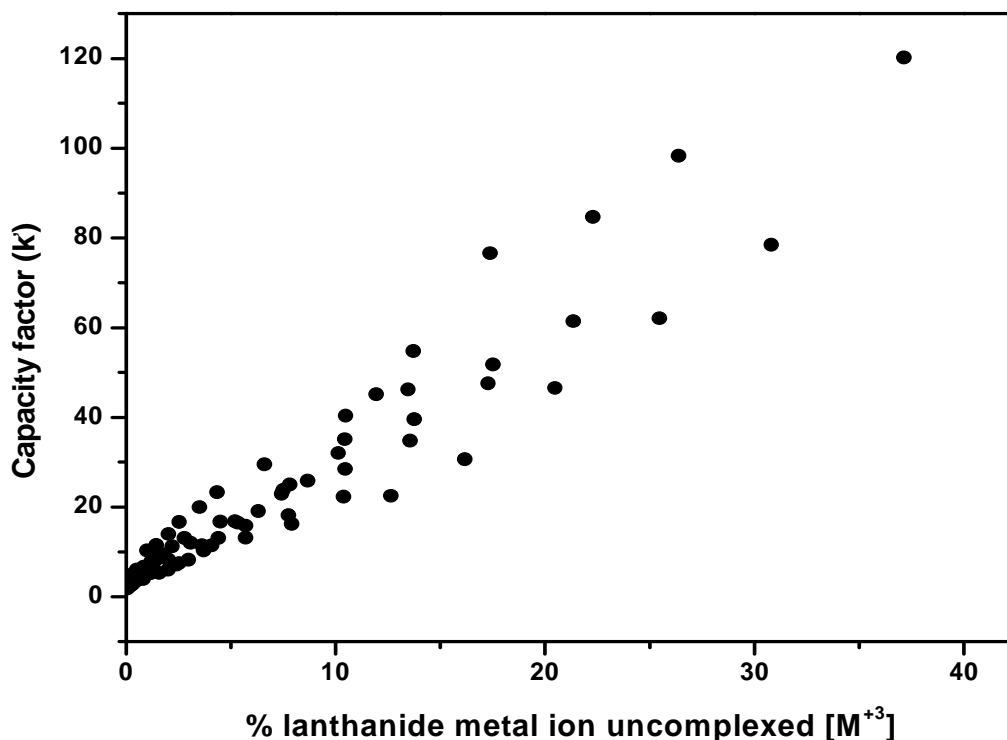


Fig.6.4. Plot of uncomplexed $[M^{+3}]$ against capacity factor for all the lanthanides. Mobile phase: CSA (0.01 M) and α -HIBA (0.1 M). Experiment was carried out in the pH region of 2.6 to pH 3.1 at 0.1 increments.

6.3.5 Correlation of retention with stability constant – estimation of stability constant at different ionic strengths

Most of the chromatographic studies were carried out in the present work at an ionic strength ~ 0.1 M. The same chromatogram was used for estimating stability constants at different ionic strengths, e.g., 0.5 M (**Table.6.10**). A good agreement was established with the literature values, i.e., estimated stability constants were for an ionic strength, similar to that of the calibrants. Similarly, lanthanide separations were also performed in the present study at α -HIBA concentrations of 0.05 M. Stability constant of calibrants at 0.2 M / 0.5 M

ionic strength were employed for estimation of stability constants of unknowns (**Table.6.11** & **Table.6.12**).

Table.6.10. Stability constant of lanthanide - HIBA complexes (method-1), estimated at 0.5 M ionic strength at 25°C

Lit.data (R. Portanova *et al*, 2003 [192]): for 0.5 M ionic strength and 25°C.

Exp: 0.005 M CSA + 0.1 M HIBA; pH 2.6 & 2.7 (25°C).

Sm-calibrant.

lanthanides	log β_1		log β_2	
	Lit.data	Present study	Lit.data	Present study
La	2.22	2.36(6.30)	3.67	4.01(9.26)
Ce	2.37	2.40(1.26)	4.01	4.25(5.98)
Pr	2.48	2.44(1.61)	4.12	4.38(6.31)
Nd	2.54	2.48(2.36)	4.32	4.45(3.01)
Sm	2.63	2.55(3.04)	4.60	4.68(1.74)
Eu	2.71	2.60(4.06)	4.92	4.81(2.23)
Gd	2.71	2.63(2.95)	4.97	4.87(2.01)
Tb	2.87	2.75(4.18)	5.21	5.02(3.64)
Dy	2.95	2.85(3.39)	5.32	5.13(3.57)
Ho	2.98	2.91(2.35)	5.42	5.20(4.06)
Er	3.03	3.02(0.33)	5.54	5.27(4.87)
Tm	3.13	3.09(1.28)	5.62	5.33(5.16)
Yb	3.18	3.20(0.63)	5.76	5.39(6.42)
Lu	3.21	3.27(1.87)	5.85	5.42(7.35)
Am ⁺³	**	2.54	**	4.58
Pu ⁺³	**	2.51	**	4.56

** lit data not available.

Parenthesis: % Deviation from literature data.

Table.6.11. Stability constant of lanthanide -HIBA complexes (method-1 & method-2), estimated at 0.2 M ionic strength at 25°C

Lit.data (R. Portanova *et al*, 2003[192]): for 0.2 M ionic strength and 25°C.

Exp: 0.008 M CSA + 0.05 M HIBA.

Sm-calibrant (method-1) & Pr, Gd, Ho and Lu- calibrants (method-2)

Lanthanide (III)	method-1		Lanthanide	method-2			
	log(β_1)	log(β_2)		log(β_1)	log(β_2)	log(β_3)	log(β_4)
La	2.60(2.30)	#(4.04)	La	2.28(2.30)	4.28(4.04)	4.98(**)	# (**)
Ce	2.61(2.55)	#(4.08)	Ce	2.46(2.55)	4.27(4.08)	5.34(5.49)	# (**)
Pr	2.65(2.59)	#(4.37)	Pr	2.57(2.59)	4.35(4.37)	5.62(5.60)	#(6.38)
Nd	2.76(2.74)	3.98(4.42)	Nd	2.63(2.74)	4.45(4.42)	6.23(5.98)	#(6.58)
Sm	2.74(2.75)	4.80(4.77)	Sm	2.76(2.75)	4.77(4.77)	6.48(6.17)	6.18(7.38)
Eu	2.76(2.79)	4.95(4.86)	Eu	2.81(2.79)	4.95(4.86)	6.56(6.34)	6.80(7.59)
Gd	2.78(2.90)	5.01(4.98)	Gd	2.84(2.79)	5.03(4.98)	6.69(6.50)	8.11(7.65)
Tb	2.81(2.92)	5.21(5.24)	Tb	2.90(2.92)	5.27(5.24)	7.03(6.86)	7.92(8.09)
Dy	2.85(2.94)	5.35(5.45)	Dy	2.94(2.94)	5.44(5.45)	7.27(7.29)	8.47(8.50)
Ho	2.90(2.98)	5.40(5.54)	Ho	2.97(2.98)	5.53(5.54)	7.40(7.44)	8.74(8.74)
Er	2.88(3.01)	5.54(5.70)	Er	3.00(3.01)	5.66(5.70)	7.58(7.58)	9.13(9.03)
Tm	2.90(3.10)	5.63(5.79)	Tm	3.03(3.10)	5.77(5.79)	7.73(7.71)	9.42(9.33)
Yb	2.91(3.13)	5.74(5.87)	Yb	3.07(3.13)	5.89(5.87)	7.89(7.94)	9.74(9.72)
Lu	2.93(3.18)	5.79(6.05)	Lu	3.09(3.18)	5.96(6.05)	7.98(8.07)	9.89(9.99)
Am ⁺³	2.63(**)	4.93(**)	Am ⁺³	2.60(**)	4.55(**)		
Pu ⁺³	2.70(**)	4.73(**)	Pu ⁺³	2.67(**)	4.68(**)		

Literature data [R. Portanova et al, 2003] in parenthesis.

*** data not available in literature.*

unable to estimate from fit.

% deviations from lit.data: 0.36 to 13.00 % (method-1) 0.18 to 16% (method-2).

Table.6.12. Stability constant of lanthanide-HIBA complexes (method-1 & method-2), estimated at 0.5 M ionic strength at 25°C

Lit.data (R. Portanova *et al*, 2003 [192]): for 0.5 M ionic strength and 25°C.

Exp: 0.008 M CSA + 0.05 M HIBA.

Sm-calibrant (method-1) & La, Gd, Ho and Lu- calibrants (method-2)

Lanthanide (III)	method-1		Lanthanide	method-2		
	log(β_1)	log(β_2)		log(β_1)	log(β_2)	log(β_3)
La	2.40(2.22)	3.94(3.67)	La	2.21(2.22)	3.61(3.67)	# (**)
Ce	2.42(2.37)	4.23(4.01)	Ce	2.37(2.37)	4.17(4.01)	# (**)
Pr	2.45(2.48)	4.37(4.12)	Pr	2.47(2.48)	4.41(4.12)	# (**)
Nd	2.46(2.54)	4.46(4.32)	Nd	2.52(2.54)	4.53(4.32)	# (**)
Sm	2.56(2.63)	4.67(4.60)	Sm	2.66(2.63)	4.82(4.60)	# (**)
Eu	2.61(2.71)	4.82(4.92)	Eu	2.72(2.71)	4.95(4.92)	# (5.91)
Gd	2.64(2.71)	4.86(4.97)	Gd	2.75(2.71)	5.02(4.97)	# (6.01)
Tb	2.76(2.87)	5.04(5.21)	Tb	2.84(2.87)	5.20(5.21)	# (6.19)
Dy	2.87(2.95)	5.16(5.32)	Dy	2.90(2.95)	5.33(5.32)	7.42(7.16)
Ho	2.91(2.98)	5.22(5.42)	Ho	2.94(2.98)	5.40(5.42)	7.55(7.41)
Er	3.00(3.03)	5.27(5.54)	Er	3.00(3.03)	5.51(5.54)	7.74(7.56)
Tm	3.08(3.13)	5.34(5.62)	Tm	3.06(3.13)	5.61(5.62)	7.87(7.84)
Yb	3.20(3.18)	5.40(5.76)	Yb	3.13(3.18)	5.72(5.76)	8.03(8.02)
Lu	3.27(3.21)	5.42(5.85)	Lu	3.17(3.21)	5.78(5.85)	8.10(8.21)
Am ⁺³	2.51(**)	4.40(**)	Am ⁺³	2.56(**)	4.41(**)	
Pu ⁺³	2.54(**)	4.43(**)	Pu ⁺³	2.54(**)	4.37(**)	5.28(**)

Literature data (R. Portanova et al, 2003[192]) in parenthesis.

*** data not available in literature.*

unable to estimate from fit.

% deviations from lit.data: 0.63 to 8.10 % (method-1) 0.12 to 3.63% (method-2).

A good agreement has been established with the literature data in both the cases. These studies established that, even though the absolute value of capacity factors is a function of ionic strength, the trend of relative variation of capacity factor with mobile phase composition remains more or less similar and least affected by ionic strength variation. **Fig.6.5** depicts stability constant of lanthanide-HIBA complexes at two different ionic strengths. An important and significant observation established in these studies is that the same chromatogram can be used to estimate stability constants of metal ions at various ionic strengths and a single chromatogram is generally adequate.

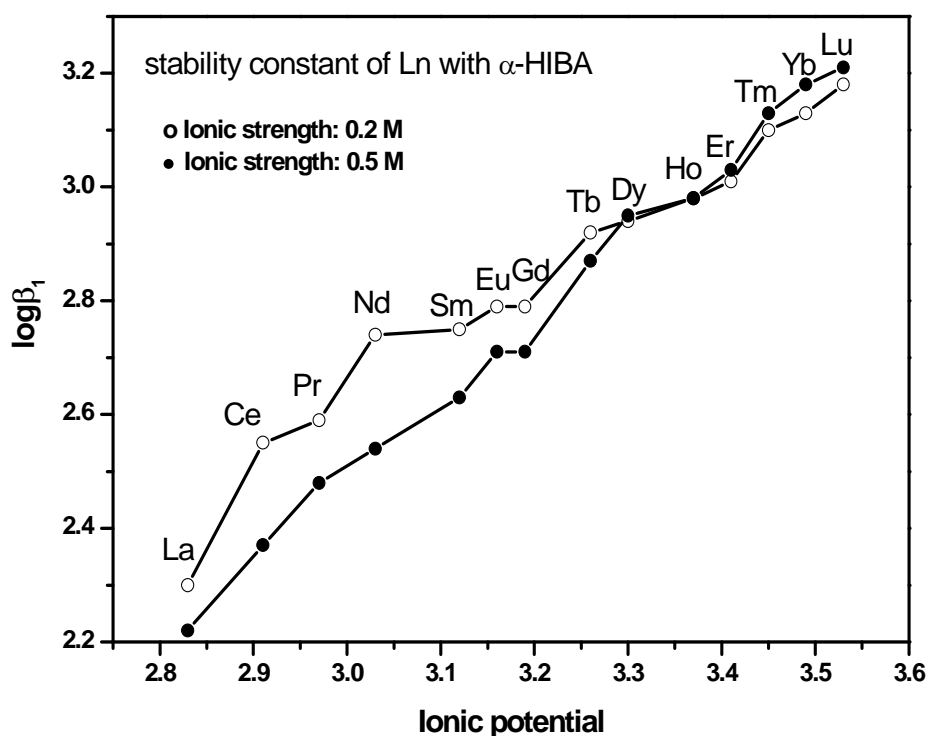


Fig.6.5. Stability constant of lanthanide-HIBA complexes ($\log\beta_1$) at two different ionic strengths [192].

6.3.6 Estimation of stability constant of transition metal ions, Th(IV) and Pu(IV)

Method-2 approach was also employed to estimate stability constant of transition metal ions such as Mn^{+2} , Fe^{+2} , Co^{+2} , Ni^{+2} , Cu^{+2} , Zn^{+2} and Cd^{+2} with HIBA. Calibrants

chosen from this group e.g. Mn^{+2} , Ni^{+2} , and Cu^{+2} enabled the estimation of stability constant of transition metal ions only (**Table.6.13**). Th(IV) retention and stability constant data [192] was used to estimate stability constant of Pu(IV) and Zr(IV) [204]. The $\log\beta_1$ and $\log\beta_2$ for Pu(IV)-HIBA complexes were estimated and found to be 6.48 and 8.72 respectively.

Table.6.13. Stability constant of transition metal complexes with HIBA (method-2), estimated for 1 M ionic strength

Lit.data: for 1.0 M ionic strength at 25°C

Chromatographic exp. conditions: HIBA: 0.1 M; CSA: 0.001 M, pH: 2.49; (25°C)

Calibrants: Mn, Ni, Cu

Transition metals	$\log(\beta_1)$		$\log(\beta_2)$		$\log(\beta_3)$	
	*Lit.data	Exp. data	Lit.data	Exp. data	Lit.data	Exp. data
Mn(II)	0.96	1.3	1.54	2.00	1.74	2.14
Fe(II)	**	1.51	**	2.75	**	3.14
Co(II)	1.45	1.46	2.43	2.62	2.73	3.02
Ni(II)	1.67	1.51	2.80	2.75	3.20	3.14
Cu(II)	2.74	2.75	4.34	4.36	4.74	4.75
Zn(II)	1.70	1.57	2.97	2.88	3.39	3.28
Cd(II)	1.24	1.26	2.16	2.3	2.4	2.14

* Literature data (Portanova et al, 75 (2003)495[192]).

** lit. data not available

The stability constant of Zr-HIBA complexes are found to be in good agreement with the literature data ($\pm 10\%$). K_s , which is the stability constant of the analyte with CSA, varies significantly for the +2, +3 and +4 oxidation states and hence demanded a different calibrant. These studies established that the estimation of stability constant is generally

applicable within a group of metal cations with similar properties, e.g. lanthanides and actinides of +3 oxidation states and demands different calibrant for different group of metal ions.

6.3.7 The advantages and limitations of estimation of stability constant by chromatographic retention correlation

The stability constant values estimated in the present study are found to be in very good agreement with the experimental data reported in the literature. The chromatographic method is fast and estimation of stability constant can be done in a very short time, which is an additional advantage, especially in dealing with radioactive elements. A single chromatogram can be used for estimation of stability constant at various ionic strengths. The experimental data also demonstrate that the method can be applied for the estimation of stability constant of metal ions with a ligand, whose value is not reported. The estimation of stability constant of actinide biological complexes is of great importance and liquid chromatographic technique developed in the present study offers an alternate method of estimation.

One calibrant data is required for the correlation of retention with the stability constant. These studies established that the estimation of stability constant is generally applicable within a group of metal cations with similar properties, e.g., lanthanides and actinides of +3 oxidation states and demands different calibrant for different group of metal ions.

6.3.8 Speciation of actinides and their retention behavior on reversed phase chromatography

Estimated stability constants data using present study were employed for speciation of Pu(III), Pu(IV) and PuO_2^{+2} with α -HIBA as a function of pH (**Fig.6.6**). In the case of Pu(III), dominant species are, dipositive species, $[\text{Pu}(\text{IBA})^{+2}]$ at pH 2.8, monopositive $[\text{Pu}(\text{IBA})_2^+]$ from pH 3 to 3.5 and neutral species, $[\text{Pu}(\text{IBA})_3]$ at pH 4. The anionic species, $[\text{Pu}(\text{IBA})_4]^-$ increase from 0.3 to about 9.6% when pH was altered from 2.8 to 4. In the case of Pu(IV), dominant species is the neutral one, $[\text{Pu}(\text{IBA})_4]$ from pH 2.8 to 4. In the case of PuO_2^{+2} , dominant species are, monopositive $[\text{PuO}_2(\text{IBA})^+]$ at pH 2.8 and neutral species, $[\text{PuO}_2(\text{IBA})_2]$ from pH 3 to 4. The anionic species $[\text{PuO}_2(\text{IBA})_3]^-$ increase from 4.4 to 35% when pH was raised from 2.8 to 4. The speciation of behaviour of Am(III)-HIBA complexes was more or less similar to Pu(III) / Nd(III), the neutral species content increases when pH was raised to 4 (**Fig.6.7**).

Retention of Pu(III), Pu(IV) and PuO_2^{+2} , Am(III) along with UO_2^{+2} , and Th(IV) species was investigated on reversed phase based monolith support. In this study, 0.1 M α -HIBA solutions of pH 2.8, 3, 3.5 and 4 were employed as the mobile phase and the results are shown in **Fig.6.8**. Retention of all species in general increases with mobile phase pH. It was observed that at pH: 4, PuO_2^{+2} has higher retention compared to Th(IV), UO_2^{+2} , Pu(IV) and Pu(III). Elution behavior of these elements can be explained based on the speciation diagram generated from the stability constant data. It was observed that the percentage of uncomplexed species decreases and that of ionic / neutral species increases with increase of pH. The total percentage of anionic and neutral species for PuO_2^{+2} , Pu(IV) and Pu(III) with α -HIBA are 90, 96 and 58 % respectively.

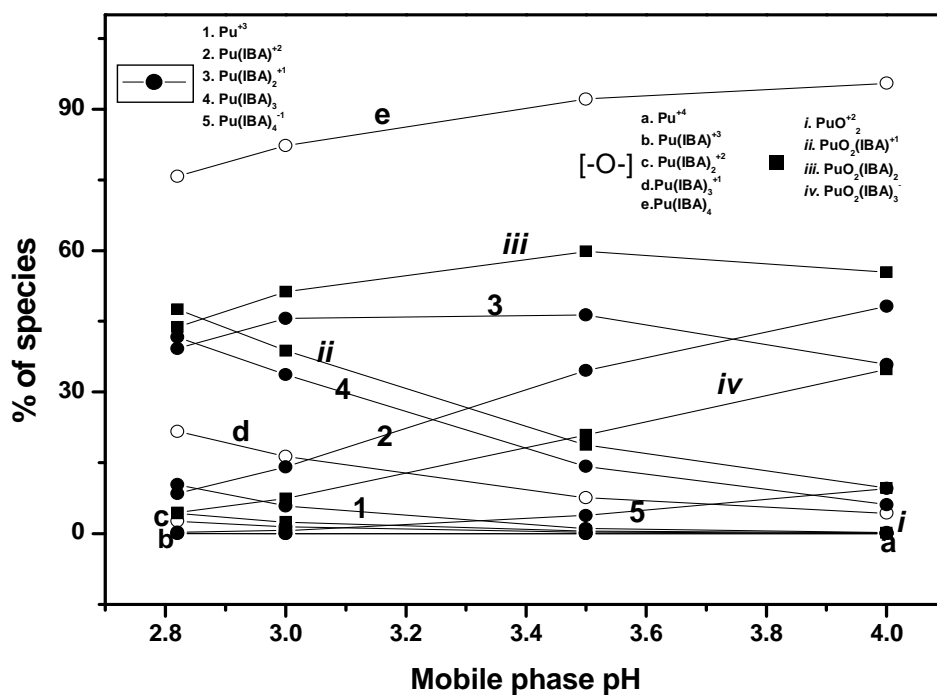


Fig.6.6. Speciation of (a) Pu(III)-HIBA, (b) Pu(IV)-HIBA and (c) PuO_2^{+2} -HIBA complexes as a function of mobile phase (0.1 M α -HIBA) pH.

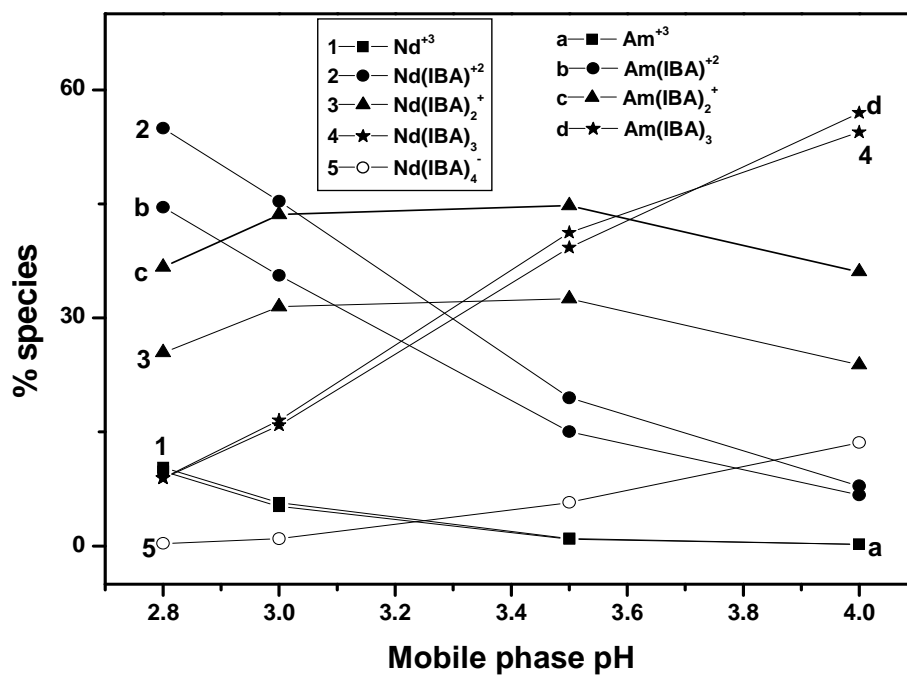


Fig.6.7. Speciation of Nd(III)-HIBA and Am(III)-HIBA complexes as a function of mobile phase (0.1 M α -HIBA) pH.

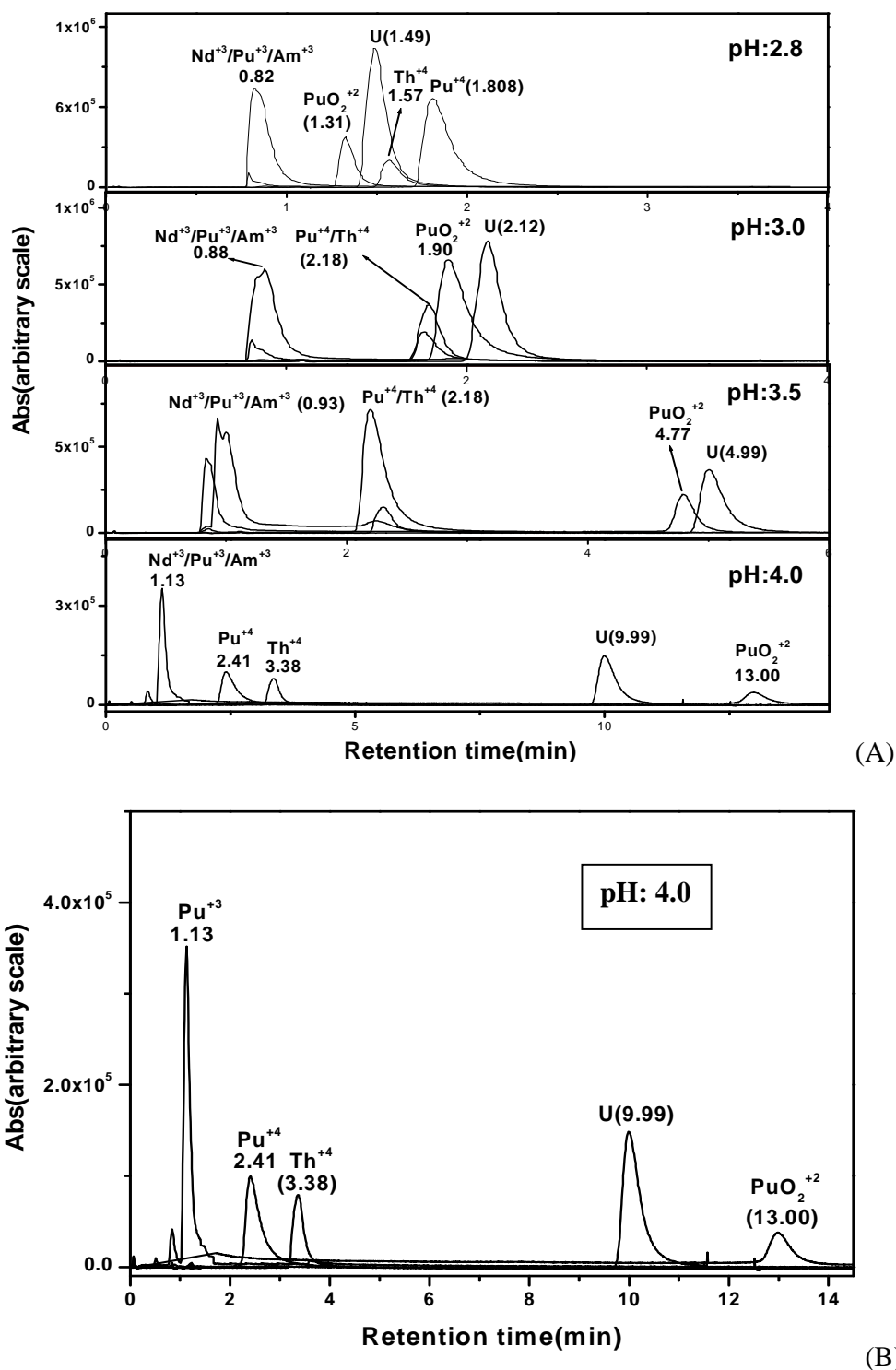


Fig.6.8. (A) Elution behaviour of Pu(III), Pu(IV), PuO₂⁺², Am(III), UO₂⁺² and Th(IV) on a reversed phase HPLC as a function of pH. (B) Elution behaviour at pH:4. Mobile phase: 0.1 M α -HIBA; Flow rate: 2 mL/min; Column: 10 cm monolith support; Detection: PCR with arsenazo(III) at 655 nm; Sample: U(28 ppm), Th(20 ppm) and Pu(~ 20 ppm).

Table.6.14. Percentage of total species (neutral + anionic) of Nd(III)-HIBA, Am(III)-HIBA, Pu(III)-HIBA, Pu(IV)-HIBA, Th(IV)-HIBA, UO₂⁺²-HIBA and PuO₂⁺²-HIBA – elution sequence of lanthanide and actinides

pH	%Neutral + % Anionic species of actinides and lanthanide with HIBA							Elution order
	Nd ⁺³	Am ⁺³	Pu ⁺³	Pu ⁺⁴	Th ⁺⁴	UO ₂ ⁺²	PuO ₂ ⁺²	Elution Sequence
2.8	9.3	8.9	8.7	76.0	75.7	45.7	48.2	(Pu ⁺³ , Am ⁺³ , Nd ⁺³), PuO ₂ ⁺² , UO ₂ ⁺² , Th ⁺⁴ & Pu ⁺⁴
3	17.5	15.9	14.8	82.2	58.0	58.0	58.8	(Pu ⁺³ , Am ⁺³ , Nd ⁺³), (Pu ⁺⁴ , Th ⁺⁴), PuO ₂ ⁺² & UO ₂ ⁺²
3.5	46.9	39.2	38.4	92.1	92.1	83.5	80.7	(Pu ⁺³ , Am ⁺³ , Nd ⁺³), (Pu ⁺⁴ , Th ⁺⁴), PuO ₂ ⁺² & UO ₂ ⁺²
4	68.1	56.9	57.8	95.5	95.5	93.0	90.2	(Pu ⁺³ , Am ⁺³ , Nd ⁺³), Pu ⁺⁴ , Th ⁺⁴ , UO ₂ ⁺² , & PuO ₂ ⁺²

* Separation carried out on a monolith support; 0.1 M α -HIBA- used for elution.

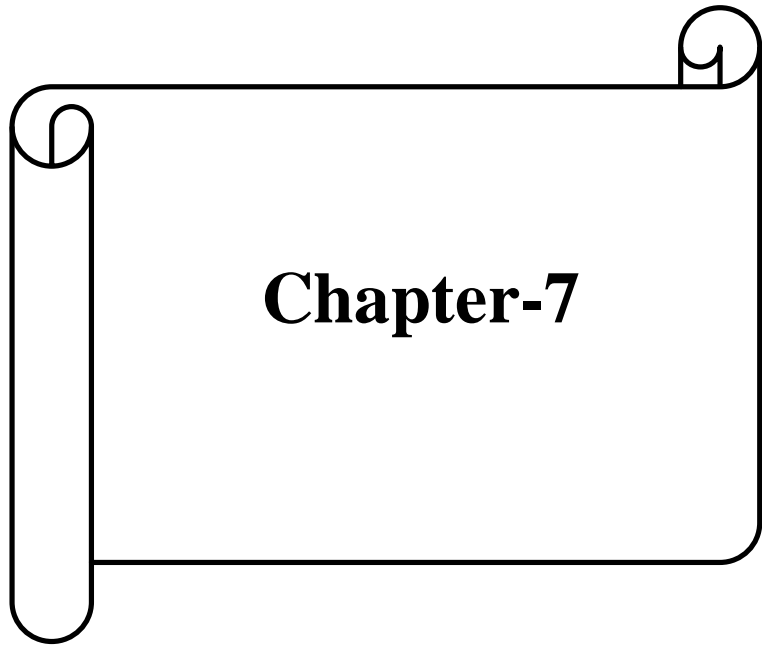
* (Pu⁺³, Am⁺³, Nd⁺³)-have least retention during reversed phase chromatographic experiments and elute together

The retention of actinides e.g., plutonium on the reversed phase support was attributed to the formation of both neutral and anionic species with HIBA (Table.6.14), e.g., in the case of PuO₂⁺²-HIBA complexes, both species, [PuO₂(IBA)₂] and [PuO₂(IBA)₃]⁻ become dominant with the increase of pH from 2.8 to 4. Despite, [PuO₂(IBA)₃]⁻ being anionic, it is sufficiently hydrophobic (higher carbon moiety) and exhibit reversed phase retention through dispersion forces (i.e., van der Waal forces) on a hydrophobic C₁₈ surface. The monopositive species, [PuO₂(IBA)]⁺ has the least retention compared to the other two species on a hydrophobic support. The retention of PuO₂⁺² / Pu(IV) is higher compared to

Pu(III) species in the reversed phase chromatography. Though percentage of total species i.e. neutral for Pu(IV) is marginally higher compared to PuO_2^{+2} , the lower retention of Pu(IV) was observed possibly due to hydrolysis of Pu(IV)-HIBA complex.

6.4 Conclusion

A chromatographic method has been demonstrated for the correlation of capacity factor with the stability constant of lanthanides, and some actinide complexes. The stability constants estimated using chromatographic studies are found to be in very good agreement with the established experimental methods of literature. The chromatographic method is fast and estimation of stability constant can be done in a very short time which will be an added advantage in dealing with radioactive elements. The experimental data also demonstrate potential application of the method for the estimation of stability constants of metal ions with a ligand whose value is not reported.



Chapter-7

Chapter-7

Influence of Temperature on the Elution Behaviour of Lanthanides and Some Actinides on Reversed Phase Supports

7.1 Introduction

Temperature plays an important role in liquid chromatographic technique for improving the separation efficiency [205-206]. Generally, mobile phase viscosity decreases with increase in temperature, leading to reduction in column back pressure. Knowledge of temperature effect on thermodynamic and kinetic aspects of chromatographic separation is also essential for method development. The effect of temperature on solute retention of metal ions such as alkali, alkaline-earth and transition metals was studied and reported [207-208]. Effect of temperature on ion chromatographic separation of lanthanides was also investigated [209-211].

In chromatography, temperature effect on solute retention can be expressed by simplified van't Hoff equation [212-214] and it relates the capacity factor (k') of solute to the temperature via enthalpy and entropy of exchange of solute between two phases. The modified version of van't Hoff equation $\left(\ln k' = \frac{-\Delta H}{RT} + \frac{\Delta S}{R} + \ln \phi \right)$ has been derived from relation between capacity factor (k') and thermodynamic equilibrium constant (K) [215] and is shown in equation 7.1

$$\ln k' = \ln K + \ln \phi \dots\dots\dots(7.1)$$

where

k' = Capacity factor ($k' = t_r - t_0 / t_0$),

K = Equilibrium constant for the distribution of solute between mobile and

stationary phase,

ϕ = Phase ratio (volume of the stationary phase divided by the volume of mobile phase).

Parameters, such as enthalpy and entropy, can be obtained from van't Hoff plot, $\ln(k')$ vs. $1/T$. These parameters can determine the sorption process of solute between mobile phase and stationary phase during chromatographic separation. van't Hoff plot can be linear as well as nonlinear depending on the parameters such as ΔH and phase ratio on temperature. Linear plot of $\ln k'$ vs. $1/T$ was observed when phase ratio is constant and ΔH is independent of temperature. However, nonlinear plot of $\ln k'$ vs. $1/T$ was reported with assumption of temperature dependent behaviour of ΔH and changes in phase ratio [216-221].

This chapter describes the influence of temperature (25°C to 85°C) on the retention of lanthanides and some actinides on dynamic ion-exchange and reversed phase based chromatographic systems. The retention of uranium and thorium was investigated on a reversed phase based support using α -HIBA, mandelic acid and lactic acid as a function of temperature. Capacity factors of lanthanides, U and Th were correlated with the temperature using van't Hoff plot. The enthalpy of sorption ($\Delta H_{\text{sorption}}$) of lanthanides, uranium and thorium was calculated and these results are discussed.

7. 2 EXPERIMENTAL

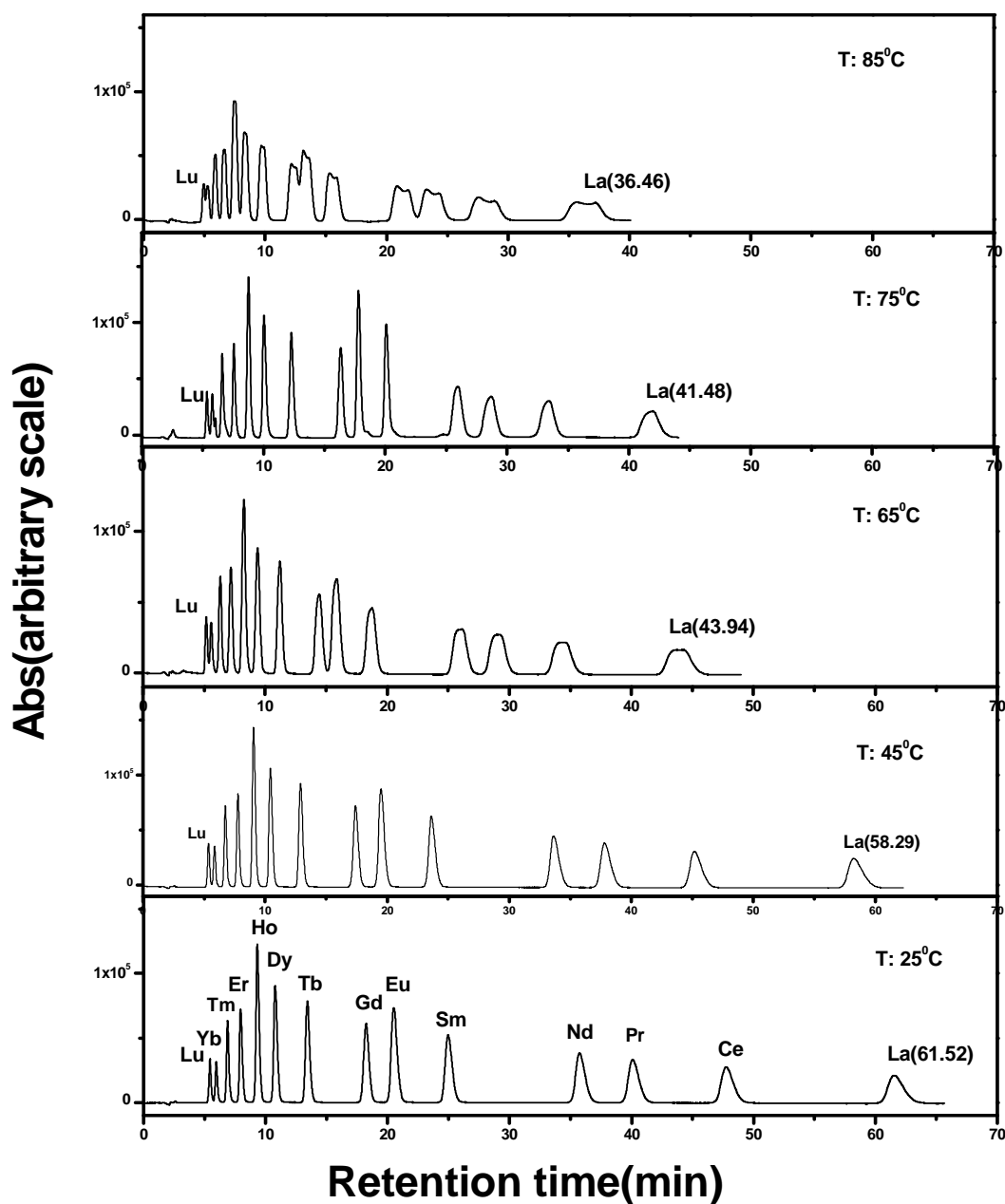
The HPLC column was kept inside a thermostat compartment/oven (HPLC technology) and allowed to equilibrate to the desired temperature (± 1 °C) for at least 30 min prior to sample injection. Mobile phase employed was also heated to desired temperature using an oil bath. The post column reagent was cooled to $\sim 10^0$ °C to reduce the temperature of column effluent before reaching the detector.

7.3 RESULTS AND DISCUSSION

7.3.1 Effect of temperature on chromatographic separation of lanthanides and some actinides on reversed phase support

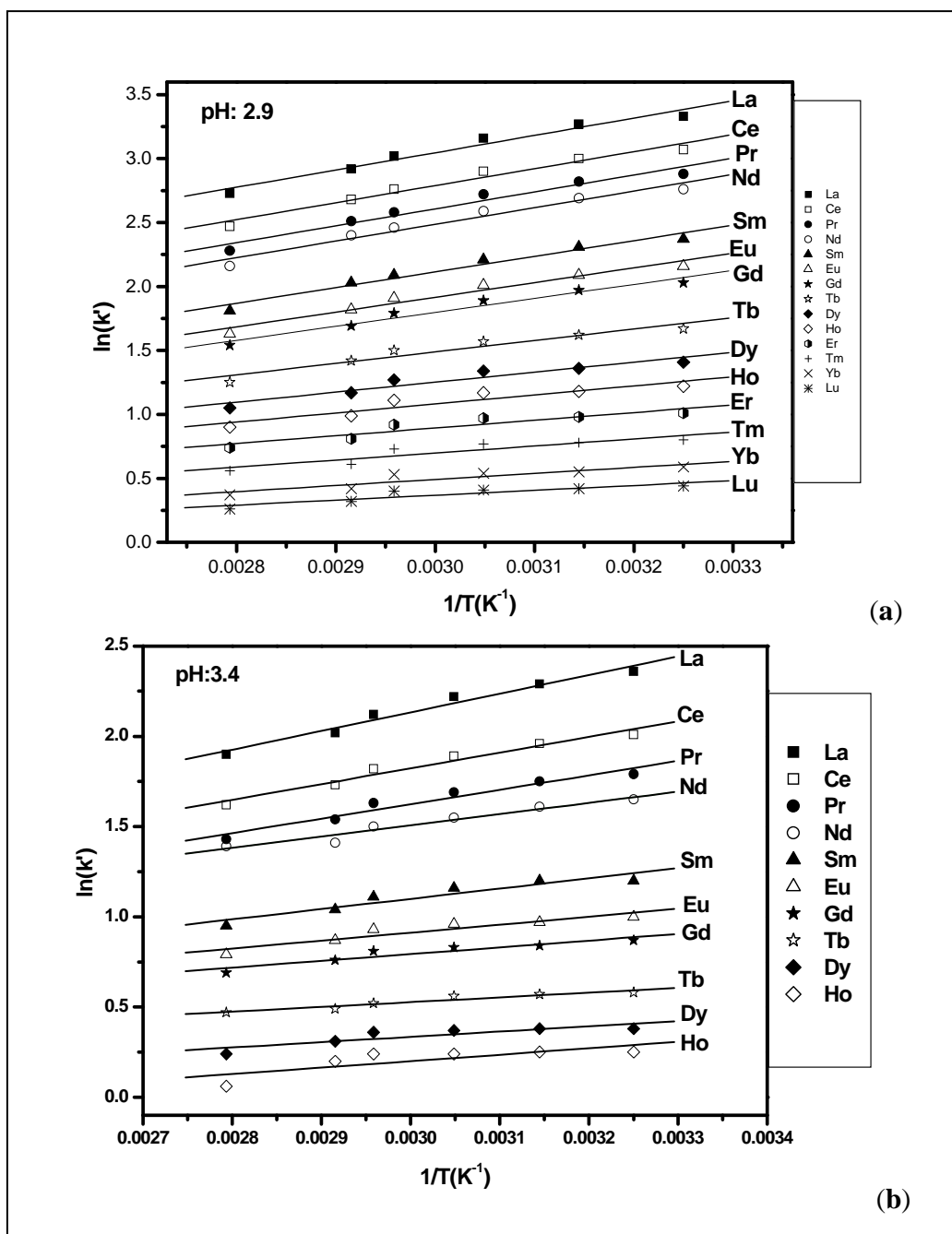
7.3.1.1 Isocratic elution of lanthanides on 25 cm (5 μm) and 3 cm (1.8 μm) length reversed phase supports

In these studies, retention of lanthanides was investigated on 25 cm length (5 μm) and 3 cm length (1.8 μm) reversed phase supports under dynamic ion-exchange conditions as a function of temperature. Influence of temperature on the separation of lanthanides was studied in the temperature range of 25⁰C to 85⁰C. In a typical study, mobile phase employed for the individual separation of lanthanides was a solution made of α -HIBA (0.1 M) and CSA (0.015 M) with pH 2.9 and 3.4. Under typical experimental condition, total separation time of lanthanides was about 62 min at 25⁰C and 36 min at 85⁰C (**Fig.7.1**). A reduction of retention time of lanthanides by a factor of 1.8 times was observed with increase of temperature, from 25 to 85⁰C. This is due to faster analyte mass transfer at higher temperatures as viscosity of mobile phase decreases with increase in temperature. Peak broadening was noticed in the case of some lighter lanthanides, e.g., Nd-La especially above 65⁰C; splitting of peak, e.g., for La-Gd was observed at 85⁰C. A linear variation of $\ln(k')$ vs $1/T$ plot was obtained at pH 2.9 and 3.4 for all lanthanides (**Fig.7.2**).



* Retention time of broader peak (i.e., lighter lanthanides peak at higher temperature) was measured from the center of the top of the peak

Fig.7.1. Isocratic elution of lanthanides on 25 cm length support as a function of temperature. Mobile phase: 0.1 M α -HIBA + 0.015 M CSA; pH: 2.9; Column: 25 cm length (5 μ m) reversed phase support; Flow rate: 3 mL/min; PCR flow rate: 2 mL/min; Detection: 655 nm; Sample: lanthanides (20 ppm) in 0.01 N HNO₃; Injected volume: 20 μ L



* pH change at higher temperature is assumed to be constant

Fig.7.2. Plot of $\ln(k')$ vs $1/T$ for lanthanides from a 25 cm length column. Mobile phase: 0.1 M α -HIBA + 0.015 M CSA; (a) pH: 2.9 and (b) pH: 3.4; Column: 25 cm length (5 μ m) reversed phase support; Flow rate: 3 mL/min; PCR flow rate: 2 mL/min; Detection: 655 nm; Sample: lanthanides (20 ppm) in 0.01 N HNO_3 ; Injected volume: 20 μ L

van't Hoff plot was linear with positive slope for all lanthanides indicating exothermic sorption process for these ions between stationary phase and mobile phase. Exothermic behaviour indicates favorable desorption process compared to the adsorption process at elevated temperatures. Enthalpy of sorption ($\Delta H_{\text{sorption}}$) of lanthanides was obtained from slope of van't Hoff plots and the values are shown in **Table.7.1**.

Table.7.1 Slope from van't Hoff plot and enthalpy of sorption of lanthanides on 25 cm and 3 cm length supports

Lanthanides	25 cm length (5 μm) support				3 cm length (1.8 μm) support	
	pH:2.9		pH:3.4		pH:3.2	
	Slope from van't Hoff plot ($-\Delta H/R$) (K)	Enthalpy of sorption ($\Delta H_{\text{sorption}}$) (kJ/mol)	Slope from van't Hoff plot ($-\Delta H/R$) (K)	Enthalpy of sorption ($\Delta H_{\text{sorption}}$) (kJ/mol)	Slope from van't Hoff plot ($-\Delta H/R$) (K)	Enthalpy of sorption ($\Delta H_{\text{sorption}}$) (kJ/mol)
La	1353 \pm 124	-11.0 \pm 1.0	1033 \pm 89	-8.6 \pm 0.7	1573 \pm 105	-13.17 \pm 0.03
Ce	1328 \pm 119	-11.1 \pm 1.0	872 \pm 82	-7.2 \pm 0.7	1550 \pm 6	-12.9 \pm 0.05
Pr	1320 \pm 135	-11.0 \pm 1.1	800 \pm 92	-6.6 \pm 0.7	1496 \pm 96	-12.4 \pm 0.8
Nd	1301 \pm 129	-10.8 \pm 1.1	621 \pm 73	-5.2 \pm 0.6	1488 \pm 124	-12.4 \pm 1.0
Sm	1222 \pm 120	-10.2 \pm 1.0	568 \pm 100	-4.7 \pm 0.7	1312 \pm 267	-10.9 \pm 2.2
Eu	1152 \pm 117	-9.6 \pm 1.0	442 \pm 80	-3.7 \pm 0.6	1224 \pm 210	-10.8 \pm 1.7
Gd	1092 \pm 105	-9.1 \pm 0.9	373 \pm 66	-3.1 \pm 0.5	1163 \pm 69	-9.7 \pm 0.6
Tb	895 \pm 125	-7.4 \pm 1.0	356 \pm 138	-2.9 \pm 1.1	870 \pm 420	-7.2 \pm 3.5
Dy	781 \pm 124	-6.5 \pm 1.0	293 \pm 83	-2.5 \pm 0.7	746 \pm 397	-6.2 \pm 3.3
Ho	707 \pm 135	-5.9 \pm 1.1	264 \pm 39	-2.2 \pm 0.3	661 \pm 416	-5.5 \pm 1.9
Er	604 \pm 121	-5.0 \pm 1.0	#	#	664 \pm 235	-5.5 \pm 3.5
Tm	549 \pm 126	-4.6 \pm 1.0	#	#	639 \pm 60	-5.3 \pm 0.5
Yb	473 \pm 105	-3.9 \pm 0.9	#	#	619 \pm 297	-5.1 \pm 2.5
Lu	383 \pm 91	-3.2 \pm 0.7	#	#	580 \pm 3	-4.82 \pm 0.03

could not calculated

* Error in slope/ ΔH estimated from the error of linear fit of $\ln(k')$ vs $1/T$

It can be seen from **Table.7.1** that at pH: 2.9, the enthalpy of sorption ($-\Delta H_{\text{sorption}}$) decreased from 11.0 ± 1.0 kJ/mol for lanthanum to 3.2 ± 0.7 kJ/mol for lutetium. The decrease in $\Delta H_{\text{sorption}}$ from La to Lu with the decrease in capacity factor from La to Lu correlates well with the increasing ionic potential of lanthanide cations, from La to Lu. Increase in ionic potential across the lanthanide series results in enhanced complexation with complexing agent, e.g. α -HIBA across the series, i.e., from La^{+3} to Lu^{+3} .

Separation of individual lanthanides on dynamically modified 3 cm length ($1.8 \mu\text{m}$) support was also studied as function of temperature and the results are shown in **Fig.7.3**.

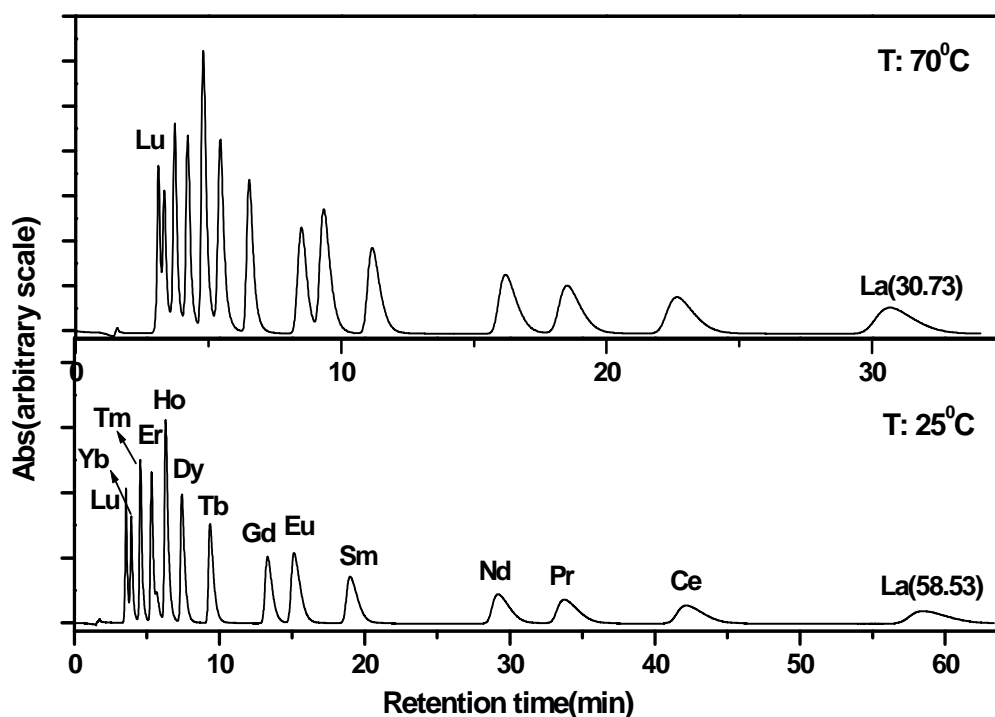


Fig.7.3. Elution behaviour of lanthanides on 3 cm length support as a function of temperature. Mobile phase: 0.05 M α -HIBA + 0.01 M CSA; pH: 3.2; Column: 3 cm length ($1.8 \mu\text{m}$) reversed phase support; Flow rate: 2 mL/min; PCR flow rate: 2 mL/min; Detection: 655 nm; Sample: lanthanides (~ 20 ppm) in 0.01 N HNO_3 ; Injected volume: 20 μL

Total retention time was reduced to approximately half of its initial time at 70°C compared to one at 25°C . In this study, at temperature $> 75^\circ\text{C}$, broadening of lighter

lanthanides peak was also observed. The mobile phase employed was a mixture of solution of CSA (0.01 M) as ion-pairing reagent and α -HIBA (0.05 M, pH 3.2). Enthalpy of sorption ($\Delta H_{\text{sorption}}$) of lanthanides on dynamically modified 3 cm length (1.8 μm) reversed phase support was calculated from slope of van't Hoff plots (**Fig.7.4**). **Table.7.1**. shows the value of $\Delta H_{\text{sorption}}$ for lanthanides. These values are varying from -13.17 ± 0.03 kJ/mol (La^{+3}) to -4.82 ± 0.03 kJ/mol (Lu^{+3}).

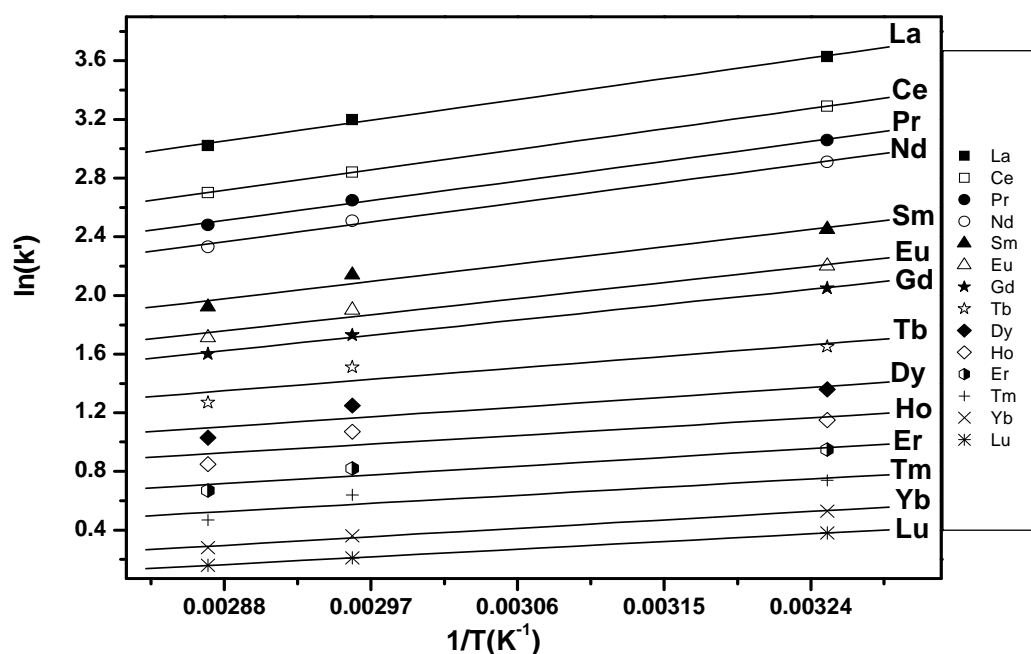


Fig.7.4. Plot of $\ln(k')$ vs $1/T$ for lanthanides from a 3 cm length (1.8 μm) column. Mobile phase: 0.05 M α -HIBA + 0.01 M CSA; pH: 3.2; Column: 3 cm length (1.8 μm) reversed phase support; Flow rate: 2 mL/min; PCR flow rate: 2 mL/min; Detection: 655 nm; Sample: lanthanides (12 ppm) in 0.01 N HNO_3

A temperature gradient was also employed to separate individual lanthanides in an isocratic mode. In this method, with a constant mobile phase composition, i.e., isocratic mode, temperature of the column was altered from 25°C to 85°C during a chromatographic run. Lanthanides were separated from each other in about 17 min (**Fig.7.5**) in these studies.

In another study, separation of lanthanides was also carried out at lower temperature, i.e., 10⁰C. Mobile phase employed for separation of individual lanthanides was a mixture of solution of CSA (0.01 M) and α -HIBA (0.05 M) with pH of 3.2. However, there was no noticeable change in separation time compared to the one obtained at 25⁰C.

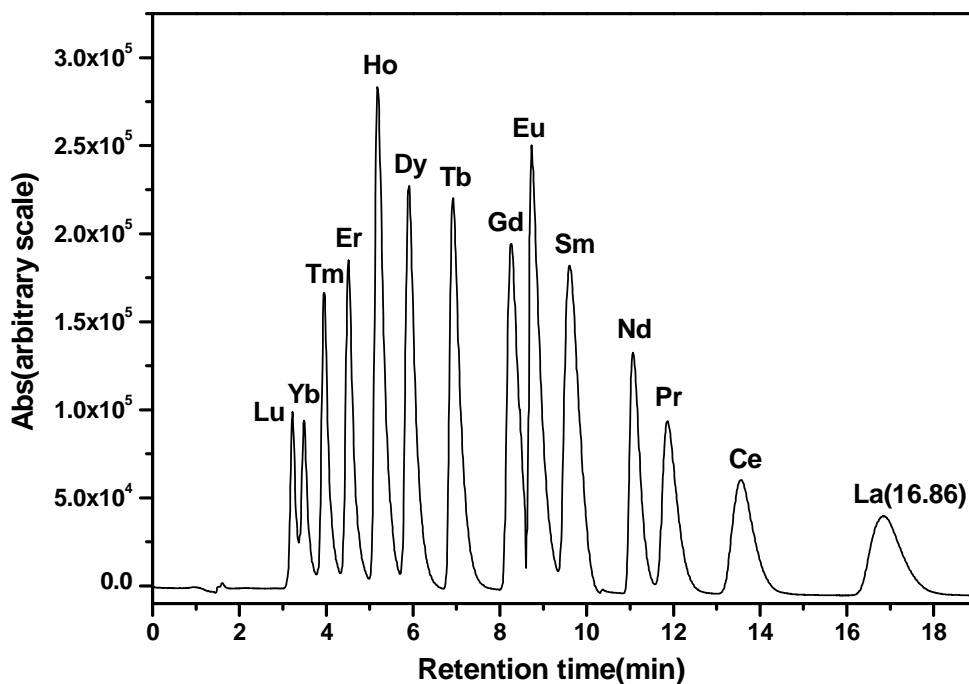


Fig.7.5. Elution of lanthanides using temperature gradient (25⁰C-90⁰C). Mobile phase: 0.05 M α -HIBA + 0.01 M CSA; pH: 3.2; Column: 3 cm length (1.8 μ m particle) reversed phase support; Flow rate: 2 mL/min; PCR flow rate: 2 mL/min; Detection: 655 nm; Sample: lanthanides (~20 ppm) in 0.01 N HNO₃; Injected volume: 20 μ L
*Temperature was raised from 25⁰C to 90⁰C in a span of 9 minutes (8⁰C raise per min)

7.3.1.2 Separation of U & Th on 25 cm (5 μ m) and 3 cm (1.8 μ m) length reversed phase supports as a function of temperature

The effect of temperature on retention of actinides such as uranium and thorium on reversed phase support was also investigated in the temperature range of 25⁰C to 85⁰C. A solution of 0.1 M α -HIBA with pH 3.25, 3.60 and 4.00 was used as eluent for separation of U & Th on a 25 cm length reversed phase column (**Fig.7.6**).

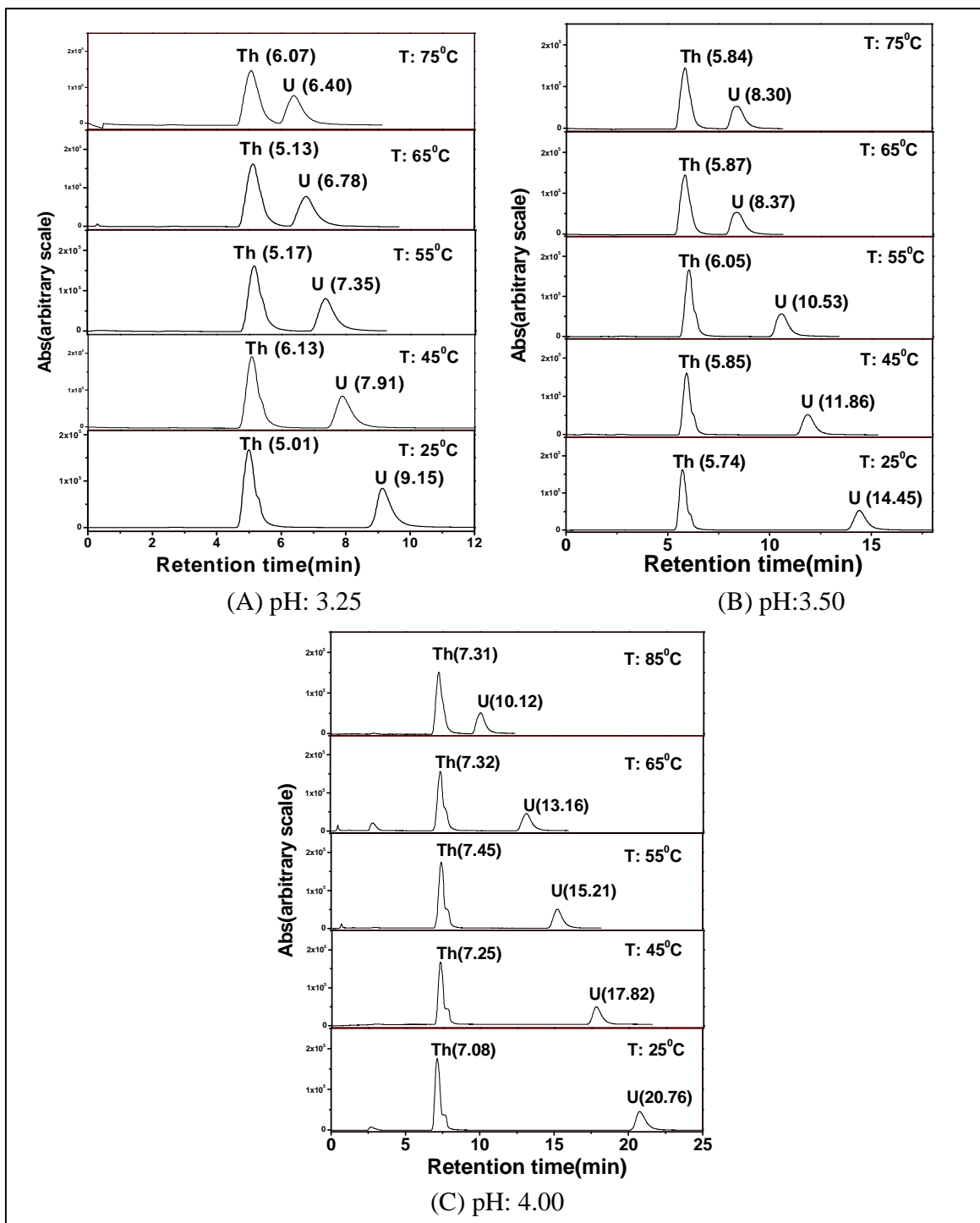


Fig.7.6. Retention of U & Th - HIBA complexes on a 25 cm length reversed phase support as a function of temperature. Mobile phase: 0.1 M α -HIBA; pH: (A) pH: 3.25, (B) pH: 3.50 and (C) pH: 4.00; Column: 25 cm length (5 μ m) reversed phase support; Flow rate: 2 mL/min; PCR flow rate: 2 mL/min; Detection: 655 nm; Sample: U (65 ppm) & Th (75 ppm) in 0.01 N HNO₃; Injected volume: 20 μ L.

It was observed that the retention of uranium reduced appreciably with raise in column temperature whereas retention of Th almost more or less unchanged with raise in temperature. **Fig.7.7** shows van't Hoff plots of U and Th with 0.1 M α -HIBA with pH 3.25, 3.50 and 4.00. In the case of uranium, van't Hoff plot was observed with positive slope, indicating exothermic behaviour of sorption process. However, slope of van't Hoff plot was negative for thorium, indicating endothermic behaviour of sorption process. Enthalpy of sorption ($\Delta H_{\text{sorption}}$) for uranium and thorium was also calculated from slope of van't Hoff plots and the values are shown in **Table.7.2**.

The elution behaviour of uranium and thorium was also studied on a 3 cm length (1.8 μm) reversed phase support as function of temperature (25⁰C-75⁰C). In these studies, retention of uranium decreased with increase of temperature whereas retention of thorium marginally increased with raise in temperature (**Fig.7.8**). In these studies, van't Hoff plots of $\ln(k')$ vs $1/T$ for U and Th were observed with positive and negative slope respectively (**Fig.7.9**). Enthalpy of sorption ($\Delta H_{\text{sorption}}$) of uranium and thorium was calculated from slope of van't Hoff plots and the values are shown in **Table.7.3**.

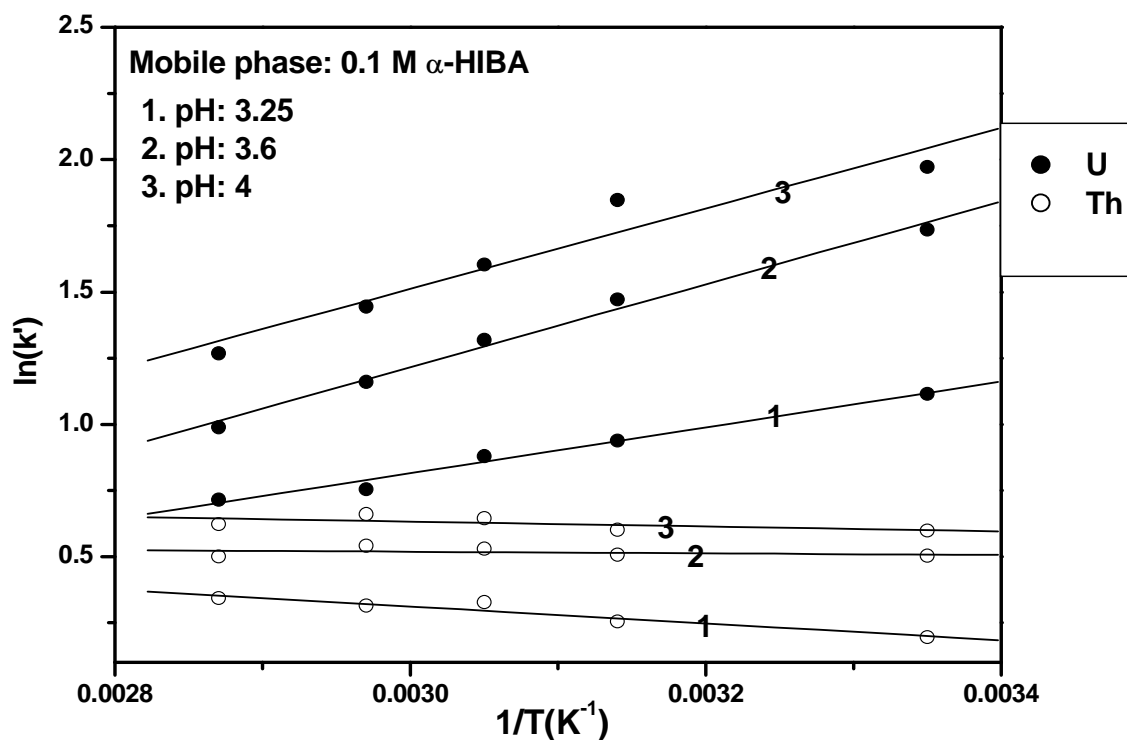


Fig.7.7. Plot of $\ln(k')$ vs $1/T$ for U and Th for 25 cm length column. Mobile phase: 0.1 M α -HIBA; pH: 3.25, 3.50 & 4.00; Column: 25 cm length (5 μ m) reversed phase support; Flow rate: 2 mL/min; PCR flow rate: 2 mL/min; Detection: 655 nm; Sample: U (65 ppm) & Th (75 ppm) in 0.01 N HNO_3

Table.7.2 Enthalpy of sorption of U & Th on 25 cm length reversed phase support

Actinides	0.1 M α -HIBA		
	Enthalpy of sorption ($\Delta H_{\text{sorption}}$)(kJ/mol) at pH:3.25	Enthalpy of sorption ($\Delta H_{\text{sorption}}$) (kJ/mol) at pH:3.5	Enthalpy of sorption ($\Delta H_{\text{sorption}}$) (kJ/mol) at pH:4
U	-7.2 \pm 0.5	-16.2 \pm 0.6	-16.1 \pm 1.1
Th	2.64 \pm 0.02	0.25 \pm 0.06	0.9 \pm 0.7

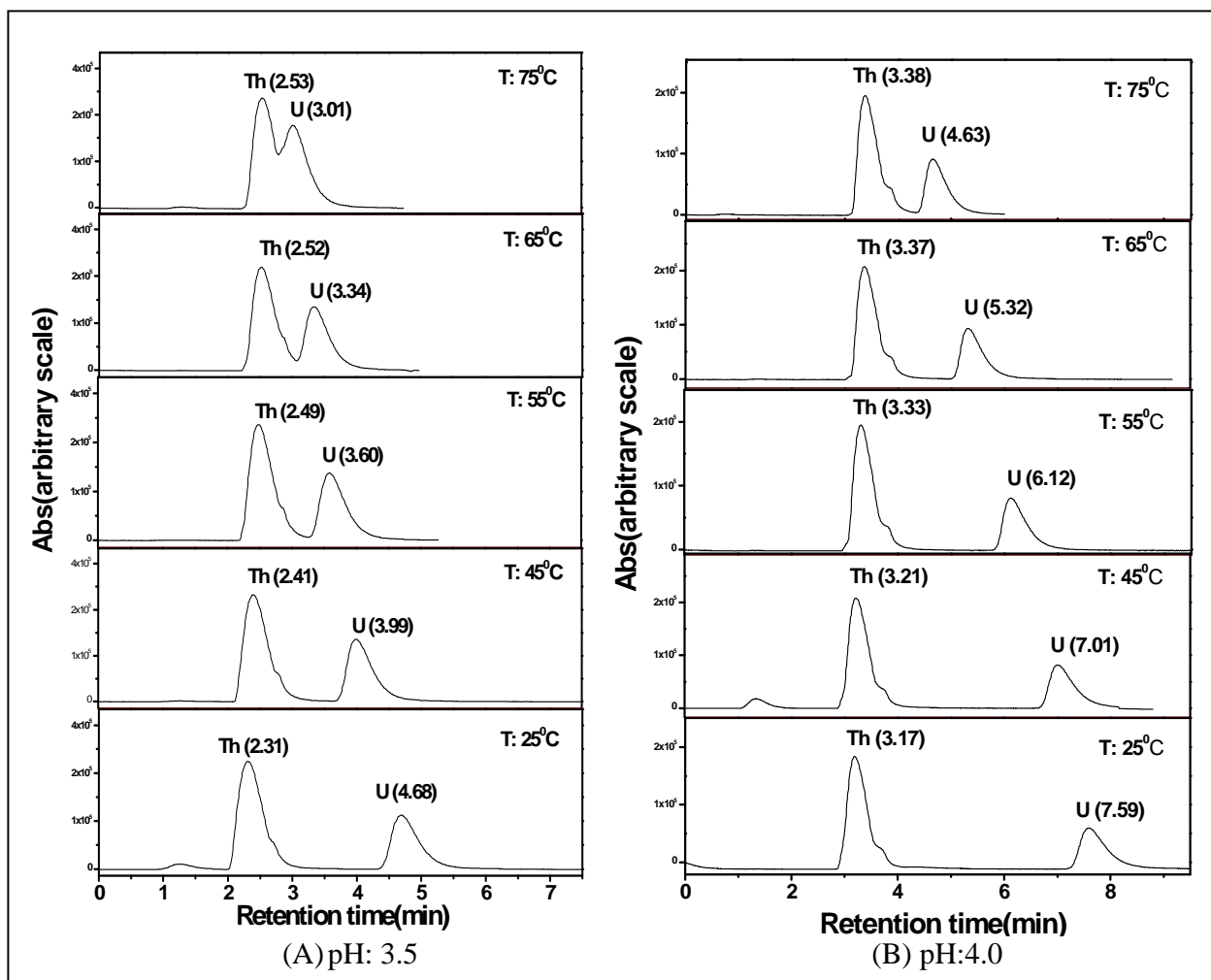


Fig.7.8. Retention of U & Th – HIBA complexes on 1.8 micron reversed phase support as function of temperature. Mobile phase: 0.1 M α -HIBA; pH: (A) pH: 3.5, (B) pH: 4.0; Column: 3 cm length (1.8 μ m) reversed phase support; Flow rate: 2 mL/min; PCR flow rate: 2 mL/min; Detection: 655 nm; Sample: U (65 ppm) & Th (75 ppm) in 0.01 N HNO₃; Injected volume: 20 μ L

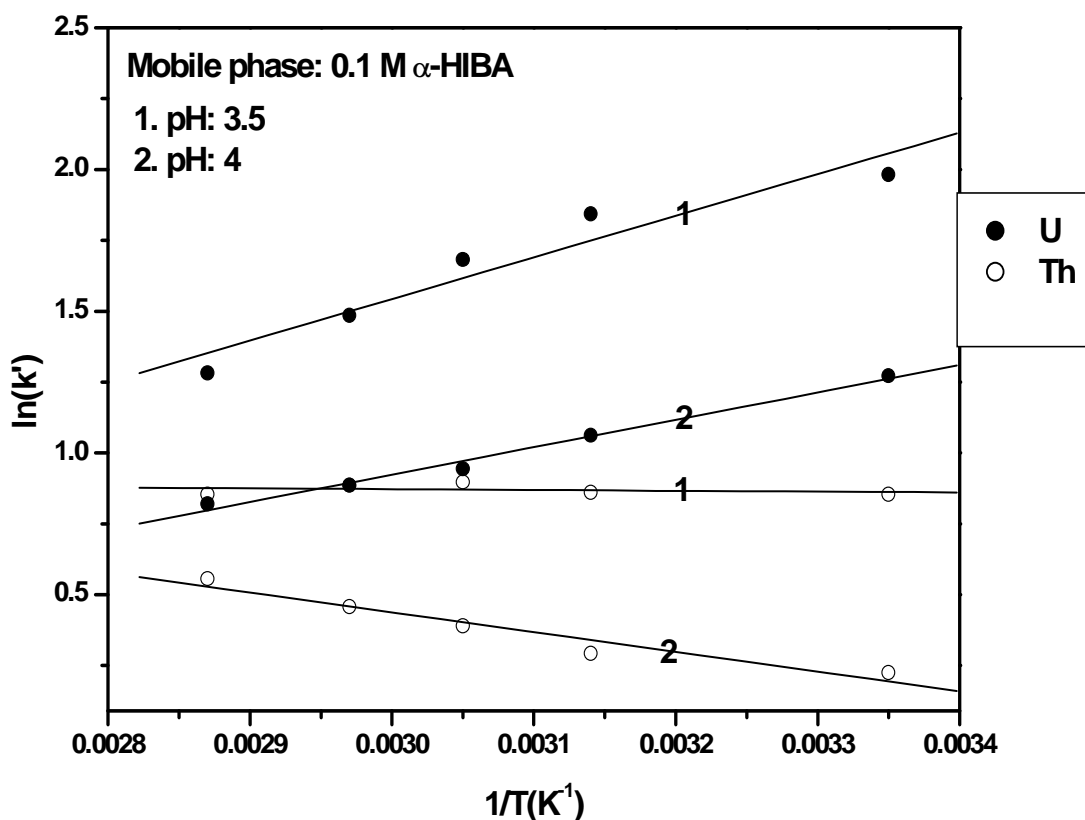


Fig.7.9. Plot of $\ln(k')$ vs $1/T$ for U and Th for 3 cm length 1.8 micron reversed phase column. Mobile phase: 0.1 M α -HIBA; pH: 3.50 & 4.00; Column: 3 cm length (1.8 μ m) reversed phase support; Flow rate: 2 mL/min; PCR flow rate: 2 mL/min; Detection: 655 nm; Sample: U (65 ppm) & Th (75 ppm) in 0.01 N HNO_3

Table.7.3 Enthalpy of sorption of U & Th on 3 cm length (1.8 μ m) reversed phase support

Actinides	0.1 M α -HIBA		0.1 M mandelic acid	0.1 M lactic acid
	Enthalpy of sorption ($\Delta H_{\text{sorption}}$) (kJ/mol) at pH:3.5	Enthalpy of sorption ($\Delta H_{\text{sorption}}$) (kJ/mol) at pH:4	Enthalpy of Sorption ($\Delta H_{\text{sorption}}$) (kJ/mol) at pH:2.79	Enthalpy of Sorption ($\Delta H_{\text{sorption}}$) (kJ/mol) at pH:4
U	-8.0 \pm 0.5	-14.1 \pm 1.4	-3.2 \pm 1.2	-9.0 \pm 0.8
Th	5.8 \pm 0.8	~ 0.2	1.2 \pm 0.1	5.2 \pm 0.3

In some experiments, mandelic and lactic acids were also employed as complexing agents for elution of uranium and thorium. In the case of mandelic acid (0.1 M with pH 2.80), retention of thorium-mandelate complexes was found to be higher than that of uranyl-mandelate complexes (**Fig.7.10**). Higher retention of Th compared to U could be explained from speciation of U and Th- mandelate complexes (**Fig.7.11**). Complexation of uranyl ion (UO_2^{+2}) with mandelic acid results in formation of various species such as UO_2^{+2} , $[\text{UO}_2(\text{mandelate})]^+$, $[\text{UO}_2(\text{mandelate})_2]$ and $[\text{UO}_2(\text{mandelate})_3]^-$. Similarly, thorium ion (Th^{+4}) can also form species such as Th^{+4} , $[\text{Th}(\text{mandelate})]^{+3}$, $[\text{Th}(\text{mandelate})_2]^{+2}$, $[\text{Th}(\text{mandelate})_3]^+$ and $[\text{Th}(\text{mandelate})_4]$. In the case of U, dominant species is, monopositive species, $[\text{UO}_2(\text{mandelate})]^+$ at pH 2.8 and pH 3.0, neutral species, $[\text{UO}_2(\text{mandelate})_2]$ at pH 3.5 and anionic species, $[\text{UO}_2(\text{mandelate})_3]^-$ at pH 4.0. In case of Th, dominant species is, neutral species, $[\text{Th}(\text{mandelate})_4]$ at pH 2.8, 3.0, 3.5 and 4.0. At pH 2.8, higher retention of Th is due to the species $[\text{Th}(\text{mandelate})_4]$ (77.60%), which has 4 mandelate moieties resulting in stronger hydrophobic interaction, i.e. induced dipole-induced dipole with the reversed phase support. The lower retention of uranium is due to $[\text{UO}_2(\text{mandelate})^{+2}]$ species (49.93%), which has only one mandelate moiety resulting in relatively lower hydrophobic interaction with the reversed phase support. Total separation time of uranium and thorium was 41.7 min at pH: 2.80. U and Th separation was also investigated at pH: 3.5, U elution was observed in about 7 min. However, Th was not eluted from the column even after 100 min. Hence, experiments on the effect of temperature on retention of uranium and thorium were carried out at pH 2.80. The retention of uranium was reduced from 3.4 to 2.9 min with increase in temperature (25°C to 75°C), whereas, retention time of thorium increased from 41.7 min to 45.1 min and more or less remained constant after that. Linear correlation of van't Hoff plot of $\ln(k')$ vs $1/T$ with positive slope was

observed in case of U and negative slope in the case of Th (**Fig.7.12**). Enthalpy of sorption ($\Delta H_{\text{sorption}}$) of uranium and thorium was calculated from slope of van't Hoff plots and are shown in **Table.7.3**.

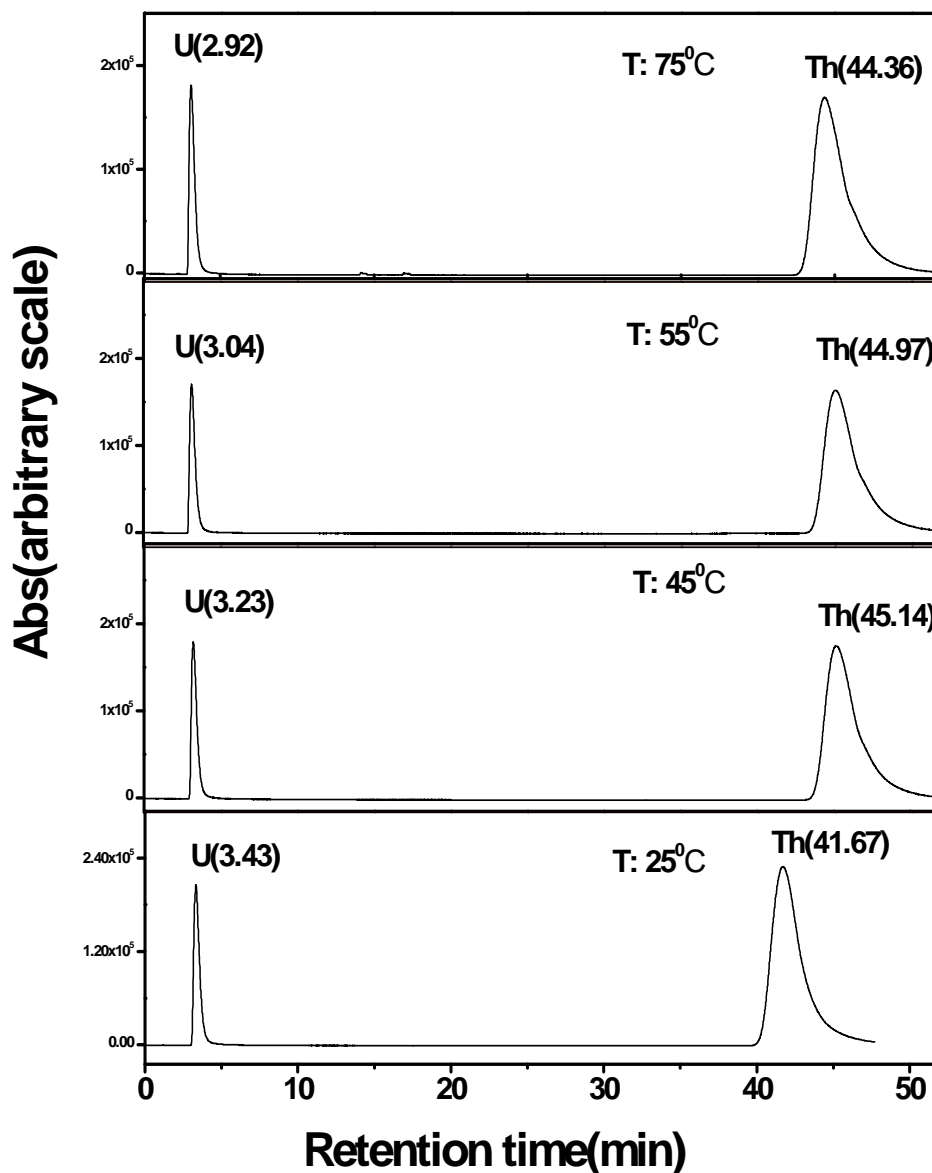


Fig.7.10. Retention of U & Th – mandelate complexes on a reversed phase HPLC as a function of temperature. Column: 3 cm length (1.8 μm) reversed phase support; Mobile phase: 0.1 M mandelic acid; pH: 2.79; Flow rate: 2 mL/min; PCR flow rate: 2 mL/min; Detection: 655 nm; Sample: U (65 ppm) & Th (75 ppm) in 0.01 N HNO_3 ; Injected volume: 20 μL

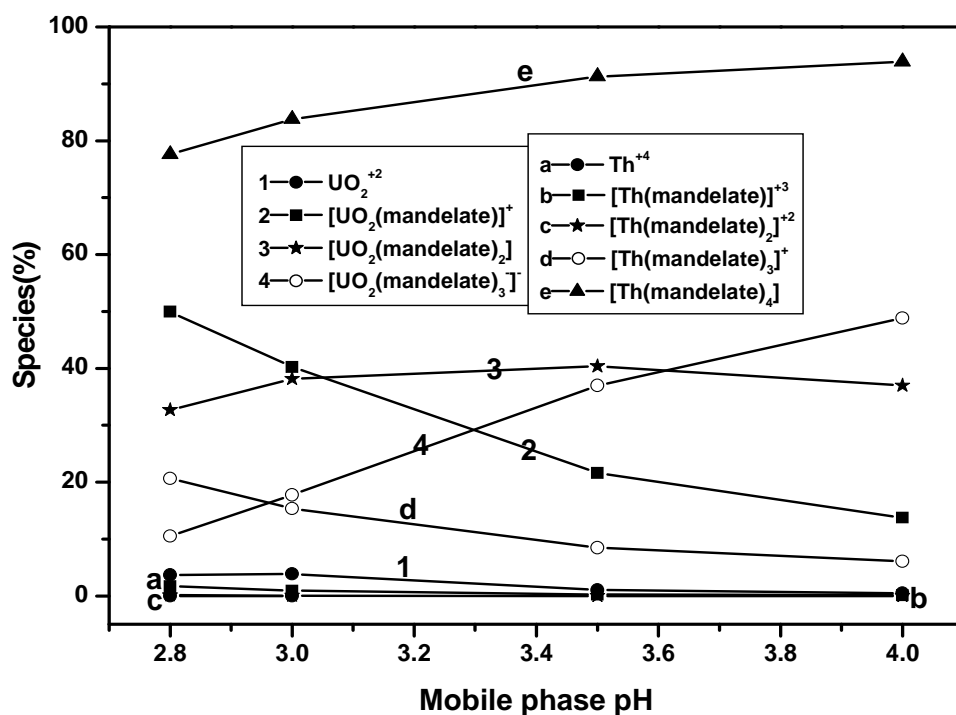


Fig.7.11. Speciation of U & Th with mandelic acid as a function of pH

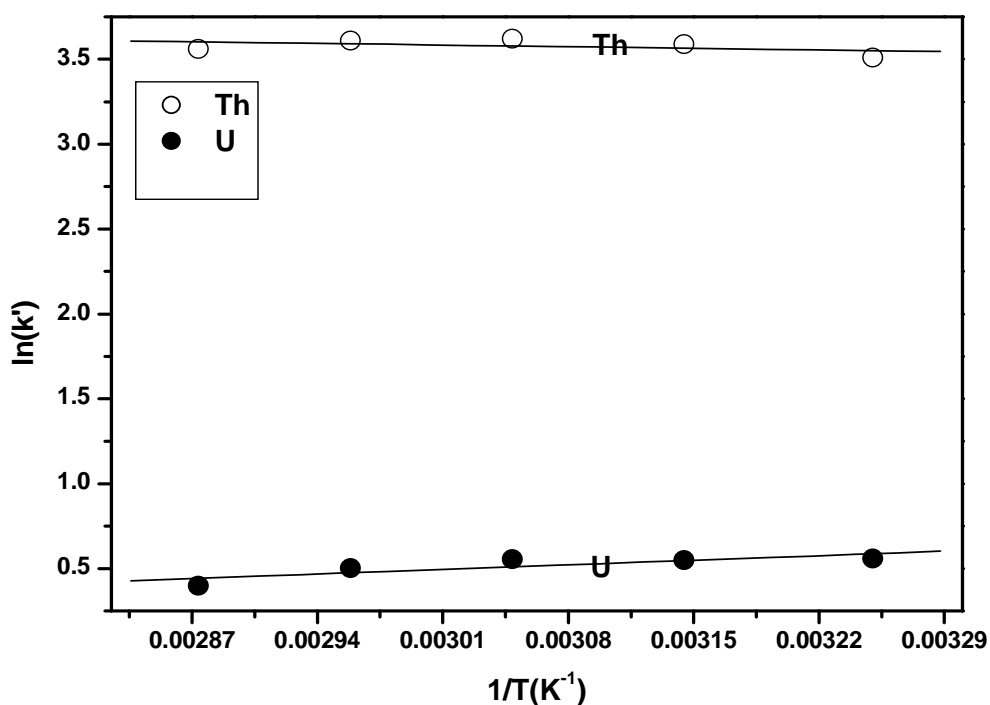


Fig.7.12. Plot of $\ln(k')$ vs $1/T$ for U and Th with mandelic acid. Mobile phase: 0.1 M mandelic acid; pH: 2.79; Column: 3 cm length (1.8 μm) reversed phase support; Flow rate: 2 mL/min; PCR flow rate: 2 mL/min; Detection: 655 nm; Sample: U (65 ppm) & Th (75 ppm) in 0.01 N HNO_3

The retention of uranyl-lactate and thorium-lactate complexes is more or less similar to retention behaviour of U & Th-HIBA complexes. In a typical experiment, 0.1 M lactic acid (pH 4.00) was employed for the separation of uranium and thorium. Uranium-lactate complex retention was higher than that observed with the Th-complex. In these studies, retention of uranium and thorium was investigated in the temperature range of 25⁰C to 75⁰C (Fig.7.13).

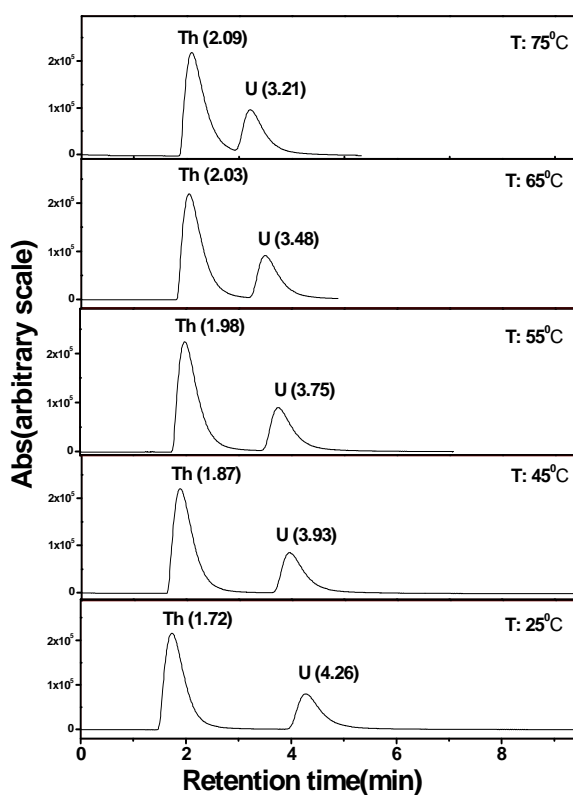


Fig.7.13. Retention behaviour of U & Th-lactate complexes on a reversed phase chromatography as a function of temperature. Mobile phase: 0.1 M lactic acid; pH: 4; Column: 3 cm length (1.8 μ m) reversed phase support; Flow rate: 2 mL/min; PCR flow rate: 2 mL/min; Detection: 655 nm; Sample: U (65 ppm) & Th (75 ppm) in 0.01 N HNO₃; Injected volume: 20 μ L

Retention time of uranium was reduced from 4.26 to 3.21 min, whereas that of Th was increased from 1.72 to 2.09 min with raise in (25⁰C-75⁰C). Linear correlation of van't

Hoff plot of $\ln(k')$ vs $1/T$ was also observed with positive slope in case of U and negative slope in case of Th (**Fig.7.14**). Enthalpy of sorption ($\Delta H_{\text{sorption}}$) of uranium and thorium was calculated from slope of van't Hoff plots and the values are shown in table (**Table.7.3**).

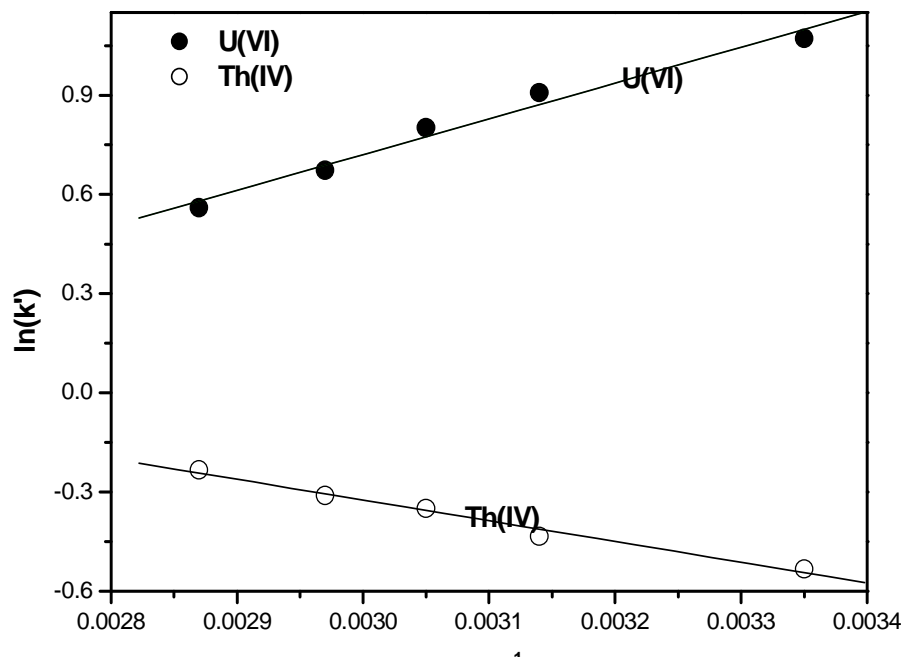
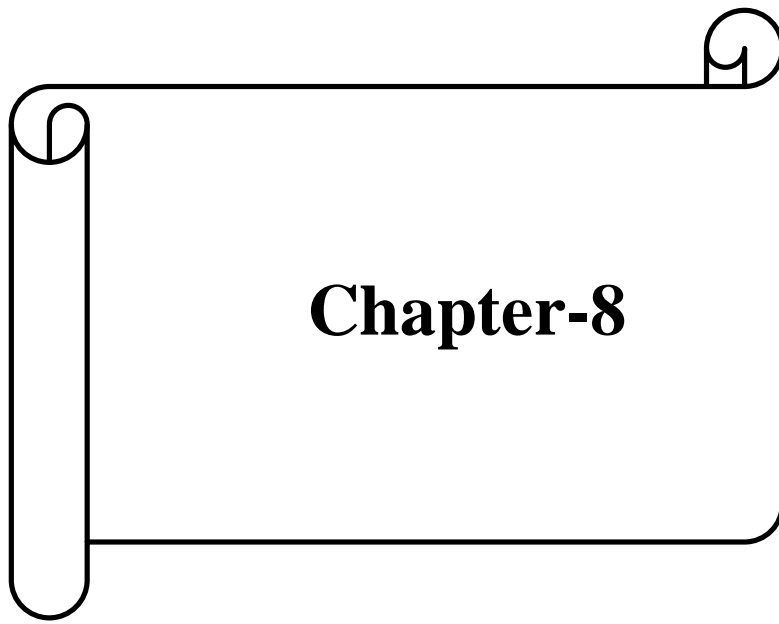


Fig.7.14. Plot of $\ln(k')$ vs $1/T$ for U and Th with lactic acid. Mobile phase: 0.1 M lactic acid; pH: 4; Column: 3 cm length (1.8 μm) reversed phase support; Flow rate: 2 mL/min; PCR flow rate: 2 mL/min; Detection: 655 nm; Sample: U (65 ppm) & Th (75 ppm) in 0.01 N HNO_3

Dybczynski *et al* has studied elution sequence of lanthanides using ion chromatographic system [209]. In these studies, an increase in retention of lanthanides with increase in temperature was reported with citric acid as well as tartaric acid as the complexing agents. Use of nitrilo triacetic acid resulted in the reduction in overall separation time with increase in temperature [209]. However, in our studies an overall reduction in separation time was observed at elevated temperature when HIBA has been employed for the isolation of individual lanthanides.

7.4. Conclusion

Influence of temperature on the retention of lanthanides in a dynamic ion-exchange mode and retention of uranium and thorium complexes on a reversed phase chromatographic mode was investigated in detail. Linear correlation of van't Hoff plot of $\ln(k')$ vs $1/T$ for lanthanides and actinides such as U and Th was observed. Enthalpy of sorption of lanthanide and actinides were calculated. The results of these studies indicated potential use of high temperature liquid chromatography for the development of high performance separations. Use of small particle support (e.g. 1.8 micron) at elevated temperatures can be employed to reduce the over all separation time. Dynamic ion-exchange studies at elevated temperature resulted in an overall reduction in separation time of individual lanthanides as well as U from Th by a factor of ~ 2 . The back pressure reduces considerably at higher temperatures and the columns can also be operated at much higher flow rates compared to one at room temperature for reducing the overall separation time. Use of temperature gradient also provides new avenues for altering the separation efficiency. Further studies are required to understand the endothermic behaviour of sorption process for thorium.



Chapter-8

Chapter-8

Task-Specific Ionic Liquids in Liquid Chromatography-Studies on the Retention Behaviour of Lanthanides and Some Actinides

8.1 Introduction

The cationic or anionic part of room temperature ionic liquids functionalized covalently with organic moieties that perform a target specific application are known as task specific ionic liquids (TSILs) [222]. The presence of organic moiety in TSILs results in the unique and synergistic properties of both room temperature ionic liquid and organic functionality. TSILs are suitable for wide variety of applications in synthesis, catalysis and separation technology [223]. Protonated betaine bis(trifluoromethyl-sulfonyl)imide [Hbet][NTf₂] (**Fig.8.1A**) is a task specific ionic liquid, reported to be a solvent for dissolving oxides of some lanthanides and actinides [223-224]. The carboxyl group attached to the cationic moiety of [Hbet][NTf₂] binds with metal ion through mono- or bidentate coordination, which is reported to facilitate the dissolution of oxides. Similarly, 1-butyl-3-methylimidazolium benzoate (bmim benzoate) is a TSIL as it contains carboxylate ion in the anionic part of ionic liquid as shown in **Fig.8.1B**.

In the present study, retention of uranium, thorium and lanthanides was investigated on reversed phase support modified with TSIL with α -HIBA as the complexing reagent for elution of metal ions. Elution profiles of uranium, thorium and lanthanides were studied as a function of the ionic liquid concentration, α -HIBA concentration and its pH. Task-specific ionic liquids such as bmim benzoate, [Hbet][NTf₂] and its precursor [Hbet] Cl, were employed along with α -HIBA on a reversed phase support to study the sorption behaviour of uranium, thorium and lanthanide ions. The separation factors for U-Th as well as

adjacent lanthanides were measured under various experimental conditions. For the first time, ionic liquids were investigated for chromatographic separation of individual lanthanides and also for the isolation of uranium from thorium.

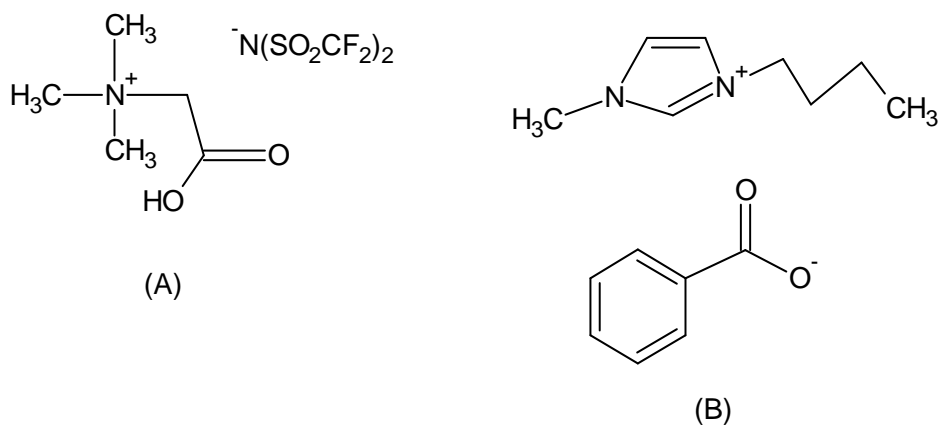


Fig.8.1. Structure of ionic liquids, (A) Betaine NTf₂ (B) Bmim-benzoate

8.2. EXPERIMENTAL

Standard solutions of U and Th were injected in to the HPLC system for preparing the calibration plots. For e.g., in a typical study, a mobile phase consisting of 0.01 M betaine chloride, 0.05 M α -HIBA (pH: 2.42) was employed; a mobile phase flow rate of 2 mL/min was used for preparing calibration plots (**Fig 8.2**).

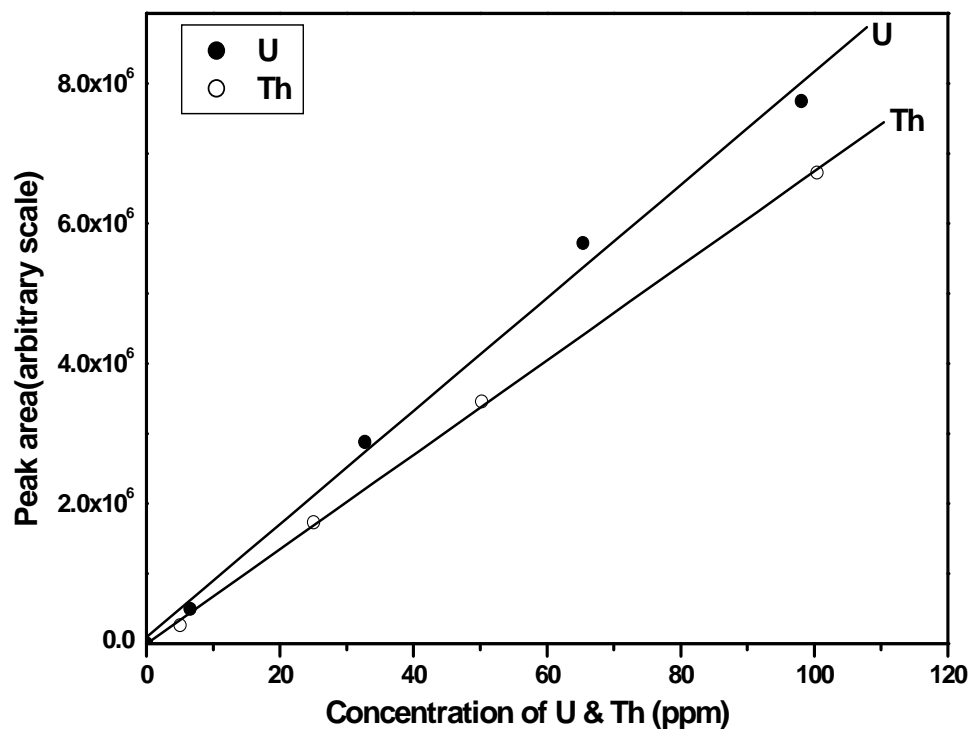


Fig.8.2. Calibration plot for U and Th using ionic liquid as mobile phase. Mobile phase: 0.01 M betaine chloride + 0.05 M α -HIBA; pH: 2.42; Column: 25 cm length (5 μ m) C₁₈ support; Sample: U & Th (5-100 ppm) in 0.01 N HNO₃; Det: 655 nm, Sample injected: 20 μ L

8.3 RESULTS AND DISCUSSION

8.3.1 Retention behavior of U and Th in the presence of TSIL+ α -HIBA system

Retention of uranium and thorium was investigated using ionic liquids, e.g., betaine chloride, betaine NTf₂ and bmim-benzoate as the mobile phase. In a typical experiment, mobile phase employed was a solution of 0.001 M betaine chloride and 0.05 M α -HIBA. A good base-line separation of U-Th was established (**Fig.8.3**). Retention of uranium and thorium was also investigated using ionic liquid, betaine NTf₂ on a modified reversed phase support (**Fig.8.4**). U and Th separation using ionic liquid, bmim-benzoate was also studied under various experimental conditions and the results are shown in **Fig.8.5**.

U-Th separation factors for TSILs in the presence of α -HIBA as a function of mobile phase pH are shown in **Fig.8.6**. Highest separation factor is achieved with bmim-benzoate. The separation factors increase with increase of mobile phase pH.

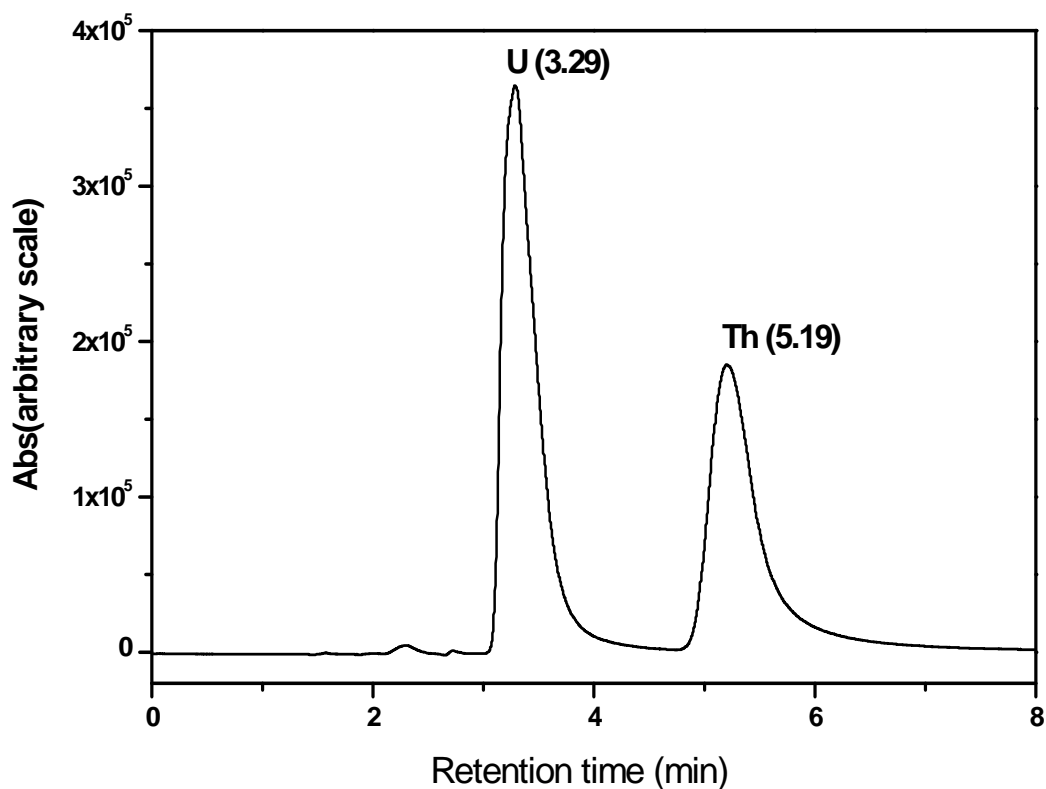


Fig.8.3. Separation of uranium from thorium (~25 ppm) using ionic liquid, betaine chloride. Column: 25 cm length (5 μ m) reversed phase support; Mobile phase: 0.001 M betaine chloride + 0.05 M α -HIBA; pH: 2.94; Flow rate: 2 mL/min. PCR flow rate: 1 mL/min; Sample: U & Th (25 ppm) in 0.01 N HNO₃; Detection: PCR with arsenazo(III) at 655 nm; Loop: 20 μ L

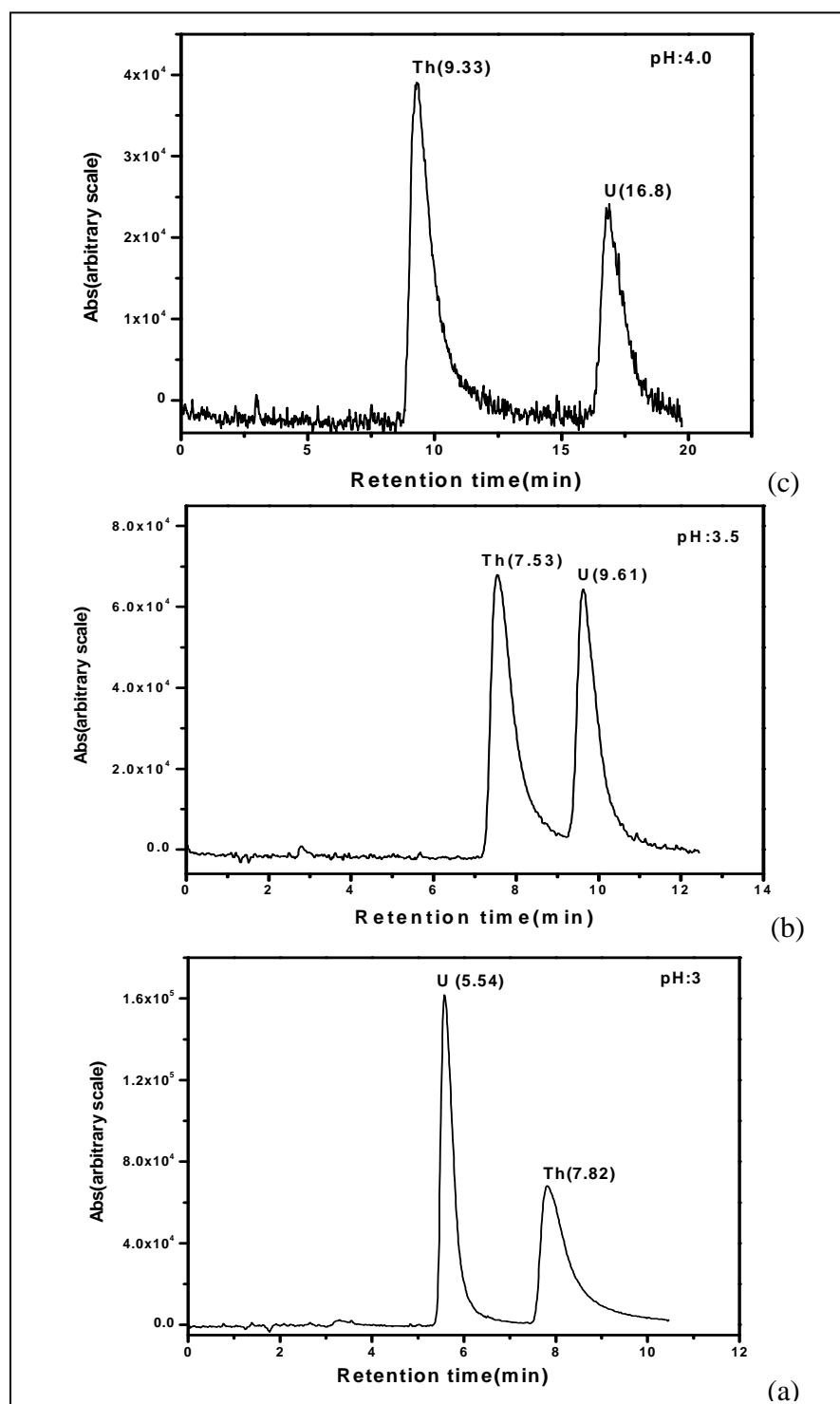


Fig.8.4. Separation of uranium from thorium (25 ppm) using ionic liquid, betaine NTf_2 . Column: 25 cm length ($5 \mu\text{m}$) reversed phase support; Mobile phase: 0.001 M betaine NTf_2 + 0.05 M HIBA; pH: (a) 3.0 (b) 3.5 and (c) 4.0; Flow rate: 2 mL/min. PCR flow rate: 1 mL/min; Sample: U & Th (25 ppm) in 0.01 N HNO_3 ; Detection: PCR with arsenazo (III) at 655 nm; Loop: 20 μL

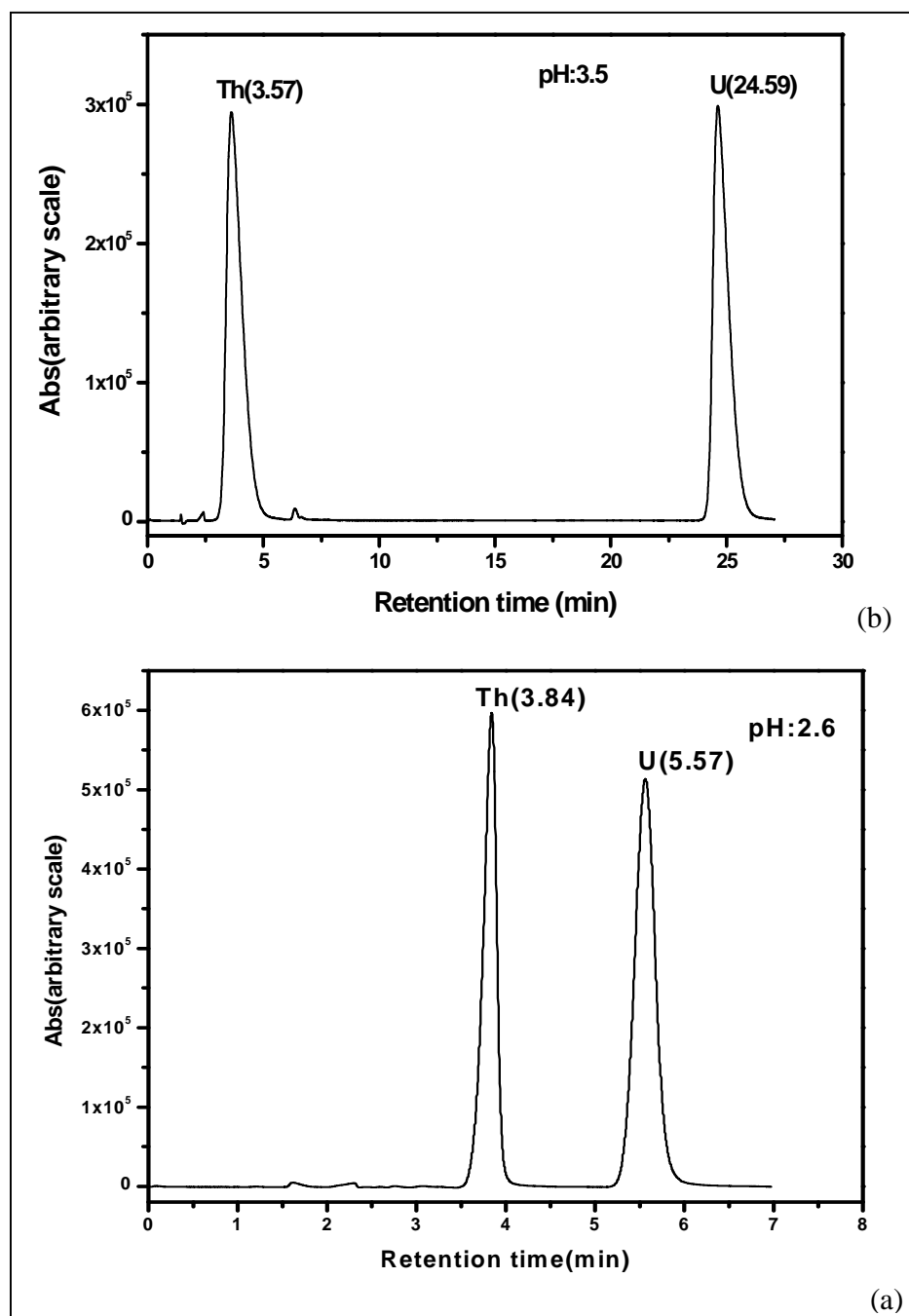


Fig.8.5. Separation of uranium from thorium (~ 50 ppm) using bmim-benzoate + α -HIBA. Column: 25 cm length (5 μ m) reversed phase support; Mobile phase: 0.001 M bmim- benzoate + 0.15 M α -HIBA, pH: (a) 2.6 and (b) 3.5; Flow rate: 2 mL/min. Sample: U & Th (50 ppm) in 0.01 N HNO₃; Detection: PCR with arsenazo(III) at 655 nm.

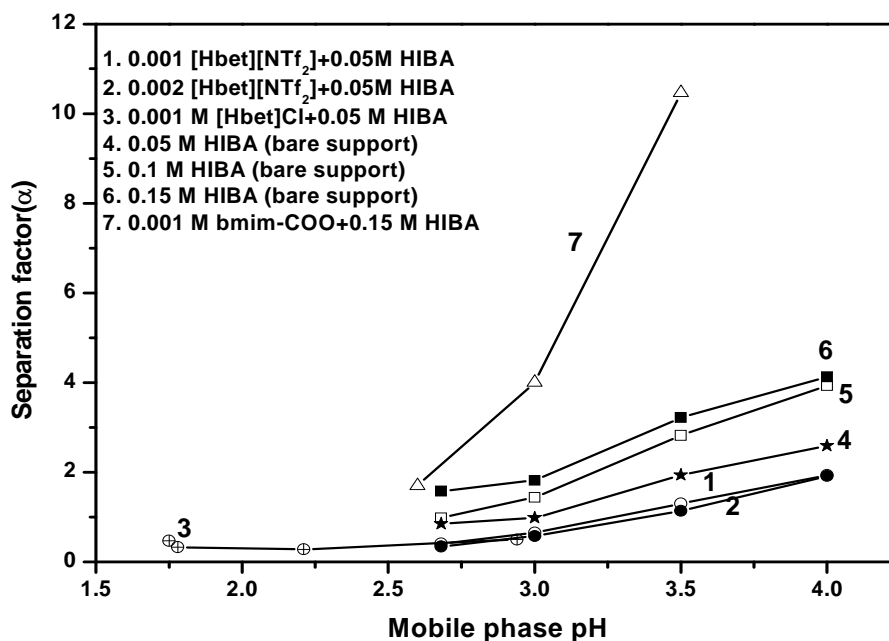


Fig.8.6. Separation factors for U-Th as a function of mobile phase pH.

8.3.1.1 Retention mechanism of U and Th in the presence of TSIL on the reversed phase support

Retention for uranium and thorium – hydroxyl isobutyrate complexes on a bare C₁₈ reversed phase column decreases with increase in α -HIBA concentration, but increases with increase in mobile phase pH. At lower pH (pH < 3), uranium and thorium elute together as these complexes are mainly of positively charged species; at pH \geq 3, retention of uranium is much higher compared to that of thorium complexes; under these conditions, the predominant complex of uranium with α -HIBA is the anionic species, [UO₂(IBA)₃]⁻ which has higher hydrophobicity than the corresponding thorium complex, [Th(IBA)₄(OH)₂]²⁻. This results in enhanced affinity for uranium complex over thorium species on the reversed phase support, mainly through induced dipole-induced dipole interactions. When TSILs are used in the mobile phase along with α -HIBA, retention of U and Th complexes increases when mobile phase pH were raised from 3 to 4. Highest separation factor was observed

when Bmim benzoate was employed in the mobile phase. In some cases, early elution of uranium over thorium was observed, especially when the mobile phase pH was kept at or below 3 in experiments where betaine NTf₂ / betaine chloride were employed with α -HIBA. This is possibly due to the dominance of cation exchange mechanism over hydrophobic interaction (induced dipole interaction).

8.3.2 Retention behavior of lanthanides using ionic liquid, betaine NTf₂ as mobile phase

The retention of lanthanides was also examined using TSILs, betaine chloride, betaine NTf₂ and bmim benzoate with α -HIBA as a complexing agent for elution. The retention of lanthanides with ionic liquid, betaine NTf₂ is shown in **Fig.8.7**. Unlike with the dynamic ion exchange system, lanthanides were not baseline resolved from each other.

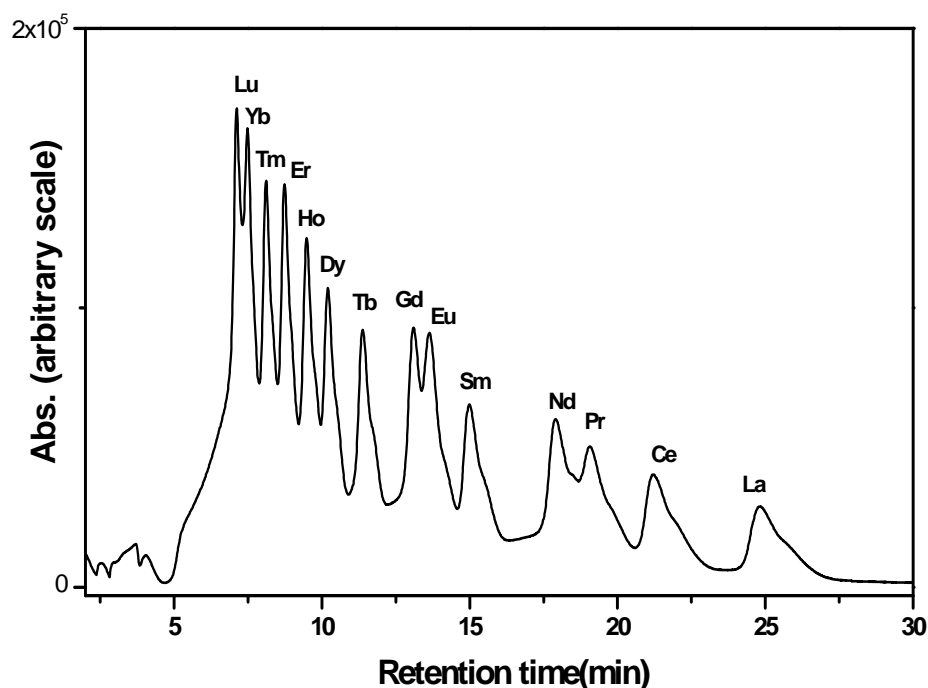


Fig.8.7. Separation of lanthanides using ionic liquid [Hbet][NTf₂] with α -HIBA as mobile phase on reversed phase support. Column: 25 cm length (5 μ m) reversed phase support; Mobile phase: 0.002 M betaine NTf₂ + 0.05 M HIBA, pH: 2.68; Flow rate: 2 mL/min. Sample: lanthanides (20 ppm) in 0.01 N HNO₃; Detection: PCR with arsenazo(III) at 655 nm.

The reason for the shift in baseline has not been established and further studies are required to understand this profile. However, when Lu^{+3} alone was injected, the baseline of chromatogram has not been affected significantly (**Fig.8.8**).

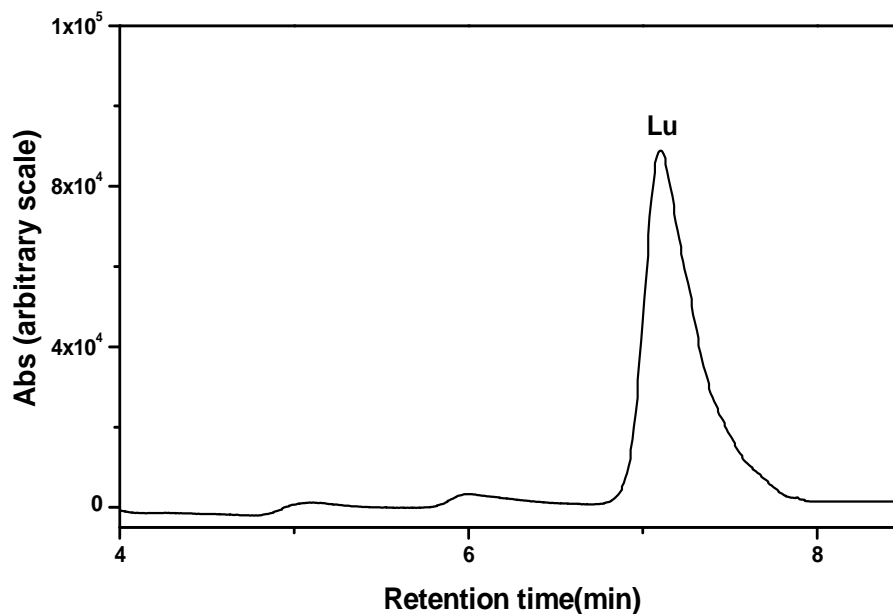


Fig.8.8. Retention behaviour of lutetium using ionic liquid [Hbet][NTf₂] with α -HIBA as mobile phase on reversed phase support. Column: 25 cm (5 μm) length reversed phase support; Mobile phase: 0.002 M betaine NTf₂ + 0.05 M HIBA, pH: 2.68; Flow rate: 2 mL/min. Sample: Lu (20 ppm) in 0.01 N HNO₃; Detection: PCR with arsenazo(III) at 655 nm.

The separation factors for adjacent lanthanides were calculated and shown in **Table.8.1**. The elution order observed is similar to one observed in a dynamic ion-exchange system where Lu^{+3} is eluted first and La^{+3} is eluted last. This could be due to strong complexation of Lu^{+3} -HIBA system over La^{+3} -HIBA system. It is possible that TSIL, betain NTf₂ through cation exchange would have complexed Lu^{+3} preferentially over La^{+3} . The stability constant of Lu^{+3} -HIBA complex is far higher compared to that of La^{+3} -HIBA complex; hence Lu^{+3} - complex eluted first and La^{+3} complex eluted at the end. These studies clearly established strong influence of ionic liquid, betaine NTf₂ in its complexation

with lanthanides. The absence of ionic liquid in the mobile phase, i.e., only with α -HIBA in the mobile phase, resulted in a single peak with all lanthanides eluting together. The use of TSIL offers new avenues for improving the separation factors by introduction of task specific ionic liquids into the chromatographic system.

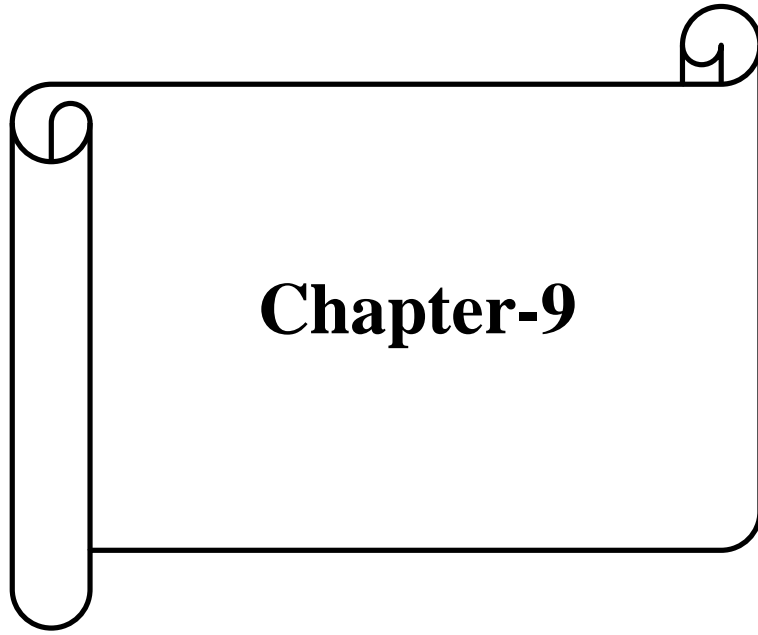
Table.8.1 Separation factors for adjacent lanthanides

Lanthanides	Separation factor
La:Ce	1.19
Ce:Pr	1.13
Pr:Nd	1.07
Nd:Sm	1.24
Sm:Eu	1.13
Eu:Gd	1.06
Gd-Tb	1.20
Tb-Dy	1.15
Dy-Ho	1.09
Ho-Er	1.11
Er-Tm	1.10
Tm-Yb	1.10
Yb-Lu	1.07

Mobile phase: 0.002 M [Hbet][NTf₂] with 0.05 M α -HIBA, pH:2.68

8.4 Conclusion

Preliminary investigations were carried out in the present work using TSIL as the mobile phase. These studies indicated potential application of ionic liquids for the development of separation procedures for isolation of individual lanthanides and also for the isolation of uranium from thorium. These studies established that TSIL can be employed for selective sorption of uranium over thorium. Task specific ionic liquids can be synthesized and anchored on a chromatographic support for selective sorption and separation metal ions of interest.



Chapter-9

Chapter-9

Summary and Conclusion

This chapter summarises the results of the investigations carried out in the present work. Following studies were carried out for the development of high performance separation of lanthanides and actinides.

- Development of rapid separation methods for the isolation of individual lanthanides and some actinides on small particle (1.8 μm) based reversed phase and monolith based supports. These methods were demonstrated for the measurement of atom percent burn-up of nuclear reactor fuels.
- A single stage coupled column HPLC technique has been developed and demonstrated for separation and determination of lanthanides in uranium matrix. This method was applied for the determination of atom percent burn-up of nuclear reactor fuels; the method can be employed to estimate lanthanide impurities in samples of UO_2 (1 in 10^6) without removal of uranium matrix.
- The retention of lanthanides and actinide complexes was correlated with their stability constant; based on these investigations, a HPLC technique has been developed for estimation of stability constant of ligands with lanthanides and actinides. Stability constants were also estimated for different ionic strengths. Speciation of lanthanides and actinides was carried out using stability constant data; the retention behavior of actinide complexes during reversed phase chromatographic technique has been explained based on the speciation data.

- Influence of temperature on the elution behaviour of lanthanides and actinides was investigated. It was observed in the present study that use of elevated temperature (40-80°C) resulted in overall reduction in separation time.
- Retention of lanthanides and some actinides was investigated using task-specific ionic liquids. Separation of uranium from thorium was demonstrated; similarly, individual separation of lanthanides was also carried out using TSIL.

9.1 Rapid separation of lanthanides and actinides on small particle based reversed phase supports

High performance liquid chromatographic separation of individual lanthanides as well as uranium from thorium was investigated for the first time on small particle (1.8 μm) based reversed phase supports. Based on these studies, a dynamic ion-exchange chromatographic separation technique was developed using camphor-10-sulfonic acid as the ion-pairing reagent and α -HIBA as the complexing reagent for the isolation of individual lanthanides as well as for the separation of uranium from thorium. Capacity factor of lanthanides was measured as a function of CSA, HIBA and mobile phase pH. Based on these studies, separation factor of adjacent lanthanides was measured under various experimental conditions. The lanthanides could be isolated from each other in 3.6 min from 1.8 μm based support using gradient elution. Use of 1.8 micron particle column resulted in faster separation of individual lanthanides compared to the use of 5 micron particle of 25 cm length support, which has resulted in 7.9 min. The column efficiency observed with 1.8 μm based 3 cm length reversed phase support ($N \sim 100,000$ plates per meter) is much higher than the column efficiency of 5 μm based 25 cm length reversed phase support ($N \sim 37,000$ plates/meter). Thus use of shorter column length with smaller particle support has been

demonstrated in the present study to achieve rapid separations maintaining more or less similar separation factor between adjacent lanthanides.

Reversed phase HPLC technique was demonstrated for the isolation and quantitative determination of uranium from thorium as well as lanthanide group from uranium. Rapid separation of lanthanide group from thorium and uranium was achieved in about a minute. The rapid separation technique was demonstrated for separation and determination of lanthanides in uranium matrix (typically La:U~1:2000) of salts of pyrochemical process samples.

9.2 Liquid chromatographic behavior of lanthanides and actinides on monolith supports

The retention of lanthanides, and some actinides was studied on a reversed phase monolith supports. Individual separation of lanthanides was carried out using a dynamic ion-exchange technique in isocratic and gradient elution modes. Capacity factor and separation factor of lanthanides was measured as a function of α -HIBA, CSA and mobile phase pH. A Rapid separation of individual lanthanides (2.77 min) was demonstrated using monolith support and this could be the fastest LC technique reported as of now in literature, to the best of my knowledge. The column efficiency of modified monoliths is ~44,000 plates per meter. The back pressure observed with monolith supports is far too low compared to the one observed with small particle supports. Hence monolithic columns were operated at higher flow rates in the present study to achieve rapid separation of individual lanthanides.

The reversed phase retention behaviour of uranium and thorium was also investigated on the reversed phase monolith supports of 10 cm length column as well as 5 cm length column. The retention behavior was also investigated on monolith support

modified with bis-2-ethylhexyl succinamic acid (BEHSA), using α -HIBA as well as HNO_3 as the mobile phase. Elution profiles of uranium and thorium were studied as a function of the BEHSA concentration, mobile phase composition, and its flow rate. The separation factor for U/Th was determined under various experimental conditions. Uranium could be isolated from thorium in about 0.34 min using 0.01 N HNO_3 as the mobile phase. Thus modified monolith supports were employed in the present study for the rapid separation of lanthanides and actinides.

9.3 Burn-up measurement on nuclear reactor fuels using HPLC

The dynamic ion-exchange techniques using small particle based support as well as monolith support were demonstrated for determining the concentrations of lanthanide fission products such as La, Ce, Pr, Nd and Sm in the dissolver solution of nuclear reactor fuels. Direct injection of dissolver solution on a monolithic support was demonstrated for the first time for the determination of atom percent burn-up without pre-separation of matrix uranium and plutonium.

Uranium was separated from Pu(III) as well as Pu(IV) by reversed phase as well as dynamic ion-exchange HPLC technique. A reversed phase chromatographic technique has been developed for the assay of uranium and plutonium present in the dissolver solution of nuclear reactor fuels.

9.4 Single stage coupled column HPLC technique for separation and determination of lanthanides in uranium matrix - application to burn-up measurement on nuclear reactor fuel

Single stage coupled column chromatographic method was demonstrated for the first time towards separation and determination of lanthanides in uranium matrix. Tri-n-octylphosphine oxide modified reversed phase column connected in series with a

dynamically modified cation exchange monolithic column accomplished the task of individual isolation of lanthanides from uranium matrix. The proposed method eliminates the step of uranium matrix removal for the determination of lanthanides. Samples with lanthanide to uranium ratio, as high as 1: 10^6 , were directly injected into the “coupled double column” for the quantitative determination of lanthanides without uranium matrix removal. Samples of lanthanides in uranium matrix could be injected as much as 45 times consecutively into the HPLC system for determination of lanthanides without any uranium elution. The retention behaviour of Pu(IV), Pu(III), Am(III) and various fission products such as Zr, Mo, Cs, Ba, Sr, Ru, Rh, Pd and lanthanides was also studied on the TOPO modified reversed phase support. The single stage coupled column chromatographic technique was also demonstrated for the separation and determination of lanthanide fission products in the dissolver solution of PHWR and fast reactor spent fuels for the determination of atom percent burn-up.

9.5 Correlation of retention of lanthanide and actinide complexes with stability constants and their speciation

Correlation on retention of lanthanide and some actinide complexes on a chromatographic column with their stability constant have been investigated in the present study. Large number of chromatograms were recorded under various experimental conditions. From these studies, a correlation has been established between capacity factor of a metal ion, concentration of ion-pairing reagent and complexing agent with the stability constant of metal complex.

Based on these studies, it has been shown that the stability constant of lanthanide and actinide complexes can be estimated using a single lanthanide calibrant. Validation of the method was carried out with the complexing agents such as α -HIBA, mandelic acid and

lactic acid. It was also demonstrated that data from a single chromatogram can be used for estimation of stability constant at various ionic strengths and the estimated stability constant data are found to be in very good agreement with the experimentally determined values. These studies also demonstrated that the method can be applied for estimation of stability constant of actinides with a ligand whose value is not reported yet. The chromatographic separation method is fast and the estimation of stability constant can be done in a very short time, which is a significant advantage especially in dealing with radioactive elements. The stability constant data was also employed to compute speciation of plutonium in different oxidation states as well as that of americium with α -HIBA. The elution behavior of actinides such as Pu and Am from reversed phase chromatographic technique could be explained based on these studies.

9.6 Influence of temperature on the elution behaviour of lanthanides and some actinides using HPLC

The effect of temperature (25°C to 85°C) on the retention of lanthanides and some actinides on chromatographic supports was investigated. Dynamic ion-exchange and reversed phase chromatographic techniques were employed for the individual separation of lanthanides and actinides such as uranium and thorium. It was observed from these studies that total retention time was reduced to approximately half of its initial time at 85°C compared to the one at 25°C for individual separation of lanthanides. A temperature gradient was also employed to separate the individual lanthanides in an isocratic mode in ~ 16 min. The retention of actinides such as uranium and thorium was also investigated on a reversed phase based support using α -HIBA, mandelic acid and lactic acid as a function of temperature from 25°C to 85°C.

Capacity factors of lanthanides, U and Th were correlated as a function of temperature using van't Hoff plot and linear correlation has been established; from this study, enthalpy of sorption ($\Delta H_{\text{sorption}}$) of lanthanides, uranium and thorium has been computed. These studies demonstrated potential use of carrying dynamic ion-exchange/reversed phase chromatographic techniques at elevated temperature for achieving rapid separations.

9.7 Task-specific ionic liquids in liquid chromatography-Studies on the sorption behaviour of lanthanides and some actinides

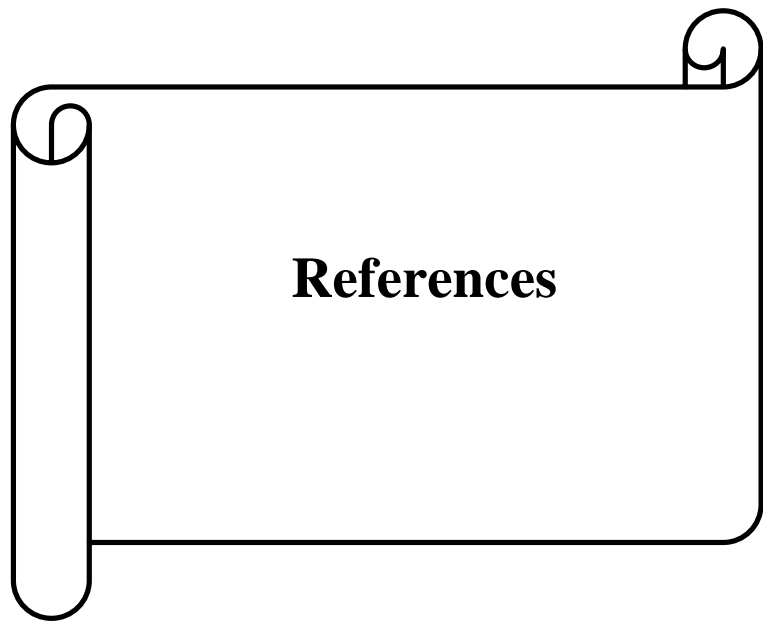
Task-specific ionic liquids such as 1-butyl-3-methylimidazolium benzoate (bmim-benzoate), protonated betaine bis(trifluoromethylsulfonyl)imide ([Hbet][NTf₂]) and its precursor betaine chloride ([Hbet] Cl) were examined for the first time as mobile phase along with complexing reagent, i.e., α -hydroxy isobutyric acid to study the sorption behaviour of uranium, thorium and lanthanides on reversed phase chromatographic supports. Retention behavior of uranium and thorium was investigated with ionic liquids, 1-butyl-3-methylimidazolium benzoate and betaine chloride. The separation factors for U-Th as well as adjacent lanthanide pairs were measured under various experimental conditions. Highest separation factor for separation of uranium and thorium was obtained with 1-butyl-3-methylimidazolium benzoate as an ionic liquid. Individual separation of lanthanides was observed with task specific ionic liquid, protonated betaine bis(trifluoromethylsulfonyl)imide [Hbet][NTf₂], though the separation efficiency was not on par with the one achieved with dynamic ion exchangers.

Future Studies

The results obtained in this present study indicated some promising research areas for the future work. They are listed below.

1. The stability constant of lanthanides and actinides with new ligands can be estimated in shortest possible time. Precisely predicting retention of actinides, e.g. curium and americium can be employed to collect their valuable fractions during their isolation from various stages of nuclear fuel cycle.
2. Single stage dual column chromatography can be employed to estimate lanthanide poisons in the samples of UO_2 without the removal of uranium matrix. Similarly, development of extraction chromatographic methods will be of immense interest and use for the determination of various metal ion impurities in plutonium matrix.
3. Preliminary experiments on the use of ionic liquids as mobile phase for separation of lanthanides and actinides indicated promising results. Ionic liquids as well as task specific ionic liquids can be incorporated into the stationary phase for isolation of specific metal ions.
4. The use of high temperature liquid chromatographic technique can be examined for development of superior isolation procedures for lanthanides and actinides.
5. The dynamic ion-exchange techniques can be extended for the preparative scale purification of actinides such as Am and Cm; similarly, bulk scale isolation of uranium from thorium matrix can be examined.

These studies eventually may pave way for the development of superior isolation procedures of lanthanides and actinides.



References

References

- [1] P. A. Sewell, B. Clarke, *Chromatographic separations, analytical chemistry by open learning*, John Wiley & Sons, New York, 1987.
- [2] L. R. Snyder, J. J. Kirkland, *Introduction to modern liquid chromatography*, 2nd Edn, John Wiley & Sonc, Inc, New York, 1979.
- [3] E. Heftmann, *Chromatography (6th ed): Fundamentals and applications of chromatography and related differential migration methods; Part B: applications*, Elsevier, Vol. 69, New York, 2004.
- [4] A. Striegel, W. W. Yau, J. J. Kirkland, and D. D. Bly (2nd), *Modern size-exclusion liquid chromatography: Practice of gel permeation and gel filtration chromatography*, John-Wiley & Sons, USA, 2009.
- [5] M. S. Tswett, *Ber. Dtsch. Botan. Ges.*, 24 (1906) 316-323.
- [6] M. S. Tswett, *Ber. Dtsch. Botan. Ges.*, 24 (1906) 384-393.
- [7] M. S. Tswett, *Ber. Dtsch. Botan. Ges.*, 44 (1911) 1124-1127.
- [8] A. P. J. Martin, R. L. M. Synge, *Biochem. J.*, 35 (1941) 1358-1368.
- [9] H. H. Strain, J. Sherma, *J. Chem., Educ.*, 44 (1967) 235-237.
- [10] K. Sakodynskii, K. Chmutov, *Chromatographia*, 5 (1972) 471-476.
- [11] L. S. Ettre, "Evolution of liquid chromatography-a historical overview"-In Cs. Horvath (ed), *high performance liquid chromatography-advances and prospectives*, Academic Press, New York, Vol. 1, 1980.
- [12] E. Stahl, "75 years of chromatography-a historical dialogue"- In L. S. Ettre, A. Zlarkis (eds) Elsevier, Amsterdam, 1979.
- [13] A. C. Roque, C. R. Lowe, *Methods Mol. Biol.*, 421 (2008) 1-21.
- [14] Y. V. Shostenkot, V. P. Georgievskii, M. G. Levin, *J. Anal. Chem.*, 55 (2000) 904-905.

- [15] H. Small, Ion chromatography, Plenum Press, New York and London, 1989.
- [16] D. T. Gjerde, J. S. Fritz, Ion Chromatography, 3rd ed., Weinheim, Wiley-VCH, New York, 2000.
- [17] M. C. Breadmore, S. Shrinivasan, J. Karlinsey, J. P. Ferrance, P. M. Norris, J. P. Landers, Electrophoresis, 24 (2003) 1261-1270.
- [18] E. Katz, K. L. Ogan, R. P. W. Scott, J. Chromatogr., 270 (1983) 51-75.
- [19] S. Ahuja, M. W. Dong (ed), Handbook of pharmaceutical analysis by HPLC, Elsevier/Academic Press, Amsterdam, 2005.
- [20] Y. V. Kazakevich and R. Lobrutto (ed.), HPLC for pharmaceutical scientists, John Wiley and Sons. Inc, New Jersey, Canada, 2007
- [21] G. Guiochon, S. G. Shizazi and A. M. Katti, "Fundamentals of preparative and nonlinear chromatography", Academic Press, Boston, 1994.
- [22] F. Svec, J. M. L. Frechet, Anal. Chem., 64 (1992) 820-822.
- [23] H. Zou, X. Huang, M. Ye, Q. Luo, J. Chromatogr., 954 (2002) 5-32.
- [24] A. M. Siouffi, J. Chromatogr., 1000 (2003) 801-818.
- [25] K. Cabrera, J. Sep. Sci., 27 (2004) 843-852.
- [26] I. Mihelic, T. Koloini, A. Podgornik, M. Barut, A. Strancar, Acta Chim. Slov., 48 (2001) 551-564
- [27] N. Tanaka, H. Kobayashi, K. Nakanishi, H. Minakuchi, N. Ishizuka, Anal. Chem., 73 (2001) 420A-429A.
- [28] D. Lubda, K. Cabrera, W. Kraas, C. Schaefer, D. Cunningham, R. E. Majors, LC.GC Europe, December 2001.
- [29] H. Minakuchi, K. Nakanishi, N. Soga, N. Ishizuka, N. Tanaka, Anal. Chem., 68 (1996) 3498-3501.

- [30] F. Svec, *J. Chromatogr.*, 1228 (2012) 250-262.
- [31] E. Sugrue, P. N. Nesterenko, B. Paull, *Anal. Chim. Acta*, 553 (2005) 27-35
- [32] J. Scancar, R. Milacic, *Trends in Anal. Chem.*, 28 (2009) 1048-1056.
- [33] R. Giovannini, R. Freitag, T. B. Tennikova, *Anal. Chem.*, 70 (1998) 3348-3355
- [34] M. Vodopivec, A. Podgornik, M. Berovic, A. Strancar, *J. Chromatogr. Sci.*, 38 (2000) 489-495
- [35] A. Podgornik, M. Barut, J. Jancar, A. Strancar, T. B. Tennikova, *Anal. Chem.*, 71 (1999) 2986-2991
- [36] A. Podgornik, M. Barut, J. Jancar, A. Strancar, *J. Chromatogr.*, 848 (1999) 51-60
- [37] J. J. Arnikaar, *Essentials of nuclear chemistry*, New Age International, 4th edn, India, 1995.
- [38] *Atomic data and nuclear data tables: Fission product yields from neutron induced fission*, E. A. C. Crouch, Academic Press, New York and London, 1977.
- [39] K. A. Gschneidner, L. Eyring, *Handbook on the physics and chemistry of rare earths*, vol. 9, Elsevier, Amsterdam, 1987.
- [40] S. A. Cotton, *Lanthanides and actinides*, Macmillan, London, 1991.
- [41] F. H. Spedding, A. H. Daane, *The rare earths*, Wiley, New York, 1961.
- [42] C. K. Gupta, N. Krishnamurthy, *Extractive metallurgy of rare earths*, CRC Press, (2004).
- [43] S. Kobayashi, R. Anwender, *Lanthanides: Chemistry and use in organic synthesis*, Springer, Verlag, Berlin, Heidelberg, 1999.
- [44] B. G. Wybourne, L. Smentek, *Optical spectroscopy of lanthanides: magnetic and hyperfine interactions*, CRC Press, 2007.
- [45] J. C. G. Bunzli, G. R. Choppin, *Lanthanide probes in life, chemical and earth Sciences:*

- Theory and practice, Elsevier, Amsterdam, 1989.
- [46] C. Preinfalk, G. Morteani, Special publication of the society for geology applied to Mineral Deposits, 7 (1989) 359-370.
- [47] N. R. Larsen, J. Radioanal. Chem., 52 (1979) 85-91.
- [48] C. H. Knight, R. M. Cassidy, B. M. Recoskie, L.W. Green, Anal. Chem., 56 (1984) 474-478.
- [49] N. Sivaraman, S. Subramaniam, T.G. Srinivasan, P. R. Vasudeva Rao, J. Radioanal. Nucl. Chem., 253 (2002) 35-40.
- [50] J. J. Katz, G. T. Seaborg, L. R. Morss, The chemistry of the actinide elements, Chapman and Hall Publishers, London, New York, 1986.
- [51] S. Ahrland, J. O. Liljenzin, J. Rydberg, The actinides solution chemistry, Comprehensive inorganic chemistry, Pergamon Press, Oxford, 1973.
- [52] G. R. Choppin, Radiochim. Acta, 32 (1983) 42-53.
- [53] R. A. Beauvais, S. D. Alexandratos, React. Funct. Polym., 36 (1998) 113-123.
- [54] R. C. Martin, J. B. Knauer, P. A. Balo, Appl. Radiat. Isotopes, 53 (2000) 785-792.
- [55] V. Sarma Mallela, V. Ilankumaran, N. S. Rao, Indian Pacing Electrophysiol. J. 4 (2004) 201-212.
- [56] W. J. Maeck, W. A. Emel, J. E. Delmore, F. A. Duce, L. L. Dickerson, J. H. Keller, R. L. Tromp, Report No. EY-76-C-07-1540, 1976.
- [57] W. N. Bishop, Nuclear Regulatory Commission, Washington D.C., Vol. 1, Report NUREG/CP 004, p. 469, 1977.
- [58] B. Saha, R. Bagyalakghmi, G. Periaswami, V. D. Kevimandan, S. A. Chitambar, H. C. Jain, C. K. Mathews, Determination of nuclear fuel burn-up using mass spectrometric techniques, Report No. B.A.R.C-891, India, 1976

- [59] Y. B. Novikov, V. Y. Gabeskiriya, V. V. Gryzina, V. V. Tikhomirov, *Atomic Energy*, 43 (1977) 871-874.
- [60] M. Iqbal, T. Mehmood, S. K. Ayazuddin, A. Salahuddin, S. Pervez, *Annals of Nuclear Energy*, 28 (2001) 1733-1744.
- [61] K. Suyama, H. Mochizuki, *Annals of Nuclear Energy*, 33 (2006) 335-342.
- [62] C. Willman, A. Hakansson, O. Osifo, A. Backlin, S. J. Svard, *Annals of Nuclear Energy*, 33 (2006) 427-438.
- [63] J. E. Rein, B. F. Rider, Burn-up determination of nuclear fuels, AEC Research and Development report, Report TID-17385, TID-4500 (18th Ed.), 1963.
- [64] A. J. Fudge, A. J. Wood, M. F. Banham, Report TID-7629, p. 152, 1961.
- [65] ASTM Standards E 321 – 96 (Reapproved 2005); “Standard Test Method for Atom Percent Fission in Uranium and Plutonium Fuel (Neodymium-148 Method)”, PA 19428-2959, United States.
- [66] P. Deregge, R. Boden, *J. Radioanal. Chem.*, 35 (1977) 173-184.
- [67] D. Karunasagar, M. Joseph, B. Saha, C. K. Mathews, *Sep. Sci. Tech.*, 23 (1988) 1949-1957.
- [68] R. M. Cassidy, S. Elchuk, N. L. Elliot, L. W. Green, C. H. Knight, B. M. Recoskie, *Anal. Chem.*, 58 (1986) 1181-1186.
- [69] P. Henderson, *Rare earth element geochemistry*, Elsevier, Amsterdam, 1984.
- [70] E. R. Tompkins, J. X. Khym, W. E. Cohn, *J. Am. Chem. Soc.*, 69 (1947) 2769-2777.
- [71] F. H. Spedding, A. F. Voigt, E. M. Gladrow, N. R. Sleight, *J. Am. Chem. Soc.*, 69 (1947) 2777-2781.
- [72] J. A. Marinsky, L. E. Glendenin, C. D. Coryell, *J. Am. Chem. Soc.*, 69 (1947) 2781-2785.

- [73] D. H. Harris, E. R. Tompkins, *J. Am. Chem. Soc.*, 69 (1947) 2792-2800.
- [74] B. H. Ketelle, G. E. Boyd, *J. Am. Chem. Soc.*, 69 (1947) 2800-2812.
- [75] F. H. Spedding, E. I. Fulmer, T. A. Butler, E. M. Gladrow, M. Gobush, P. E. Porter, J. E. Powell, J. M. Wright, *J. Am. Chem. Soc.*, 69 (1947) 2812-2818.
- [76] S. W. Mayer, E. R. Tompkins, *J. Am. Chem. Soc.*, 69 (1947) 2866-2874.
- [77] G. R. Choppin, R. J. Silva, *J. Inorg. Nucl. Chem.*, 3 (1956), 153-154.
- [78] S. G. Thompson, USAEC Report. UCRL-8615, Lawrence Berkeley Laboratory, University of California, Berkeley, California, 1959.
- [79] L. S. Clesceri, A. E. Greenberg, R. R. Trussell, M. A. M. Franson (Eds), *Standards methods for the Examination of water and waste water*, Edn 17th, American public health Association , Washington, DC, part 3000, 1998.
- [80] L. S. Clesceri, A. E. Greenberg, R. R. Trussell, M. A. M. Franson (Eds), *Standards methods for the examination of water and waste water*, Edn 20th, American public health association , Washington, DC, part 7000, 1998.
- [81] R. R. Greenberg, H. M. Kingston, *Anal. Chem.*, 55 (1983) 1160-1165.
- [82] Y. Igarashi, C. K. Kim, Y. Takatu, K. Shiraishi, M. Yamamoto, N. Ikeda, *Anal. Sci.*, 6 (1990) 157-164.
- [83] J. Korkisch, *Modern methods for the separation of rarer metal ions*, Chapter 3, Pergamon Press, Oxford, 1969.
- [84] K. L. Nash, M. P. Jensen, *Sep. Sci. and Tech.*, 36 (2001) 1257-1282.
- [85] D. H. Sisson, V. A. Mode, D. O. Campbell, *J. Chromatogr.*, 66 (1972) 129-135.
- [86] M. Schadel, N. Trautmann, G. Herrmann, *Radiochim. Acta*, 24 (1977) 27-31.
- [87] S. Elchuk, R. M. Cassidy, *Anal. Chem.*, 51, (1979) 1434-1438.
- [88] D. O. Campbell, *J. Inorg. Nucl. Chem.*, 35 (1973), 3911-3919.

- [89] B. H. Ketelle, G. E. Boyd, *J. Am. Chem. Soc.*, 69 (1947) 2800-2812.
- [90] K. Yoshida, H. Haraguchi, *Anal. Chem.*, 56 (1984) 2580-2585.
- [91] J. E. Girard, *Anal. Chem.*, 51 (1979) 836-839.
- [92] P. Dufek, M. Vobecky, J. Valaek, *J. Chromatogr.*, 435 (1988) 249-252.
- [93] G. J. Sevenich, J. S. Fritz, *Anal. Chem.*, 55 (1983) 12-16.
- [94] S. Elchuk, K. I. Burns, R. M. Cassidy, C. A. Lucy, *J. Chromatogr.*, 558 (1991) 197-207.
- [95] M. N. Raut, P. G. Jaison, S. K. Aggarwal, *J. Chromatogr.*, 1052 (2004) 131-136.
- [96] J. M. Schwantes, R. S. Rundberg, W. A. Taylor, D. J. Vieira, *J. Alloys and Compd.*, 418 (2006) 189-194.
- [97] A. Tsuyoshi, K. Akiba, *Anal. Sci.*, (2000) 843-846
- [98] B. A. Bidlingmeyer, *J. Chromatogr. Sci.*, 18 (1980) 525-539.
- [99] B. A. Bidlingmeyer, S. N. Deming, W. P. J. Price, B. Sachok, M. Petrussek, *J. Chromatogr.*, 186 (1979) 419-434.
- [100] N. Sivaraman, R. Kumar, S. Subramaniam, P. R. Vasudeva Rao, *J. Radioanal. Nucl Chem.*, 252 (2002) 491-495.
- [101] P. R. Haddad, P. E. Jackson, *Ion chromatography-principles and applications*, *J. Chromatogr. Libr.*, Vol. 46, Elsevier, New York, 1990.
- [102] D. J. Barkley, L. A. Bennett, J. R. Charbonneau, L.A. Pokrajac, *J. Chromatogr.*, 606 (1992) 195-201.
- [103] F. Hao, P. R. Haddad, P. E. Jackson, J. J. Carnevale, *J. Chromatogr.*, 640, (1993) 187-194.
- [104] V. Vidyalakshmi, M. S. Subramanian, N. Sivaraman, T. G. Srinivasan, P. R. Vasudeva Rao, *J. Liq. Chromatog. Relat. Technol.*, 27 (2004) 2269-2291.

- [105] M. A. Maheswari, D. Prabhakaran, M. S. Subramanian, N. Sivaraman, T. G. Srinivasan, P. R. Vasudeva Rao, *Talanta*, 72 (2007) 730–740.
- [106] C. S. K. Raju, M. S. Subramanian, N. Sivaraman, T. G. Srinivasan, P. R. Vasudeva Rao, *J. Chromatogr.*, 1156 (2007) 340–347.
- [107] S. P. Verma, R. Garcia, E. Santoyo, A. Aparicio, *J. Chromatogr.*, 884 (2000) 317-328.
- [108] D. N. Cvjeticanin, M. M. Vucetic, *J. Chromatogr.*, 103 (1975) 305-310.
- [109] V. T. Hamilton, W. Dale Spall, B. F. Smith, E. J. Peterson, *J. Chromatogr.*, 469, (1989) 369-377.
- [110] F. Hao, B. Paull, P. R. Haddad, *J. Chromatogr.*, 739, (1996) 151-161.
- [111] P. G. Jaison, V. M. Telmore, P. Kumar, S. K. Aggarwal, *J. Chromatogr.*, 1216 (2009) 1383–1389.
- [112] D. J. Barkley, M. Blanchette, R. M. Cassidy, S. Elchuk, *Anal. Chem.*, 58 (1986) 2222-2226.
- [113] R. M. C. Sutton, S. J. Hill, P. Jones, A. Sanz-Medel, J. I. Garcia-Alonso, *J. Chromatogr.*, 816, (1998) 286-291.
- [114] M. P. Harrold, A. Siriraks, J. Riviello, *J. Chromatogr.*, 602 (1992) 119-125.
- [115] G. R. Choppin, *J. Radioanal. Nucl. Chem.*, 273 (2007) 695-703.
- [116] D. M. Nelson, R. P. L. W. R. Penrose, Chemical speciation of plutonium in natural waters, *Proc. Symp., USDOE, Washington D. C.*, p. 27, (1987).
- [117] E. Ansoborlo, O. Prat, P. Moisy, C. D. Auwer, P. Guilbaud, M. Carriere, B. Gouget, J. Duffield, D. Doizi, T. Vercouter, C. Moulin, V. Moulin, *Biochim.*, 88 (2006) 1605-1618.
- [118] G. Shtacher, *J. Inorg. Nucl. Chem.*, 28 (1966) 845-861.

- [119] L. Chen, M. Bos, P. D. J. Grootenhuis, A. Christenhusz, E. Hoogendam, D. N. Reinhoudt, W. E. Van Der Linden, *Anal. Chim. Acta*, 201 (1987) 117-125.
- [120] P. Janos, *J. Chromatogr.*, 641 (1993) 229-234
- [121] L. Harju, *Talanta*, 34 (1987) 817-820.
- [122] T. Welton, *Chem. Rev.*, 99 (1999) 2071-2084.
- [123] P. Wasserscheid, T. Welton, *Ionic liquids in synthesis*, Wiley-VCH, Weinheim, Germany, 2002.
- [124] P. A. Z. Suarez, J.E.L. Dullius, S. Einloft, R. F. De Souza, *Polyhedron*, 15 (1996) 1217-1219.
- [125] M. J. Earle, K. R. Seddon, C. J. Adam, G. Roberts, *Chem. Commun.*, 19 (1998) 2097-2098.
- [126] C. J. Adam, M. J. Earle, K. R. Seddon, *Green. Chem.*, 2 (2000) 21-24.
- [127] S. T. Handy, X. L. Zhang, *Org. Lett.*, 3 (2001) 233-236.
- [128] J. G. Huddleston, H. D. Willauer, R. P. Swatloski, A. E. Visser, R. D. Rogers, *Chem. Commun.*, 16 (1998) 1765-1766.
- [129] G. Mamantov, A. I. Popov, *Chemistry of nonaqueous solvents: current progress*, VCH, New York, 1994.
- [130] I. W. Sun, C. L. Hussey, *Inorg. Chem.*, 28 (1989) 2731-2737.
- [131] K. A. Venkatesan, T. G. Srinivasan, P. R. Vasudeva Rao, *J. Nucl. Radiochem. Sci.*, 10 (2009) R1-R6
- [132] J. L. Anderson, D. W. Armstrong, *Anal. Chem.*, 75 (2003) 4851-4858.
- [133] D. W. Armstrong, L. He, Y. S. Liu, *Anal. Chem.*, 71 (1999) 3873-3876.
- [134] A. Berthod, L. He, D. W. Armstrong, *Chromatographia*, 53 (2001) 63-68.
- [135] C. F. Poole, S. K. Poole, *J. Sep. Sci.*, 34 (2011) 888-900.

- [136] J. Flieger, *Anal. Lett.*, 42 (2009) 1632–1649.
- [137] M. P. Marszall, R. Kaliszan, *Crit. Rev. Anal. Chem.* 37 (2007) 127-140.
- [138] C. F. Poole, B. R. Kersten, S. S. J. Ho, M. E. Coddens, K. G. Furton, *J. Chromatogr.*, 352 (1986) 407-425.
- [139] Y. Wang, M. Tian, W. Bi, K. H. Row, *Int. J. Mol. Sci.* 10 (2009) 2591-2610
- [140] D. Parriott, *A Practical Guide to HPLC Detection*, Academic Press, San Diego, 1993.
- [141] G. Schwarzenbach, *Standardization of lanthanides with EDTA in complexometric Titrations*, Interscience, New York, USA, pp 77-82, 1957.
- [142] J. Mendham, R. C. Denney, J. D. Barnes, M. J. K. Thomas, *Vogel's: Textbook of quantitative chemical analysis*, 6th Edn, Pearson Education Ltd, Asia, 2002.
- [143] A. Suresh, T. G. Srinivasan, P. R. Vasudeva Rao, *Solvent Extr. Ion Exch.* 12 (1994) 727-744.
- [144] O. A. Vita, C. R. Walker, E. Litteral, *Anal. Chim. Acta*, 64 (1973) 249-257.
- [145] K. Robards, S. Clarke, E. Patsalides, *Analyst*, 113 (1988) 1757-1779.
- [146] M. Kumar, *Analyst*, 119 (1994) 2013-2024.
- [147] R. M. Cassidy, S. Elchuk, *Anal. Chem.*, 54 (1982) 1558-1563.
- [148] P. R. Vasudeva Rao, N. Sivaraman, T. G. Srinivasan, *Studies on the lanthanide separation using HPLC*, *Encyclopedia of Chromatography*, (2005).
- [149] J. Cowan, M. J. Shaw, E. P. Achterberg, P. Jones, P. N. Nesterenko, *Analyst*, 125 (2000) 2157-2159.
- [150] S. Vavilov, T. Kobayashi, M. Myochin, *J. Nucl. Sci. Tech.*, 41, (2004) 1018-1025.
- [151] W. Davies, W. Gray, *Talanta*, 11 (1964) 1203-1211.
- [152] S. Hjerten, J. L. Liao, R. Zhang, *J Chromatogr.*, 473 (1989) 273-275.
- [153] S. Xie, F. Svec, J. M. Frechet, *J. Chromatogr.*, 775 (1997) 65-72.

- [154] N. Tanaka, H. Kobayashi, N. Ishizuka, H. Minakuchi, K. Nakanishi, K. Hosoya, T. Ikegami, *J. Chromatogr.*, 965 (2002) 35-49.
- [155] H. Minakuchi, K. Nakanishi, N. Soga, N. Ishizuka, N. Tanaka, *J. Chromatogr.*, 762 (1997) 135-146.
- [156] W. Gao, G. Yang, J. Yang, H. Liu, *Turk. J. Chem.*, 28 (2004) 379-385.
- [157] H. Minakuchi, K. Nakanishi, N. Soga, N. Ishizuka, N. Tanaka, *J. Chromatogr.*, 797 (1998) 121-131.
- [158] K. Cabrera, D. Lubda, H-M. Eggenweiler, H. Minakuchi, K. Nakanishi, *J. High Resolut. Chromatogr.*, 23 (2000) 93-99.
- [159] H. Minakuchi, N. Ishizuka, K. Nakanishi, N. Soga, N. Tanaka, *J. Chromatogr.*, 828 (1998) 83-90.
- [160] N. Tanaka, H. Nagayama, H. Kobayashi, T. Ikegami, K. Hosoya, N. Ishizuka, H. Minakuchi, K. Nakanishi, K. Cabrera, D. Lubda, *J. High Resolut. Chromatogr.*, 23 (2000) 111-116.
- [161] K. Cabrera, G. Wieland, D. Lubda, K. Nakanishi, N. Soga, H. Minakuchi, K. K. Unger, *Trend Anal. Chem.*, 17 (1998) 50-53.
- [162] T. Ikegami, N. Tanaka, *Curr. Opin. Chem. Biol.*, 8 (2004) 527-533.
- [163] E. A. Mowafy, H. F. Aly, *J Radioanal. Chem.*, 250 (2001) 199-203.
- [164] G. Thiollet, C. Musikas, *Solvent Extr Ion Exch* 7 (1989) 813-827.
- [165] V. Vidyalakshmi, M. S. Subramanian, T. G. Srinivasan, P. R. Vasudeva Rao, *Solvent Extr. Ion Exch.*, 19, (2001) 37-49.
- [166] Ch. S. K. Raju, M. S. Subramanian, T. G. Srinivasan, P. R. Vasudeva Rao, *Radiochim. Acta*, 94 (2006) 351-356.
- [167] W. J. Maeck, R. P. Larsen, J. E. Rein, A review and status of the nuclear data and

- analytical chemistry methodology requirements, U.S. Atomic Energy Commission, 1973.
- [168] J. E. Rein, *Analytical Methods in the Nuclear Fuel Cycle*, IAEA –SM-149, IAEA, Vienna, 1972.
- [169] R. M. Cassidy, *Trace Anal.*, 1 (1981) 121-192.
- [170] R. M. Cassidy, S. Elchuck, L. W. Green, C. H. Knight, F. C. Miller, B. M. Recoskie, *J. Radioanal. Nucl. Chem.*, 139 (1990) 55-64.
- [171] M. A. Floyd, R. W. Morrow, R. B. Farrar, *Spectrochim. Acta B*, 38 (1983) 303-308.
- [172] K. Satyanarayana, S. Durani, *J. Radioanal. Nucl. Chem.*, 285 (2010) 659-665.
- [173] P. G. Jaison, N. M. Raut, and S. K. Aggarwal, *J. Chromatogr.*, 1122 (2006) 47-53
- [174] C. A. Lucy, L. Gureli, and S. Elchuk, *Anal. Chem.*, 65, (1993) 3320-3325.
- [175] J. D. Navratil, W. W. Schulz, *Actinide separations*, ACS Symposium Series, Vol 117, Chapter 8, Washington D.C., 1980.
- [176] P. G. Manning, *Can J. Chem.*, 40, (1962)1684-1689.
- [177] T. H. Siddall, *J. Inorg. Nucl. Chem.*, 26, (1964)1991-2003.
- [178] E. P. Horwitz, D. J. Kalina, H. Diamond, D. G. Vandegrift, W.W. Schulz, *Solvent Extr Ion Exch.*, 3 (1985) 75-109.
- [179] M. R. Yaftian, M. Burgard, C. Wieseir, D. Matt, *Solvent Extr. Ion Exch.* 16, (1998) 1131-1149.
- [180] F. Arnaud-Neu, J. K. Browne, D. Byrne, D. J. Marrs, M. A. Mckervey, P. Ohagan, M. J. Schwing-Weill, A. Walker, *Chem–Eur. J.*, 5, (1999) 175-186.
- [181] M. Shamsipur, A. R. Ghiasvand, Y. Yamini, *Anal. Chem.*, 71, (1999) 4892-4895.
- [182] A. R. Ghiasvand, E. Mohagheghzadeh, *Anal Sci* 20, (2004) 917-919.
- [183] T. Ishimori, K. Kimura, T. Fujino, H. Murakami, *Nippon Genshiryoku Gakkaishi*

- (Japan), 4 (1962) 117-126.
- [184] F. H. Lin, C. Horvath, *J Chromatogr.*, 589 (1992) 185-195.
- [185] C. Y. Li, J. Z. Gao, G. H. Zhao, J. W. Kang, H. H. He, *Chromatographia*, 46 (1997) 489-494.
- [186] V. V. Nikonorov, *J. Anal. Chem.*, 65 (2010) 359-365.
- [187] P. Janos, *J Chromatogr.*, 1037 (2004) 15-28.
- [188] M. C. Bruzzoniti, E. Mentasti, C. Sarzanini, *J Chromatogr.*, 717 (1998) 3-25.
- [189] P. Janos, *J Chromatogr.*, 737 (1996) 129-138.
- [190] P. Janos, *J Chromatogr.*, 789 (1997) 3-19.
- [191] N. Yoza, *J. Chem. Educ.*, 54 (1977) 284-287.
- [192] R. Portanova, L. H. J. Lajunen, M. Tolazzi, J. Piispanen, *Pure Appl. Chem.*, 75 (2003) 495-540.
- [193] G. R. Choppin, J. A. Chopporian, *J. Inorg. Nucl. Chem.*, 22 (1961) 97-113.
- [194] P. Carpenter, C. B. Monk, R. J. Whewell, *J. Chem. Soc. Faraday Trans I*, 73 (1977) 553-557.
- [195] A. L. J. Rao, M. Singh, S. Sehgal, *Rev. Anal. Chem.*, 8 (1986) 283-312.
- [196] C. W. Davies, *Ion association*, Butterworths, London 1961.
- [197] C. B. Monk, *Electrolytic dissociation*, Academic Press, London 1961.
- [198] K. Bukietynska, A. Mondry, E. Osmeda, *J. Inorg. Nucl. Chem.*, 43 (1981) 1311-1319.
- [199] S. Andersson, K. Eberhardt, C. Ekberg, J. O. Liljenzin, M. Nilsson, G. Skarnemark, *Radiochim. Acta*, 94 (2006) 469-474.
- [200] D. Wenming, Z. Hongxia, H. Meide, T. Zuyi, *Appl. Radiat. Isot.*, 56 (2002) 959-965.
- [201] Z. Y. Tao, Z. J. Guo, W. M. Dong, *J Radioanal Nucl Chem*, 256 (2003) 575-580.
- [202] R. M. C. Dawson, *Data for biochemical research*, Clarendon press, Oxford, 1959.

- [203] J. Bjerrum, *Stability constants*, Chemical society, Vol.1, London, 1958.
- [204] H. F. Aly, M. A. El-Haggan, M. A. Abdel-Rassoul, *J. Radioanal. Chem.*, 30 (1976) 81-91
- [205] F. V. Jr. Warren, B. A. Bidlingmeyer, *Anal Chem.*, 60 (1988) 2821-2824.
- [206] J. W. Dolan, *LC-GC North America*, 20 (2002) 524-530.
- [207] M. G. Kolpachnikova, N. A. Penner, P. N. Nesterenko, *J. Chromatogr.*, 826 (1998) 15-23.
- [208] W. Bashir, E. Tyrrell, O. Feeney, B. Paull, *J. Chromatogr.*, 964 (2002) 113-122.
- [209] R. S. Dybczynski, K. Kulisa, *Sep. Sci. Tech.*, 46 (2011) 1767-1775.
- [210] R. S. Dybczynski, K. Kulisa, *Chromatographia*, 61 (2005) 573-580.
- [211] R. S. Dybczynski, K. Kulisa, *Chem. Anal. (Warsaw)*, 54 (2009) 437-457
- [212] B. Paull, W. Bashir, *Analyst*, 128 (2003) 335-344.
- [213] V. L. McGuffin, C. E. Evans, S. H. Chen, *J. Microcol. Sep.*, 5 (1993) 3-10.
- [214] N. E. Fortier, J. S. Fritz, *Talanta*, 34 (1987) 415-418.
- [215] T. Fornstedt, *J. Chromatogr.*, 1217 (2010) 792-812.
- [216] T. L. Chester, J. W. Coym, *J. Chromatogr.*, 1003 (2003) 101-111.
- [217] P. Hatsis, C. A. Lucy, *J. Chromatogr.*, 920 (2001) 3-11.
- [218] Y. Mao, P. W. Carr, *Anal. Chem.*, 72 (2000) 110-118.
- [219] R. G. Smith, P. A. Drake, J. D. Lamb, *J. Chromatogr.*, 546 (1991) 139-149.
- [220] Y. Baba, N. Yoza, S. Ohashi, *J. Chromatogr.*, 348 (1985) 27-37.
- [221] K. A. Krous, R. J. Raridon, *J. Phys. Chem.*, 63 (1959) 1901-1907.
- [222] J. H. Davis, *J. Chem. Lett.*, 33 (2004) 1072-1077
- [223] P. Nockemann, B. Thijs, S. Pittois, J. Thoen, C. Glorieux, K. V. Hecke,
L. V. Meervelt, B. Kirchner, K. Binnemans, *J. Phys. Chem. B*, 110 (2006) 20978-20992.
- [224] Ch. Jagadeeswara Rao, K. A. Venkatesan, K. Nagarajan, T. G. Srinivasan, *Radiochim. Acta*, 96 (2008) 403-409.



**List of Publications,
Awards / Honors**

Publications

List of publications based on the work described in this thesis is given below.

Journals

1. Rapid Separation of Lanthanides and Actinides on Small Particle Based Reverse Phase Supports; **Arpita Datta**, N. Sivaraman, T. G. Srinivasan and P. R. Vasudeva Rao; Radiochim. Acta, 98, (2010) 277-285.
2. Liquid Chromatographic Behaviour of Actinides and Lanthanides on Monolith Supports; **Arpita Datta**, N. Sivaraman, T. G. Srinivasan and P. R. Vasudeva Rao; Radiochim. Acta, 99, (2011) 275-283.
3. High Performance Separation and Supercritical Extraction of Lanthanides and Actinides; **Arpita Datta**, K. Sujatha, R. Kumar, N. Sivaraman, T. G. Srinivasan and P. R. Vasudeva Rao; Energy Procedia, Elsevier, 8, (2011) 425-430.
4. Single Stage Coupled Column HPLC Technique for the Separation and Determination of Lanthanides in Uranium Matrix-Application to Burn-up Measurement on Nuclear Reactor Fuel; **Arpita Datta**, N. Sivaraman, T. G. Srinivasan and P. R. Vasudeva Rao; Nuclear Technology (2013, TN-12-45).
5. Correlation of Retention of Lanthanide and Actinide Complexes with Stability Constant and Their Speciation; **Arpita Datta**, N. Sivaraman, K. S. Viswanathan, Suddhasattwa Ghosh, T. G. Srinivasan and P. R. Vasudeva Rao; Radiochimica Acta (0.1524/ract.2013.2005).

6. Influence of Temperature on the Elution Behaviour of Lanthanides and Some Actinides on Reversed Phase supports; **Arpita Datta**, N. Sivaraman, Suddhasattwa Ghosh, T. G. Srinivasan and P. R. Vasudeva Rao (manuscript to be submitted).

National and International Conferences

1. Retention Behaviour of Uranium and Thorium on N, N-di(2-ethylhexyl)isobutyramide Reverse Phase Support; **Arpita Datta**, N. Sivaraman, T. G. Srinivasan and P. R. Vasudeva Rao; Nuclear and Radiochemistry Symposium (NUCAR-2009), Mumbai, India, p 487-488, 2009.

2. Task-Specific Ionic Liquids as Mobile Phase in Liquid Chromatography-Studies on the Sorption Behaviour of Uranium, Thorium and Lanthanides; **Arpita Datta**, N. Sivaraman, K. A. Venkatesan, T. G. Srinivasan and P. R. Vasudeva Rao, Nuclear and Radiochemistry Symposium (NUCAR-2009), Mumbai, India, p 489-490, 2009.

3. Liquid Chromatographic Behaviour of Actinides on Monolith Supports; **Arpita Datta**, N. Sivaraman, T. G. Srinivasan and P. R. Vasudeva Rao; Biennial Symposium on Separation Science and Technology (SESTEC-2010), Kalpakkam, India, p 463-464, 2010.

4. Fast Separation of Lanthanides and Actinides on Small Particle Support; **Arpita Datta**, N. Sivaraman, T. G. Srinivasan and P. R. Vasudeva Rao; Biennial Symposium on Separation Science and Technology (SESTEC-2010), Kalpakkam, India, p 465-466, 2010.

5. High Performance Separation and Supercritical Extraction of Lanthanides and Actinides; **Arpita Datta**, K. Sujatha, R. Kumar, N. Sivaraman, T. G. Srinivasan and P. R. Vasudeva Rao; 2nd International Conference on Asian Nuclear Prospects (ANUP-2010), Mamalapuram, India, p FR8, 2010.

6. Liquid Chromatographic Behavior of Lanthanides and its Application on Burn-up Measurement; **Arpita Datta**, N. Sivaraman, T. G. Srinivasan and P. R. Vasudeva Rao; Nuclear and Radiochemistry Symposium (NUCAR-2011), Visakhapatnam, India, p 144-145, 2011.
7. High Performance Separation Studies on Lanthanides and Actinides, **Arpita Datta**, N. Sivaraman, T. G. Srinivasan and P. R. Vasudeva Rao; Chemistry Research Scholar Meet (CRSM- 2011), Kalpakkam, India, 111, 2011.
8. Lanthanides and Actinides Separation Studies using Liquid Chromatography; **Arpita Datta**, N. Sivaraman, T. G. Srinivasan and P. R. Vasudeva Rao; International Conference on Vistas in Chemistry (ICVC-2011), Kalpakkam, India, p 30, 2011.
9. Separation and Estimation of Lanthanides using High Performance Liquid Chromatography; **Arpita Datta**, N. Sivaraman, and P. R. Vasudeva Rao; DAE-BRNS Theme Meeting on Recent trends in Analytical Chemistry (TRAC-2012), Chennai, India, p 54-55, 2012.

Award / Honors

1. Best oral presentation award in Nuclear and Radiochemistry symposium (NUCAR-2009) held at Mumbai, India.
2. Best Poster presentation award in DAE-BRNS Theme Meeting on Recent trends in Analytical Chemistry (TRAC-2012), held at Chennai, India.